

INFORMATION TO USERS

This manuscript has been reproduced from the microfilm master. UMI films the text directly from the original or copy submitted. Thus, some thesis and dissertation copies are in typewriter face, while others may be from any type of computer printer.

The quality of this reproduction is dependent upon the quality of the copy submitted. Broken or indistinct print, colored or poor quality illustrations and photographs, print bleedthrough, substandard margins, and improper alignment can adversely affect reproduction.

In the unlikely event that the author did not send UMI a complete manuscript and there are missing pages, these will be noted. Also, if unauthorized copyright material had to be removed, a note will indicate the deletion.

Oversize materials (e.g., maps, drawings, charts) are reproduced by sectioning the original, beginning at the upper left-hand corner and continuing from left to right in equal sections with small overlaps.

Photographs included in the original manuscript have been reproduced xerographically in this copy. Higher quality 6" x 9" black and white photographic prints are available for any photographs or illustrations appearing in this copy for an additional charge. Contact UMI directly to order.

**Bell & Howell Information and Learning
300 North Zeeb Road, Ann Arbor, MI 48106-1346 USA
800-521-0600**

UMI[®]

Molecular Signaling Pathways Regulating Cation Channels in Ocular Epithelial Cells

By

Jennifer Susan Ryan

Submitted to the Faculty of Graduate Studies
in partial fulfillment of the requirements
for the degree of Doctor of Philosophy
at
Dalhousie University
Halifax, Nova Scotia
Canada

(December, 1998)

© Copyright by Jennifer Susan Ryan, 1998



National Library
of Canada

Acquisitions and
Bibliographic Services

395 Wellington Street
Ottawa ON K1A 0N4
Canada

Bibliothèque nationale
du Canada

Acquisitions et
services bibliographiques

395, rue Wellington
Ottawa ON K1A 0N4
Canada

Your file *Votre référence*

Our file *Notre référence*

The author has granted a non-exclusive licence allowing the National Library of Canada to reproduce, loan, distribute or sell copies of this thesis in microform, paper or electronic formats.

The author retains ownership of the copyright in this thesis. Neither the thesis nor substantial extracts from it may be printed or otherwise reproduced without the author's permission.

L'auteur a accordé une licence non exclusive permettant à la Bibliothèque nationale du Canada de reproduire, prêter, distribuer ou vendre des copies de cette thèse sous la forme de microfiche/film, de reproduction sur papier ou sur format électronique.

L'auteur conserve la propriété du droit d'auteur qui protège cette thèse. Ni la thèse ni des extraits substantiels de celle-ci ne doivent être imprimés ou autrement reproduits sans son autorisation.

0-612-49289-3

Canada

DALHOUSIE UNIVERSITY

FACULTY OF GRADUATE STUDIES

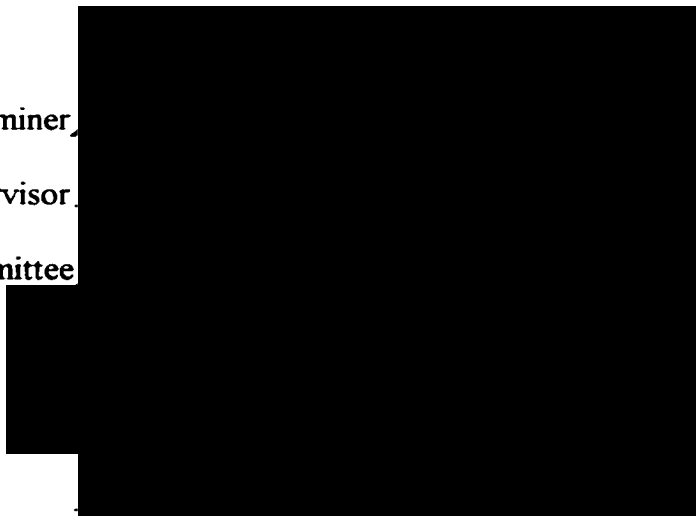
The undersigned hereby certify that they have read and recommend to the Faculty of Graduate Studies for acceptance a thesis entitled "Molecular Signaling Pathways Regulating Cation Channels in Ocular Epithelial Cells"

by Jennifer Susan Ryan

in partial fulfillment of the requirements for the degree of Doctor of Philosophy.

Dated: January 11, 1999

External Examiner
Research Supervisor
Examining Committee



DALHOUSIE UNIVERSITY

DATE: January 1999

AUTHOR: Jennifer Susan Ryan

TITLE: Molecular Signaling Pathways Regulating Cation Channels

in Ocular Epithelial Cells

DEPARTMENT OR SCHOOL: Department of Pharmacology

DEGREE: Ph.D CONVOCATION: May YEAR: 1999

Permission is herewith granted to Dalhousie University to circulate and to have copied for non-commercial purposes, at its discretion, the above title upon the request of individuals or institutions.


Signature of Author

THE AUTHOR RESERVES OTHER PUBLICATION RIGHTS, AND NEITHER THE THESIS NOR EXTENSIVE EXTRACTS FROM IT MAY BE PRINTED OR OTHERWISE REPRODUCED WITHOUT THE AUTHOR'S WRITTEN PERMISSION.

THE AUTHOR ATTESTS THAT PERMISSION HAS BEEN OBTAINED FOR THE USE OF ANY COPYRIGHTED MATERIAL APPEARING IN THIS THESIS (OTHER THAN BRIEF EXCERPTS REQUIRING ONLY PROPER ACKNOWLEDGEMENT IN SCHOLARLY WRITING) AND THAT ALL SUCH USE IS CLEARLY ACKNOWLEDGED.

FOR BUP: WHO SMILES ON ME FROM ABOVE
&
WHOSE SPIRIT GUIDES ME THROUGH MY DAYS

“Sith do d’ annam, is Clach air do Charn”

TABLE OF CONTENTS

LIST OF FIGURES		Page vii
LIST OF TABLES		x
ABSTRACT		xi
LIST OF ABBRIVIATIONS		xii
ACKNOWLEDGEMENTS		xvii
PUBLICATIONS		xviii
CHAPTER 1	General Introduction	1
CHAPTER 2	General Methods	45
CHAPTER 3	Voltage-dependent K ⁺ currents and a G protein-coupled nonspecific cation current in cultured rat retinal pigment epithelial cells	
	Abstract	60
	Introduction	62
	Materials and Methods	64
	Results	73
	Discussion	139
CHAPTER 4	Purinoreceptor regulation of cation channels and cytosolic [Ca ²⁺] in cultured rat retinal pigment epithelial cells	
	Abstract	160
	Introduction	162
	Materials and Methods	166
	Results	171
	Discussion	210

CHAPTER 5	Adrenergic regulation of a calcium-activated potassium current in cultured rabbit pigmented ciliary epithelial cells	
Abstract		230
Introduction		231
Materials and Methods		233
Results		236
Discussion		268
CHAPTER 6	General Discussion and Future Work	283
APPENDIX		291
REFERENCES		293

LIST OF FIGURES

CHAPTER 1

- 1.1 Schematic of RPE cells
- 1.2 Model for RPE fluid and ion transport
- 1.3 Schematic of the CBE: PCE and NPCE cells
- 1.4 Model of CE Channels and Transporters involved in AH formation
- 1.5 Heterotrimeric G proteins activation
- 1.6 G protein subtypes

CHAPTER 2

- 2.1 Schematic diagram of rat RPE cell isolation and culture
- 2.2 Schematic diagram of rabbit PCE cell isolation and culture
- 2.3 Whole-cell patch clamp recording

CHAPTER 3

- 3.1 Photomicrograph of isolated rat RPE cells in culture
- 3.2 Immunocytochemical staining of cultured rat RPE cells
- 3.3 Voltage-dependent currents in rat RPE cells
- 3.4 K^+ selectivity of outward current in rat RPE cells
- 3.5 Pharmacological blockade of K^+ currents in rat RPE cells
- 3.6 Effect of GTP γ S on whole-cell current in rat RPE cells
- 3.7 Time course for activation of the cation current by G protein analogues

- 3.8 Sensitivity of cation current to pharmacological blockers
- 3.9 GTP γ S-activates a nonspecific cation current in rat RPE cells
- 3.10 The NSC current activated by GTP γ S is impermeable to anions
- 3.11 Cation selectivity of the GTP γ S-activated NSC current
- 3.12 Involvement of intracellular Ca²⁺ in NSC current activation
- 3.13 Fluoroaluminate activates the NSC current
- 3.14 PTX blocks activation of the GTP γ S current in rat RPE cells
- 3.15 Immunofluorescent detection of anti-G α subunit proteins in rat RPE cells
- 3.16 GTP γ S -activation of the NSC current in replated rat RPE cells
- 3.17 Effect of GTP γ S on whole-cell currents in RPE cells loaded with anti-G α subunit proteins
- 3.18 Effects of protein kinase inhibitors on GTP γ S activated NSC current
- 3.19 H-7 and PD 98059 reduce NSC current activation
- 3.20 Cyclic nucleotides are not involved in NSC current activation
- 3.21. Schematic for NSC current activation by PTX-sensitive G α_i in RPE cells

CHAPTER 4

- 4.1 ATP activates two ionic conductances in rat RPE cells
- 4.2 Activation of an NSC current by ATP
- 4.3 ATP-activated NSC current is not sensitive to extracellular Ca²⁺
- 4.4 Effects of suramin and PPADS on ATP-activated NSC current
- 4.5 Activation of an outward K⁺ current by ATP
- 4.6 ATP-activates a Ca²⁺-dependent K⁺ current in rat RPE cells

- 4.7 Potency of other purine analogues on NSC current and $I_{K(Ca)}$ activation
- 4.8 ATP-evoked changes in $[Ca^{2+}]_i$
- 4.9 UTP-evoked changes in $[Ca^{2+}]_i$
- 4.10 $[Ca^{2+}]_i$ increases are selective for purinoceptors
- 4.11 Increases in $[Ca^{2+}]_i$ are not dependent on extracellular Ca^{2+}
- 4.12 Schematic for NSC current and $I_{K(Ca)}$ activation by ATP/UTP in rat RPE cells

CHAPTER 5

- 5.1 Phase and fluorescent images of rabbit CE cells in culture
- 5.2 Whole-cell current in cultured PCE cells
- 5.3 Ca^{2+} -activated K^+ current in PCE cells
- 5.4 Effect of TEA, IbTX and 0 Ca^{2+} on $I_{K(Ca)}$
- 5.5 Activation of $I_{K(Ca)}$ by ionomycin in PCE cells
- 5.6 Epinephrine activates $I_{K(Ca)}$ in PCE cells
- 5.7 Activation of $I_{K(Ca)}$ by the α_1 -adrenergic agonist phenylephrine
- 5.8 Prazosin blocks PHe-mediated activation of $I_{K(Ca)}$ in PCE cells
- 5.9 Involvement of IP_3 and intracellular Ca^{2+} release in $I_{K(Ca)}$ activation
- 5.10 Inhibition of PLC inhibits PHe-induced increases in $I_{K(Ca)}$
- 5.11 PTX-sensitive G proteins are involved in PHe-mediated $I_{K(Ca)}$ increases
- 5.12 Schematic of α_1 -adrenergic signaling pathway regulating $I_{K(Ca)}$ in rabbit PCE cells

LIST OF TABLES

1-1 Composition of extracellular and intracellular recording solutions

ABSTRACT

The pigmented cells of the retinal pigment epithelium (RPE) and the ciliary body epithelium (CBE) of the vertebrate eye are both transporting epithelia. The RPE cells perform a number of functions vital to maintaining the visual signal, including maintenance of fluid and ion homeostasis in the subretinal space and phagocytosis of shed photoreceptor outer segments. The pigmented (PCE) cells of the CBE, together with the nonpigmented epithelial cells, are responsible for the secretion of aqueous humor into the posterior chamber. In this study, receptor and G-protein-coupled signaling pathways regulating ion channels in cultured RPE and PCE cells were examined using whole-cell patch-clamp recording techniques.

Under control conditions, a TEA and 4-AP-sensitive delayed outwardly rectifying K^+ current (I_K), a Ba^{2+} -sensitive inwardly rectifying K^+ current (I_{Ki}), and an inactivating outward K^+ current were recorded in rat RPE cells. A large non-inactivating, nonselective cation (NSC) channel activated by non-hydrolyzable G protein analogues (GTP γ S or Gpp(NH)p), was also identified in rat RPE cells. This NSC current had a mean reversal potential of +5.7 mV, was permeable to several monovalent cation and was not affected by alterations in the Cl^- concentration gradient. Blocking G proteins of the $G_{i/o/v/z}$ class with pertussis toxin (PTX) or with antibodies against $G_{\alpha i}$ subunits abolished current activation, confirming involvement of a $G_{\alpha i}$ subunit protein. Further investigations revealed that intracellular Ca^{2+} and kinase-dependent phosphorylation, potentially mediated by MAP kinase, may be downstream signaling components involved in the modulation of NSC channel activation.

In rat RPE cells, application of ATP (100 μ M) activated a cation conductance via actions on purine receptors. The ATP-activated current reversed at -1.5 mV and had electrophysiological properties distinct from the GTP γ S-activated NSC current. The ATP-activated current was inwardly rectifying, cation nonselective, and insensitive to the P_{2X} receptor antagonists suramin or PPADS. The electrophysiological characteristics of this current suggests that ATP activates P_{2X} purinoceptors in rat RPE. In many cell types, ATP can also act on metabotropic P_{2Y} purinoceptors coupled to a phospholipase C (PLC)/inositol triphosphate (IP_3) signaling pathway and intracellular Ca^{2+} stores release. In 38% of rat RPE cells recorded from, ATP also activated an iberiotoxin (IbTX)-sensitive Ca^{2+} -activated K^+ current ($I_{K(Ca)}$). Using Ca^{2+} imaging techniques, both ATP and UTP elevated intracellular free $[Ca^{2+}]$ in a manner independent of extracellular Ca^{2+} influx. These data supports the presence of a P_{2Y} -purinoceptor signaling pathway linked to intracellular Ca^{2+} stores release and K channel modulation in rat RPE cells.

In cultured rabbit PCE cells, inwardly and outwardly rectifying K^+ conductances were recorded. A portion of the outward K^+ current was dependent on Ca^{2+} and was sensitive to IbTX, demonstrating the presence of $K_{(Ca)}$ channels. The adrenergic agonists epinephrine (EPI) and phenylephrine (PHe) increased $I_{K(Ca)}$. PHe-mediated increases in $I_{K(Ca)}$ activity were blocked by the adrenergic antagonist, prazosin, confirming the involvement of α -adrenoceptors. Further experiments demonstrated that a PTX-insensitive G protein linked to an PLC/ IP_3 pathway and intracellular Ca^{2+} stores release are involved in $I_{K(Ca)}$ modulation. These findings demonstrate that α_1 -adrenoceptors modulate $I_{K(Ca)}$ in rabbit PCE cells.

These studies provide evidence for the regulation of ionic conductances in the RPE and PCE cells via signaling pathways linked to G protein activation. Identifying how ionic channels are regulated in these epithelia will increase our understanding of their roles in normal ocular physiology and may provide insight into the pathogenesis of a number of ocular diseases linked to defects in ion transport pathways in these cells.

LIST OF ABBREVIATIONS

AA	arachadonic acid
AC	adenylate cyclase
ADP	adenosine diphosphate
ATP	adenosine triphosphate
Ba ²⁺	barium ion
BAPTA	[1.2-bis(o-Aminophenoxy)ethane-N,N,N',N'-tetraacetic acid]
Ca ²⁺	calcium ion
[Ca ²⁺] _i	intracellular calcium concentration
cAMP	cyclic adenosine monophosphate
CBE	ciliary body epithelium
CE	ciliary epithelium
cGMP	cyclic guanosine monophosphate
CK	cytokeratin
CSR	central serous retinopathy
DAG	diacylglycerol
Dibutryl cGMP	guanosine 3',5'-cyclic Monophosphate, N ² . 2'-O-dibutryl-, sodium
DIDS	diisothiocyano-2-2 disulphonic acid stilbene
DMEM	Dulbecco's modified Eagle's Medium
DMSO	dimethylsulfoxide
EGTA	[ethyleneglycol-bis(aminoethyl)-N,N,N',N'-tetraacetic acid]
E _k	equilibrium potential for K ⁺ ions

EPI	epinephrine
ER	endoplasmic reticulum
ERG	electroretinogram
ERK1/2	extracellular regulated protein kinase
ΔF	Change in fluorescent intensity
Fluo-3 AM	{1-[2-Amino-5-(2,7-dichloro-6-hydroxy-3-oxo-3H-xanthen-9-yl)]-2-(2'-amino-5'-methyl-phenoxy)ethane-N,N,N',N'-tetraacetic acid pentaacetoxymethyl ester}
GDP β S	Guanosine 5'-O-(2-Thiodiphosphate), Tetralithium salt
GF 109203X	Bisindolylmaleimide I {2-[1-(3-dimethylaminopropyl)-1H-indol-3-yl]-3-(1H-indol-3-yl)-maleimide}
G protein	GTP-binding protein
GPCR	G protein coupled receptor
GPP(NH)p	5'-guanylimidodiphosphate
GTP	guanosine 5' triphosphate
GTP γ S	guanosine 5'-O-(3-Thiotriphosphate), Tetralithium salt
GRB2	guanine regulatory binding protein 2
H-7	[1-(5-Isoquinolinesulfonyl)-2-methylpiperazine, HCl]
HEPES	N-(2-hydroxyethyl)- piperazine-N'-(2-ethanesulphonic acid)
IbTX	Iberitoxin (<i>Buthus tamulus</i>)
I _{K(Ca)}	calcium-activated K ⁺ current
ION	ionomycin (<i>Streptomyces conglobatus</i>)
IP ₃	D- <i>myo</i> -Inositol 1,4,5-Triphosphate
K ⁺	potassium ion

KN-92	{2-[N-(4-Methoxybenzenesulfonyl)]amino-N-(4-chlorocinnamyl)-N-methylbenzyl-amine, phosphate}
KPA	kilopascal
lb in ²	pounds per square inch
MAP	mitogen activated protein kinase
MAPKK	mitogen activated protein kinase kinase
MEK	MAP kinase kinase
α,β -methyl ATP	α,β -Methylene adenosine 5'-triphosphate dilitium
2MeSATP	2-Methylthio-ATP tetrasodium
mM	millimolar
n	number of cells in each group
Na ⁺	sodium ion
NE	norepinephrine
nm	nanometers
NMDG	N-methyl-D-glucamine
NPCE	nonpigmented ciliary epithelium
PBS	phosphate buffered saline
PCE	pigmented ciliary epithelium
PD 98509	(2'-Amino-3'-methoxyflavone)
PHe	phenylephrine
PKA	protein kinase A
PKC	protein kinase C
PLA ₂	phospholipase A ₂

PLC	phospholipase C
PLD	phospholipase D
RMP	resting membrane potential
ROS	rod outer segments
PNMT	phenylethanolamine N-methyltransferase
PPADS	pyriodoxal-phosphate-6-azophenyl-2',4'-disulphonic acid tetrasodium
PTX	pertussis toxin (<i>Bordetella pertussis</i>)
RCS	Royal College of Surgeons
RPE	retinal pigment epithelium
RT	room temperature
SE	standard error of the mean
SOS	son of sevenless
SR	smooth endoplasmic reticulum
TEA	tetraethylammonium chloride
TEP	transepithelial potential
TG	thapsigargin
U-73122	{1-[6-((17- β -Methoxyestra-1,2,5(10)-trien-17-yl)amino)hexyl]-1H-pyrrole-2,5-dione}
μ M	micomolar
UTP	uridine triphosphate
V_a	apical membrane potential
V_b	basal membrane potential
V_h	holding potential

\leq / \geq

less than or equal to/ greater than or equal to

\pm

plus/minus

ACKNOWLEDGMENTS

This thesis represents five years of an incredible journey in which many people have played a part and so deserve a word of thanks.

To all present and past members of the “Kelly Lab”: I’ll never forget all the fun, laughter, arguments, friendship and support you’ve all shown me throughout the years. Thanks to Mel for her guidance and her confidence in me when I thought it couldn’t be done. You have challenged me and given me a wealth of new experiences but most importantly you have instilled in me great personal and professional confidence which I’ll carry throughout my life. A special thanks also to Christine and Rob. How boring the lab would have been without our weekly “crisis” or the daily “Seinfeld” episodes we managed to find ourselves in. You guys always knew what to say, in good times and in bad, and I’ll never forget your friendship.

To my family, especially my Mom and Dad, who for 5 years stepped around endless papers, drove 10,000 km to the Tupper and back, pulled me through some my momentary lapses in sanity and stayed up with me to the wee hours of the morning just so I wouldn’t have to do it alone. There are no words to express how lucky I am. All my success is because of you. I would be remiss if I also didn’t thank my Nana, brother Chris, Aunt Trudy, Uncle Pat, Peter and Tori. All of you have always loved, supported and encouraged me and knew exactly when to call and what to say.

Finally, to the Department of Pharmacology, especially Sandi, Karen, Janet and Luisa who never failed to lend a hand and could always make me leave the office with a smile. To all the rest of the faculty, staff and students I’ve met along the way, thank-you for your part in a wonderful, supportive and challenging experience.

PUBLICATIONS

Parts of this thesis have been previously published:

Ryan, J.S. and Kelly, M.E.M. (1998). Patch clamp recording methods for examining adrenergic modulation of potassium channels in ocular epithelial cell. **In:** Methods in molecular biology. Walker, J. (ed). Humana Press Inc. (In Press).

Ryan, J.S., Tao-QP and Kelly, M.E.M. (1998). Adrenergic regulation of calcium-activated potassium current in cultured rabbit ciliary epithelial cells. *J. Physiol.* **511**:145-152.

Ryan, J.S. and Kelly, M.E.M. (1998). A nonselective cation channel in rat retinal pigment epithelial cells is activated by G_{ai} protein subunits. *Brit. J. Pharmacol.* **124**: 1115-1122.

Poyer, J.F., **Ryan, J.S.** and Kelly, M.E.M. (1996). G protein mediated activation of a nonselective cation current in rat retinal pigment epithelial cells. *J. Membr. Biol.* **153**: 13-26.

Ryan, J.S., Shi, C. and Kelly, M.E.M. (1998) Adrenergic Regulation of K⁺ and Cl⁻ current in rabbit ciliary epithelial cells. *Exp. Eye. Res.* **67**(1): S.8

Kelly, M.E.M., Baldrige, W.H. and **Ryan, J.S.** (1998). Purinoceptor regulation of cytosolic [Ca²⁺] and cation channels in rat retinal pigment epithelial cells. *Exp. Eye. Res.* **67**(1): S.36.

Shi, C., **Ryan, J.S.**, French, A., Coca-Prados, M. and Kelly, M.E.M. (1998). Characterization of a hypoosmotically-stimulated Cl⁻ current contributing to regulatory volume decrease in rabbit NPE cells. *Invest. Ophthalmol. Vis. Sci.*

Ryan J.S. and Kelly, M.E.M. (1997). Nucleotide-activated cation currents in rat retinal pigment epithelial cells. *Biophys. J.* **72**: A36.

Ryan J.S., Poyer, J.F. and Kelly, M.E.M. (1996). Characterization of a G protein-activated nonspecific cation current in rat retinal pigment epithelial cells. *Biophys. J.* **70**: A199.

Kelly, M.E.M. and **Ryan, J.S.** (1996). GTP γ S-activation of a non-specific cation current in rat retinal pigment epithelial cells is PTX-sensitive. *Exp. Eye Res (suppl)* **63**: S80 (261).

Ryan, J.S., Tao, Q-P., Jollimore, C.A. and Kelly, M.E.M. (1996). Adrenergic modulation of calcium-activated potassium current in rabbit pigmented ciliary epithelial cells. *Brit. J. Pharmacol.* **119**: 165P.

CHAPTER 1

GENERAL INTRODUCTION

1. Ocular Epithelia

The pigment epithelium of the retina (RPE) and the pigmented epithelium of the ciliary body (PCE) are both transporting ocular epithelia. They share a common embryonic origin, developing from a single layer of cuboidal cells that line the outer wall of the optic cup. The RPE forms as a continuous monolayer of cells and is situated between the choroidal blood supply at its basal surface and the neurosensory retina at its apical surface. The cells of the RPE monolayer begin at the edge of the optic nerve head and extend peripherally to the ora serrata. At the ora serrata, the RPE continues anteriorly as the PCE of the ciliary body (Ozanics & Jakobiec, 1982; Mund & Rodrigues, 1979). Development results in the basal surface of the PCE facing the ciliary body stroma while the apical surface of the PCE becomes opposed to the apical surface of the nonpigmented ciliary epithelium (NPCE), which forms as a continuation of the neurosensory retina (Cole, 1984; Caprioli, 1992; Streeten, 1982).

Like other epithelia, the RPE and PCE are polarized and their basal surfaces are intricately folded to produce a large surface area attachment to a thin basement membrane. However, despite shared epithelial characteristics and a common embryological origin, these pigmented ocular epithelial cells are functionally distinct. The single-layered RPE is an absorptive epithelium that has a number of specialized functions vital to the maintenance of the neural retina and the processing of the visual image in the posterior part of the eye (Bok 1988 & 1993; Zinn & Benjamin-Henkind, 1979; Steinberg & Miller, 1979). In contrast, the PCE, together with the NPCE, functions as a bilayered secretory epithelium involved in maintaining intraocular pressure (IOP) via the secretion of aqueous humor (Cole, 1984; Weiderholt *et al*, 1991; Martin-Vasallo *et al*, 1989).

The biophysical and pharmacological properties of the ion transport pathways within the RPE and PCE have been examined in an attempt to better understand the physiology of transepithelial transport in these epithelia (Chu *et al*, 1986; Hughes & Steinberg, 1990; Krupin *et al*, 1991; Jacob & Civan, 1996). These studies have also been driven by the demonstration that alterations in ocular epithelial ion transport pathways are linked to the pathogenesis of a number of ocular diseases. For example, altered fluid and ion transport by the RPE has been implicated in macular degeneration (Tso, 1988), central serous retinopathy (Chuang *et al*, 1987; Zamir, 1997), retinitis pigmentosa (Chader *et al*, 1988) and proliferative vitreoretinopathy (Topping *et al*, 1979). Similarly, in the ciliary body, changes in aqueous secretion by the PCE and NPCE cells can alter IOP. Elevated IOP is the principal modifiable risk factor for the development of open-angle glaucoma and can be treated by decreasing aqueous humor secretion by the ciliary epithelium (Dunbar-Hoskins, 1989; Jacob & Civan, 1996). Our current understanding of how ion and fluid transport may contribute to these pathologies is hampered by the lack of consistent information about basic mechanisms regulating transepithelial transport under normal physiological conditions. This includes identification of selective receptor subtypes and molecular signaling pathways contributing to ion transport across these epithelia.

Both the RPE and PCE receive paracrine and/or endocrine signals from adjacent cells, the underlying vasculature and neuronal innervation that can alter transepithelial fluid and ion transport (Negi & Marmor, 1986; Gallemore & Steinberg, 1990; Wax, 1991). Most of these signals act as ligands at G protein-coupled receptors and are linked to signaling cascades that have the potential to regulate ion channel activity through the

generation of Ca^{2+} , lipid signaling molecules and/or protein kinases. The purpose of this thesis project is to examine the effects of such ligands on the activity of ion channels in the PCE and RPE and to identify the underlying signaling pathways involved in their regulation. This information is essential, not only to provide a greater understanding of the physiology of transepithelial ion transport, but also to identify how signaling pathways are linked to ion and fluid transport and how these pathways may be altered under pathophysiological conditions.

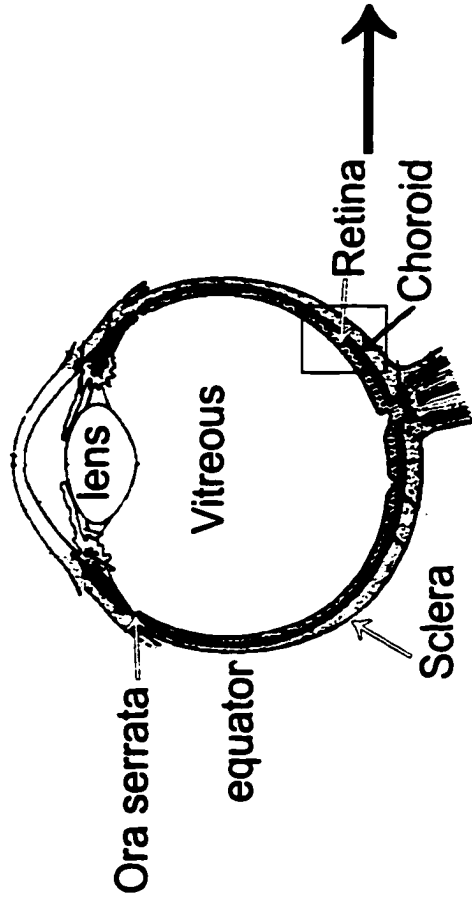
The following sections will provide background information on the general morphological and functional characteristics of the RPE and the PCE and will present current models for the transport mechanisms underlying fluid and ion transport in these ocular epithelia. The role that G protein-coupled signaling pathways play in the regulation of ion channels will be highlighted and the rationale for exploring these pathways in the RPE and PCE will be provided.

2. The Retinal Pigment Epithelium

2.1 Location, functions and structure of the retinal pigment epithelium

The retinal pigment epithelium (RPE) is a continuous monolayer of specialized epithelial cells that extends peripherally from the optic nerve to the ora serrata (Figure 1.1A). These cells form the non-neuronal component of the vertebrate retina and carry out a number of functions vital to the processing of the visual image and maintenance of retinal integrity. Within the retina, the RPE is situated between the choroid and the rod and cone photoreceptors of the neural retina. Histologically, three well-defined zones, the basal, lateral and the apical membranes, are recognized in these cells (Figure 1.1B).

A.



B.

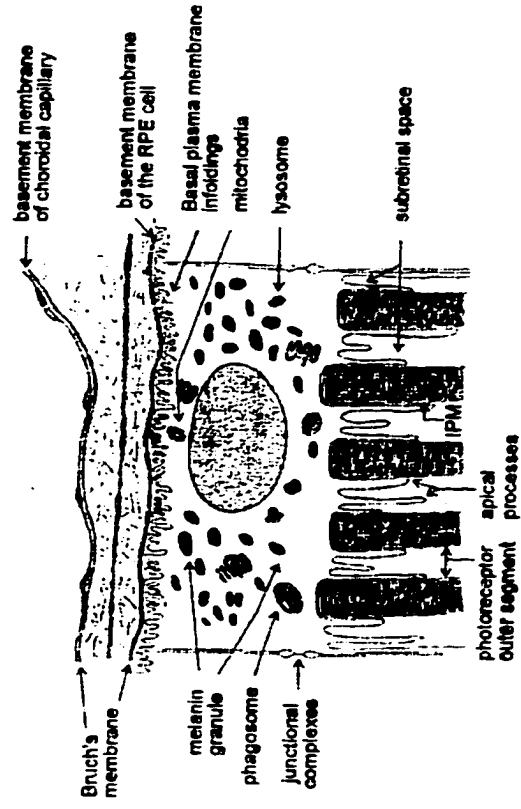


Figure 1.1. The retinal pigment epithelium (RPE) (modified from Clark, 1986)

At their basal surface, the markedly convoluted membranes of the RPE cells are functionally linked to the underlying choroid via Bruch's membrane, a specialized basement membrane composed of the basal lamina and an underlying layer of reticular fibers. The basal lamina is secreted directly by the RPE cells and serves a point of support and attachment for the epithelium in the retina. Bruch's membrane also serves as a "molecular sieve" for substances passing between the capillaries of the choroid and the retina. Laterally, the borders of the RPE cells are coupled by a series of junctional complexes that include desmosomes, gap junctions and tight junctions. The presence of gap junctional proteins between RPE cells allows the epithelium to couple both metabolically and electrically. Tight junctions exist closer to the apical end of the cell walls where they prevent the free exchange of macromolecules between the choroidal circulation and the neural retina. These tight junctions, together with the endothelium of the choriocapillaries, form the blood-retinal barrier of the vertebrate eye (Clark, 1986; Bok, 1993). By preventing the diffusion of potentially harmful substances into the neural retina, the blood-retinal barrier maintains the integrity of the visual signal. At their apices, the RPE cells face the subretinal space in which the rod and cone photoreceptors of the neural retina are located. Finger-like apical microvilli from the RPE extend into the subretinal space and interdigitate with the photoreceptor outer segments (see Fig 1.1B). An inter-photoreceptor matrix, secreted partially by the RPE cells, which surrounds the microvilli and the photoreceptor outer segments keeps the RPE cells tightly apposed, yet not anatomically joined, to the neural retina. Since the neural retina has no true site of firm attachment in the eye, apical interdigitation of the RPE with the photoreceptor outer segments is functionally important for maintaining retinal attachment. It has also been

suggested that this inter-photoreceptor matrix provides an important medium for the exchange of substances between the neural retina and the nonneuronal RPE (Zinn & Benjamin-Henkind, 1979; Bird, 1989; Marmor, 1989).

Similar to other eukaryotic cells, the cells of the RPE possess a number of intracellular organelles (mitochondria, smooth and rough endoplasmic reticulum, golgi apparatus) that are necessary for normal cellular activities (Bok, 1988). These cells also contain a number of other organelles and cytoplasmic inclusions that tend to be polarized in their distribution. For example, RPE cells possess melanin granules (melanosomes) which give these cells their characteristic brown coloration. These granules tend to be absent in the basal region of the RPE but are highly concentrated in the apical region, especially in the apical microvilli. By absorbing stray light scatter in the retina, these granules prevent degradation of the visual image and maintain visual acuity. RPE cells are also phagocytic, a role which is vital for retinal function (see below). As a consequence of this activity, phagosomes are also commonly found in the cytoplasm of RPE cells. These organelles tend to have an apical distribution consistent with the involvement of the apical microvilli in phagocytosis. Lipofuscin granules are also common cytoplasm inclusions in the RPE. These granules, which contain the residual bodies of phagocytized particles, tend to cluster near the nucleus (Bok, 1988).

One function of the RPE that is vital to the maintenance of retinal integrity is phagocytosis of detached distal portions of rod and cone photoreceptors. As a part of a normal renewal process, photoreceptors undergo a circadian shedding of their outer segments (OS) into the subretinal space which is accompanied by the assembly of new membrane at their proximal ends (Bok, 1993). Shed OS are rapidly recognized, bound

and ingested by the RPE in an incompletely understood process. The importance of this RPE function is highlighted in the Royal College of Surgeons rat model and in the human disorder Retinitis Pigmentosa where failure of the RPE to phagocytize OS leads to the build up of debris in the subretinal space, photoreceptor degeneration and eventually loss of vision (Chader *et al*, 1988; Heth *et al*, 1995). Photoreceptor function is also sustained by RPE-mediated processing of retinoids (Bok, 1993). The RPE serves as the cellular site for regeneration of 11-*cis*-retinal, the chromophore for the visual pigments in rod and cone photoreceptors. During the visual cycle, 11-*cis*-retinal is photoisomerized to 11-*trans*-retinol then released from the OS into the subretinal space. Retinol is then taken-up, re-isomerized and oxidized to 11-*cis* retinal in the RPE before being returned to the photoreceptors for subsequent use in the visual cycle. The RPE can also obtain retinol from the choroidal circulation via receptor-mediated up-take. This retinol can be stored in esterified form by binding to cellular retinol binding proteins (CRBP) until required by the photoreceptors (Bok, 1993). Processing, storing and recycling of retinoids by the RPE ensures an adequate supply of chromophore for visual transduction.

The retinal pigment epithelium is also responsible for the net flow of ions and water from the retina to the choroid (Bok, 1988 & 1993; Clark, 1986; Steinberg & Miller, 1979; Zinn & Benjamin-Henkind, 1979). Ion and fluid transport across the RPE plays a major role in maintaining a constant ionic milieu in the subretinal space, a role that is integral for photoreceptor function. The following section will highlight our current knowledge of the various pumps, transporters and ion channels present in the RPE and provide a model of how ion and fluid movement across this epithelium maintains a

homeostatic environment in the subretinal space to preserve visual processing in the neural retina.

2.2. Apical and basal membrane ion transport mechanisms in the RPE

A variety of studies on intact RPE-choroid preparations and isolated single RPE cells have identified that there is an asymmetrical distribution of both active and passive ion transport mechanisms between the apical and basolateral membranes of RPE cells. The co-ordinated action of these ion transport pathways in the mammalian RPE maintains an apical-side positive transepithelial potential (TEP) of ~ 6 mV promoting absorptive solute-coupled fluid transport from the subretinal space to the choroid (Joseph & Miller, 1991).

Transepithelial isotope flux and microelectrode studies on RPE-choroid preparations have identified several transport mechanisms localized to the apical and/or basolateral cell membranes. In a variety of mammalian species, studies have demonstrated that an ouabain-sensitive electrogenic Na^+/K^+ -ATPase pump is located exclusively on the apical membrane of the RPE (Bok, 1993; Ernst *et al.*, 1986). Localization of this pump to the apical RPE membrane allows for the net flux of KCl to occur in the retina-to-choroid direction. The apical RPE membrane also contains a bumetanide-sensitive electroneutral $\text{Na}^+/\text{K}^+/\text{Cl}^-$ co-transporter that is involved in uptake of KCl from the subretinal space. In addition to Na^+ , K^+ and Cl^- , isotope flux studies in RPE have also identified putative transport pathways for HCO_3^- in the RPE. In frog RPE, both an apical $\text{Na}^+/\text{HCO}_3^-$ co-transporter and a basolateral $\text{HCO}_3^-/\text{Cl}^-$ exchanger have

been identified and are proposed to play a role in cellular acid extrusion (Miller & Steinberg, 1977; Lin & Miller, 1992). An apical amiloride-sensitive $\text{Na}^+\text{-H}^+$ exchanger identified in frog RPE also makes a small contribution to acid extrusion and finally, an apical $\text{Na}^+\text{-Ca}^{2+}$ exchange mechanism is proposed to contribute to the regulation of both intracellular and subretinal Ca^{2+} concentration (Kenyon *et al*, 1991; Fujisawa *et al*, 1992).

In addition to KCl, net transfer of Na^+ across the RPE may occur. Net Na^+ absorption is accomplished exclusively by paracellular absorption of Na^+ driven by the apical side positive TEP (Edelman & Miller, 1991). Na^+ may also be transported into the RPE by the various transporters/exchangers on the apical membrane, however, efflux pathways for Na^+ have not yet been identified on the basolateral membrane. The action of the Na^+/K^+ -ATPase pump is therefore very important for providing an efflux pathway for Na^+ from the RPE back to the subretinal space. By maintaining a Na^+ gradient in the subretinal space, the Na^+/K^+ -ATPase pump also ensures the proper function of Na^+ -dependent transport mechanisms in both the RPE and the closely opposed photoreceptors.

In addition to pumps and transporters, studies on freshly isolated and cultured RPE cells have identified a variety of ion channels on both the apical and basolateral membranes. Information obtained from patch-clamp studies has demonstrated that mammalian RPE exhibit multiple types of K^+ -selective ion channels (Fox *et al*, 1988; Strauß *et al*, 1993; Strauß *et al*, 1994; Tao *et al*, 1994). Both inward and outwardly rectifying Ba^{2+} -sensitive voltage-dependent K^+ conductances dominate the apical and basolateral membranes of the RPE. Several aspects of RPE transport are controlled by these conductances. For example, K^+ channels provide passive efflux pathways for the return of K^+ ions to the subretinal space which entered via the Na^+/K^+ -ATPase pump and

the Na^+ - K^+ - Cl^- co-transporter. Apically located inwardly rectifying K^+ channels play primary roles in establishing the apical membrane potential and thus influence transepithelial transport of these ions, the movements of which are dependent upon transmembrane voltage (Hughes & Steinberg, 1990). In addition to K^+ channels, the basolateral membrane of the RPE has been shown to possess a DIDS-sensitive Cl^- conductance (Botchkin & Mathews, 1993; Ueda & Steinberg, 1994). This conductive pathway allows for the basolateral exit of Cl^- ions that were transported into the cell by the apical $\text{Na}^+/\text{K}^+/\text{Cl}^-$ cotransporter. This efflux of Cl^- , in parallel with the efflux of cation (K^+), into the choroid space drives net transepithelial transport of ions and water. In addition to K^+ and Cl^- conductances, voltage-dependent Ca^{2+} channels have been described in both fresh and cultured RPE cells (Ueda & Steinberg, 1993; Strauß & Wienrich, 1993), a voltage-dependent TTX-sensitive Na^+ current has been described in cultured rat RPE cells (Botchkin & Mathews, 1994) and a nonselective cation channel has been identified in cultured human RPE cells (Fox *et al*, 1988). The role of these conductances in fluid and ion transport has not yet been determined.

A model of RPE ion transport, incorporating both active and passive pathways, is presented in Figure 1.2.

2.3. Physiological role of ion transport in subretinal homeostasis

Any change in the external and/or internal ion concentration may alter the TEP and thus affect ion and fluid movement across the RPE. The most significant physiological change in RPE transepithelial ion transport occurs during light/dark adaptation in the retina. In the intact eye, the subretinal concentration of K^+ ($[\text{K}]_o$) changes abruptly from 5 mM to 2 mM during the transition from dark to light. This drop

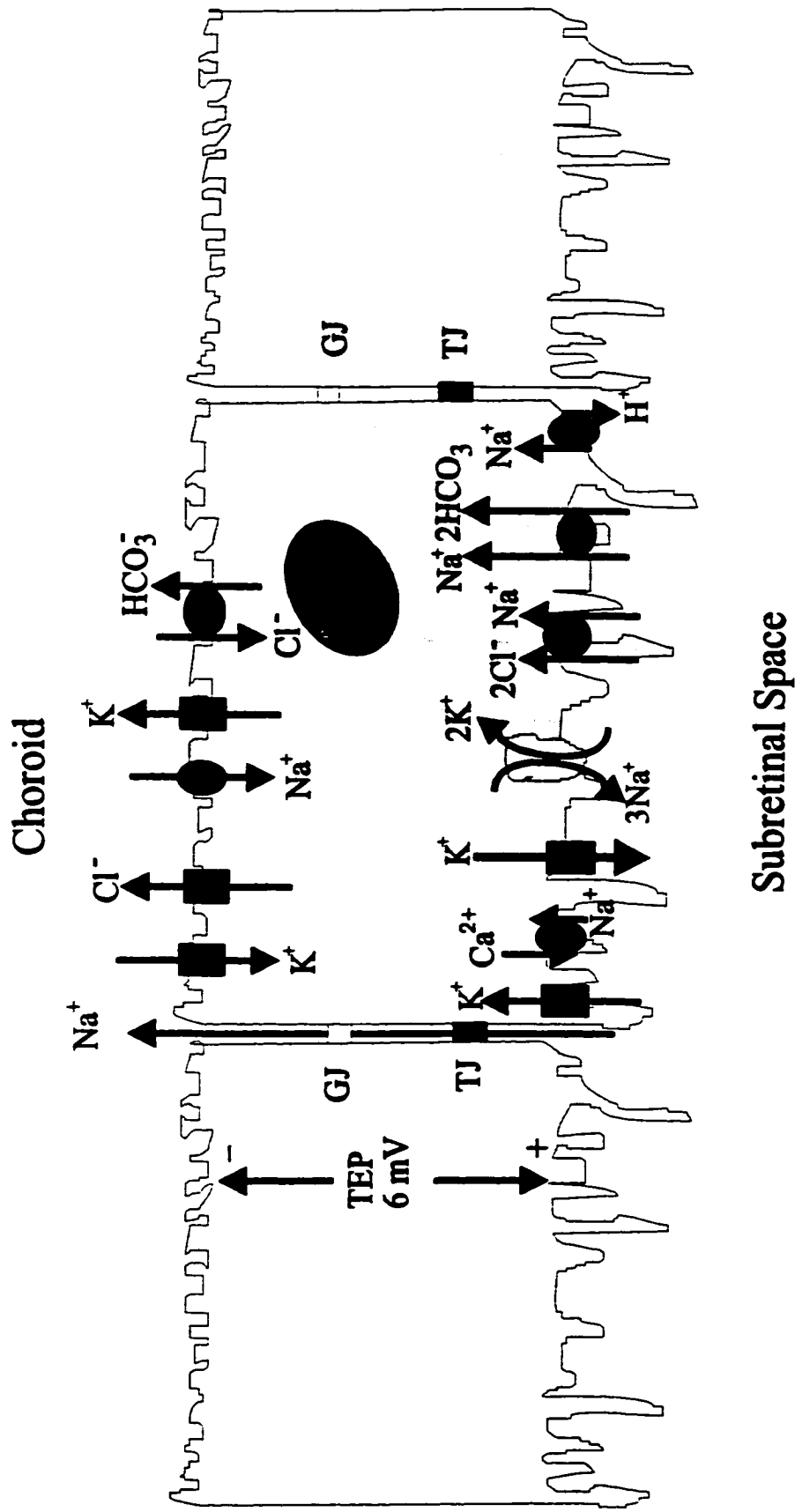


Figure 1.2. Model of ion transport in the RPE. GJ= gap junction ; TJ= tight junction; TEPP=trans-epithelial potential. See text for details. (Modified from Edelman & Miller, 1991)

in subretinal $[K^+]_o$ occurs as a result of light-evoked hyperpolarization of the photoreceptor membrane that closes cation channels and stops K^+ efflux. This subretinal $[K^+]_o$ change acts as an important paracrine signal to significantly alter RPE transport. As a result, $[K^+]_o$ rebounds, limiting the effect of photoreceptor hyperpolarization and thus maintaining subretinal homeostasis.

In vitro, mimicking the dark to light decrease in subretinal $[K^+]_o$, results in three well defined phases of transepithelial transport changes in intact RPE-choroid preparations (Joseph & Miller, 1991). Within seconds of the decrease in $[K^+]_o$ an apical hyperpolarization can be recorded in the RPE which is operationally defined as phase 1. Apical hyperpolarization, accompanied by an increase in TEP, is driven by the increased K^+ diffusion potential across the membrane and K^+ efflux into the subretinal space via apical K^+ channels. This efflux contributes to the rebound of K^+ in the subretinal space and buffers the photoreceptor-induced decrease in $[K^+]_o$. Decreased $[K^+]_o$ would cause concomitant inhibition of the apical Na^+/K^+ ATPase pump and the $Na^+/K^+/Cl^-$ cotransporter. Pump inhibition would tend to oppose apical hyperpolarization and decrease the effect of K^+ efflux. Decreased driving force for ion entry via the cotransporters would slow Cl^- influx and thus reduce Cl^- efflux at the basolateral membrane. This lower diffusion gradient for basolateral Cl^- efflux underlies the transepithelial potential change observed for phase 2 of the light response. During phase 2, apical hyperpolarization is shunted to the basolateral membrane and the TEP begins to decrease. Delayed hyperpolarization results from decreased intracellular $[Cl^-]$ which leads to the inhibition of passive Cl^- efflux through basolateral Cl^- channels. The final phase of transmembrane change in response to light onset is depolarization of both the apical and

basolateral membranes of the RPE. Apical depolarization is thought to result from reduced intracellular $[K^+]_i$ and decreased apical K^+ conductance as the subretinal $[K^+]_o$ rebounds to normal levels (Jospeh & Miller, 1991). An increased Cl^- conductance is believed to underlie the observed basolateral depolarization (Gallemore & Steinberg, 1989). By the end of phase 3 both apical and basolateral membrane potentials have returned to near resting values.

Clinically, these membrane changes of the RPE in the transition from dark to light are measured as distinct components of the DC-recorded electroretinogram (DR-ERG) (Marmor, 1991). The ERG is a noninvasive recording of the electrical signals from the retina elicited by a flash of light (Berson, 1992). Three components of the ERG originate from the RPE (Linsenmeier & Steinberg, 1984). The C wave corresponds to the phase 1 apical hyperpolarization in response to the drop in subretinal $[K^+]_o$. This ERG component is initiated 5 sec after light onset and is followed by the fast oscillation (FO) component that peaks 20 sec after light onset. The FO component represents the delayed RPE basolateral hyperpolarization measured *in vitro* during the phase 2 transepithelial response. The light peak is the final ERG component originating from the RPE and thought to result from the increased basolateral Cl^- conductance of the phase 3 *in vitro* response (Fujii *et al*, 1991). The light peak follows the FO component and peaks 5 min after light onset. Many components of the ERG find use as sensitive clinical indicators of generalized retinal degeneration as well as several types of human RPE dystrophy (Marmor & Lurie, 1979; Marmor, 1991).

3. The Ciliary Body Epithelium

Like the cells of the RPE, ion and fluid transport across the epithelial cells of the ciliary body also plays an important role in the vertebrate eye. The structure, transport mechanisms and function of the ciliary body epithelium (CBE) in the anterior segment of the eye will be the focus of the following section

3.1 Location, functions and structure of the ciliary body epithelium

The ciliary body is part of the uveal tract of the eye. It is triangular in shape and lies between the ora serrata at its posterior end and the iris root at its anterior end (Figure 1.3A). The ciliary body can be divided into three major parts: the ciliary stroma, the ciliary muscle and the ciliary epithelium. The ciliary epithelium forms the inner surface covering of the ciliary body and is composed of two different epithelial cell layers: a non-pigmented ciliary epithelial (NPCE) cell layer and a pigmented ciliary epithelial (PCE) cell layer (Caprioli, 1992; Streeten, 1982). During development both epithelial cell layers form as a forward continuation of the retina. The PCE cells and their basement membrane are continuous with the RPE and Bruch's membrane of the non-neuronal retina whereas the nonpigmented cells are continuous, although in attenuated form, with the neural retina. During embryonic development, the epithelial cells are arranged in a bilayer with the basolateral membrane of the PCE cell layer facing the vascular connective tissue stroma and the basolateral membrane of the NPCE cells facing the posterior and vitreal spaces of the vertebrate eye (Ozanics & Jakobiec, 1982; Mund & Rodrigues, 1979). (Figure 1.3B).

Histologically, PCE cells are cuboidal and are characterized by both the presence of numerous melanosomes and relative lack of intracellular organelles. In contrast, NPCE

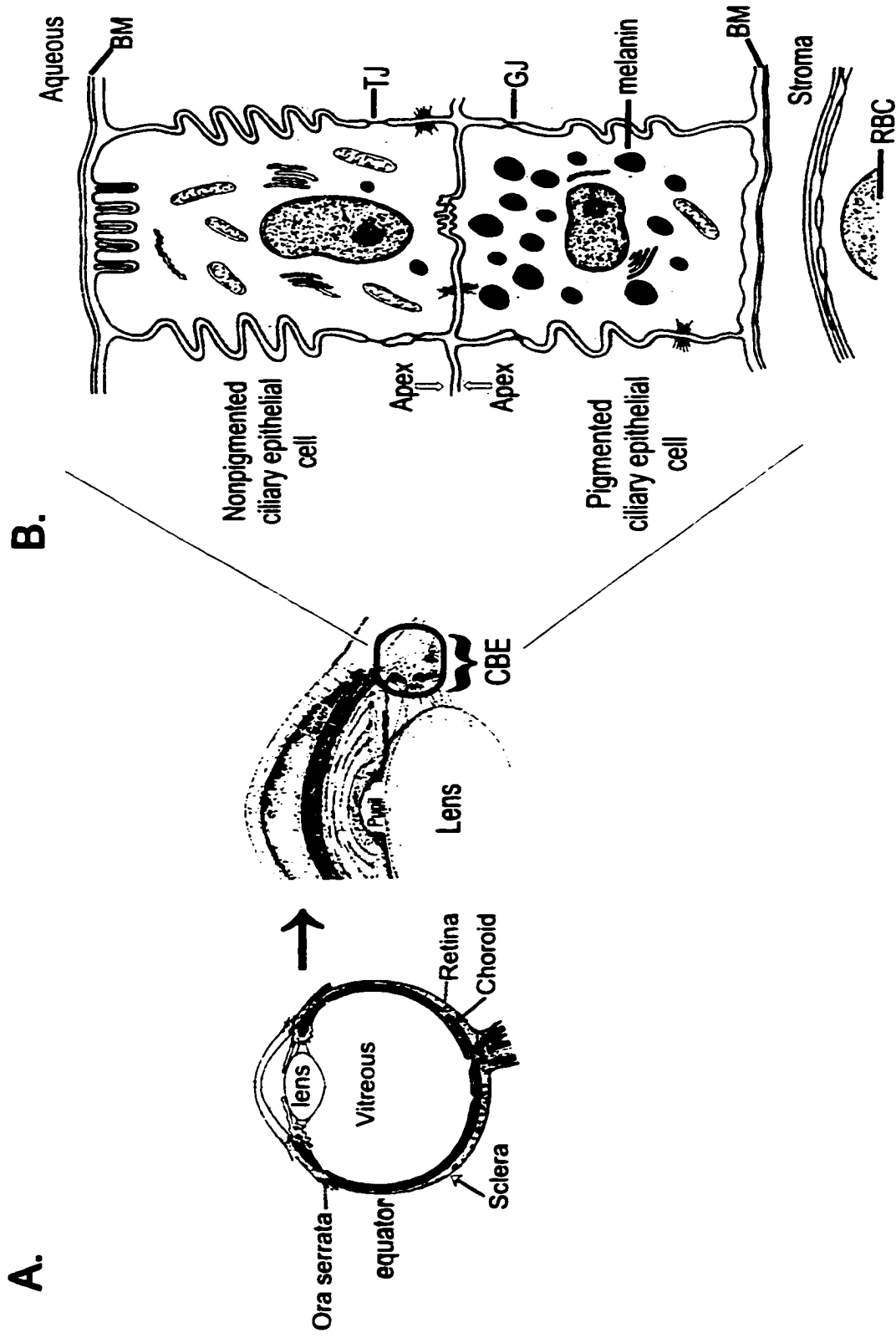


Figure 1.3. Schematic of the ciliary body epithelium(CBE). See text for details. GJ= gap junction; TJ= tight junction; BM= basement membrane; RBC= red blood cell. Figure reproduced with permission from Caprioli, 1987.

cells are columnar with numerous basal infoldings, are devoid of melanosomes and are rich in mitochondria and endoplasmic reticulum as compared to PCE cells. At their apical facing membranes the PCE and NPCE cells are tightly apposed and coupled via a series of junctional complexes that include numerous desmosomes and gap junctions (Ravioli & Ravioli, 1978). Gap junctions also couple PCE cells at their lateral surfaces but are less frequent between the lateral surfaces of the NPCE cells. The presence of gap junctions between PCE-PCE and PCE-NPCE cells allows the bilayer to function as both a metabolic and transport syncytium. The major protein of these junctions, connexon 43, has been demonstrated to be the target for modulation by a variety of pharmacological agonists, therefore suggesting that coupled ion transfer between the cells of the CBE may be regulated (Sears *et al*, 1997). One specialization of the lateral borders of the NPCE cell membranes is the presence of intercellular tight junctions. These tight junctions prevent the free passage of serum proteins from the blood (stroma) into the posterior chamber of the eye via the paracellular pathway. This diffusional barrier, along with the nonfenestrated iris vessels, comprises an important structural component of the blood aqueous-barrier of the eye. By preventing free diffusion of substances from the stroma the blood-aqueous barrier maintains the optical integrity of the eye (Raviola & Raviola, 1978; Caprioli, 1992).

Anatomically, the CBE can be divided into two main segments: the anterior pars plicata and the posterior pars plana. The pars plicata contains the numerous fingerlike projections of the ciliary processes, which are villiform ridges that radiate inward toward the pupil. The PCE and NPCE cells that line the surface of the ciliary processes are involved in the production of aqueous humor (AH). The formation of AH occurs

primarily by active secretion of electrolytes from the CB stroma, across the PCE-NPCE epithelial bilayer, into the posterior chamber of the eye. The aqueous secreted into the posterior chamber is an isotonic solution composed primarily of water, Na^+ , Cl^- and HCO_3^- (Cole, 1984; Caprioli, 1992). Once secreted into the posterior chamber, the aqueous passes through the pupil into the anterior chamber. On its path through the eye the AH serves three major functions: 1) delivers oxygen and nutrients and removes waste products from the anterior segment tissues; (2) flushes away blood, macrophages and other inflammatory cells and products from the anterior segment; (3) retains the shape and internal structure of the eye (Chong, 1996; Cole, 1984).

The majority of the aqueous secreted into the posterior chamber eventually drains from the eye through the trabecular meshwork and the canal of Schlemm, however a small amount of drainage is provided via exit through uveoscleral or uveovascular pathways (Davson, 1984; Cole, 1984). The balance between the rate and quantity of AH produced and AH escape from the eye via drainage pathways is the primary determinant of intraocular pressure (IOP). Under normal conditions IOP is maintained at 15 mmHg, slightly higher than normal atmospheric pressure (Davson, 1984; Hart, 1992). Elevated IOP, due to either increased rates of AH inflow or increased resistance to AH outflow, is a common risk factor for the development of glaucoma (Dunbar-Hoskins, 1989; Brubaker, 1992; Hart, 1992). Current medical therapies for glaucoma are most successfully directed at decreasing IOP by pharmacologically reducing AH secretion by the CE cells. Therefore, studies examining the mechanisms of the cell transport pathways underlying AH secretion are of great importance due to the fact that alterations in these pathways may result in a clinically desirable reduction of IOP in the treatment of

glaucoma. To date, however, our understanding of the processes underlying AH formation is limited. Recent transport data from intact and dispersed ciliary epithelial tissue suggests that PCE cells have solute uptake properties and are functionally coupled to the NPCE cells which have solute efflux properties (Wiederholt *et al*, 1991; Edelman *et al*, 1994). In this cell coupled model, ion and water from the stroma are taken up by PCE cells and passed to the NPCE cells via apical gap junctions, where they are secreted at the basolateral membrane into the posterior chamber as aqueous humor. Despite our understanding of this functional coupling between CE cells, the exact cellular transport mechanisms involved in fluid and ion secretion remain unresolved. Part of the difficulty in resolving the underlying cellular mechanisms derives from the complexity of the epithelial bilayer itself. Many new details on ion transport mechanisms are now being elucidated through the use of both primary cell cultures of NPCE and PCE cells as well as immortalised cell lines (for review see Jacob & Civan, 1996). The following section will highlight our current knowledge of solute-coupled fluid transport across this epithelium and will attempt to incorporate studies at the single cell level with those from intact preparations into a model for secretion of salt and water into aqueous humor.

3.2. Ion transport mechanisms in the ciliary epithelium

Studies in iris-ciliary body (I-CB) preparations from a number of mammalian species have demonstrated that in the CE, as in other epithelia, the inward Na^+ gradient is maintained by the Na^+ pump with electrogenic and electroneutral ion entry (Edelman *et al*, 1994). Immune staining and ion flux studies have determined that both PCE and NPCE cells have a Na/K-ATPase in their basolateral membranes. In the PCE cells the Na/K-ATPase resides adjacent to the stroma and in the NPCE cells it faces the posterior

chamber (Coco-Prados & Lopez-Briones, 1987; Ghosh *et al*, 1990). This symmetry in pump distribution has led to the suggestion that the PCE cells are absorptive and are coupled via gap junctions to the NPCE cells which are secretory (Edelemen *et al*, 1994). The major route for uptake of Na^+ , K^+ and Cl^- into the PCE cells from the stroma is thought to be via a basolateral bumetamide-sensitive electroneutral $\text{Na}^+/\text{K}^+-2\text{Cl}^-$ symport. The ions then diffuse through gap junctions to the basolateral membrane of the NPCE cells where they are released into the aqueous phase via the Na^+/K^+ pump and parallel K^+ and Cl^- channels. The ciliary epithelium is a “leaky” epithelium and, as such, also allows for significant ion movement through a paracellular pathway. The small aqueous-side negative TEP (~ 1 mV) plays a major role in providing the net electrochemical driving force for ion movement from the stroma to the aqueous via this route. Thus, the rate of net Na^+ transfer through the paracellular pathway is also a major determinant of aqueous formation. In all vertebrate species studied, both the magnitude and the sign of the TEP are dependent upon the presence of bicarbonate (HCO_3^-), suggesting a central role for HCO_3^- in aqueous secretion (Wolosin *et al*, 1991; McLaughlin *et al*, 1998). It has been proposed that HCO_3^- modulates the electrical driving force to favour net paracellular Na^+ secretion and thus aqueous formation. Passive water movement accompanies net Na^+ flow via the paracellular and/or transcellular pathways.

Figure 1.4 schematically represents the major transport elements in CE cells responsible for the secretion of salt and water into the aqueous phase. A number of other ion channels and transporters have been identified on both PCE and NPCE cells, however the roles they play in solute-coupled fluid secretion across this epithelium are less well defined. For example, PCE and NPCE cells exhibit whole-cell Cl^- currents as well as

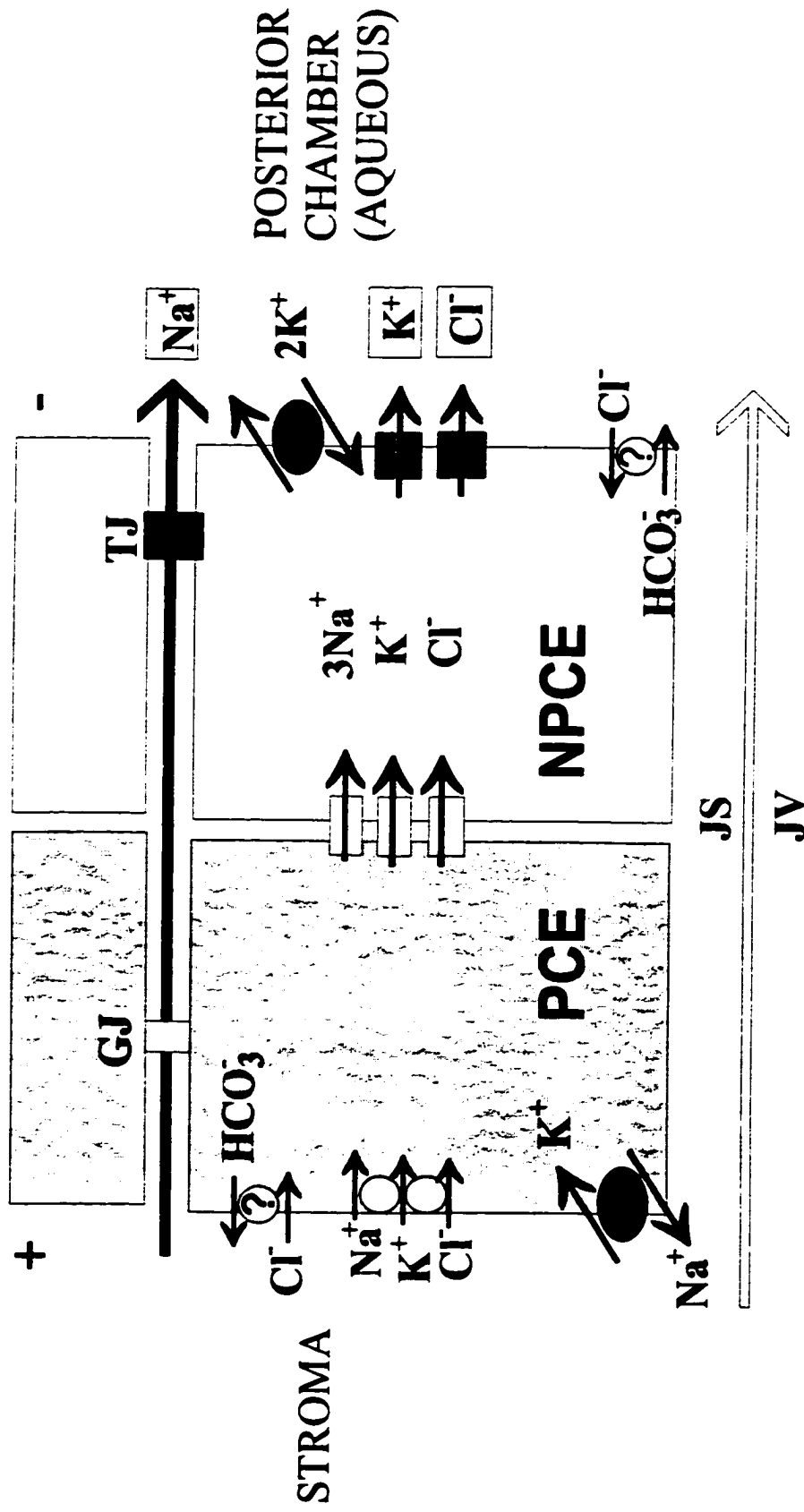


Figure 1.4. Model of ion transport across the CBE. GJ= gap junction;

TJ= tight junction; J_S = net solute; J_V = net volume. See text for details.

(Modified from Jacob & Civan, 1996)

volume-activated Cl^- currents associated with regulatory volume decrease (RVD) (Coca-Prados *et al*, 1995; Jacob & Civan, 1996; Chen & Sears, 1997). Cl^- channel activity in the CBE has been proposed to be rate-limiting in the secretion of aqueous humor. Therefore, activation of Cl^- channels, most notably basolateral NPCE channels, would promote aqueous secretion into the posterior chamber (Coca-Prados *et al*, 1995). Voltage-dependent L-type Ca^{2+} channels (PCE and NPCE) and T-type Ca^{2+} channels (PCE only) have also been described in the CBE (Jacob, 1991a; Jacob & Civan, 1996). As in other cell types, activation of these channels in CE cells would modulate intracellular Ca^{2+} levels and thus potentially regulate a number of cellular events. One potential role of PCE-located T-type Ca^{2+} currents would be the activation of Ca^{2+} -sensitive K^+ channels ($\text{K}_{(\text{Ca})}$) (Jacob, 1991a). T-type Ca^{2+} channels are active at the normal potential of PCE cells and thus could provide sufficient Ca^{2+} influx to activate these channels. $\text{K}_{(\text{Ca})}$ channel activation would cause membrane hyperpolarization towards E_{K} , increasing the driving force for Cl^- exit and thus the rate of aqueous humor formation into the posterior chamber.

In addition to Ca^{2+} -activated K^+ channels, mammalian CE cells also possess voltage-activated delayed rectifying and inward rectifying K^+ currents (Stelling & Jacob, 1991; Fain & Farahbakhsh, 1989; Jacob & Civan, 1996). Functionally, activation of inwardly rectifying K^+ currents helps to maintain the resting potential of CE cells and increases the driving force for Cl^- secretion into the aqueous phase by hyperpolarizing the cell membrane towards E_{K} . The role of delayed rectifying K^+ currents in this epithelium has not been resolved. Unlike $\text{I}_{\text{K}(\text{Ca})}$ they are not thought to play an important role in ion transport as they are inactivated at the resting potential of the cells and can only be

activated at depolarized levels (30-40 mV from rest) that the tissue will not normally reach. A number of nonselective cation and anion channels have also been identified in PCE and NPCE cells. These channels have been proposed to play a role in Ca^{2+} entry, cation loading, volume regulation and the translocation of anionic drugs (Jacob & Civan, 1996). Finally, TTX-sensitive and amiloride-sensitive Na^+ channels have been described in isolated CE cells (Fain & Farahbakhsh, 1989; Jacob & Civan, 1996). The role of these channels in aqueous humor formation remains unknown.

4. Heterotrimeric G proteins

In the eye, ion channels of the RPE and CE are subject to modulation by autocrine/paracrine and hormonal signals coming from adjacent tissue, nerves or blood supply. These extracellular signals can initiate a series of intracellular events that leads to changes in a variety of cell functions including ion channel activity. Probably the best studied signals are those that act as ligands at receptors that couple to heterotrimeric G proteins. The following sections will briefly describe how ion channels may be regulated by G protein coupled receptors and will review our current knowledge on how transepithelial responses in the RPE and CE are modulated via signaling pathways linked to activation of these receptors.

4.1. Heterotrimeric G proteins: structure

Heterotrimeric G proteins link the activities of extracellular stimuli to intracellular response and consist of three heterologous polypeptide subunits: α , β , and γ . In their inactive state, these subunits form a stable membrane-associated $\alpha\beta\gamma$ heterotrimer, with

GDP tightly bound to the α subunit. This heterotrimer is tethered to the membrane by prenylation of the carboxyl terminus of the γ subunit and myristoylation and palmitoylation of the amino terminus of the α subunit (Conklin & Bourne, 1993; Neer, 1995). The α subunit is composed of a GTPase domain that contains the GTP-GDP binding pocket as well as binding sites for receptors, effectors and the $\beta\gamma$ subunit and an alpha helical domain whose function is not entirely clear. In its inactive state, the α subunit contacts the β subunit at two sites, one near the N-terminal of the α subunit and the other at the GTPase domain. The β subunit consists of an N-terminal region (the so-called "coiled-coil") and 7 repeating units of 43 amino acids which form the so-called WD repeat region. The β subunit binds the middle region of the alpha helical γ subunit by making extensive contacts via its coiled-coil N-terminus region. These subunits bind each other so tightly that they can only be separated by denaturants and thus function as a monomer (for review see; Clapham, 1996).

In their inactive GDP-bound state, $G\alpha$ subunits have a high affinity for the tightly complexed β and γ subunit. $\beta\gamma$ binds and stabilizes only the GDP-bound form of α occluding any interaction of the subunits (α and/or $\beta\gamma$) with downstream effectors. This inactive trimeric state of the G protein is maintained by the slow rate of GDP dissociation from the α subunits. However, receptor activation catalyzes the exchange of bound GDP for GTP on the α subunit. The GTP-bound form of the heterotrimer is unstable and heterolytically dissociates to form the active GTP- α and $\beta\gamma$ complexes. Once dissociated, free $G\alpha$ -GTP and $G\beta\gamma$ subunits, acting either co-ordinately or independently, can both bind and regulate intracellular signaling molecules (Clapham & Neer, 1993; Neer, 1995;

Hamm, 1998). Termination of the signaling pathway is dependent upon the intrinsic GTPase activity of the α subunit which hydrolyzes $G\alpha$ -GTP to $G\alpha$ -GDP. Hydrolysis results in dissociation of the α subunit from effectors and promotes reassociation with the $\beta\gamma$ dimer. All α subunits isoforms are GTPases, although the rate of GTP hydrolysis varies greatly from one type to another. The rate of $G\alpha$ -GTP hydrolysis is also regulated by interaction of the α subunit with a specific family of GTP-ase activating proteins (or GAPs) known as regulators of G protein signaling (or RGS proteins) (Koelle, 1997; Berman & Gilman, 1998). RGS act at the level of the dissociated $G\alpha$ -GTP to stimulate GTPase activity and thus facilitate deactivation by hydrolyzing GTP to GDP. Once the heterotrimer is reformed, the G protein can reassociate with the receptor, which primes the system to undergo a new cycle of signal transduction. Figure 1.5 shows a schematic representation of the activation/inactivation cycle for heterotrimeric G proteins.

4.2. Heterotrimer G proteins: activation by receptors

Receptors that are known to transduce extracellular signals via activation of heterotrimeric G proteins are coined G protein coupled receptors (GPCRs) (Watson & Arkininstall, 1994). These receptors comprise the largest known family of cell surface receptors containing more than 1000 recognized members. GPCRs mediate cellular responses to highly selective ligands as diverse as hormones, neurotransmitters, odorants and photons. Once activated they promote interaction between the receptor and the G protein on the intracellular side of the membrane to initiate a complex cascade of intracellular signaling events.

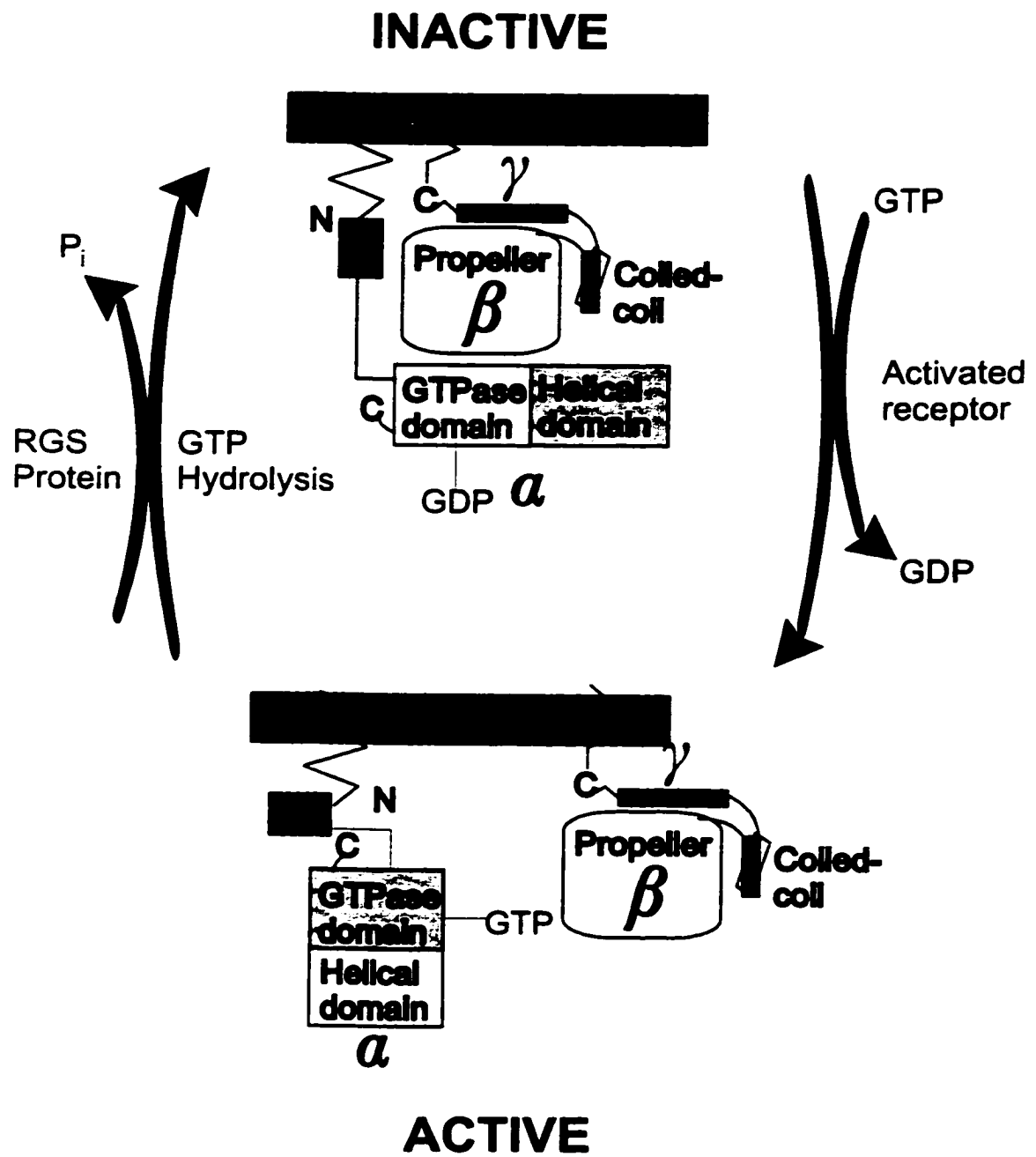


Figure 1.5. Heterotrimeric G protein activation

GPCRs share a common structural motif consisting of seven transmembrane α helices joined by three intracellular and three extracellular loops, an extracellular N-terminal tail and an intracellular C-terminal tail (Watson & Arkininstall, 1994; Wess, 1997). Despite this structural homology, GPCRs can selectively activate specific G proteins by discriminating among structural features of both $\beta\gamma$ and $G\alpha$ subunits. This specificity in G protein-receptor interaction defines the range of responses that a cell is able to make. Recent investigations have demonstrated that the intracellular loops of GPCRs have conformations such that they can only accommodate certain G-protein trimers. All three subunits of the G protein are thought to make contact with the receptor (Bourne 1997; Wess, 1997). The best-characterized contact is between the carboxy terminus of $G\alpha$ with the C terminus of the third intracellular loop of the receptor. Contacts between the $\beta\gamma$ subunit and the receptor have been reported but are less well characterized.

Biochemical and mutagenesis experiments suggest that transmembrane segments and 6 of GPCRs undergo conformational changes upon activation by ligand binding (for review see; Gether & Kobilka, 1998; Bourne, 1997). These conformational change uncover previously masked G protein binding sites and promote receptor/G protein interaction. G-protein binding to its receptor results in activation and exchange of GDP for GTP on the α subunit. It is not well understood how G protein activation results in the release of GDP. It has been suggested that receptor binding causes a conformational change in the shape of the $G\alpha$ subunit which, in turn, decreases GDP affinity and allows for GTP binding to the active site. The GTP-bound activated conformation of the α subunit has a lower affinity for $G\beta\gamma$ and the trimer dissociates to start the cycle described

above. Once this cycle of receptor-G protein activation has been initiated, mechanisms must exist to ensure proper magnitude and specificity of intracellular responses. At the receptor level, three major mechanisms exist: desensitization, downregulation and sequestration (Ferguson *et al*, 1996; Krupnick & Benovic, 1998; Carmen & Benovic, 1998). Desensitization of GPCRs occurs primarily by kinase-dependent receptor phosphorylation mediated by second messenger responsive protein kinases (ie. PKC, PKA) and specific G protein-coupled receptor kinases (GRKs). Downregulation and sequestration involves the physical removal of receptor protein from the plasma membrane. During sequestration, the receptor protein is temporally internalized into the cytosolic compartment of the cell, whereas during downregulation, there is an overall reduction in the total cellular level of receptor protein. The coordinated action of these pathways allows for tight regulation of the intracellular responses linked to GPCR activation.

4.3. Heterotrimeric G protein: classes and effectors

The family of heterotrimeric G proteins includes over 30 isoforms, which amounts to at least 20 α , 6 β and 12 γ gene products (Hamm, 1998). This diversity allows for a wealth of heterogeneity in subunit combinations, although the functional significance of this possibility is not yet understood. Once activated, G protein subunits can interact specifically with hundreds of different receptors and more than a dozen effectors providing another vast source of heterogeneity. These effectors include molecules such as cyclic nucleotides, phospholipases, protein kinases, phosphodiesterases and ion channels.

G protein α subunits have been divided into 4 main classes (G_s , G_i , G_q and G_{12}) based in part on their sequence homology and effector interactions. The 4 classes can be subdivided into specific subtypes (Figure 1.6). Studies have suggested that individual cells contain at least four or five different $G\alpha$ subtypes (reviewed by Neer, 1994). These subunits tend to have a wide tissue expression, with the exception of a few (α_t , α_{olf} , α_{16} , α_o and α_{gust}), which are more regionally tissue specific. It is the activated conformation of specific α -GTP subunits that provides new surfaces for interaction with highly specific effectors. For example, G_{α_s} proteins stimulate adenylyl cyclase (AC), $G_{\alpha_{i/o}}$ family members are sensitive to pertussis toxin (PTX) and often mediate inhibition of adenylyl cyclase and G_q and G_{11} proteins are PTX-insensitive and frequently couple receptors to activation of phospholipase C (PLC) isoforms. Despite this apparent rigid selectivity for G protein-effector interaction, a plethora of studies now supports multiple cross talk between GPCR signaling pathways (for reviews see; Hamm, 1998; Selbie & Hill, 1998). For example, in smooth muscle, stimulation of both G_i and G_q can augment PLC and PKC activity to promote contraction. GPCR activation of $G\alpha$ and $G\beta\gamma$ subunits can also regulate receptor tyrosine-kinase-mediated signaling pathways both at the receptor level and at the level of downstream signaling components (Selbie & Hill, 1998; Luttrell *et al.*, 1997; van Biesen, 1996). Therefore, it is no longer practical to view the cascade from receptor-G protein-effector as a specific linear sequence of events as multiple interactions at all levels of receptor-mediated signaling pathways continue to be elucidated.

Five β subunits and six γ subunits isoforms have been identified and sequenced. β isoforms share between 53-90% homology whereas γ isoforms have less homology than either α or β subtypes. Despite all the potentially different dimer combinations that

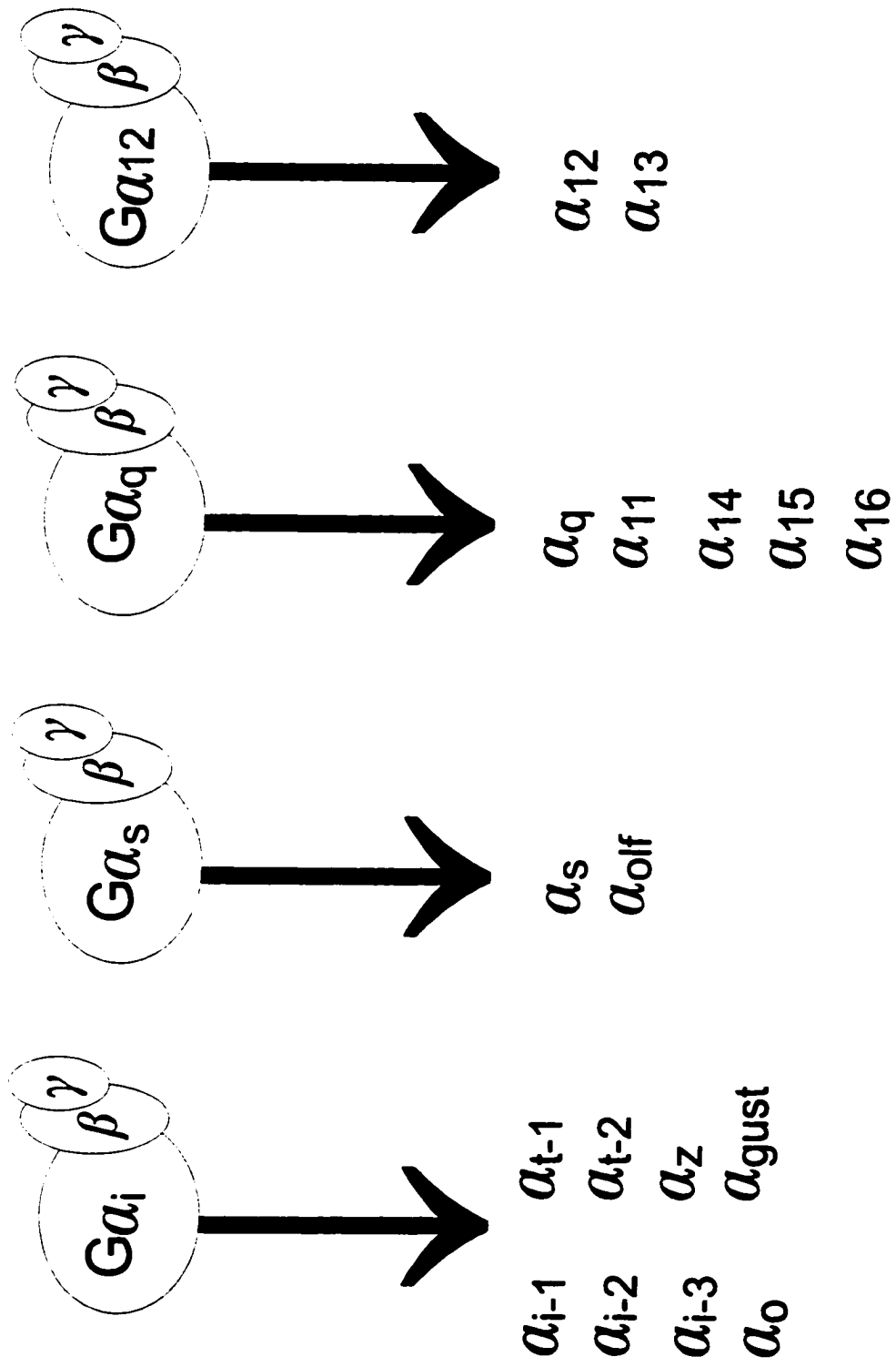


Figure 1.6. Heterotrimeric G protein α subtypes

these isoforms could generate, there is a certain degree of specificity in $\beta\gamma$ dimer formation (for review see; Neer, 1995). For example, $\beta 1$ and $\beta 2$ share a high degree of homology yet only $\beta 1$ can interact with $\gamma 1$. Selectivity is thought, at least in part, to be mediated by multiple sites in the WD repeat regions of the β subunit and a stretch of 14 amino acids in the middle of the γ subunit. For a long time it was thought that $\beta\gamma$ dimers acted simply as negative regulators of α -GTP subunits. Subsequently, the $\beta\gamma$ dimers have been shown to be positive regulators of a large number of effectors including receptors, AC, PLC β , PLA $_2$, PI3-kinase, β ARK and ion channels (reviewed by Clapham & Neer, 1993). As proposed for activated GTP- α subunits, receptor activation and release of the G protein $\beta\gamma$ is thought to uncover previously masked sites for direct protein-protein interaction of the dimer with specific effectors.

5. Regulation of ion channels by Heterotrimeric G proteins

The diversity of signaling cascade initiated by GPCRs provides a wealth of ways in which downstream effectors may be regulated. Ion channels are very common effectors of G protein-coupled signaling pathways. Regulation of ion channel activity by G protein activation has been shown to be essential for generating electrical impulses in excitable cells, for eliciting our sense of vision, taste and smell and for regulating growth and secretory activities in nonexcitable cells (reviewed by Wickman & Clampham, 1995a and b). The next section highlights the two main ways in which activated G proteins can modulate ion channel activity and provides evidence for these pathways in regulating transepithelial ion fluxes in the RPE and CE.

5.1. Membrane delimited and second messenger-mediated regulation

Ion channel regulation by GPCRs may be mediated by either G protein-coupled second messenger cascades and/or a direct “membrane delimited” G protein subunit interaction with the channel protein. The plethora of second messengers and other intracellular signaling molecules that can be activated by GPCRs underscores the diverse ways in which ion channels can be regulated. G protein-mediated elevations in intracellular Ca^{2+} , generation of cyclic nucleotides (cAMP, cGMP), lipid compounds (arachidonic acid) and stimulation of protein kinases (PKC, PKA, CaM kinase, MAP kinase) have all been shown to be signaling components involved in the regulation of ion channel activity (for see reviews; Jan & Jan, 1997; Finn *et al*, 1996; Wickman & Clapham, 1995).

Elevations in intracellular Ca^{2+} can induce changes in the activity of a variety of ion channels. For example, a number of calcium-activated K^+ , Cl^- and nonselective cation (NSC) channels found in both excitable and nonexcitable cells are targets for modulation by agonists that stimulate receptors coupled to Gq proteins (REF). Gq activation stimulates PLC to generate IP_3 and DAG with subsequent IP_3 -mediated Ca^{2+} release from intracellular stores (reviewed by; Exton, 1996 and 1997). Elevated cytosolic-free Ca^{2+} can then bind directly to channel proteins to induce opening. Cyclic nucleotides (cAMP, cGMP), generated by G protein activation of intracellular enzymes, can also directly bind to ion channels and alter their activity. A variety of nonselective cation channels have been identified that are directly activated by cyclic-nucleotide binding (reviewed by; Finn *et al*, 1996). In vertebrate olfactory neurons, activation of the G_{olf} protein-mediated signaling cascade stimulates adenylate cyclase to produce cAMP, which can directly bind

and activate a nonselective cation channel. Similar nonselective cation channels that are activated by direct binding of cGMP have been identified in retinal rods and cones, photoreceptors and in retinal Müller cells (Kusaka *et al*, 1996; Wei *et al*, 1996).

One of the most ubiquitous mechanisms of ion channel regulation is kinase-mediated phosphorylation. G protein-coupled signaling pathways can activate all major classes of protein kinases to regulate ion channels. For example, Gq proteins activate protein kinase C (PKC) via the generation of diacylglycerol (DAG) and elevation in $[Ca^{2+}]_i$. Stimulation of Gs proteins coupled to adenylate cyclase and cAMP production activates protein kinase A (PKA) and G proteins coupled to elevations in intracellular $[Ca^{2+}]$ can activate Ca^{2+} -calmodulin (CaM)-dependent protein kinases. More recently, PTX-sensitive Gi proteins and PTX-insensitive Gq proteins have been shown to activate MAP kinase. All protein kinases cause covalent modification of the channel structure through the addition of a charged phosphate group from ATP to serine, threonine and/or tyrosine residues (Jonas & Kaczmarek, 1996). Direct phosphorylation can result in changes in the activation/activation kinetics of ion channels, can alter levels of channel protein at the plasma membrane and/or can acutely alter current amplitude with little or no change in kinetics (Jonas & Kaczmarek, 1996; Smart, 1997).

The role of G protein stimulated phospholipid-derived compounds in ion channel regulation is less well documented than Ca^{2+} and/or kinase-dependent channel modulation. Activation of Gi and Gq family members has been demonstrated to result in activation of PLA₂ with subsequent PLA₂-mediated generation of arachadonic acid (AA). AA and its metabolites are powerful modulators of both cardiac and neuronal K⁺ currents (Zinn *et al*, 1998), volume sensitive Cl⁻ channels in osteoblastic cells (Gosling *et al*,

1996) and large-conductance Ca^{2+} -activated K^+ currents in chromaffin cells (Twitchell *et al*, 1997). In most cases, modulation of ion channel activity by AA and/or its metabolites appears to be direct without the involvement of kinase or Ca^{2+} -dependent processes (Twitchell *et al*, 1997). More detailed information on the mechanisms involved in G protein-activated lipid modification of ion channel activity and the roles that other lipid-derived molecules may play awaits further investigation.

Regulation of ion channel activity by a G protein-coupled pathway independent of any soluble intracellular signaling element has also been proposed. This so-called “membrane-delimited” pathway has now been described for the modulation of inwardly and outwardly rectifying K^+ channels, voltage-gated Ca^{2+} channels, inwardly rectifying Cl^- channels, and amiloride-sensitive Na^+ channels (reviewed by Hille, 1994; Wickman & Clampham, 1995). Generally, a membrane-delimited route is proposed whenever agonists, G protein analogues or purified G protein subunits can regulate ion channel activity in excised patch recordings where cytosolic signaling elements are absent. It has been suggested that in the absence of cytosolic second messengers ion channels are activated/inhibited by the direct binding of either the activated $\text{G}\beta\gamma$ subunit and/or $\text{G}\alpha$ subunit directly to the channel protein. Activated $\beta\gamma$ subunits have been demonstrated to directly modulate the activity of cardiac and neuronal I_{KACH} channels and voltage-gated N-type Ca^{2+} channels (reviewed by Dolphin, 1998). Similarly, a primary role for activated $\text{G}\alpha$ subunits in membrane delimited regulation of the cardiac ATP-sensitive K^+ channel ($\text{G}_{\alpha\text{i}}$), the epithelial amiloride-sensitive Na^+ channels ($\text{G}_{\alpha\text{i}3}$) and voltage-dependent L-type Ca^{2+} channels ($\text{G}_{\alpha\text{s}}$ and $\text{G}_{\alpha\text{o}}$) has also been proposed (Wickman & Clampham, 1995).

Despite the description of the two distinct G protein-mediated pathways regulating ion channel function, one should bear in mind that this artificial separation between membrane-delimited versus second-messenger-mediated does not occur *in vivo*. Studies have demonstrated that ion channels can be modulated at a number of sites by multiple G protein pathways acting in concert. Multiple modulation may provide fine-tuning of ion channel activity by allowing for versatile regulation in response to a variety of extracellular and/or intracellular stimuli.

5.2 Ion channel regulation in the RPE

In the eye, the basal surface of the RPE is in close approximation to the choriocapillaries, whereas the apical membrane of the RPE interacts with the photoreceptors of the neural retina. Paracrine and/or hormonal factors emanating from either of these tissues may modulate transepithelial responses. Biochemical and electrophysiological studies on the RPE have demonstrated that adrenergic, muscarinic, purinergic and dopaminergic agonists can modulate both transepithelial ion and fluid transport as well as other RPE functions including phagocytosis (Deary *et al*, 1990; Gregory *et al*, 1994; Gallemore & Steinberg, 1990). These agonists couple via GPCRs to signaling pathways that alter intracellular phospholipid, Ca^{2+} and cyclic nucleotide levels. Studies investigating the role(s) that these signaling elements play in the regulation of ion channel activity are integral for our understanding of the basic transport mechanisms at work in the RPE as well as how modulation of these ion transport pathways may ultimately lead to alteration in RPE function.

A number of studies have examined the effects of intracellular signaling molecules on RPE fluid and ion transport by bypassing GPCR activation. For example, in isolated bullfrog RPE-choroid preparations, elevations in intracellular cAMP stimulates active NaCl secretion and K⁺ absorption as a result of active Cl⁻ transport inhibition and a stimulation of active K⁺ and Na⁺ transport (Hughes *et al*, 1987; Hughes & Edelman, 1988). Similar results have been found in the chick RPE-choroid preparation, where basolateral Cl⁻ conductances were shown to be inhibited by elevated intracellular cAMP (Kuntz *et al*, 1994). These effects of elevated cAMP levels on ion channels in the RPE suggests that ligands linked to a G_s-mediated signaling pathway may be very important paracrine signals for the modulation of transepithelial ion transport.

In rabbit and bovine RPE, ion transport studies have shown that epinephrine, acting on apical G protein-coupled α_1 -adrenoceptors, stimulates fluid absorption across the RPE (Joseph & Miller, 1992). This absorptive pathway involves stimulation of apical Na⁺-K⁺-2Cl⁻ co-transporters and Cl⁻ conductive pathways at the basolateral membrane. One consequence of ion-coupled fluid absorption in the RPE is a reduction in subretinal fluid volume. Thus, epinephrine may play an important role in retinal adhesion by acting as a paracrine signal to regulate hydration in the subretinal space. A paracrine role for extracellular ATP, neuropeptide Y (NPY), and dopamine in regulating transepithelial fluid and ion transport has also been proposed in the RPE. Extracellular ATP acting via putative G_q-coupled P2Y purinoceptors affects the activity of both an apical K⁺ and a basolateral Cl⁻ current (Petersen *et al*, 1997). This change in channel activity is correlated with an increase in both intracellular free [Ca²⁺] and fluid absorption across the apical surface. Thus, in a manner similar to epinephrine, the effect of ATP on ion channels in

the RPE is linked to the regulation of subretinal ion composition and fluid volume. NPY receptor subtypes have also been identified on the RPE. These receptors couple to a variety of G proteins including G_i , G_o and G_q . Functionally, activation of these receptors stimulates elevations in intracellular Ca^{2+} and cAMP levels. Studies in bovine and human RPE-choroid preparations have demonstrated that NPY-mediated elevations in $[Ca^{2+}]_i$ increases the transepithelial potential, as a result of the activation of a basolateral Ca^{2+} -sensitive Cl^- conductance (Ammer *et al*, 1998). This finding suggests that, like epinephrine and ATP, NPY-mediated activation of a basolateral Cl^- conductance may be involved in altering Cl^- and fluid transport across the RPE. A similar effect for dopamine on basolateral Cl^- conductances in the RPE has also been reported (Gallemore & Steinberg, 1990).

In addition to traditional peptide agonists, a recent study has demonstrated that the simple phospholipid lysophosphatidic acid (LPA) can alter ionic conductances in isolated rat RPE cells (Thoreson & Chacko, 1997). LPA has been shown to act at membrane receptors coupled to PTX-sensitive G_i proteins (reviewed by; Moolenaar *et al*, 1997). The effect of LPA on transepithelial transport has not yet been investigated. In rat RPE cells however, LPA does activate a nonselective cation current and an outwardly rectifying K^+ current in a PTX-sensitive manner suggesting the involvement of G_i proteins. Receptors for a variety of other agonists including: carbachol, serotonin, vasopressin, melatonin and atrial natriuretic peptide have all been demonstrated in the RPE (Friedman *et al*, 1991; Osborne *et al*, 1993; Wolfensberger *et al*, 1994; Nash & Osborne, 1995; Nash & Osborne, 1996). Within the epithelium, these agonists activate GPCRs to mediated PI turnover, elevations in intracellular $[Ca^{2+}]$ and cyclic nucleotide (cAMP, cGMP)

generation. Due to the fact that the generation of these intracellular signaling molecules has been previously linked to changes in ion and fluid transport it appears likely that the RPE is modulated by a number of paracrine signals, which via cross-talking pathways, tightly regulate ion and fluid transport.

5.3. Rationale for studying ion channel regulation by G protein-coupled signaling pathways in the RPE

RPE fluid and ion movement is vital not only to RPE function but is also inextricably linked to the maintenance of retinal function. Therefore, identifying the role(s) that agonists and signaling pathways may play in modulating ion/fluid movement under physiological conditions may augment our understanding of the underlying causes of altered RPE function under pathophysiological conditions. This rationale is supported by the observation that a number of the signaling pathways in the RPE linked to altered ion transport have been implicated in ocular disorders. For example, G protein-coupled signaling pathways linked to, cAMP, IP₃ and elevations in [Ca²⁺]_i have been found to be altered in the RPE from Royal College of Surgeons (RCS) rats (Heth & Marescalchi, 1994; Heth *et al*, 1995). This rat strain has an autosomal recessive mutation that results in marked retinal degeneration due to a phagocytic defect in the RPE. Retinal degeneration in RCS rats is commonly used as a model for the retinal degeneration associated with the human disorder Retinitis Pigmentosa (Nash & Osborne, 1995). Changes in IP₃ and [Ca²⁺]_i signaling in RPE cells from RCS rats was correlated to alterations in both Cl⁻ and Ca²⁺ conductances as compared with nondystrophic control rats (StrauB *et al*, 1996). Since phagocytic ability has been linked to changes in ion channel activity in other cell

types (Ince *et al*, 1987 & 1988), these findings raise the interesting possibility that signaling defects in the RPE from RCS rats may cause functional changes in ion channels that are involved in phagocytosis. A similar role for signaling-mediated changes in ion channel function in the RPE has been proposed in the genesis of central serous retinopathy (CSR). CSR is characterized by fluid accumulation in the subretinal space which eventually leads to retinal detachment and blindness (Marmor, 1988). Subretinal accumulation is believed to occur as a result of defective fluid and ion transport by the RPE, suggesting that this epithelium plays a central role in the pathogenesis of this ocular disease. In a recent study, elevations in intracellular cAMP levels mediated by activation of G protein-coupled receptors was shown to cause ion pump dysfunction and reversal of ionic flow in the RPE (Zamir, 1997). Flow reversal would abolish net fluid absorption and cause fluid accumulation in the subretinal space. Therefore, these findings support the possibility that a signaling pathway(s) linked to alterations in cAMP may play a role in the genesis of CSR.

In light of the important role G protein coupled signaling pathways play in the normal physiology of the RPE and their potential role in ocular pathologies such as Retinitis Pigmentosa and CSR the main objectives of this thesis section are:

- i. To examine the effect of G protein activation on whole-cell currents in isolated rat RPE cells.**
- ii. To identify and characterize G protein activated channels in rat RPE cells and examine the signaling pathway(s) involved in their regulation.**

- iii. **To examine the actions of purinergic receptor-coupled signaling pathways in modulating cation currents and intracellular Ca^{2+} in isolated rat RPE cells.**

5.4 Ion channel regulation in the CE

The ciliary epithelium has a vast array of ion channels, pumps and transporters that play a vital role in the formation of aqueous humor. Within the eye, the sympathetic nervous system is an important common pathway in the regulation of aqueous humor flow. Sympathetic nerve fibers are present throughout the iris stroma and have also been observed in the ciliary muscle, where their function is not well understood (Wax, 1992; Caprioli, 1992). Given the close approximation of the epithelia cells to the stroma and underlying muscle, ion channels in the CE may be targets for modulation by neurotransmitters released from adrenergic nerve endings. The ciliary body also receives fibers from the parasympathetic nerves that innervate the ciliary muscle suggesting that cholinergic regulation of ion channels in the CE may also affect aqueous humor formation. It has been demonstrated that both parasympathetic and sympathetic nerves are present in the ciliary processes within the vicinity of the epithelial cells (Caprioli, 1992). In addition to transmitter release, circulating catecholamines or other factors may also reach the CE via the major arterial circle located in the ciliary body. In support of this hypothesis, studies have demonstrated that catecholamines are present throughout the uveal tract especially around the blood vessels within the CB (Kramer *et al*, 1972). There is also evidence to suggest that the CE may synthesize, process and release certain peptides into the aqueous humor where they could alter ion channel function through an

autocrine and/or paracrine manner (Trope & Rumley, 1985; Trope *et al*, 1987). Thus, paracrine and or autocrine signals from a number of sources have the potential to regulate ion channels in the CE.

Therapeutically, both adrenergic agonists and antagonists lower intraocular pressure (IOP) via actions on aqueous humor production and outflow (Ross & Drance, 1970; Krupin *et al*, 1980). While the net effect may be a reduction in IOP, the action of these agents at the level of the CE is still incompletely understood. Studies on isolated iris-CB preparations from a number of mammalian preparations have demonstrated that adrenergic selective agonists affect transepithelial electrical measurements (Krupin *et al*, 1991). Both α and β agonists decreased short circuit current (SCC) in a dose-dependent fashion. A change in SCC indicates that ionic movement through the CE is altered however, it does not permit an identification of whether this change represents an increase or decrease in net ion transfer. These studies were the first to suggest that adrenergic receptors were present in the CE and that their activation was linked to changes in ion channel activity. All adrenergic receptors are G protein-coupled and radioligand binding studies in the CE have established that both α ($\alpha_2 > \alpha_1$) and β ($\beta_2 > \beta_1$)-receptor subtypes are present (Nathanson, 1981; Wax & Molinoff, 1986; Huang *et al*, 1995; Bylund *et al*, 1997; Jin *et al*, 1994). Studies on intact dog CE bilayer further demonstrate that β -adrenergic receptor-mediated elevations in cAMP stimulate aqueous humor formation through the activation a Cl^- conductance thereby promoting Cl^- efflux (Chen *et al*, 1994). As mentioned above (section 3.2), Cl^- efflux plays a major role in AH formation and therefore any factor that alters Cl^- conductances may affect both the rate and quantity of aqueous humor secreted. Thus, there is good evidence to suggest that

activation of β -adrenergic receptors coupled to Gs-stimulated signaling pathways may play an important role in ion channel regulation in the CE. However, despite a role in modulating SCC, the effect of α -adrenergic signaling pathway(s) on ion channels in the CE remains undefined.

Like adrenergic agonists, parasympathomimetic agents have also been found to reduce IOP, although this effect is predominantly due to an increase in outflow (Kaufman, 1984). At the level of aqueous secretion however, their role is less clearly defined. The identification of muscarinic receptors in both isolated NPCE cells and intact iris-CB preparations suggests that these agents may act at the level of the CE to alter aqueous secretion. However, conflicting reports have found no effect, stimulation or inhibition of AH formation. The first report demonstrating an effect of cholinergic agonists on ion channels in the CE was demonstrated in cultured human NPCE cells. Acetylcholine was shown to transiently hyperpolarize the membrane potential via activation of an outwardly rectifying Ca^{2+} -sensitive K^+ current by mobilization of Ca^{2+} from intracellular stores (Helbig *et al*, 1989). The authors of this paper hypothesized a basolateral locale for this channel and proposed that it may be involved in the recycling of K^+ pumped into the cell and thus indirectly influence the rate of Na^+ transport. Similar to the findings in NPCE cells, carbachol-mediated increase in $[\text{Ca}^{2+}]_i$ also transiently activated an outward K^+ current via stimulation of M_3 receptors in isolated bovine PCE cells (Stelling & Jacob, 1993). In this paper, the authors suggested that activation of this current in PCE cells would hyperpolarize NPCE cells, provide a driving force for Cl^- exit and thus increase aqueous secretion. The lack of a clear effect of parasympathomimetic agents on AH secretion *in vivo* makes it difficult to assign a role for cholinergic-activated

K^+ current in coupled ion/fluid secretion. These studies do suggest however, that ACh acting at GPCRs linked to elevations in intracellular Ca^{2+} may be an important paracrine signal for the regulation of ion flow across this epithelium.

A variety of other receptors that couple to G protein-mediated signaling pathways have also been demonstrated in the CE. These include receptors for adenosine, ATP, histamine, vasoactive intestinal peptide and endothelin (Crook *et al*, 1991; Farahbaksh & Cilluffo, 1996). Activation of these receptors in isolated PCE and NPCE cells may cause stimulation of PLC, phospholipid generation, mobilization of intracellular Ca^{2+} , changes in cAMP levels and production of PGE_2 . Based on evidence that demonstrates a role for these intracellular signaling elements in altered ion channel activity, the CE, like the RPE, is poised to receive and respond to signals from multiple G protein-coupled pathways. Currently, little is known about how these signaling pathways target ion channels in the CE to affect aqueous humor secretion.

5.5. Rationale for studying ion channel regulation by G protein-coupled signaling pathways in the CE

Decreasing aqueous production is still the major target in the pharmacological management of glaucoma. Autonomic drugs and carbonic anhydrase inhibitors are widely used in the treatment of glaucoma but their use is limited by a number of side effects. Therefore, exploring alternative ways to suppress secretion and reduce IOP without the unwanted side effects of current therapies is an area of intense interest. However, attempts to alter AH secretion are frequently hampered by a relative lack of understanding of the precise cellular mechanisms that underlie this process. Thus,

identifying the selective receptor subtypes and molecular signaling pathways involved in regulating ion transport in the CE will not only enhance our knowledge of the basic physiology of aqueous humor formation, but may also provide specific targets for the development of selective drugs with fewer side effects. Therefore, the objectives of this thesis section are:

- i. To examine the effect of adrenergic agonists on whole-cell currents in isolated pigmented ciliary epithelial (PCE) cells.**
- ii. To determine the receptor subtype(s) and signaling pathway(s) mediating adrenergic regulation of cation and/or anion channels in isolated PCE cells.**

CHAPTER 2

GENERAL METHODS

1. Cell Dissociation and Culture

1.1 Retinal Pigment Epithelial Cells

Long Evans rats (age 8 to 14 days) were anaesthetized using halothane, sacrificed by decapitation, and the eyes enucleated. Rats were maintained and anaesthetized in accordance with the ARVO Statement for the Use of Animals in Ophthalmic and Vision Research. The RPE cells were isolated using a modification of the method of Wang, Koutz and Anderson (1993). Enucleated eyes were placed in calcium-free Hank's solution containing EDTA (CFHE; Gibco BRL, Burlington, Ontario). The connective tissue was removed and the globes were bisected along the equator just above the ora serrata so that the neural retina remained attached to the posterior eyecup. The anterior portion of the eye containing the cornea, lens and vitreous was discarded. The posterior eye cup was then placed in calcium-free HANK's EDTA containing 220 U/ml hyaluronidase type III (Sigma Chemical Company, St. Louis) and 65 U/ml collagenase A (Boehringer Mannheim, Laval, Quebec) for 10 minutes at 37°C. Under a dissecting microscope, in fresh CFHE without enzyme, the neural retina was cut at its attachment to the optic nerve head and was gently peeled from the eye cup using forceps. The remaining posterior segment was incubated at 37°C for 5 minutes in CFHE enzyme solution to facilitate the dissociation of the RPE from Bruch's membrane. Following a second transfer to fresh CFHE, the RPE was gently removed from the remaining eyecup using forceps so as not to disturb the underlying choroid, and collected using a fire-polished Pasteur pipette. RPE tissue was triturated through a narrow-bore fire-polished Pasteur pipette to yield a suspension of single cells and small clumps of

RPE tissue. The cell suspension was washed and resuspended in 500 μ l of Dulbecco's Modified Eagle's Medium (DMEM) plus 20% fetal calf serum, 0.5% penicillin-streptomycin (Gibco BRL, Burlington, Ontario), and gentamicin (50 μ g/ml; Sigma Chemical Company, St. Louis). The cell viability was estimated using trypan blue exclusion and was generally greater than 90%. The cells were seeded onto glass coverslips (12 mm diameter) in 4-well culture dishes and placed in a 37°C incubator with an atmosphere of 5%CO₂/95% O₂. The medium was changed to DMEM containing 10% fetal calf serum and antibiotics 24 hours following the initial plating (Figure 2.1).

1.2 Pigmented Ciliary Epithelial Cells

Eyes were enucleated from 5-10 week old pigmented rabbits (Reimens, Ontario) in accordance with the ARVO statement for the Use of Animals in Ophthalmic and Vision Research. Rabbits were euthanized with 0.3 ml/kg of Euthanol (sodium-pentobarbital; MTC pharmaceuticals, Cambridge, Ontario) by intravenous injection into the marginal ear vein. Enucleated eyes were placed in sterile Dulbecco's phosphate-buffered saline (D-PBS; Gibco, Grand Island, NY) and the ciliary body was freed from the iris by an incision between the iridal and ciliary processes. The epithelium was then dissected from the underlying stroma and treated for 30-40 minutes with D-PBS containing collagenase (1.5 mg/ml; Sigma) and pronase (1 mg/ml; Boehringer Manneheim). Epithelial pieces were triturated gently to yield single PCE and NPCE cells and small tissue explants. The cell suspension was centrifuged at 5000 g for 5 min, washed with enzyme-free D-PBS and then re-centrifuged. Cells were seeded onto glass coverslips (12 mm diameter) and incubated at

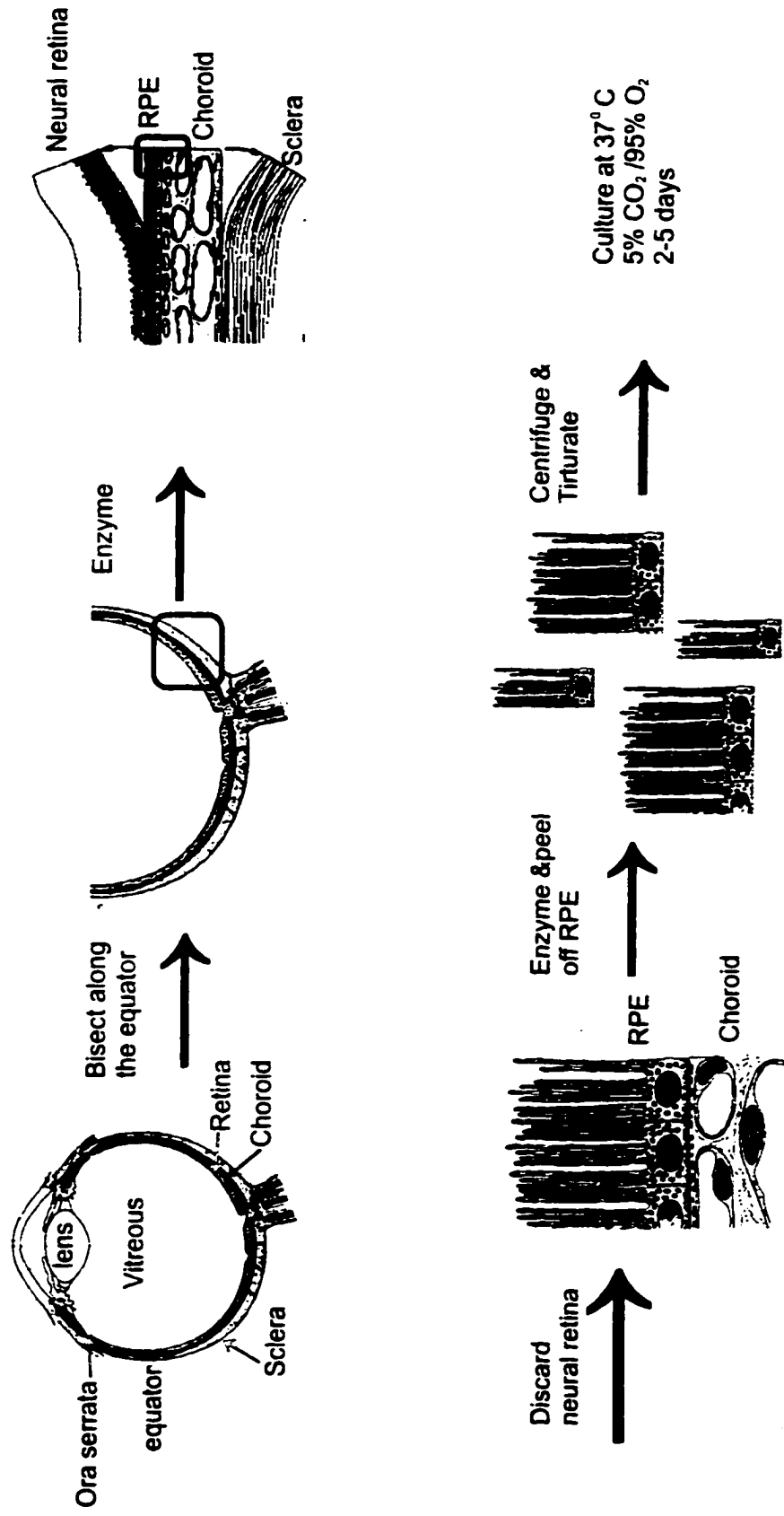


Figure 2.1. Schematic diagram of rat RPE isolation and culture. See text for details.

37°C in DMEM containing 5 or 10% fetal calf serum and placed an atmosphere of 5% CO₂/95% O₂ (Figure 2.2).

2. Immunocytochemistry

RPE or PCE cells, plated on glass coverslips, were washed three times with PBS to remove the culture medium and then fixed by the rapid addition of precooled methanol for 2-5 min at -20°C and washed three times for 10 min with 2% bovine serum albumin (BSA) in PBS at RT. The cells were then permeabilized and endogenous endoperoxidases blocked by incubation for 20 min at RT in 0.3% TritonX100 + 3% H₂O₂ in PBS. The cells were then washed (3X10 min) with 2% BSA in PBS and treated for 1 hour with donkey serum at RT to block any non-specific binding. The cells were then incubated overnight at 4°C with primary antibody at the appropriate dilution. Cells were then washed 3X10 min with PBS before incubation at RT for 1 hour with the appropriate IgG secondary antibody conjugated with the reactive fluorescent dye Cy3 or Cy2. The cells were then washed 3X5 min with PBS, mounted onto glass slides with aqueous mount (1:3; PBS/glycerol) and fluorescently labeled cells were visualized under epifluorescence illumination (Nixon Diaphot) and photographed on Kodax 400 film. For nuclear immunofluorescence, fixed cells were rinsed with PBS 3X 5min at RT. Cells were then incubated with 1µg/ml of Hoescht Reagent (Sigma) for 20 min at RT in the dark. Cells were washed (PBS 3X 5min) and mounted onto glass slides with aqueous mount.

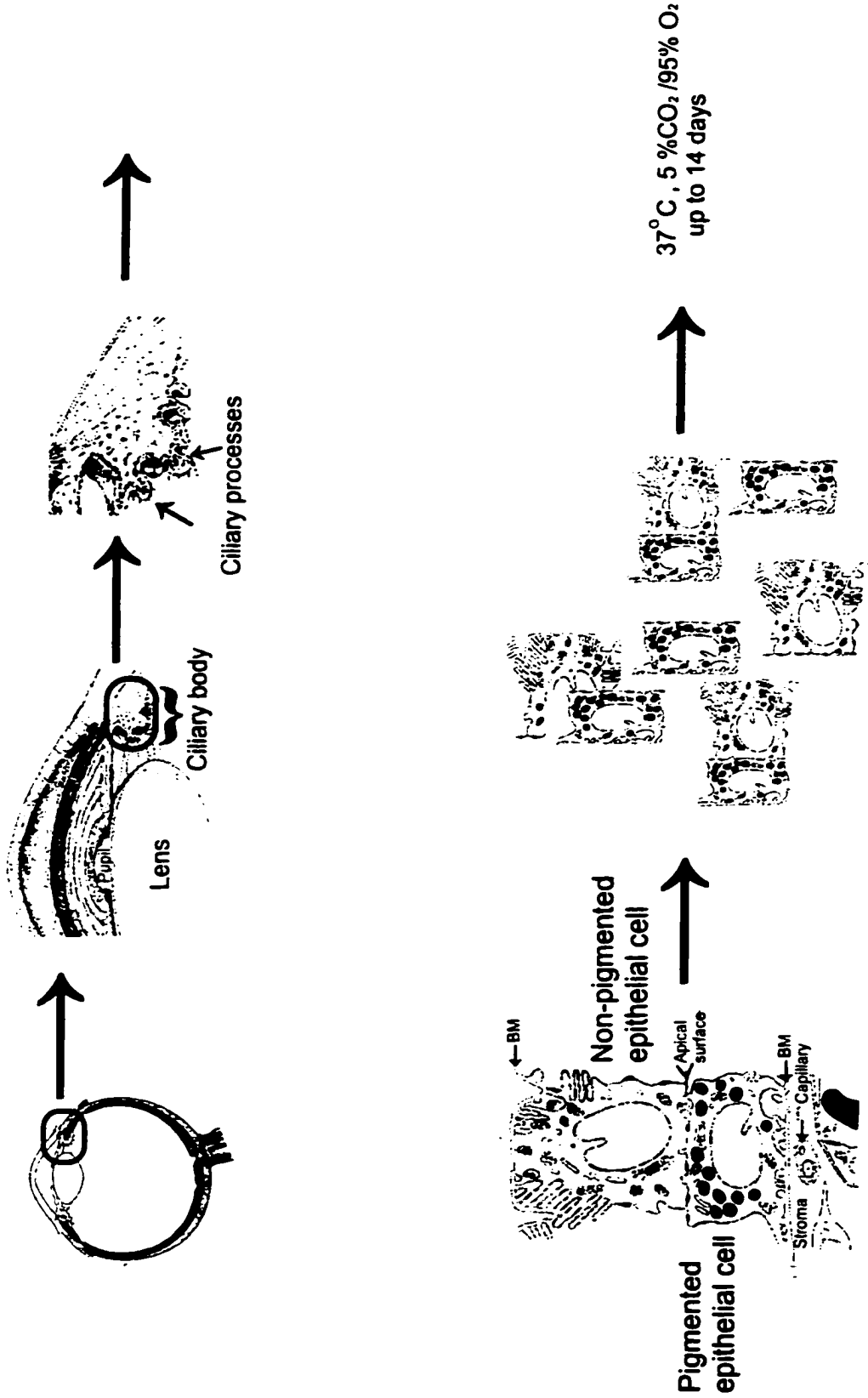


Figure 2.2. Schematic diagram of rabbit PCE isolation and culture. See text for details.

For all immunofluorescent experiments, substituting PBS for primary antibody in one coverslip of cells controlled for non-specific background fluorescence. All other steps remained the same.

3. Electrophysiological Recording

3.1 Solutions

RPE cells, attached to glass coverslips, were placed in a shallow recording chamber (volume 1 ml) and positioned on the stage of a Nikon inverted microscope (Nikon Canada Instruments Inc). The recording chamber was superfused (1 - 2 ml/min) with a variety of solutions via gravity inflow from elevated reservoirs. The flow rate was regulated by a series of valves. Perfusands containing NaHCO_3 were continuously bubbled with 5% CO_2 /95% O_2 . All extracellular and intracellular solutions were adjusted to pH 7.3 - 7.4, and the osmolarity was measured by freezing point depression (Osmette A, Fischer Scientific, Nepean, Ont.). Extracellular solutions had a final osmolarity of 330 - 340 mOsm and the osmolarity of intracellular solutions was between 310 - 320 mOsm. The use of a slightly hyperosmotic external solution was found to be effective in eliminating transient changes in ionic conductances, which occurred as a result of osmotic changes during the initial period of whole-cell recording. Table 1 lists the various extra- and intra-cellular solutions used. These solutions were used in numerous combinations to isolate and study specific ionic currents in ocular epithelial cells and will be discussed separately in the following chapters.

TABLE 1.1 Composition of extracellular solutions (mM)

	A	B	C	D	E	F	G	H
NaCl	130	-	-	-	-	30	130	30
KCl	5	5	5	5	145	5	5	5
Na - HEPES	10	10	10	10	10	10	10	10
Glucose	10	10	10	10	10	10	10	10
MgCl ₂	1	1	1	1	1	1	1	1
CaCl ₂	1	1	1	1	1	1	0.2	0.2
NaHCO ₃	10	-	-	-	-	10	10	10
Choline - Cl	-	140	-	-	-	-	-	-
TRIS - Cl	-	-	140	-	-	-	-	-
NMDG - Cl	-	-	-	140	-	-	-	-
EGTA	-	-	-	-	-	-	1.5	1.5
Na ⁺ -aspartate	-	-	-	-	-	100	-	100

Composition of intracellular solutions (mM)

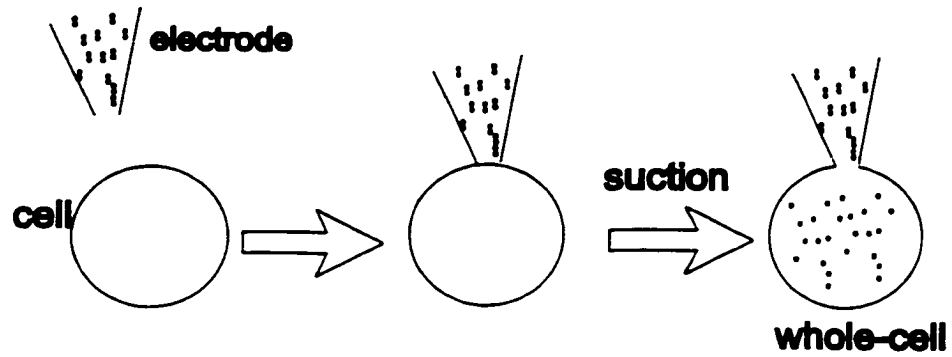
	I	J	K	L	M
NaCl	-	-	30	30	-
KCl	140	30	-	-	-
Na ⁺ - HEPES	-	-	10	10	-
HEPES acid	20	20	-	-	20
MgCl ₂	1	1	1	1	1
CaCl ₂	0.4	0.4	0.4	0.4	0.1
EGTA	1	1	1	1	1
K ⁺ -aspartate	-	110	-	-	140
Cs ⁺ -aspartate	-	-	100	-	-
BAPTA	-	-	-	-	10
CsCl	-	-	-	110	-
ATP	1	1	1	1	1
GTP	0.1	0.1	0.1	0.1	0.1

3.2 Whole-cell Patch Clamp Technique

We used the whole-cell patch clamp technique to measure currents in isolated RPE cells (Hamill *et al.*, 1981). Figure 2.3 A and B shows a schematic diagram of this recording technique. Patch electrodes were pulled from borosilicate glass micropipettes with diameters of 1.5 mm outside and 1.1 mm inside (Sutter Instruments, Novato, CA) using a two-stage vertical microelectrode puller (Narishige model PP83, Tokyo, Japan). Electrodes were coated with beeswax in order to reduce input capacitance (Rae & Levis, 1984) and had resistances of 2-3 M Ω when filled with intracellular solution and placed in the extracellular bathing solution. The reference electrode used was a sealed electrode/salt bridge combination (Dri-Ref-2; World Precision Instruments, Sarasota, FL). Offset potentials were nulled using the amplifier circuitry before seals were made on cells.

A seal of gigaohm resistance was then formed between the pipette and a small patch of the cell membrane by pressing the pipette to the membrane and applying negative pressure. The capacitive transient arising due to pipette capacitance was cancelled using the capacitance compensation circuitry on the amplifier. A further pulse of suction was then applied which ruptures the patch of membrane but leaves the giga-seal intact. In this whole-cell configuration, the pipette interior is in direct contact with the cell interior. The additional capacitive transient that arises upon attaining whole-cell configuration (reflecting the product of the pipette resistance and the cell membrane) is cancelled, and the total response of all ion channels in the cell can now be investigated and recorded.

A. Whole-Cell Configuration



B. Whole-Cell Voltage Clamp

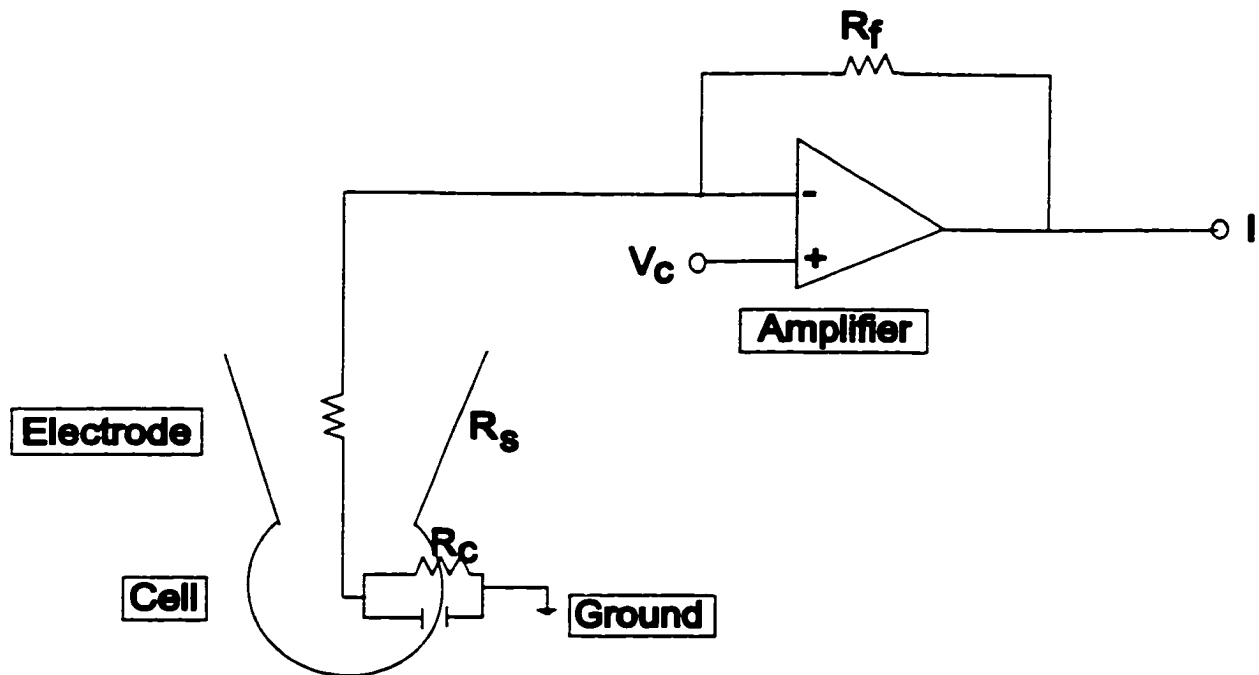


Figure 2.3. (A). Schematic diagram of whole-cell patch clamp configuration. (B). Schematic diagram for whole-cell patch clamp recording. See text for details.

Membrane potential and ionic currents were recorded with an Axopatch 1D amplifier (Axon Instruments, Foster City, CA). Voltage step commands were generated with CLAMPEX (pClamp software, Axon Instruments). To restrict the bandwidth of extraneous noise, yet to still allow adequate signal resolution, currents were filtered with a 4-pole low-pass Bessel filter (-3 dB at 1 kHz). Currents were digitized at a sampling frequency of 5 kHz using pCLAMP software (Axon Instruments). Current and voltage were displayed on a Gould TA240 chart recorder and were stored on computer disk. Values for cell capacitance were obtained from the capacitance compensation circuitry on the amplifier. Measures of series resistance were obtained directly from the amplifier and were always less than 15 M Ω . All experiments were conducted at room temperature (20-22°C).

3.3 Liquid Junction Potentials

Liquid junction potentials exist whenever two solutions of different composition come into contact. These potentials arise as a result of the different mobilities of the ions that make up the solutions. Mobility is determined by the frictional resistance to ion movement which results from the dimension of the ion and the viscosity of the medium through which they move (Barry & Lynch, 1991). In whole-cell patch clamp experiments, LJPs of significant magnitude can arise between pipette and bath solutions that differ in their concentration and composition of ions (Ng & Barry, 1995; Neher, 1992). These LJPs cannot be eliminated by the initial procedure in whole-cell patch clamp whereby the patch-amplifier is offset (or “zeroed”) prior to seal formation (see above).

Liquid junction potentials (LJP) between the bath and patch clamp electrodes were measured experimentally and defined as the potential of the bath solution with respect to the pipette solution (Barry & Lynch, 1991). For whole-cell recording the membrane potential of the cell, V_m , was then calculated as $V_m = V_p - \text{LJP}$. To confirm experimentally generated measurements, LJPs were also calculated with a software program (JPCalc, Version 2.00; P.H. Barry, Sydney, Australia) which uses the generalized Henderson equation for N polyvalent ions,

$$\text{LJP} = (RT/F) S_F \ln \left\{ \frac{\sum_{i=1}^N z_i^2 u_i a_i^P}{\sum_{i=1}^N z_i^2 u_i a_i^S} \right\} \quad (1)$$

where

$$S_F = \frac{\sum_{i=1}^N [z_i u_i (a_i^S - a_i^P)]}{\sum_{i=1}^N [z_i^2 u_i (a_i^S - a_i^P)]}$$

where LJP represents the potential of the solution (S) with respect to the pipette (P) and u , a and z represent the mobility, activity and valency (including sign) of each ion species (i); R is the gas constant, T is the temperature in K and F is the Faraday, so that $RT/F \ln = 58.2 \log_{10}$ in mV at a temperature of 20°C . All the data shown in results (Chapter 3-5) have been corrected for LJPs and the values for the various combinations used.

3.4 Pharmacological Treatment

Drugs were first dissolved in Millipore water or dimethylsulfoxide (DMSO) depending on their solubility to make concentrated stock solutions. Stock solutions were stored at -20°C until use when they were then diluted to the appropriate concentration in extracellular or intracellular solution. The final concentration of DMSO in the experimental solutions was always less than 0.05%, a concentration at which DMSO is

reported to have no significant effect on the electrical properties of rat RPE cells (Ueda & Steinberg, 1994).

Drugs diluted in intracellular solution were dialysed directly into the cells via inclusion in the patch pipette. Those drugs diluted into extracellular solution were applied to the cells by bath superfusion or pneumatic pressure ejection from a micropipette (see Methods section in chapters for details). Drugs included in the intracellular recording solution were allowed to dialyse for 10 min after achieving whole-cell configuration before electrophysiological recordings were made. Bath superfused test solutions were applied for a minimum of five and usually for ten complete (1 ml) bath exchanges. For application of test substances by pressure ejection, micropipettes (≥ 2 mm in diameter) were positioned 50-100 μm from the cell and 2-5 lb in^2 (~ 14 -34 kPa) pressure was applied to the back of the micropipette using a Picospritzer II (General Valve Corp., Fairfield, NJ, USA) for 4 - 40 sec. Pressure ejection of extracellular solution in the absence of drug was routinely performed to control for any changes in ionic currents related to this method of drug application.

3.5 Quantitative analysis

Analysis of whole-cell data was performed using CLAMPFIT (Axon pClamp Ver.5.5.1 or 6.0 Software). All current-voltage plots were obtained by averaging the current amplitude measured over 50 ms prior to the cessation of the depolarizing step commands. All I-V plots were constructed in Excel (Microsoft) or Origin (MicroCal Software Inc.). Final composite figures were constructed using CorelDraw (Corel Corp., Ontario, Canada). To account for variation in cell size most data have been normalized by

dividing current (pA) by cell capacitance (pF). In some records, the current traces were corrected for a linear “leakage” current. This linear and time-independent current was obtained by measuring the current amplitude at hyperpolarized potentials at which no voltage-dependent currents should be present. When data have been leak subtracted, this is noted in the figure legends. All data has been corrected for LJPs (see above).

4. Statistical Analysis

Data are presented as mean \pm S.E.M. mean and analysed by use of Student’s unpaired t test unless otherwise noted. A significance level of $P \leq 0.05$ was accepted.

CHAPTER 3

Activation of voltage-dependent K⁺ currents and a nonspecific cation current in cultured rat retinal pigment epithelial cells

This work has been previously published by Poyer, J., Ryan, J.S. and Kelly, M.E.M (1996). *J. Membr. Biol.* **153** :13-26 and Ryan, J.S. and Kelly, M.E.M. (1998). *Brit. J. Pharmacol.* **124**:1115-1122.

ABSTRACT

Whole-cell patch-clamp recording techniques were used to investigate the G protein subtype and related signaling molecules involved in activation of a nonspecific cation (NSC) current in cultured rat retinal pigment epithelial (RPE) cells. Using 140 mM KCl intracellular and 130 mM NaCl extracellular solutions, rat RPE cells exhibited inward and outward K^+ currents. Upon addition of the non-hydrolyzable guanine triphosphate analogue, guanosine-5'-O-(3-thiophosphate)(GTP γ S, 0.1 mM), to the recording electrode, a non-specific cation (NSC) current was elicited. The NSC current had a mean reversal potential of +5.7 mV in 130 mM extracellular NaCl with Cs^+ -aspartate in the pipette, and was not affected by alterations in the extracellular Cl^- concentration or removal of extracellular Ca^{2+} . The GTP γ S-activated current was found to be permeable to several monovalent cations (K^+ , Na^+ , choline, TRIS, and NMDG). Addition of fluoroaluminate, an activator of large molecular weight heterotrimeric GTP-binding proteins (G proteins), to the intracellular recording solution activated the NSC current. The G protein involved was pertussis toxin (PTX)-sensitive, since GTP γ S failed to activate the NSC current in cells pre-treated with PTX. Loading RPE cells with an antibody (10 μ g/ml) against the α subunit of all PTX-sensitive G proteins ($G_{\alpha i/o/v/z}$) reduced NSC current activation, while loading RPE cells with antibodies directed specifically against the α subunits of the G_i subclass ($G_{\alpha i-3}$) completely abolished current activation. Investigation of the potential downstream mediators in the $G_{\alpha i}$ -NSC channel pathway suggested that activation of the NSC current was not dependent on intracellular Ca^{2+} , but that the $[Ca^{2+}]_i$ may play a modulatory role in current regulation. The NSC

current was unaffected by treatment of RPE cells with the selective protein kinase C inhibitor GF 109203X (3 μ M) or the selective CAM kinase II inhibitor KN-93 (50 μ M). However, current activation was delayed and current amplitude reduced in the presence of the nonselective kinase inhibitor H-7 (100 μ M), or the selective inhibitor of MAPKK (MEK) activation, PD 98059 (50 μ M). In the absence of GTP γ S, the NSC current was not activated by superfusion of the cells with the cGMP kinase activator dibutyryl-cGMP or with the adenylate cyclase activator forskolin. These results support the involvement of a G protein of the G $_{\alpha i}$ subclass in the activation of a NSC current in rat RPE cells, and suggest a potential modulatory role for [Ca $^{2+}$] $_i$ and MAP kinase-dependent phosphorylation in current regulation. Activation of the NSC current would depolarize RPE cells and lead to the activation of outward K $^+$ currents. This could provide a mechanism by which these cells could rid themselves of accumulated K $^+$.

INTRODUCTION

The retinal pigment epithelium (RPE) is a specialized monocellular layer of epithelial cells that lies external to the neurosensory retina. The RPE serves a number of functions essential to the viability of the outer retina and the photoreceptors (Zauberman, 1979). Fluid and ion transport by the RPE are thought to be essential to the maintenance of retinal attachment and optical clarity, as well as being intergral components in the regulation of ion homeostasis in the subretinal space between the photoreceptors and the RPE (Steinberg & Miller, 1979; Zauberman, 1979). Patch-clamp recordings from freshly isolated and cultured RPE cells in both amphibians and mammals have identified a variety of ion channels. Several voltage-dependent K^+ selective (Fox, Pfeffer & Fain, 1988; Strauss, Richard & Wienrich, 1993; Strauss, Weiser & Wienrich, 1994; Tao, Rafuse & Kelly, 1994) and Ca^{2+} -selective ion channels (Ueda & Steinberg, 1993; Strauss & Wienrich, 1993), as well as anion channels have now been described (Botchkin & Matthews, 1993; Ueda & Steinberg, 1994). The activity of these ion channels is important in the modulation of net fluid and ion transport, light-evoked responses, and phagocytosis by this epithelium. Understanding how these ion channels are regulated may, therefore, aid in our understanding of the mechanisms controlling various RPE functions.

GTP-binding proteins (G proteins) are known to directly couple a variety of receptors to intracellular effectors, and considerable evidence now confirms that ion channels are common effector proteins in G-protein mediated signaling pathways (for review see Breitwieser, 1991; Rodbell, 1992). Ion channels can be modulated indirectly by G proteins, via activation of downstream soluble second messengers or protein kinase

phosphorylation pathways. In addition, a pathway independent of soluble second messengers involving direct membrane delimited G protein regulation of ion channels has also been suggested (Brown, 1993; Wickman & Clapham, 1995)

Several G protein alpha subunits (G_{α}) have been shown to be expressed in RPE cells (Jiang *et al.*, 1991). Activation of G protein-coupled signaling pathways, linked to a variety of intracellular signaling pathways, has been shown to modulate a number of RPE functions (Nao-i *et al.*, 1990; Gallanmore & Steinberg, 1990; Gregory, Abrams & Hall, 1992). The roles that these G proteins and their associated signaling pathways may play in regulating specific ionic conductances in the RPE, however, have not been fully elucidated. However, regulation of ion channel activity by G protein-coupled signaling pathways is important for the control of fluid and ion transport and phagocytosis in RPE cells. Therefore, our purpose was to examine the role of G proteins in regulating ionic conductances in RPE cells and to investigate the potential role of other downstream signaling components in this regulation.

MATERIALS AND METHODS

1. Cell Dissociation and Culture

Long Evans rats (age 8 to 12 days) were anaesthetised using halothane, sacrificed by decapitation, and the eyes enucleated as previously described (see GENERAL METHODS, section 1.1). RPE cells were maintained in culture for 2 - 5 days prior to electrophysiological recording. This culture period was chosen as cells maintained longer in culture (>2 weeks) were observed to lose pigmentation, de-differentiate and form a confluent epithelial monolayer (see RESULTS, Figure 3.1A-C). Isolated differentiated RPE cells maintained in culture for 2-5 days were identified by their dense pigmentation and the presence of apical microvilli. Cultured cells were stained for the epithelioid cell marker cytokeratin and were identified to be of rat RPE origin by positive staining for RET-PE10 and RET-PE2 monoclonal antibodies, which recognize RPE-specific epitopes (see RESULTS, Figure 3.2A-C) (Neill & Barnstable, 1990; Neill *et al.*, 1993).

2. Immunofluorescence

Rat RPE cells were stained for cytokeratin , RET-PE2 and RET-PE10 protein using the generalized protocol detailed in GENERAL METHODS (section 2). For cytokeratins, the primary antibody was a mouse monoclonal anti-cytokeratin 8.13 (used at a 1:100 dilution in PBS) and the secondary was anti-mouse IgG conjugated with rhodamine at a dilution of 1:100 in PBS. For RET-PE2 and RET-PE10 staining, the primary antibody was anti-mouse RET-PE2 (used at a 1:30 dilution in PBS) or anti-mouse RET-PE10 (used at a 1:10 dilution in PBS). The secondary antibody was donkey

anti-mouse IgG conjugated with Cy2 at a dilution of 1:10 in PBS for both RET-PE2 and RET-PE10.

3. G Protein Subtype Identification

3.1 Treatment of RPE cells with PTX

Pertussis toxin (PTX) is a bacterial endotoxin that inactivates G proteins of the G_i , G_o , G_t and G_z subtype by catalysing the ADP-ribosylation of cysteine residues at the GTP binding site on the α subunit (Ui, 1990). This covalent modification prevents activation of these G protein subtypes by inhibiting the exchange of GDP for GTP. To examine the potential involvement of PTX-sensitive G proteins in the activation of ionic conductances in RPE cells, freshly isolated RPE cells were cultured in DMEM for 2 days to ensure the cells were healthy and adhered firmly to the coverslips. After 2 days, the DMEM was removed and replaced with fresh DMEM containing 500 ng/ml of PTX. A control coverslip from the same culture had fresh DMEM added without PTX. The cells were then incubated at 37°C for 24 hr. prior to electrophysiological recording.

3.2 Scrape loading of RPE cells with G_α antibodies

To load RPE cells with antibodies against G_α subunits, cells were grown for 3-4 days in culture and then replated in 10 μ g/ml of either $G_{\alpha i/o/vz}$, $G_{\alpha i-3}$, or $G_{\alpha s}$ antisera. The $G_{\alpha i/o/vz}$ antibody used in these experiments was a rabbit polyclonal antibody raised against a conserved sequence near the carboxy terminus of rat $G_{\alpha z}$. This antiserum is cross reactive with all members of the G_i family, but not other G_α subunit proteins. The

rabbit polyclonal $G_{\alpha i-3}$ antibody used was raised against amino acids 345-354 at the C-terminus of rat $G_{\alpha i-3}$. This antiserum is reactive with $G_{\alpha i-1}$, $G_{\alpha i-2}$ and $G_{\alpha i-3}$, but not cross reactive with other G_{α} subunit proteins. Cells were loaded with antibodies using a variation of the scrape loading technique of McNeil *et al.* (1984). Replating is assumed to be physically equivalent to scrape loading in that during the replating process transient membrane pores are created through which antibodies can enter and gain access to the cell interior.

To replate RPE cells and load them with antibodies, cells grown for 3-4 days in culture were incubated with trypsin/EDTA for 5 min and then washed with an excess of DMEM plus 10% NCS. The cells were then centrifuged at 5000 g for 5 min, washed, resuspended and plated in 250 μ l of DMEM/NCS containing 25 μ l of antibody solution (100 μ g/ml) to give a final antibody concentration of 10 μ g/ml. Resuspended cells were allowed to replate onto glass coverslips for 12-14 hrs at 37°C in an incubator with an atmosphere of 5%CO₂/95% O₂. Control groups were: 1) cells resuspended in the absence of antisera; 2) cells replated with 10 μ g/ml of non-reactive monoclonal antiserum against glial fibrillary acidic protein (anti-GFAP) and 3) non-replated cells incubated with 10 μ g/ml G_{α} antiserum. Following electrophysiological recording, immunofluorescence was carried out with a secondary antibody raised against rabbit immunoglobulins conjugated with Cy3 to confirm G protein antibody loading.

3.3 Immunofluorescence of G_{α} subunits

Immunofluorescence detection of the anti- G_{α} proteins was performed exactly as described for rat RPE anti-cytokeratin staining (see Chapter 2 [GENERAL METHODS, Chapter 2] and section 2 , above), with the omission of the overnight incubation in primary antibody. Replated RPE cells were also labeled with a nuclear Hoescht stain by incubating fixed cells with 1ml of Hoescht reagent (see GENERAL METHODS, Chapter 2) for 20 min at RT. Cells were then rinsed 3X5 min in PBS.

4. Electrophysiological Recording

4.1 Superfusion and Solutions

Cells, attached to glass coverslips, were placed in a shallow recording chamber (volume 2 ml) and positioned on the stage of a Nikon inverted microscope. The recording chamber was superfused with various perfusands, as previously described (see GENERAL METHODS, Chapter 2). In this study, the standard extracellular solution consisted of (in mM): NaCl, 130; KCl, 5; Na^+ -HEPES, 10; NaHCO_3 , 10; MgCl_2 , 1; CaCl_2 , 1; and glucose, 10 (solution A, table 1 in GENERAL METHODS). Replacement of extracellular Na^+ was accomplished using equimolar substitution with choline chloride, TRIS-hydrochloride, N-methyl-D-glucamine (NMDG) chloride, or KCl (solutions B-E, table 1 in GENERAL METHODS). When Cl^- was reduced in the extracellular bathing medium, this was accomplished by equimolar substitution of Cl^- with aspartate ions (solution F, table 1 in GENERAL METHODS). Extracellular calcium was replaced by 0.2 mM CaCl_2 with 1.5 mM EGTA (solution G, table 1 in GENERAL

METHODS). The extracellular calcium concentration with this substitution was estimated to be <10 nM. Calcium concentration was calculated using a software program based on the algorithm of Goldstein (1979 [provided by J. Kleinschmidt]). The standard intracellular pipette solution consisted of (in mM): KCl, 140; HEPES (free acid), 20; MgCl₂, 1; CaCl₂, 0.4; EGTA, 1; ATP, 1; and GTP, 0.1 (solution I, table 1 in GENERAL METHODS). Free Ca²⁺ in the pipette solution was estimated at 100 nM. When low chloride intracellular solutions were used, 140 mM KCl was replaced with 110 mM K⁺-aspartate and 30 mM KCl (solution J, table 1 in GENERAL METHODS). Low chloride solutions were made K⁺-free by substituting 100 mM Cs⁺-aspartate, 10 mM Na⁺-HEPES, and 30 mM NaCl for K⁺-aspartate and KCl (solution K, table 1 in GENERAL METHODS). The intracellular solution was made nominally Ca²⁺-free (<10 nM) by adding 0.1 mM CaCl₂ and 10 mM BAPTA (solution M, table 1 in GENERAL METHODS).

4.2 Intracellular Dialysis of G Protein Analogues

To examine the actions of G proteins on ionic conductances in rat RPE cells we examined the effect of substituting GTP in the pipette solution with various G protein analogues. We first explored the effect of substituting GTP with 0.1 mM GTP γ S. GTP γ S is a non-hydrolyzable GTP analogue that irreversibly activates G proteins. This GTP analogue has been shown to activate a variety of ion channels when dialysed into cells by inclusion in the pipette solution (Olivia *et al*, 1988; Parson & Hartzell, 1993). We also investigated the effects of another non-hydrolyzable GTP analogue Gpp(NH)p (Allen &

Chapman, 1996; Parson & Hartzell, 1993). As with GTP γ S, 0.1 mM Gpp(NH)p was included in the pipette solution to allow dialysis directly into the cell cytosol.

Fluoroaluminate (AlF $_4^-$), as with the other nonhydrolyzable GTP analogues, has proved to be a useful tool for the activation of heterotrimeric G proteins, as opposed to the low molecular weight GTP binding proteins (Kahn, 1991). AlF $_4^-$ activates heterotrimeric G proteins reversibly by binding to the GDP-bound form of G $_{\alpha}$ and mimicking the γ phosphate of GTP. To confirm the type of G protein involved in GTP γ S and Gpp(NH)p-mediated activation of the NSC current we dialysed RPE cells with AlF $_4^-$. The fluoroaluminate complex was formed in low chloride, K $^+$ -aspartate (solution J, table 1 in GENERAL METHODS) or Cs $^+$ -aspartate (solution K, table 1 in GENERAL METHODS) intracellular solution, by the addition of 1 NaF and 25 μ M AlCl $_3$ or 10 mM NaF and 100 μ M AlCl $_3$.

In addition to G protein activators, we also explored the effect of the G protein inhibitor GDP β S on ionic currents in rat RPE cells. GDP β S is a nonhydrolyzable GDP analogue that competitively inhibits G protein activation by GTP and GTP analogues (Shuba *et al*, 1990). In our experiments, 2 mM GDP β S was substituted for GTP in the pipette solution and dialysed directly into the cell cytosol.

4.3 Pharmacology of ionic currents in RPE

A variety of drugs were employed to examine the sensitivity of native and G protein-activated currents in rat RPE cells to pharmacological blockade. Potassium channel blockers (barium, 4-aminopyridine [4-AP], tetraethylammonium [TEA], and quinine), the Na $^+$ channel blocker amiloride, the cation channel blocker, gadolinium and

the gap junction blocker, octanol, were diluted from stock solutions into the extracellular solution and superfused at concentrations cited in RESULTS.

4.4 Protein Kinase Inhibitors and Cyclic Nucleotides

To investigate the involvement of protein phosphorylation in the regulation of G protein-activated nonspecific cation (NSC) current, RPE cells were pre-incubated (20 min) and superfused during electrophysiological recording with 4 different membrane permeant protein kinase inhibitors: the non-specific kinase inhibitor, H-7; the PKC inhibitor, GF 109203X; the CaM kinase II inhibitor, KN-93 and the MEK inhibitor, PD 98059, at the concentrations cited in RESULTS.

To determine the involvement of cyclic nucleotides in the G protein activated NSC current in rat RPE cells, the cells were superfused with the membrane permeant analogue of cGMP, dibutyryl cGMP (300 μ M), or the membrane permeant adenylate cyclase activator forskolin (50 μ M) to generate cAMP. For these experiments, drugs were superfused in low Cl^- (Na^+ -aspartate) external Ringers (solution F, table 1 in GENERAL METHODS) with Cs^+ -aspartate internal electrode solution (solution K, table 1 in GENERAL METHODS), used to block any K^+ or Cl^- currents that could be activated by the cyclic nucleotide analogues.

4.5 Electrophysiological Recording Techniques

We used the whole-cell patch clamp technique to measure currents in isolated RPE cells using recording conditions as described previously (see GENERAL METHODS section 3). Liquid junction potentials (LJP) between the bath and patch

clamp electrodes were measured experimentally and confirmed using JPCalc software, as previously described. All the data and current-voltage relationships shown have been corrected for LJPs. The LJP using standard intracellular and extracellular solutions (solutions A and H, table 1 in GENERAL METHODS) was 2.5 mV. In asymmetric low chloride solution (solutions A and I, table 1 in GENERAL METHODS) the LJP was 9.7 mV and when low chloride extracellular solution and Cs^- -aspartate intracellular solution (solutions K and F, table 1 in GENERAL METHODS) were used, the LJP was 4 mV. Under experimental conditions where $[\text{Cl}^-]_{\text{out}}$ or $[\text{Cl}^-]_{\text{in}}$ was varied, the LJPs were 2.5 mV (solution F and I; solution A and I, table 1 in GENERAL METHODS) and 10 mV (solution A and J, table 1 in GENERAL METHODS), respectively. In cation-substituted extracellular solutions with Cs^+ -aspartate in the pipette, the LJPs were 15 mV (solution B,C or D and K, table 1 in GENERAL METHODS) and 5 mV (solution E and K, table 1 in GENERAL METHODS). When low calcium solutions were used (solutions G and M, table 1 in GENERAL METHODS), the LJP was 3 mV.

4.6 Permeability Ratios

The cation selectivity of the current being investigated in this study was determined by substituting extracellular Na^+ with other monovalent cations (see solutions B-E above) and measuring the reversal potential of the current in these different cation-substituted solutions. Permeability ratios (PB/PA) obtained for the current were based on experimentally measured reversal potentials, and were calculated using the following derivation of the Goldman-Hodgkin-Katz equation. The ratios are stated in the text as permeability relative to Na^+ :

$$\Delta V_r = V_r B - V_r A = 58 \log \frac{PB[B]_o}{PA[A]_o} \quad (2)$$

where V_r = reversal potential, A = Na^+ -containing extracellular solution, B = substituted extracellular solution (see table 1 in GENERAL METHODS for solutions).

5. Materials

Cy2 and Cy3-conjugated IgG were obtained from Jackson ImmunoResearch Laboratories (West Grove, PA, USA). RET-PE2 and RET-PE10 antibodies were a gift from Dr. Colin Barnstable (Yale University, School of Medicine, New Haven, Conn, USA). PTX, H-7, GF 109203X, KN-93, PD 98059, cGMP and forskolin were all purchased from Calbiochem (LaJolla, California, USA). G protein α subunit antibodies were purchased from Santa Cruz Biotechnology (Santa Cruz, California, USA). All other chemicals were from Sigma Chemical Co (St. Louis, MO, USA).

RESULTS

1. RPE cell culture and growth characteristics

Primary cultures of RPE cells were established from eyes of pigmented rats. Isolated cells exhibited the typical phenotype that has been described for RPE cells in primary culture (Wang *et al*, 1993; Mayerson *et al*, 1984). Figure 3.1A shows a freshly isolated RPE explant before mechanical dissociation. The characteristic hexagonal morphology and heavy pigmentation of the cells is evident. Trituration of the explants yielded single RPE cells that were rounded with dense pigmentation, and in most cases, prominent apical microvillous processes. RPE cells typically adhered to the coverslips within 12 hrs. Figure 3.1B shows a phase photomicrograph of RPE cells grown in culture for 3 days. These cells are representative of the type used for whole-cell patch clamp recording experiments, such that at this time in culture they retained the general morphology of RPE cells and are scattered with few contacts with neighboring cells. This low-density culture allows for adequate space-clamp of cells as it avoids any nonuniformity in voltage changes or errors in capacitive or whole-cell current measurements which may occur with more confluent cultures (see below). Rat RPE cells grown for longer periods in culture (>2 weeks) start to de-differentiate, flatten, lose their ability to synthesize melanin granules and begin to form a continuous sheet of tightly packed cells as they proliferate into confluent monolayers (Figure 3.1C). Although RPE cells *in vivo* normally form a quiescent monolayer, they still retain their ability to divide

Figure 3.1. Rat RPE cells in culture. (A) Phase-contrast photomicrograph of a freshly dissociated rat RPE explant. Cells are tightly attached to each other, hexagonal in shape and heavily pigmented. (B) Isolated RPE cells grown in culture for 3 days. These cells are representative of those used for electrophysiological recording. (C) RPE cells grown for 16 days in culture. Cells have proliferated, flattened, lost their pigment and formed a confluent monolayer. Scale bars are equal to 10 μm in (A) (B) and (C).

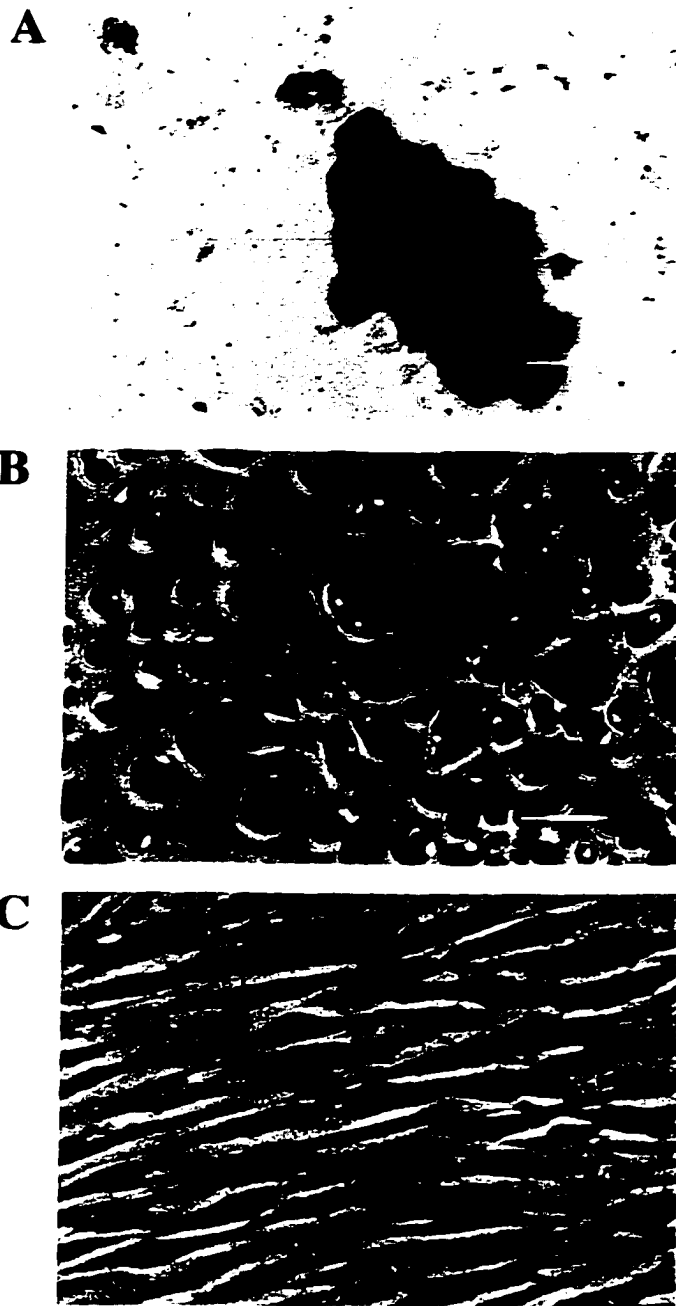


Figure 3.1

and will do so if detached from the epithelium, as occurs under culture conditions or following ocular trauma (Neill & Barnstable, 1990).

2. Identification of RPE cells

In addition to identifying RPE cells on the basis of their characteristic morphology (see above), immunofluorescent detection for specific markers of rat RPE cells in culture was also carried out. Antibodies to the intermediate filaments, cytokeratins, were used to identify putative RPE cells in our primary culture. Figure 3.2A demonstrates that RPE cells grown in culture for 10 days stain positive for cytokeratins indicative that the cells were of epithelial origin. Antibodies to cytokeratins have been used extensively as a means to identify cells with an epithelial phenotype as the presence of cytokeratins is a defining feature of this cell type (Corwin & Gown, 1989). Rat RPE cells have been demonstrated to express cytokeratins 8 and 18 as their sole intermediate filament proteins (Owaribe *et al*, 1988) and antibodies to these proteins have been used as markers of RPE cells both in tissue and cultured cells (Fuchs *et al*, 1991; Tao and Kelly, 1994). We used the broad-spectrum monoclonal antibody (anti-Cytokeratin 8.13), based on its ability to bind a common epitope in a number of cytokeratins (including 8 and 18) in cells of epithelial origin (Corwin & Gown, 1989).

Cultured rat RPE cells were also identified on the basis of positive staining for RET-PE10 (Figure 3.2B) and RET-PE2 (Figure 3.2C). RET-PE2 and RET-PE10 are cell surface antigens that can be used as specific markers for rat RPE cells in culture (Neill & Barnstable, 1990; Neill *et al*, 1993). RET-PE2 labels a 50-55 kDa cell surface protein

Figure 3.2. Immunocytochemistry of rat RPE cells in culture. (A) RPE cells grown in culture for 10 days stain positive for cytokeratins, indicative of an epithelioid phenotype. RPE cells in culture for 5 days also stain positive for the specific RPE cell markers RET-PE10 (B) and RET-PE2 (C). Scale bar equals 20 μm for panels A-C.

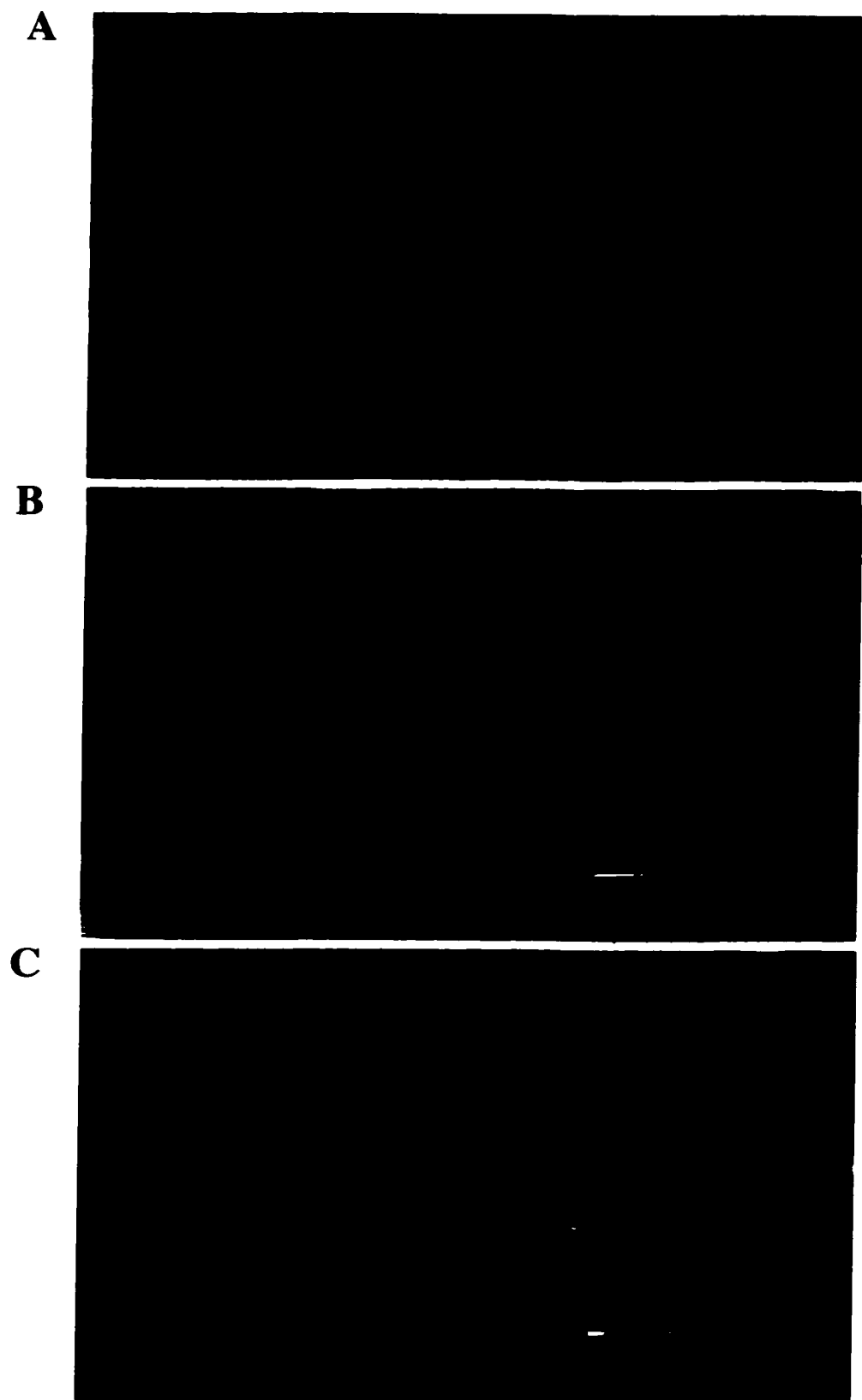


Figure 3.2

exposed on the cell surface of the RPE that is expressed during embryonic development and throughout the RPE at all ages. Similarly, RET-PE-10 also labels a cytoplasmic polypeptide epitope (61 kDa) that typically is expressed later in RPE maturation (>postnatal day 9). In our primary cultures >90 % of cells at 5 days in culture were labeled with either of the two antigens (Figure 3.2B and 3.2C), confirming their identity as RPE cells.

3. Membrane properties and whole cells current in rat RPE cells

Immediately after “break-in” to the whole-cell configuration under standard recording conditions with 130 mM NaCl extracellular (solution A, table 1 in GENERAL METHODS) and 140 mM KCl intracellular solutions (solutions I, table 1 in GENERAL METHODS), the average resting membrane potential of cultured RPE cells was -47 ± 2 mV ($n = 33$). Values for cell capacitance, obtained directly from the capacitance compensation circuitry from the amplifier, averaged 34 ± 2 pF ($n = 100$). These values for average resting membrane potential and cell capacitance are comparable to those reported in other studies for cultured mammalian RPE cells (Hughes & Steinberg, 1990; Strauß *et al.*, 1993; Strauß *et al.*, 1994; Tao *et al.*, 1994; Wen *et al.*, 1993).

Figure 3.3 shows typical whole-cell current recordings made from rat RPE cells 2- 5 days in culture with standard 130 mM NaCl extracellular and 140 mM KCl intracellular solutions. Under voltage-clamp conditions, the cells were held at -62 mV and stepped from -122 to $+58$ mV in 20 mV increments for 500 ms. In >90% of cells, the major outward current recorded was a time independent current which activated at potentials positive to -40 mV. An example of this current recorded from a representative

Figure 3.3. Whole-cell current in rat RPE cells. Whole-cell currents recorded from 3 representative RPE cells in standard 130 mM NaCl extracellular solution and standard 140 mM KCl intracellular solution, with the addition of 100 μ M GTP. The voltage-clamp protocol is shown at the top of the figure. (A) In this cell, whole-cell outward current (left panel) is activated at potentials depolarized to the holding potential (V_h) of -62 mV, with little inward current apparent at potentials hyperpolarized to V_h . The current-voltage (I-V) plot for this cell (right panel), measured over 50 ms prior to the cessation of the command pulse, is outwardly rectifying with current activated at potentials positive to -40 mV. (B) In another RPE cell (left panel), inward current was produced in response to hyperpolarizing voltage pulses with outward current activating at more positive potentials. The I-V plot for the cell in B (right panel) shows inwardly rectifying current between -122 and -62 mV and outwardly rectifying current activating positive to -40 mV. (C). Inward and outward whole-cell current was elicited in another RPE cell at potentials hyperpolarized and depolarized to V_h (-62 mV). The I-V curve for this cell (right panel) shows that outward current activated at potentials positive to -50 mV and showed time-dependent inactivation. Cell membrane capacitances were 24(A), 32(B) and 41(C). Dashed lines indicate the zero current potential in this and subsequent figures.

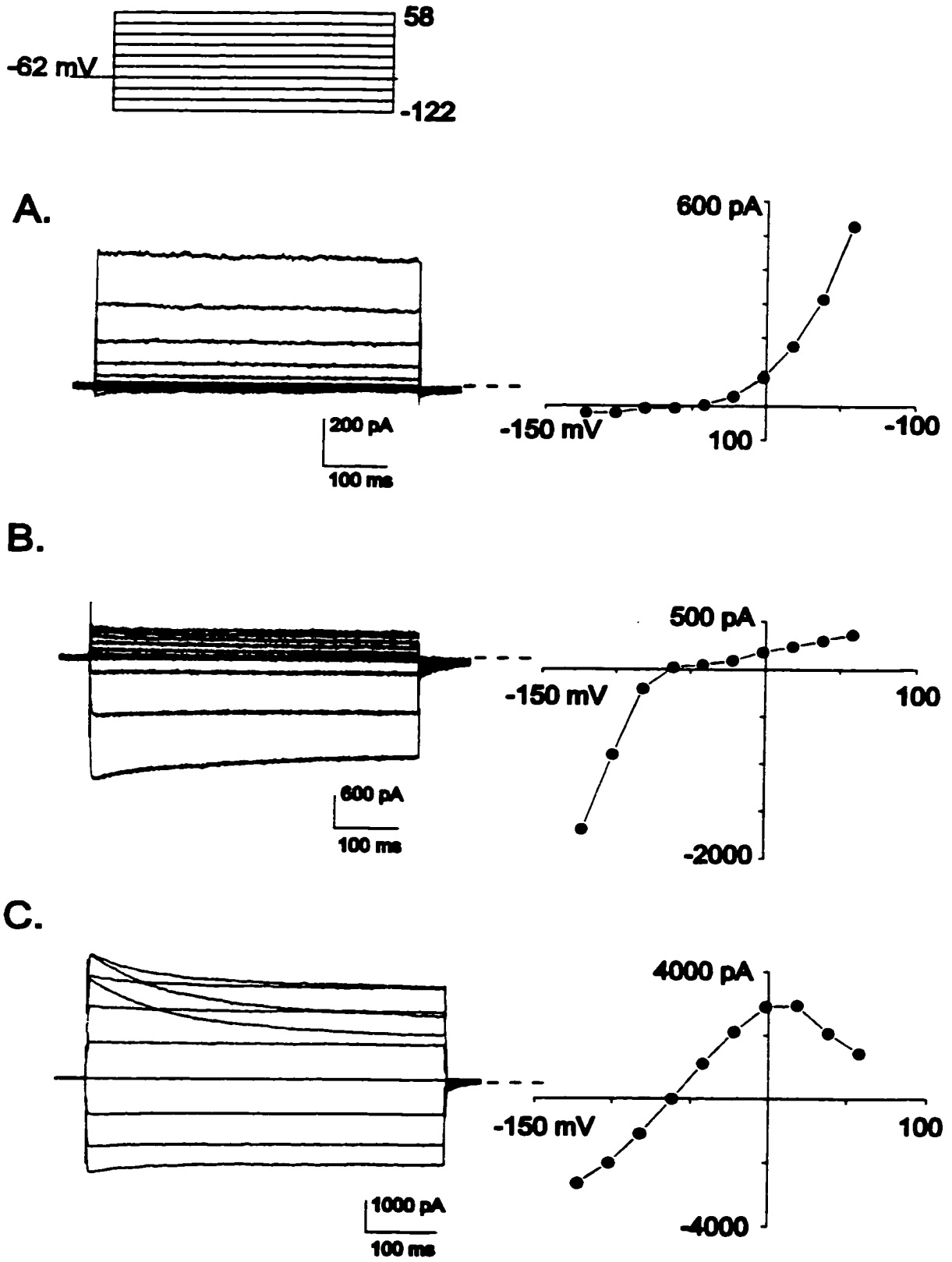


Figure 3.3

RPE cell is shown in Figure 3.3A. The I-V curve for this cell is shown in the right panel. In response to hyperpolarizing voltage commands little current is apparent, however, an outward current activates at potential positive to -40 mV and increases with increasing depolarization. The amplitude of this outward current showed little decline during the length of the depolarizing pulses. This current is similar to the delayed rectifying K^+ conductance (I_{KV}) described for cultured RPE cells in a variety of other species (Wen, Lui & Steinberg, 1993; Tao *et al*, 1994).

In 47% of RPE cells recorded from, inward current was recorded in response to voltage steps to hyperpolarized potentials between -122 and -62 mV. Figure 3.3B shows a representative RPE cell in which this hyperpolarization-activated inward current was recorded. The inward current exhibited some time-dependent decay at the more negative potential of -122 mV and slowly inactivating outward current when the membrane potential was depolarized positive to the holding potential ($V_h = -62$ mV). The I-V curve for this cell shows an inwardly rectifying current that reverses around -62 mV and an outwardly rectifying current that activates positive to -40 mV and increases with depolarization. This current is characteristic of the inwardly (anomalous) rectifying K^+ current (I_{KIR}) described in other mammalian RPE cells (Strauß *et al*, 1993; Tao *et al*, 1994).

In approximately 20% of the RPE cells recorded from, depolarizing voltage steps positive to -62 mV evoked an inactivating outward current (Figure 3.3C). The I-V for this cell illustrates that the current activates positive to -60 mV, reaches a peak and then slowly declines over the length of the voltage step. A similar inactivating outward current

has been described in cultured rabbit and turtle RPE cells (Tao *et al*, 1994; Fox & Steinberg, 1992).

4. Characterization of outward current in rat RPE cells

4.1 K⁺ selectivity of the outward current

The whole-cell current recorded in rat RPE cells was found to be primarily K⁺-selective. Confirmation of the ion selectivity of the outward current was carried out by examining the time- and voltage-dependent relaxations (tail currents) following activation of the outward current in varying extracellular K⁺ concentrations. Tail currents were recorded following activation of outward current by a 100 ms voltage step to +20 mV followed by steps to potentials between -90 and 0 mV. Representative tail currents, from a single RPE cell, recorded in 5 mM K⁺ extracellular solution at potentials between -90 and -40 mV are shown in Figure 3.4A and B. The mean (\pm SEM) reversals for tail currents were -72 ± 0.3 , -37 ± 2 , and -26 ± 2 mV when RPE cells were superfused with 5, 25, and 50 mM extracellular K⁺, respectively (n=3 cells each). A plot of the reversal potential of the tail currents vs. extracellular [K⁺] is shown in Figure 3.4C. The least-squares fit to the data has a slope of 47 mV per 10-fold change in extracellular K⁺ concentration, approaching the Nernst predicted value of 58 mV per 10-fold change in extracellular K⁺ concentration. This suggests that these currents in cultured rat RPE cells are largely carried by K⁺ ions.

Figure 3.4. Outward current in rat RPE cells is K^+ selective. (A) Representative tail currents recorded at various potentials in standard 5 mM K^+ extracellular following a step pulse to +20 mV to activate outward current. (B) Expanded view of the tail currents shown in panel A; tail currents reversed near -70 mV for this cell (see arrow). The voltage protocol for the current traces in A and B is shown at the top of the figure. (C) Plot of the mean reversal potential of the tail currents versus extracellular $[K^+]$ ($n=3$ each $[K^+]$). The slope of the line fitted by least squares is 48 mV per 10-fold change in extracellular $[K^+]$. Error bars represent S.E.M. for this and all subsequent figures.

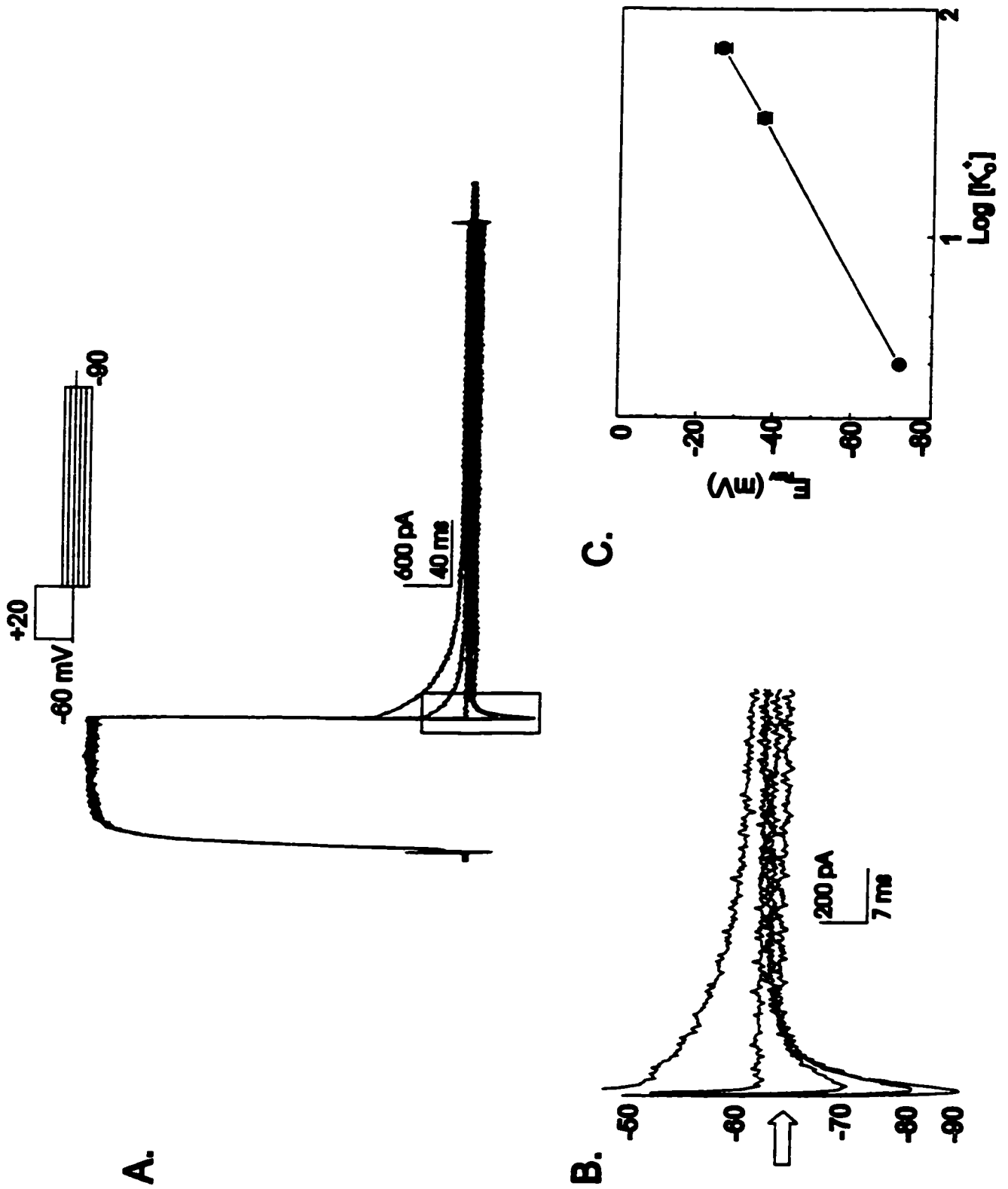


Figure 3.4

4.2 Pharmacological blockade of outward K^+ current

The most frequently observed outward K^+ current in rat RPE cells was a voltage- and time-dependent outward current (I_K) which resembled the delayed rectifier K^+ current described in fresh and cultured RPE cells from a variety of amphibian and mammalian species (Hughes & Steinberg, 1990; Strauß *et al.*, 1993; Strauß *et al.*, 1994; Tao *et al.*, 1994; Wen *et al.*, 1993). This type of K^+ conductance has been shown to be sensitive to a variety of traditional potassium channel blockers including, tetraethylammonium (TEA), 4-aminopyridine (4-AP) and barium (Ba^{2+}) (Hughes & Steinberg, 1990; Strauß *et al.*, 1993; Tao *et al.*, 1994).

In rat RPE cells, I_K was blocked ($70 \pm 8\%$, $n = 3$) by 1 mM 4-AP, and was significantly reduced ($42 \pm 4\%$, $n = 4$) by 5 mM TEA. Figure 3.5A shows whole-cell current traces obtained from a representative RPE cell before and after superfusion with 1 mM 4-AP. In this cell the outward K^+ current was almost completely blocked by 4-AP with little effect on inward current. Figure 3.5, panel B, shows the current-voltage plot for the currents in panel A, before and after superfusion with 1 mM 4-AP. Also shown is the difference current for the 4-AP-sensitive current, obtained by digital subtraction of the 4-AP blocked current from the control current. The 4-AP-sensitive current is characteristic of I_K in that it activates at potentials positive to -50 mV and increases in amplitude upon membrane depolarization.

Figure 3.5. Pharmacological Blockade of Outward Current. Whole-cell patch-clamp recordings from two representative cells showing the effect of 1 mM 4-aminopyridine (4-AP, [A,B]) and 1 mM barium (C, D) on inward and outward currents in rat RPE cells. The extracellular solution was standard 130 mM NaCl while the intracellular solution was standard 140 mM KCl with the addition of 100 μ M GTP (solutions A and I, table 1). The voltage protocol is shown at the top of panel A. Cells had a whole-cell capacitance of 25 and 20 pF for panels A and B, respectively. Data were leak subtracted at 1.6 G Ω for panel A and not leak subtracted for panel B. 4-AP virtually eliminates the outward current, while barium blocks the inward current (● control; ○ blocker (4-AP or barium); Δ difference current).

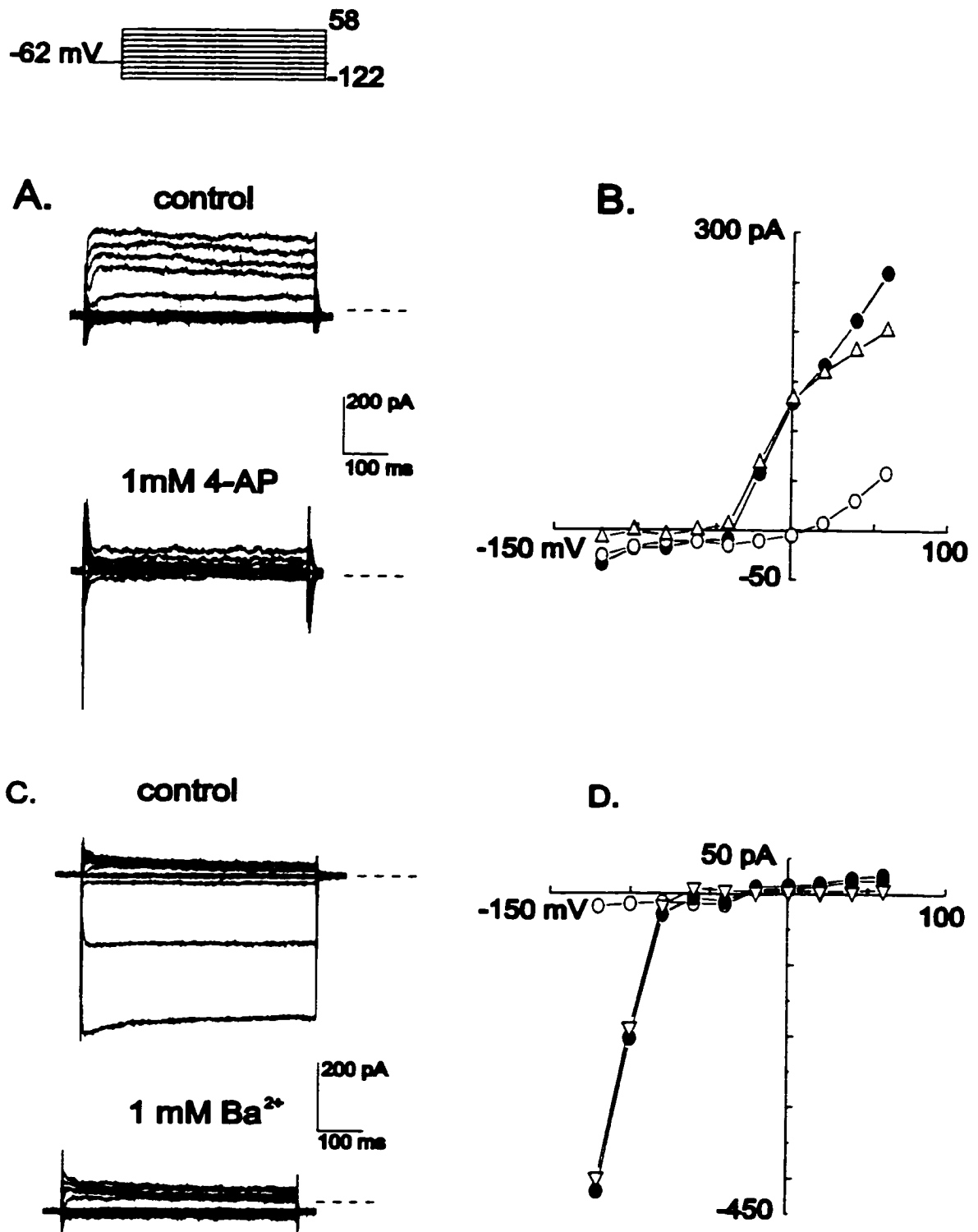


Figure 3.5

In 47% of the cultured rat RPE cells tested, inwardly rectifying current, which resembles the inwardly rectifying K^+ current (I_{K1}) described in cultured RPE cells from other species (Strauß *et al*, 1993; Tao *et al*, 1994), was also present (Figure 3.5, panel C). In mammalian RPE (Strauß *et al*, 1993; Tao *et al*, 1994) and other cell types (Cook, 1988) I_{K1} has been shown to be sensitive to blockade by external Ba^{2+} ions. For the cell shown in this figure, I_{K1} was abolished (>90% block) by 1 mM external barium leaving only a leak conductance of 3 $G\Omega$. The current-voltage plot for the control, Ba^{2+} block, and difference currents is shown in figure 3.5, panel D. The Ba^{2+} -sensitive current shows inward rectification at potentials negative to -82 mV, reverses at -78 mV (-73 ± 2 mV, $n=3$), and has a negative slope conductance between its reversal potential and -62 mV.

5. Effect of hydrolysis-resistant GTP analogues in Rat RPE

Cells

5.1 GTP γ S-activated cation current

Whole-cell recordings made after introduction of the non-hydrolyzable GTP analogue, GTP γ S (100 μ M) into the cytoplasm of cultured rat RPE cells, indicated the activation of a large non-inactivating current. Figure 3.6, panel A shows macroscopic currents recorded from a cell 1 minute after assuming the whole-cell configuration with extracellular standard 130 mM NaCl (solution A, table 1 in GENERAL METHODS) and low chloride, K^+ -aspartate solution (solution J, table 1 in GENERAL METHODS) with 100 μ M GTP γ S in the pipette. The asymmetric low chloride solutions were used to

Figure 3.6. GTP γ S activates a cation current in rat RPE cells. (A,B) Patch-clamp recording from a representative cell (whole-cell capacitance of 42 pF) taken 1 minute after assuming the whole-cell configuration. The voltage protocol is shown at the top of the figure. Data were not leak subtracted. The extracellular solution was standard 130 mM NaCl (solution A, table 1) while the intracellular solution was 110 mM K⁻-aspartate (solution I, table 1) with the addition of 100 μ M GTP γ S. Outwardly rectifying potassium current is present in this cell. (B) Same cell as shown in panel A, 15 minutes after assuming the whole-cell configuration. Large inward and outward current is apparent. (C) Current- voltage plot for the traces shown in (A) for 1 (■) and 15 min (○) after break-in. The GTP γ S-difference current (Δ) was calculated by subtracting current at 1 min from those recorded at 15 min. The activation of a cation current reversing at potential positive to E_K is apparent. Current has been normalised for cell capacitance.

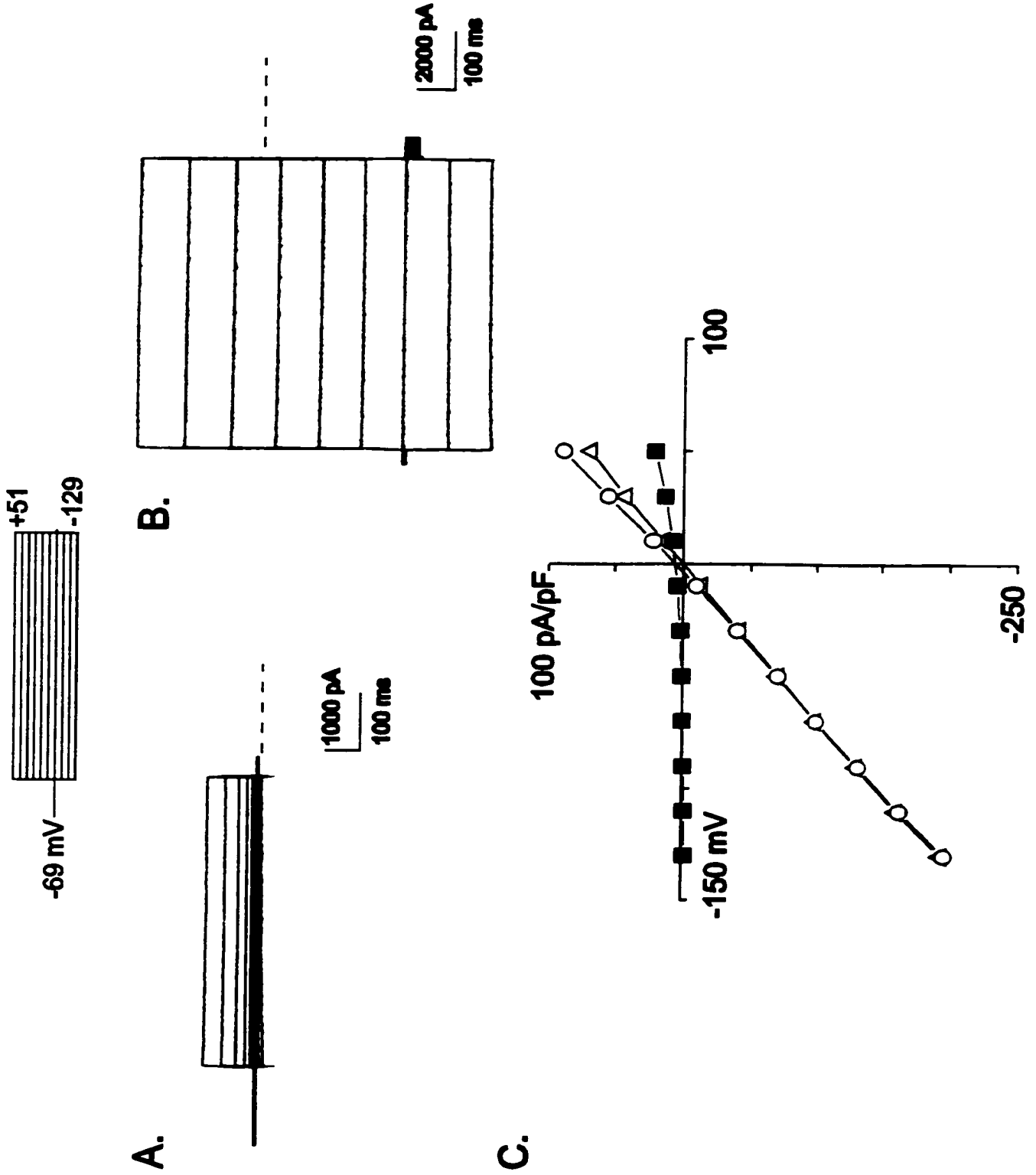


Figure 3.6

differentiate between chloride currents reversing at a potential of -38 mV from cation currents reversing at more positive potentials. Figure 3.6C shows the current-voltage plot for the whole-cell currents shown in panel A and demonstrates that, immediately after break-in, the cell exhibits outwardly rectifying current at potentials depolarized to -40 mV. This current resembles the outward K^+ current that is most predominantly seen in our cultured rat RPE cells under control conditions in the absence of GTP γ S (see Figure 3.3A). Figure 3.6, panel B shows currents recorded from the same cell 15 minutes after break-in with GTP γ S in the pipette. Large non-inactivating currents are apparent at potentials hyperpolarized and depolarized to the holding potential ($V_h = -69$ mV). The current-voltage relationship for the current measured at 15 min post-break-in and the GTP γ S-activated current, obtained by subtracting control current at 1 min after break-in from current at 15 min after break-in, are shown in Fig. 3.6C. The GTP γ S-activated current is linear and reverses at 0 mV, suggesting that GTP γ S activates a cation conductance in rat RPE cells. In 20 other cells the mean reversal potential of the GTP γ S-activated current was 2.9 ± 2 mV.

In RPE cells cultured for 2-5 days, the GTP γ S-activated current occurred in 76 % within a 15-minute period following cytosolic introduction of GTP γ S. In contrast, the GTP γ S-activated current was rarely seen in cells cultured for more extended periods of time (>5-7 days in culture). This suggests that expression and regulation of the channels giving rise to the GTP γ S-activated current may be altered in RPE cells proliferating in culture. Changes in ion channel expression for rat RPE cells in culture has been previously described and suggests that there may be a qualitative change in the electrical properties of RPE cells maintained in culture (Botchkin & Matthews, 1994; Ueda &

Steinberg, 1993). Thus, data shown in subsequent figures represents recordings made only from cells within the first 2-5 days in culture. At this time in culture, the majority of cells have not yet begun to proliferate and remain rounded and heavily pigmented (see Figure 3.1B). In many cases, truncated microvillous processes were still apparent on the apical cell surface.

5.2 Effects of other G protein analogues

Like GTP γ S, another hydrolysis-resistant GTP analogue Gpp(NH)p (100 μ M), also activated a cation current in 7 cells tested. The Gpp(NH)p-activated current had a comparable time-course of activation and was similar in magnitude to the GTP γ S-activated current. To confirm the specificity of the GTP γ S and Gpp(NH)p effects, we also tested the effects of GTP and GDP β S, a hydrolysis-resistant guanine nucleotide that does not activate G proteins. Figure 3.7 shows the time-course for currents recorded in four representative cells using standard extracellular 130 mM NaCl (solution A, table 1 in GENERAL METHODS) and K⁻-aspartate intracellular solution (solution I, table 1 in GENERAL METHODS) containing either GTP, GTP γ S, Gpp(NH)p or GDP β S, respectively. Currents were measured every 20 seconds following 100 ms voltage steps to +51 and -129 mV. Neither GTP nor the inactive GDP analogue, GDP β S, elicited any change in the outward or inward currents. However, GTP γ S and Gpp(NH)p induced similar increases in both outward and inward currents within 5 minutes of break-in. The mean activation time for the GTP γ S- and Gpp(NH)p-activated currents measured in 14 and 7 cells, respectively was 5.7 ± 0.9 and 6.0 ± 1.5 minutes.

Figure 3.7 Time course for the activation of the cation current by GTP γ S and Gpp(NH)p. Current was measured every 20 seconds from $V_h = -69$ mV using 100 ms pulses to +51 and -129 mV. Four separate representative cells are shown for intracellular solutions containing the addition of either 100 μ M GTP γ S, Gpp(NH)p, GTP, or GDP β S to a K⁻ aspartate pipette solution (solution I, table 1). The extracellular solution in all cases was standard 130 mM NaCl (solution A, table 1). The whole-cell capacitances were 24, 30, 38, and 12 pF for GTP γ S-, Gpp(NH)p-, GTP-, and GDP β S-containing cells, respectively. Neither GTP nor the inactive GDP analogue GDP β S elicited any current change, while GTP γ S and Gpp(NH)p activated a cation current.

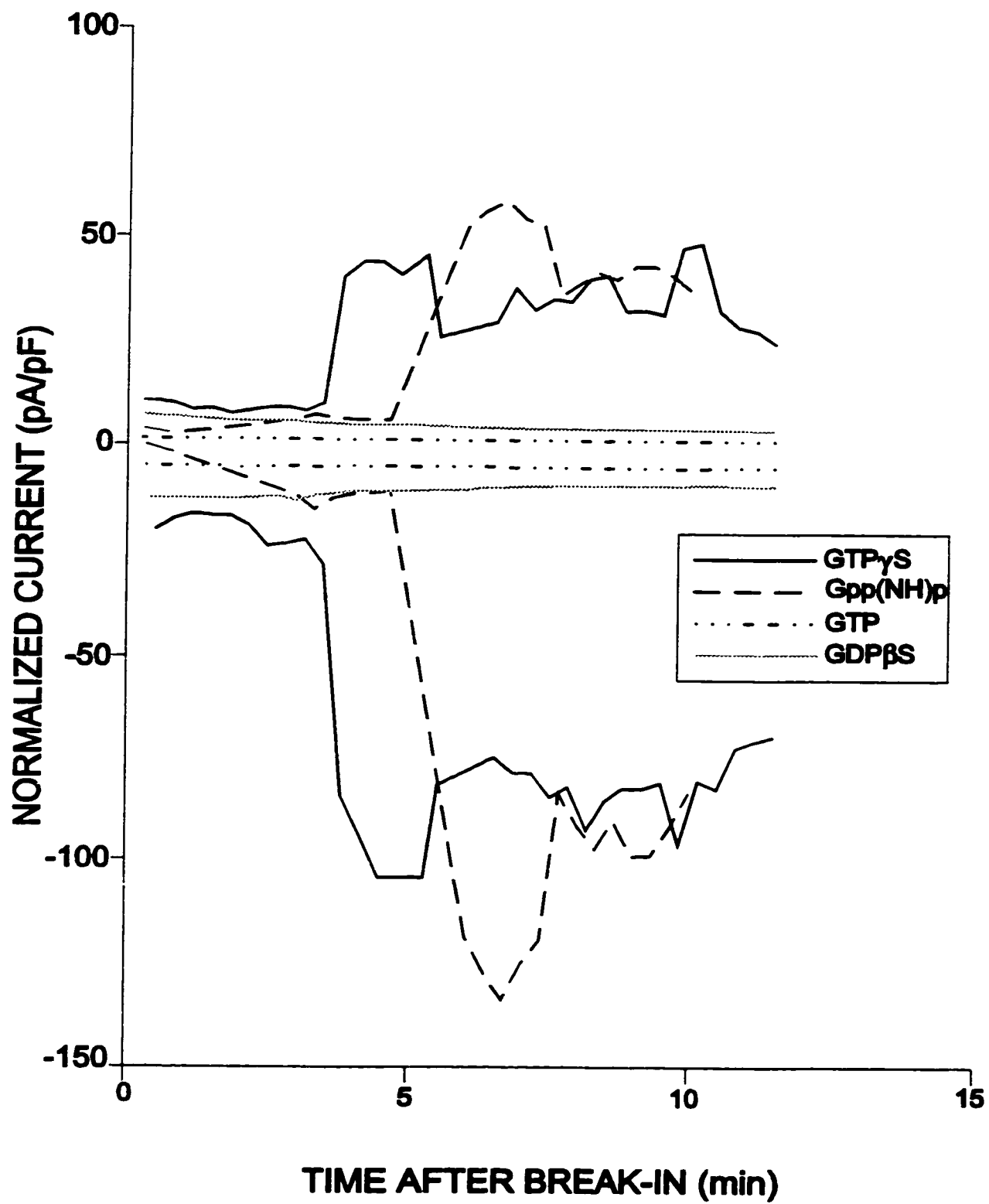


Figure 3.7

Peak current amplitudes measured for GTP γ S- and Gpp(NH)p-activated currents were 156 ± 22 and -313 ± 50 pA/pF ($n = 32$) and 95 ± 20 and -240 ± 43 pA/pF ($n = 7$) for command potentials of +51 and -129 mV. Respectively, these values were significantly greater than those measured for cells dialysed with either GTP or GDP β S. In some cells a small decline was observed in the GTP γ S- and Gpp(NH)p-activated current in the 10-15 minutes following activation, however once activated, the whole-cell current did not return to values measured immediately after break-in. The mean reversal potential of the whole-cell current in rat RPE cells measured 1 and 15 min after break-in was shifted from -38 ± 5 to -3.8 ± 2 mV in 7 cells superfused with Gpp(NH)p suggesting that like, GTP γ S, this non-hydrolyzable analogue also activated a cation current. The mean reversal potential of the whole-cell current was unaffected by intracellular dialysis with GTP or GDP β S.

6. Sensitivity of the cation current to pharmacological blockade

We attempted to determine if inward and outward rectifying K⁺ currents were still present or were suppressed by GTP γ S either prior to or following GTP γ S-activation of the cation current. For the cell shown in Figure 3.8A GTP γ S activated a cation current which reversed at -2 mV. Subsequent application of 5 mM extracellular Ba²⁺ produced a small reduction in both inward and outward current. The Ba²⁺-difference current, obtained by subtracting the whole-cell current obtained in the presence of Ba²⁺ from the current prior to Ba²⁺ exposure, revealed an inwardly rectifying K⁺ current and a small

Figure 3.8. GTP γ S may enhance an inwardly rectifying K $^+$ current. Current-voltage plot (A) for the GTP γ S-activated cation current in a representative RPE cell measured at 15 min after break-in (●) and after 10 min superfusion with 5 mM Ba $^{2+}$ (▲). The extracellular solution was low Cl $^-$ (solution F, table 1) while the intracellular solution was 110 mM K $^+$ -aspartate (solution I, table 1). The Ba $^{2+}$ difference current (□) revealed a small outward K $^+$ current and an inwardly rectifying K $^+$ current that was increased 65% over initial values recorded immediately after attaining the whole cell configuration. (B) Quinine, amiloride and gadolinium do not block the GTP γ S-activated cation current. GTP γ S-activated current (mean \pm S.E.M.) measured at -129 mV and +51 mV before and after 15 minutes of superfusion with 0.5 mM quinine (a), 0.1 mM amiloride (b) or 0.1 mM gadolinium (c).

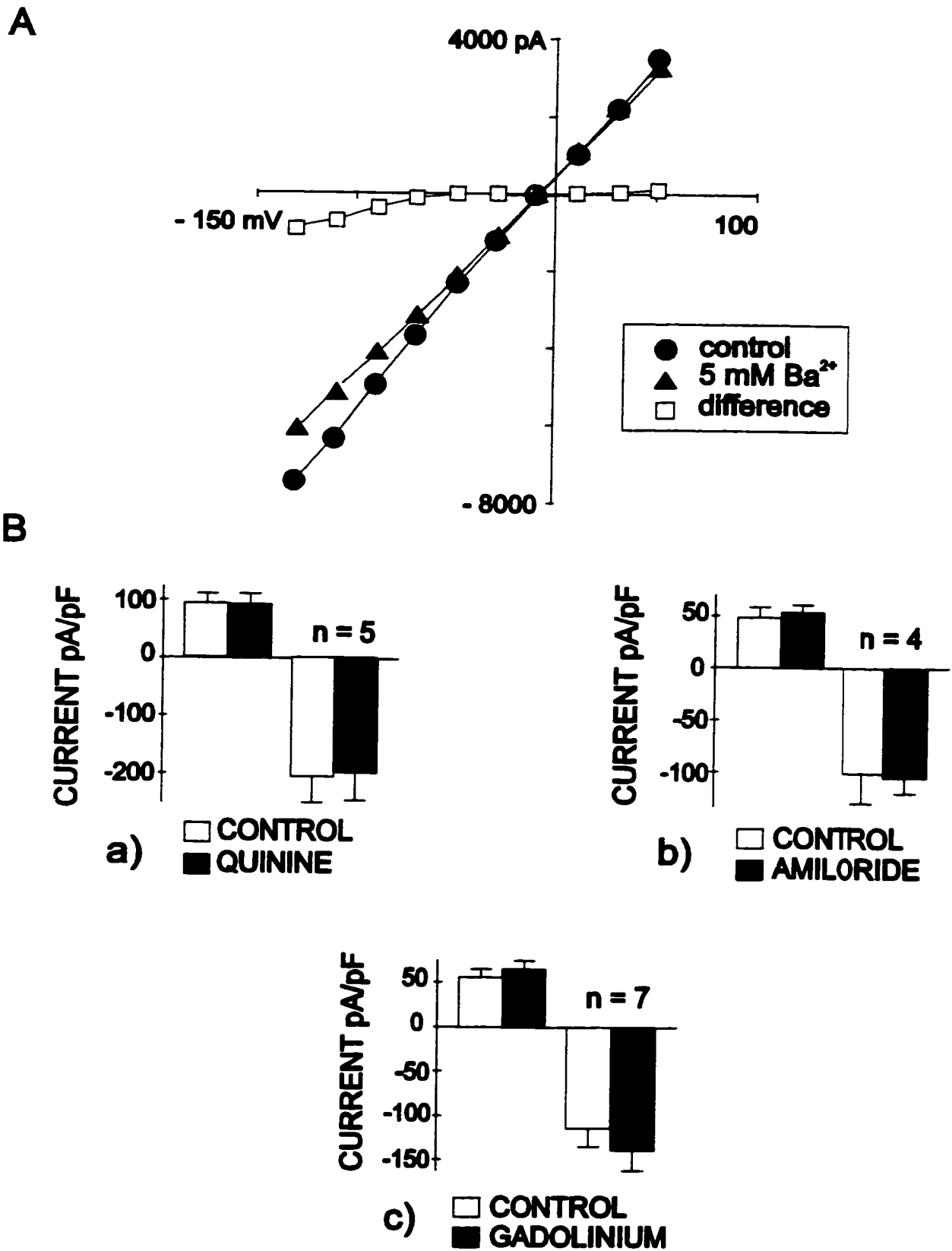


Figure 3.8

outward K^+ current. The inward K^+ current was increased by 65% over values recorded immediately after attaining the whole cell configuration. This suggests that K^+ currents were still present following GTP γ S dialysis and that GTP γ S may enhance inwardly rectifying K^+ current in rat RPE cells.

Other agents tested included; the K^+ channel blocker quinine (0.5 mM), which has also been reported to inhibit NSC currents in some cell types (Gogelein & Pfannmuller, 1989); the epithelial Na^+ channel blocker, amiloride (100 μ M) which in addition to a variety of effects on ion channels and exchangers also blocks NSC channels; and the inorganic ion, gadolinium (100 μ M) which is purported to be one of the most effective blockers of NSC channels available (Heschler & Schultz, 1993). None of these compounds was effective in significantly reducing the GTP γ S-activated cation current measured at +51 mV and -129 mV in 4-7 cells tested (see Fig. 3.8B). However, quinine slightly reduced currents measured at 0 mV ($13 \pm 5\%$, $n=5$), a potential at which outward K^+ currents would be apparent but little cation current would be present.

We also explored the possibility that activation of the cation current may be mediated via opening of gap junction hemichannels in isolated RPE cells. *In vivo*, hemichannels (connexons) on adjacent RPE cells are organised to form intercellular channels between neighbouring RPE cells which are known as gap junctions. Gap junctions allow RPE cells to be coupled both electrically and metabolically via the diffusion of small hydrophilic molecules (cGMP, cAMP) and inorganic ions (Na^+ , K^+ & Ca^{2+}) intercellularly. Under physiological conditions gap junction communication in a variety of cell types has been shown to modulated via second messenger-mediated

phosphorylation of connexons (Loewenstein, 1985; Mikalsen *et al*, 1995). Recently, it has been proposed that inhibition of gap junction permeability in cultured rat RPE monolayers may involve PKC activity (Stalmens & Himpens, 1997b). It is not known however, if putative hemichannels (connexons), connecting the cytoplasm and the extracellular space in isolated RPE cells *in vitro*, are able to open under certain conditions in response to extracellular and/or intracellular signaling molecules. To test the hypothesis that the NSC current may be mediated by flow through hemi-gap junctions we first activated the current with GTP γ S and then superfused the cell for a further 15 min with 0.5 mM octanol. Octanol and other long-chain aliphatic alcohols have been demonstrated to uncouple gap junctions in a variety of cell types (Deleze & Herve, 1983; Pott & Mechmann, 1990), including RPE (Stalmens & Himpens, 1997a). The amplitude of the GTP γ S -activated cation current measured at +51 and -129 mV in 4 cells 15 min post-break-in (94 ± 27 and -220 ± 42 pA/pF) was not significantly affected by external superfusion of the cells with octanol for 15 min (68 ± 10 and -186 ± 30 pA/pF). The small decline in current amplitude after 15 min superfusion with octanol was probably representative of the normal amplitude decrease that is observed for this current following long periods of activation (see section 5.2). The inability of octanol to significantly affect the NSC current suggests that nonselective ion flow through putative hemi-gap junctions in isolated RPE cells does not underlie the current activated by GTP γ S.

7. Ion Selectivity of the GTP γ S-activated Cation Current

7.1 Non-specificity of the cation current

To investigate the ionic selectivity of the GTP γ S-activated current for monovalent cations, we used intracellular and extracellular solutions designed to minimise Cl⁻ conductance and obliterate K⁻ currents. Figure 3.9, panel A shows currents recorded in a cell with Cs⁻-aspartate intracellular solution (solution K, table 1 in GENERAL METHODS) plus 100 μ M GTP γ S and Na⁻- aspartate bathing solution (solution F, table 1 in GENERAL METHODS). Under these recording conditions, initially very little whole-cell current is apparent (Fig. 3.9, panel A). Current recordings made at 15 minutes after break-in (Fig. 3.9, panel B), however show that cytosolic superfusion of the cell with GTP γ S, as before, activates a large non-inactivating conductance. Figure 3.9, panel C shows the I-V relationship for the currents shown in panels A and B and the GTP γ S-difference current obtained from digitally subtracting currents in A from B. The linear I-V characteristics and positive reversal potential of this current ($+5.7 \pm 1.4$ mV, $n = 18$), under conditions where contributions from K⁻ currents and chloride currents are reduced, identifies the GTP γ S-activated current as a non-specific cation (NSC) current.

7.2 Anion permeability

Further confirmation that the GTP γ S-activated current was not permeable to anion, was obtained by examining the amplitude and reversal potential for the induced current under experimental conditions where [Cl⁻]_{out} (solutions A and F, table 1 in GENERAL METHODS) or [Cl⁻]_{in} (solutions J and L in GENERAL METHODS)

Figure 3.9. The GTP γ S-activated current is a NSC current. Whole-cell from a representative RPE cell recorded 1 (A) and 15 (B) min after break-in with low chloride, K⁻-free cesium aspartate intracellular solution containing 100 μ M GTP γ S (solution K, table 1). The extracellular solution was Na⁻ aspartate Ringers (solutions F, table 1). The whole-cell capacitance was 33 pF. Data were not leak subtracted. (C) Current-voltage plot for whole-cell currents in A (■) and the GTP γ S -difference current (□). The current activated by GTP γ S is a NSC current since it was still activated in K⁻-free and low Cl⁻ conditions and reverses close to 0 mV.

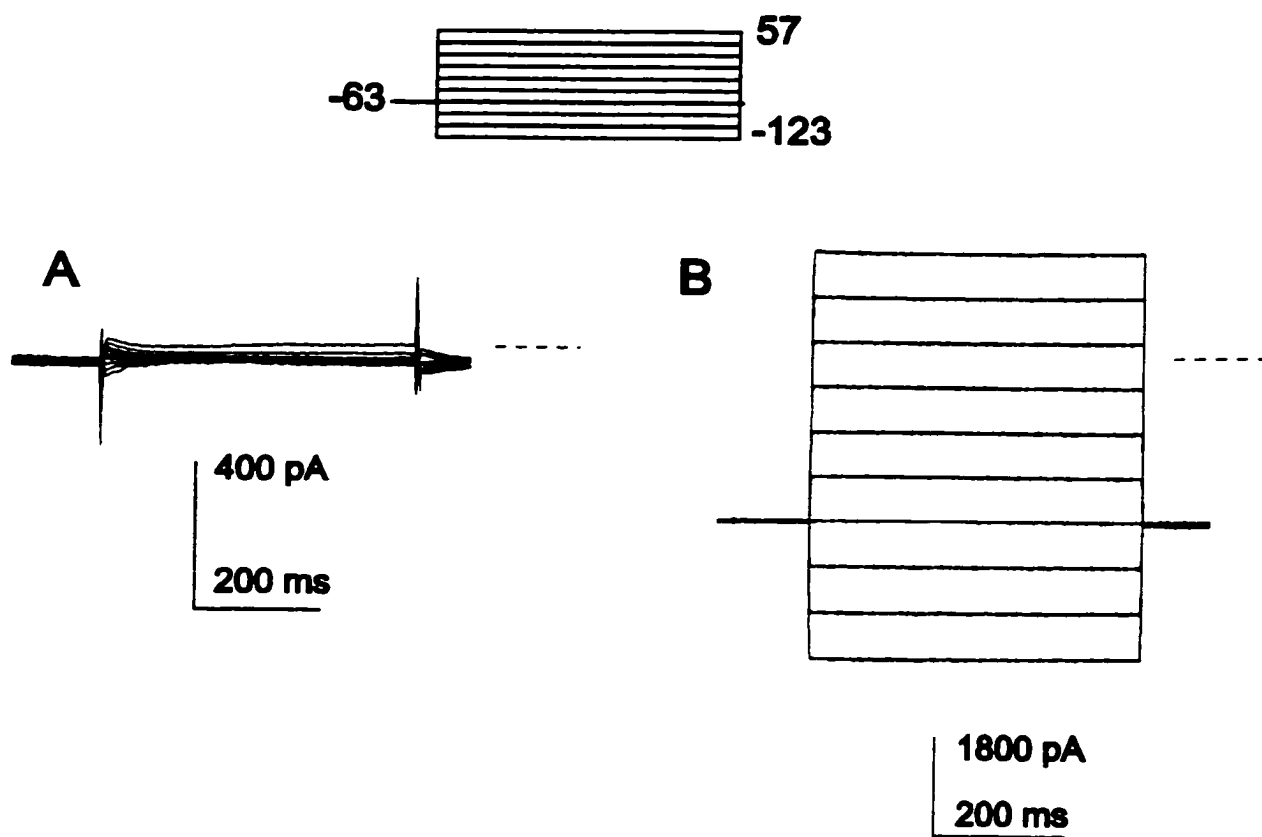


Figure 3.9

was varied. Reduction of extracellular $[Cl^-]$ from 140 mM to 40 mM did not significantly affect the amplitude of the GTP γ S-induced current measured at +51 mV (75 ± 2 pA/pF in 140 mM $[Cl^-]_{out}$ and 77 ± 4 pA/pF in 40 mM $[Cl^-]_{out}$) in 7 cells tested (Fig. 3.10, panel A). Figure 3.10, panel B, shows the measured reversal potential of the GTP γ S-activated current plotted against the theoretical E_{Cl} . The least-squares best fit of the data (continuous line) has a slope of 0.007. Also plotted (dashed line) is the relationship for a Cl^- -selective current with a slope of 1. Thus, the GTP γ S-activated conductance appears relatively impermeable to Cl^- ions, since neither the amplitude nor the reversal potential of the current is significantly affected by alterations in the Cl^- concentration gradient.

7.3 Cation selectivity of the GTP γ S-activated current

We then investigated the cation selectivity of the GTP γ S-activated cation current by substituting Na^+ in the extracellular solution with other monovalent cations. Figure 3.11 panel A shows current-voltage plots for currents recorded in a representative cell in 130 mM NaCl extracellular solution (solution A, table 1 in GENERAL METHODS) with 100 mM Cs^+ -aspartate solution in the pipette (solution K, table 1 in GENERAL METHODS). Substitution of extracellular Na^+ with TRIS, or NMDG (solutions B-E, table 1 in GENERAL METHODS) shifted the reversal potential of the NSC current to more negative potentials and reduced the current amplitude measured at -40 mV ($E_{Cl} = -38$ mV for the solutions used) from -411 pA/pF to -162 pA/pF and -60 pA/pF for TRIS solutions and NMDG solutions, respectively. Figure 3.11 panel B is a bar graph summarising the mean reversal potentials measured from 4-11 cells in the different

Figure 3.10. The GTP γ S-activated cation current is anion impermeable. (A) The amplitude of the cation current was measured at +51 mV in 7 cells with standard intracellular recording solution (solution H, table 1) and in extracellular solution in which $[Cl^-]_{out}$ was altered by substitution with aspartate (solutions A and F, table 1). The current amplitude was not affected by reduction in the external $[Cl^-]$ from 140 mM to 40 mM. (B) The reversal potential of the GTP γ S-activated current was measured in 23 cells in which $[Cl^-]_{in}$ or $[Cl^-]_{out}$ was altered by substitution with aspartate (solutions A,F,J, table 1) and plotted against the theoretical E_{Cl} . The least-squares fit of the data (continuous line) had a slope of 0.007 corresponding to a 4.8 mV per 10-fold change of $[Cl^-]_{in}/[Cl^-]_{out}$. The dashed line has a slope of 1, predicted for a Cl^- -selective current.

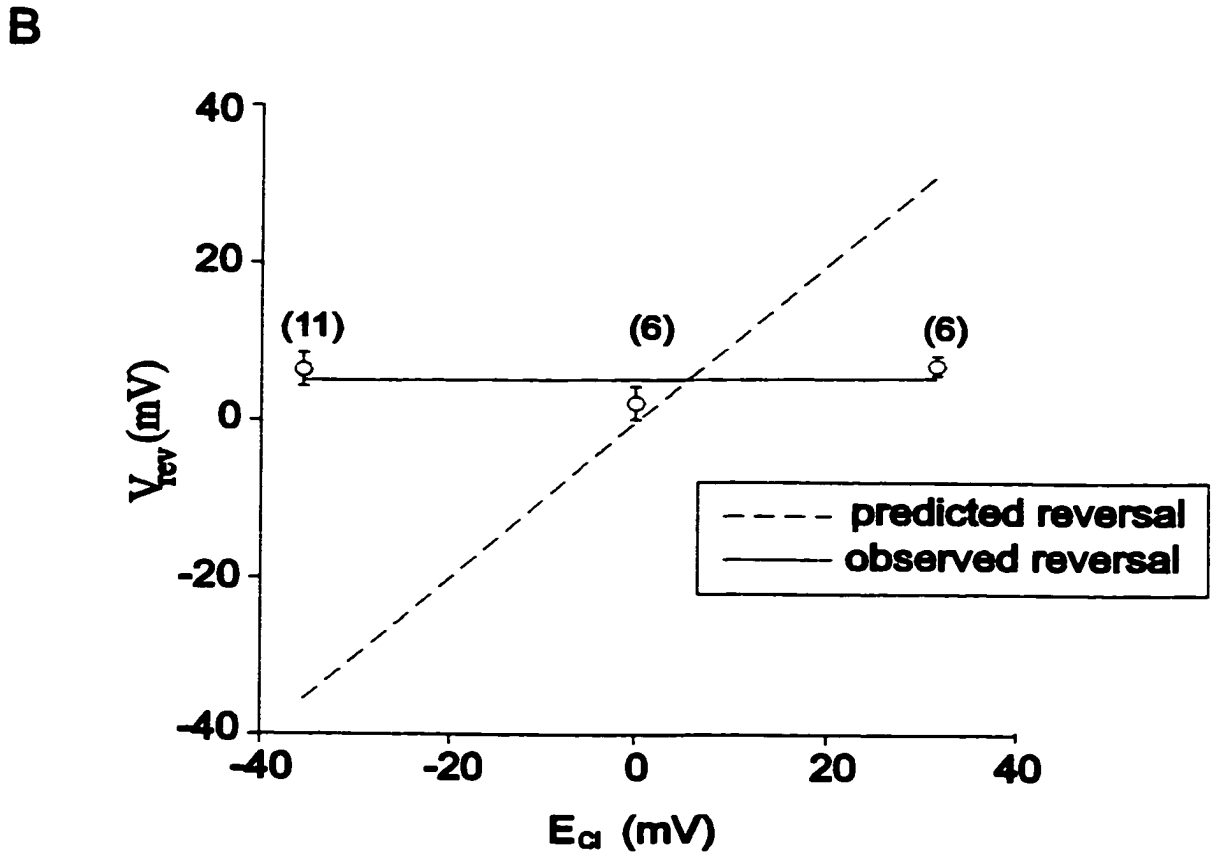
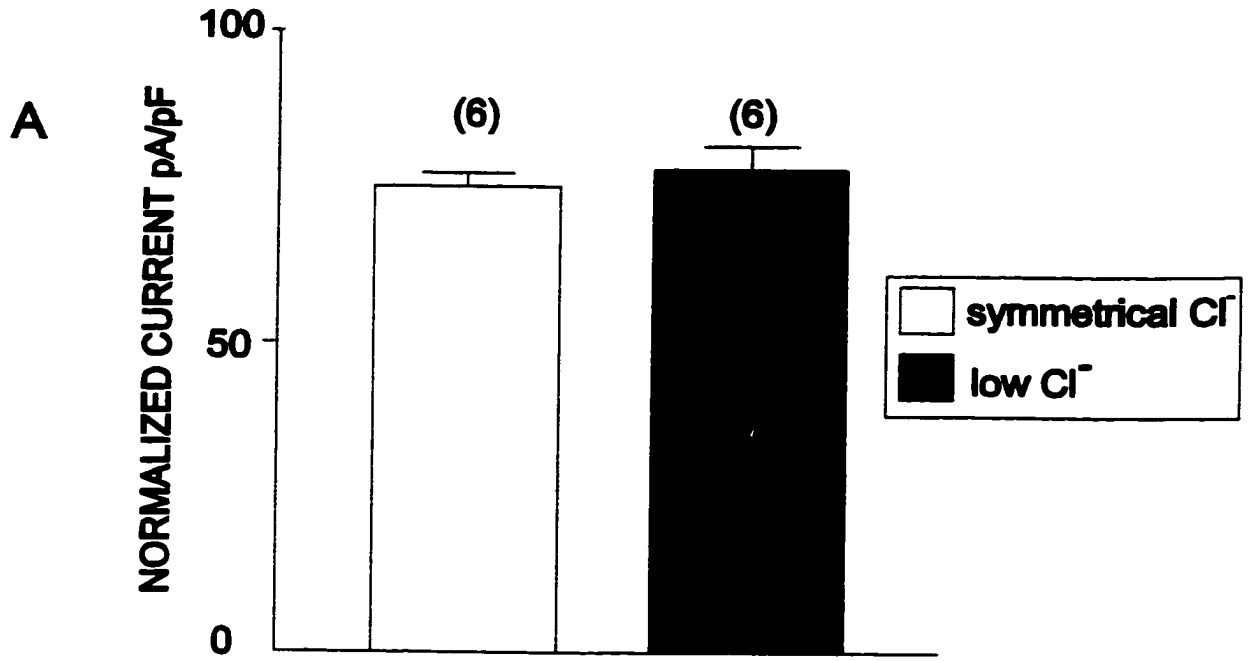


Figure 3.10

Figure 3.11. Cation selectivity of the GTP γ S-activated current. (A) Representative current-voltage curves for a rat RPE cell showing the effect of replacement of Na⁺ in the extracellular solution by several monovalent cations on the GTP γ S-activated current. The voltage protocol for the 150 mM Na⁺ trace is the same as that shown in Figure 3.6 while the protocol for the remaining traces is shown at the top of the panel. Data were not leak subtracted. The recording electrode contained solution J (table 1) with GTP γ S substituted for GTP. Current magnitude and reversal potential were altered by substitution of all but 10 mM of 150 mM extracellular Na⁺ (solution A, table 1) with either choline, TRIS, or NMDG (solutions B-D, table 1, respectively). (B) Mean \pm SEM reversal potential measured for (n) cells in the above solutions containing intracellular GTP γ S.

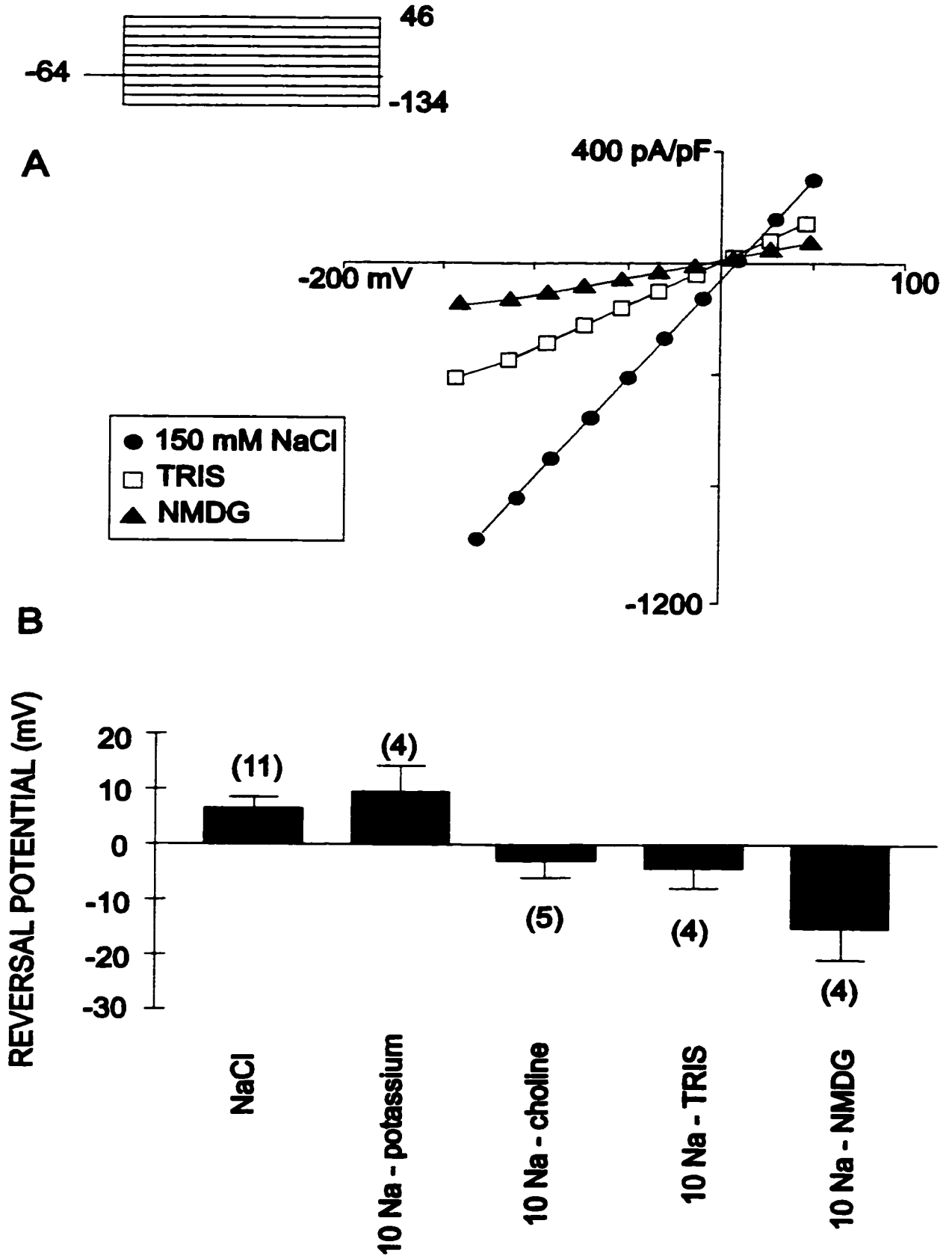


Figure 3.11

cation-substituted extracellular solutions. Permeability ratios (relative to Na^+ and shown in parenthesis) for K^+ (1.07), choline (0.51), TRIS (0.42) and NMDG (0.34) were calculated using equation (2) (see METHODS). Thus, the permeability sequence for the rat RPE NSC channel is $\text{K}^+ = \text{Na}^+ \gg \text{choline} > \text{TRIS} > \text{NMDG}$.

7.4 Effects of extracellular Ca^{2+}

Nonselective cation channels described in other cell types have been found to fall into two groups with respect to their Ca^{2+} permeability: those which are impermeable to Ca^{2+} (Rea & Levis, 1984; Lipton, 1986) and those with varying degrees of Ca^{2+} permeability (Petersen & Maruyama, 1983; von Tscharner *et al*, 1986). Permeability of the NSC channel in rat RPE cells to divalent cations was not investigated, however, reduction of extracellular Ca^{2+} concentration from 1 mM to < 10 nM (solution G, table 1 in GENERAL METHODS) did not significantly alter the amplitude of the GTP γ S-activated current nor the mean reversal potential. These results indicate that extracellular Ca^{2+} is not required for activation of the GTP γ S-activated NSC current.

8. Role of $[\text{Ca}^{2+}]_i$ and PTX-Sensitive G Proteins in NSC

Current Activation

8.1 Involvement of intracellular Ca^{2+} and ATP in NSC current activation

Many NSC channels are sensitive to activation by second messengers such as cytosolic Ca^{2+} . In a variety of cell types, including other epithelia (Gogelein & Greger, 1986), NSC channels have been described whose activation is dependent upon elevations

in intracellular Ca^{2+} (Partridge & Swandulla, 1988). We tested the involvement of $[\text{Ca}^{2+}]_i$ in the activation of the NSC current in rat RPE cells by dialysing cells with GTP γ S in 10 mM BAPTA pipette solution (solution M, Table 1 in GENERAL METHODS, free $\text{Ca}^{2+} < 10$ nM) and nominally Ca^{2+} -free (solution G, table 1 in GENERAL METHODS) bath solution. Under these conditions, GTP γ S still activated the NSC current in 57 % of the cells (4/7) examined. The GTP γ S-activated difference current recorded in low Ca^{2+} conditions had a mean current amplitude of -113 ± 40 pA/pF at -129 mV and 40 ± 15 pA/pF at $+51$ mV ($n=4$), which was significantly ($p < 0.05$) reduced compared to the GTP γ S-activated difference current recorded at -129 mV (-278 ± 29 pA/pF) and $+51$ mV (113 ± 11 pA/pF) in 29 cells with standard pipette solution ($[\text{Ca}^{2+}]_{in} \approx 10^{-7}$ M). Figure 3.12A shows the I-V plot for the mean GTP γ S-activated difference current in standard and low Ca^{2+} /BAPTA intracellular recording solution. The current amplitude of NSC current was reduced at all potentials when the $[\text{Ca}^{2+}]_i$ was reduced to less than 10 nM. The reversal potential of the NSC current activated in low $[\text{Ca}^{2+}]_i$ (7 ± 2 mV) however, was not significantly different from the NSC current activated under control conditions (2 ± 1.4 mV). Thus, while it did not appear that an increase in $[\text{Ca}^{2+}]_{in}$ was required for activation of the NSC current by GTP γ S, the significant decrease in current amplitude under low Ca^{2+} conditions suggests that intracellular Ca^{2+} may play some regulatory role in modulating current activity.

Since some NSC channels are sensitive to the modulatory effects of internal ATP (Rae et al., 1990), we also investigated whether exclusion of ATP (10^{-4} M) from the pipette solution affected the magnitude of the NSC conductance in rat RPE cells. In the 3

Figure 3.12. Involvement of $[Ca^{2+}]_i$ in NSC current activation. (A) Mean current was unaffected by decreased $[Ca^{2+}]_i$, but the current amplitude was significantly decreased. Current-voltage plot for the GTP γ S -difference current (\pm S.E.M) was recorded in standard extracellular 130 mM NaCl solution (solution A, table 1) and intracellular 110 mM K⁻-aspartate solution (solution J, table 1) (\circ ; n=29) or in nominally Ca²⁺- free extracellular (solution G, table 1) and intracellular solution (solution M, table 1) (\blacktriangle ; n=4). All currents have been normalized for cell capacitance. V_{rev} of the NSC current was unaffected by decreased $[Ca^{2+}]_i$, but the current amplitude was significantly decreased.

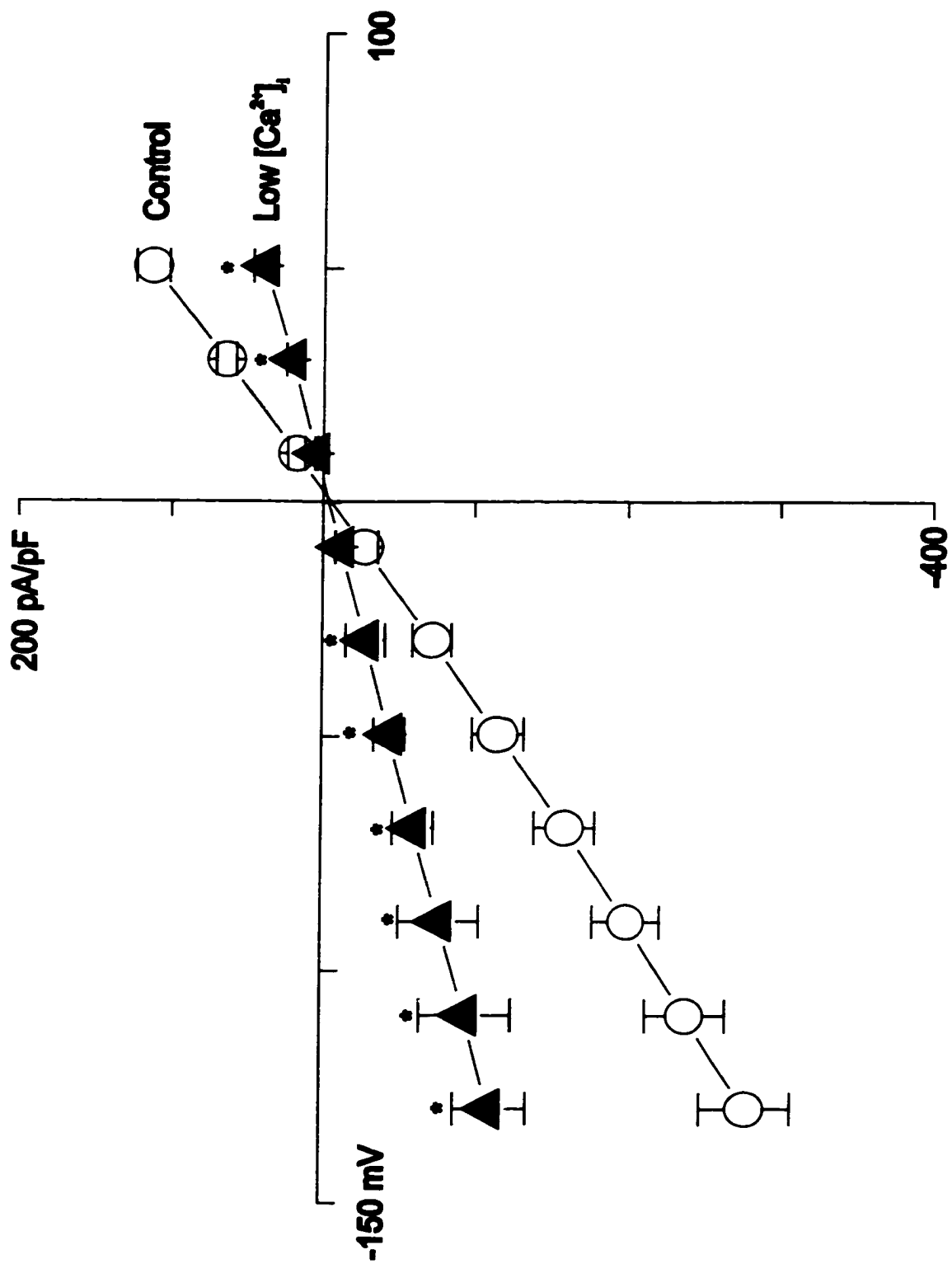


Figure 3.12

cells tested the GTP γ S-activated NSC conductance was not significantly affected by exclusion of ATP from the pipette solution.

8.2 Activation of the NSC current by fluoroaluminate

Fluoroaluminate (AlF_4^-), as with the nonhydrolyzable GTP analogues, has proved to be a useful tool for the activation of heterotrimeric G proteins as opposed to the low molecular weight GTP binding proteins (Kahn, 1991). To confirm the type of G protein involved in GTP γ S and Gpp(NH)p-mediated activation of the NSC current we dialysed RPE cells with AlF_4^- . In 20 cells tested, inclusion of NaF (1 mM) and AlCl_3 (25 μM) in either Cs^- -aspartate (solution K, table 1 in GENERAL METHODS) or K^- -aspartate pipette solution (solution J, table 1 in GENERAL METHODS) containing Mg^{2+} , failed to activate a sustained cation current. However, increasing the concentration of NaF to 10 mM and AlCl_3 to 100 μM , resulted in activation of a large conductance in 5 cells tested. Even at the higher concentration however, AlF_4^- did not appear as effective as GTP γ S, as the NSC current was activated in only 33% (5/15) of the cells dialysed with AlF_4^- . The AlF_4^- -activated current, shown in Figure 3.13 panel A, had properties similar to the GTP γ S-activated cation current, although the activation of this current was somewhat delayed (10.8 ± 1.4 min; $n=5$) with respect to that seen with GTP γ S in the pipette (5.7 ± 0.9 min; see Figure 2.7). This delay in activation may reflect the time required to form an adequate concentration of the active AlF_4^- complex from its inactive components (NaF and AlCl_3). Figure 3.13 panel B shows that the AlF_4^- -activated current had a linear I-V relationship and the current reversed close to 0 mV (-1.1 ± 0.4 mV; $n=5$). The mean

Figure 3.13 Fluoroaluminate activates the NSC current. (A) Whole-cell current recorded in a rat RPE cell with K^+ aspartate pipette solution (solution J, table 1) and 130 mM NaCl bathing solution (solution A, table 1). Dialysis of the cell interior with 10 mM NaF and 100 μ M $AlCl_3$ activated both inward and outward current at 9 min after breaking into the whole-cell recording configuration. (B) I-V relationships for the fluoroaluminate-difference current obtained immediately after turn-on (\circ), and 10 min later (\blacktriangle) for the cell shown in panel A. Fluoroaluminate activates a large current 10 min after break-in that reverses at 0 mV and has similar I-V characteristics to the $GTP\gamma S$ -activated NSC current (\circ). The amplitude of NSC current activated by fluoroaluminate declined over a 10 min period following its activation (\blacktriangle). The capacitance of the cell shown is 22 pF.

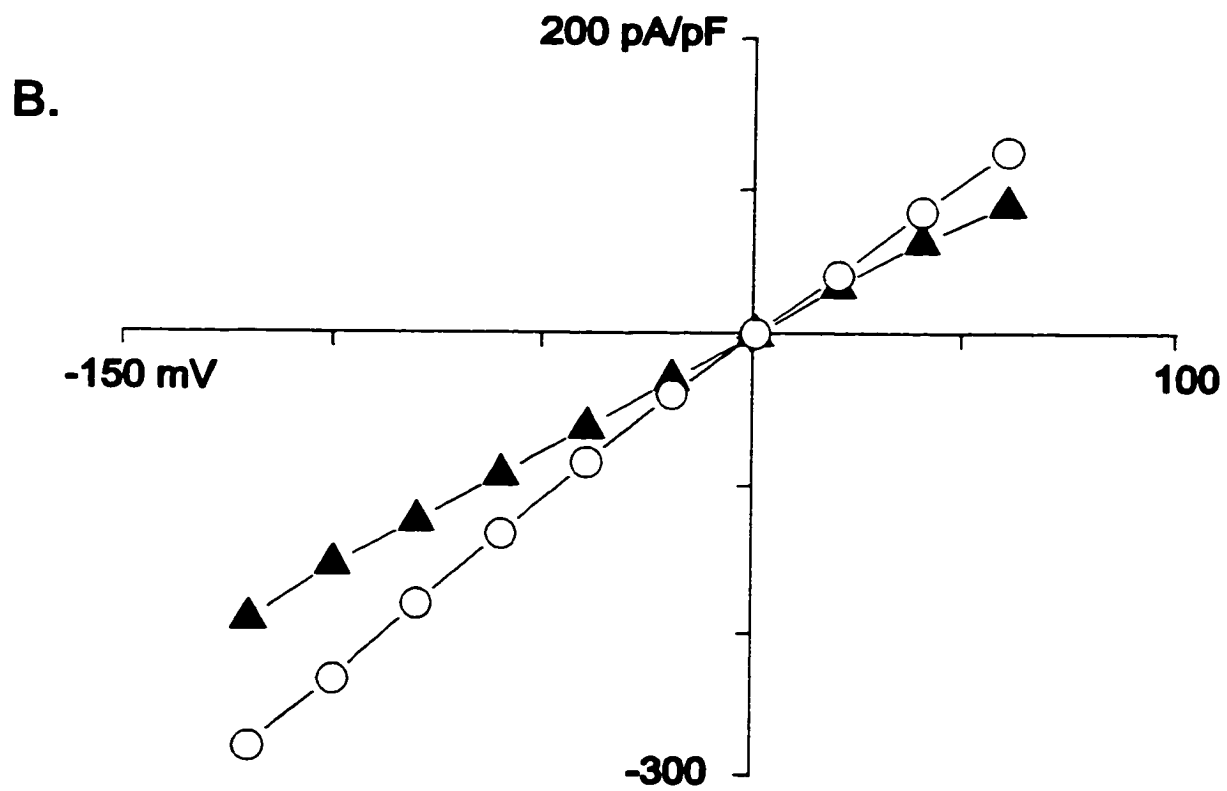
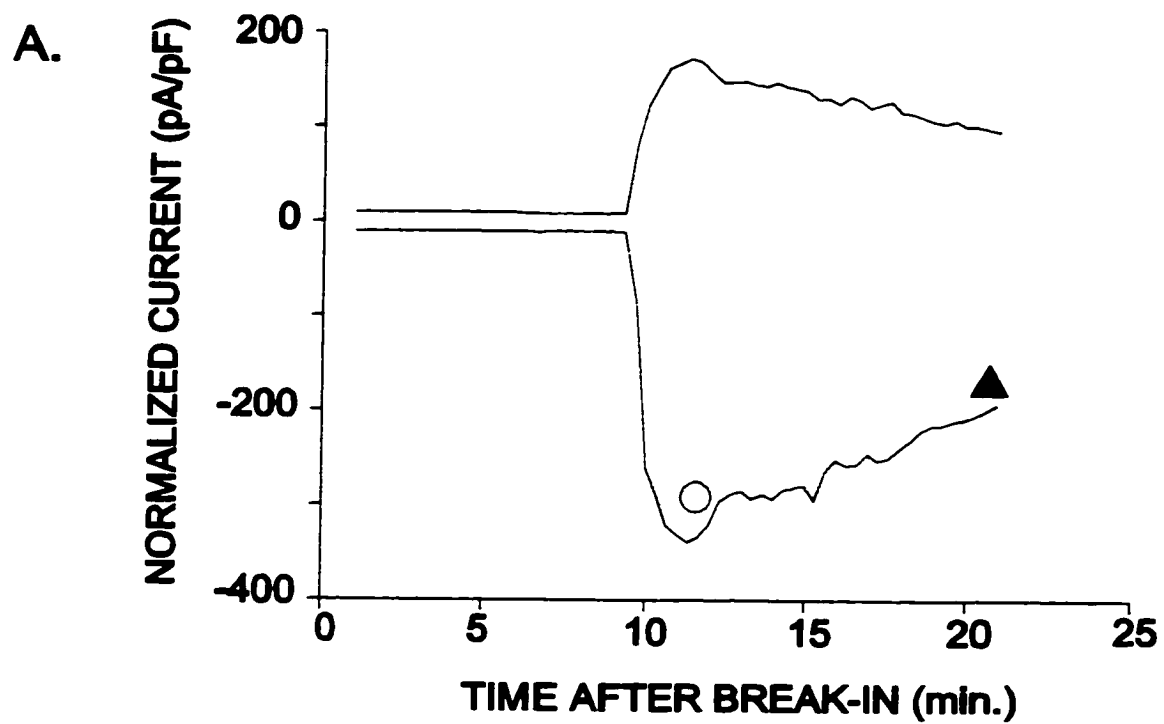


Figure 3.13

current amplitude of the AlF_4^- -activated current, measured 15 min after break-in at +51 (60 ± 13) and -129 mV (-133 ± 37), was slightly reduced and tended to decline much more rapidly in the 10-15 min following activation, as compared to the $\text{GTP}\gamma\text{S}$ -activated cation current. In one cell, activation of the NSC current by AlF_4^- was completely reversed within 15 min. These observations may reflect the rapid, reversible nature by which AlF_4^- activates G proteins, as compared with the essentially irreversible effects of $\text{GTP}\gamma\text{S}$ (Higashijima *et al.*, 1987 & 1991; Kahn, 1991).

These data do indicate however, that in the presence of an adequate concentration of NaF, AlF_4^- mimics the effects of $\text{GTP}\gamma\text{S}$ in activating the NSC current in rat RPE cells. This finding is consistent with previous findings demonstrating activation of G_α subunits by AlF_4^- (for review see Rodbell, 1992, also Higashijima *et al.*, 1991), and further implicates the involvement of heterotrimeric G proteins in the regulation of the NSC current.

8.3 Sensitivity of the $\text{GTP}\gamma\text{S}$ -activated NSC current to PTX

Different G proteins can be distinguished by their susceptibility or insensitivity to pertussis toxin (PTX) inactivation. The toxin inactivates G proteins by catalyzing the ADP-ribosylation of the α subunit of G proteins (Ui, 1990). Members of the \bar{G}_i / G_o family are sensitive to PTX, whilst members of the G_s and G_q family are insensitive to PTX modification. We investigated whether activation of the NSC current in RPE cells was mediated via a PTX-sensitive or PTX-insensitive G protein by incubating cells with PTX (500 ng/ml) for 24 hours before recording. In all PTX-treated cells tested ($n=6$),

Figure 3.14. PTX blocks the activation of the GTP γ S current. Mean (\pm SEM) current amplitude measured at +51 mV and -129 mV (n=6) in cells pre-treated for 24 hrs with 500 ng/ml of PTX indicates that GTP γ S failed to activate the NCS current. In control cells without PTX treatment GTP γ S activated an NSC current with a comparable amplitude at +51 mV and -129 mV to the currents previously recorded in other cells (n=14). The mean (\pm SEM) for all control cells were compiled (n=16).

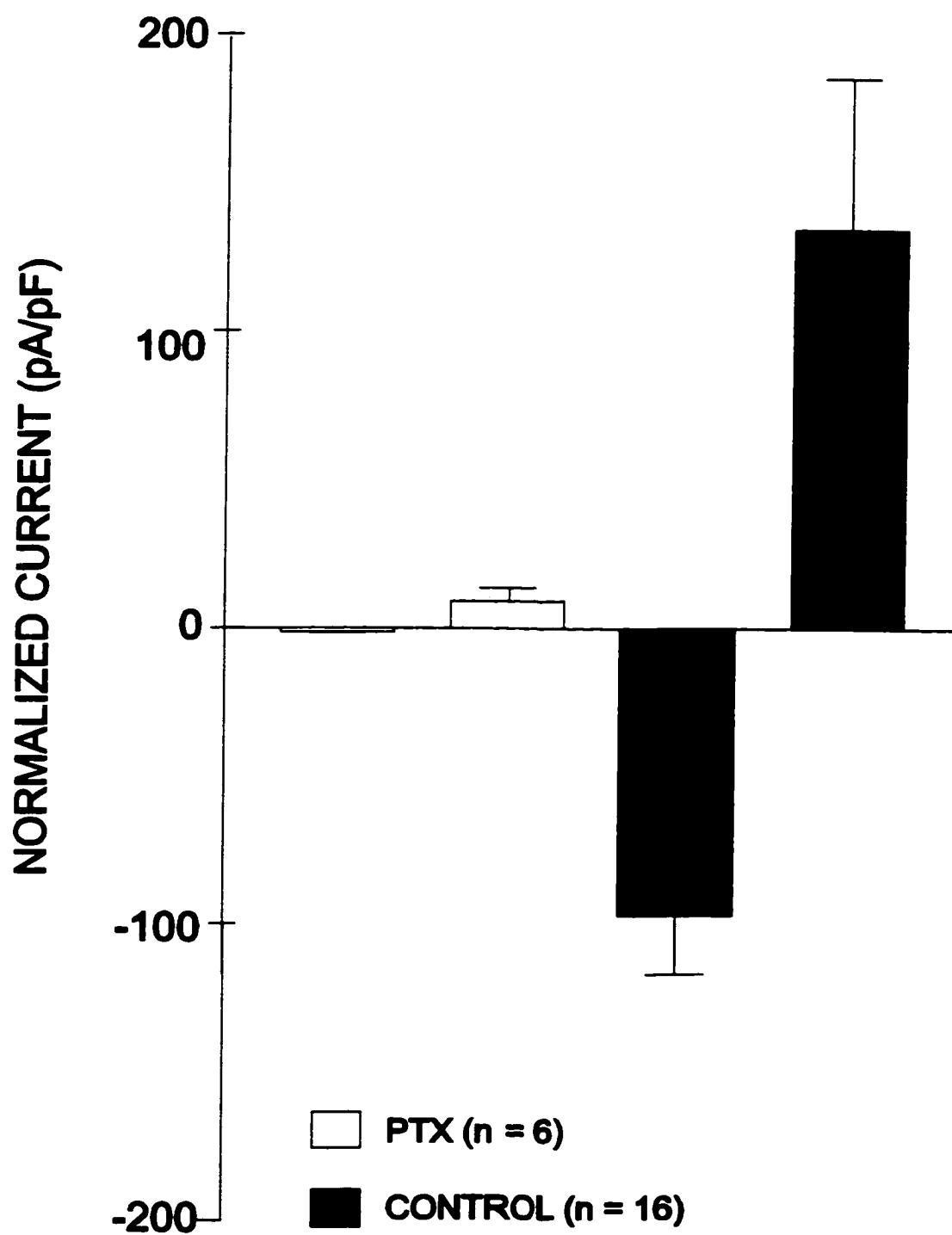


Figure 3.14

GTP γ S failed to activate the NSC current (Fig.3.14), suggesting that the G protein involved in the activation of the NSC current is of the G_i /G_o class. In another 2 cells tested from the same culture, but without PTX-pre-treatment, GTP γ S-activated the NSC current and the activated current had comparable amplitudes (-282 and -296 pA/pF at -129 mV and 122 and 158 pA/pF at +51 mV) to the current recorded previously in other cells (see above section 5.2).

9. Investigation of the PTX-sensitive G α subunit involved in NSC current activation

9.1 Morphology of scrape loaded RPE cells

As previously reported (see Figure 3.6), the introduction of the non-hydrolyzable GTP analogue GTP γ S (0.1 mM) into the cytoplasm of cultured rat RPE cells activates a NSC current. In this study, in order to investigate the PTX-sensitive G protein involved in NSC current activation, cultured RPE cells were scrape loaded with antibodies to G protein α subunits. This scrape loading technique required that the RPE cells be harvested from the coverslips using trypsin and then replated for culture in the presence of α subunit antisera.

Replated RPE cells, scrape loaded with G protein antisera, attached readily to coverslips within 2-4 hrs of trypsinization and mechanical dissociation and within 12 hrs. resume their normal morphology. Most of the replated cells remained rounded and retained their pigmentation (see Figure 3.15A). Long-term viability in culture was unaffected by scrape loading RPE cells, and if left for >12 days the cells formed a confluent monolayer, like those described for control cells (see section 1). Scrape loaded

RPE cells also exhibited whole-cell currents similar to those observed in non-replated cells (see below section 9.3). No difference was noted between the plating efficiency, morphology or electrophysiological characteristics of RPE cells scrapeloaded with antibodies compared with control cells replated in the absence of antisera.

9.2 Immunofluorescence of scape loaded G_{α} subunits

Immunofluorescent detection confirmed that all cells replated with G_{α} antisera that had reattached to the coverslips appeared to contain antibody, indicative of a loading efficiency approaching 100%. Similar loading efficiency has been reported for other cultured mammalian cells scrape loaded with antibodies (McNeil *et al*, 1984; Ortiz *et al*, 1987). Figures 3.15C and D show the phase and fluorescent images for representative rat RPE cells in culture 18 hrs after being scrape loaded with 10 $\mu\text{g/ml}$ of anti- $G_{\alpha i/\alpha U/z}$, the antibody directed against all PTX-sensitive G protein α subunits. Cells were double labelled for the G protein antibodies and a nuclear Hoescht stain. Cells were uniformly fluorescent throughout the cytoplasm of the RPE cells, but labeling tended to be excluded from the nucleus. No staining above background levels was observed in control RPE cells that were replated in the absence of antisera (Figure 3.15 B). Control cells did however, stain for the nuclear Hoescht stain indicative of the specificity of the G protein labelling. Similarly, other cells scrape loaded with anti-GFAP or non-replated controls also did not fluoresce above background (data not shown).

Figure 3.15. Immunofluorescent detection of scrape loaded G_{α} subunits. (A) Phase-photomicrograph of RPE cells 18 hrs after being replated in the absence of antisera (replated control). (B) Fluorescent image of cells shown in panel A. The nuclei of the cells are brightly stained with Hoescht reagent. No staining was observed for G protein antisera. (C) Phase-photomicrograph of RPE cells 18 hrs. after being scrape-loaded with anti- $G_{\alpha i/o/vz}$. (D) Fluorescent image of cells shown in panel C doubled labelled for G protein α subunits and nuclear Hoescht stain.

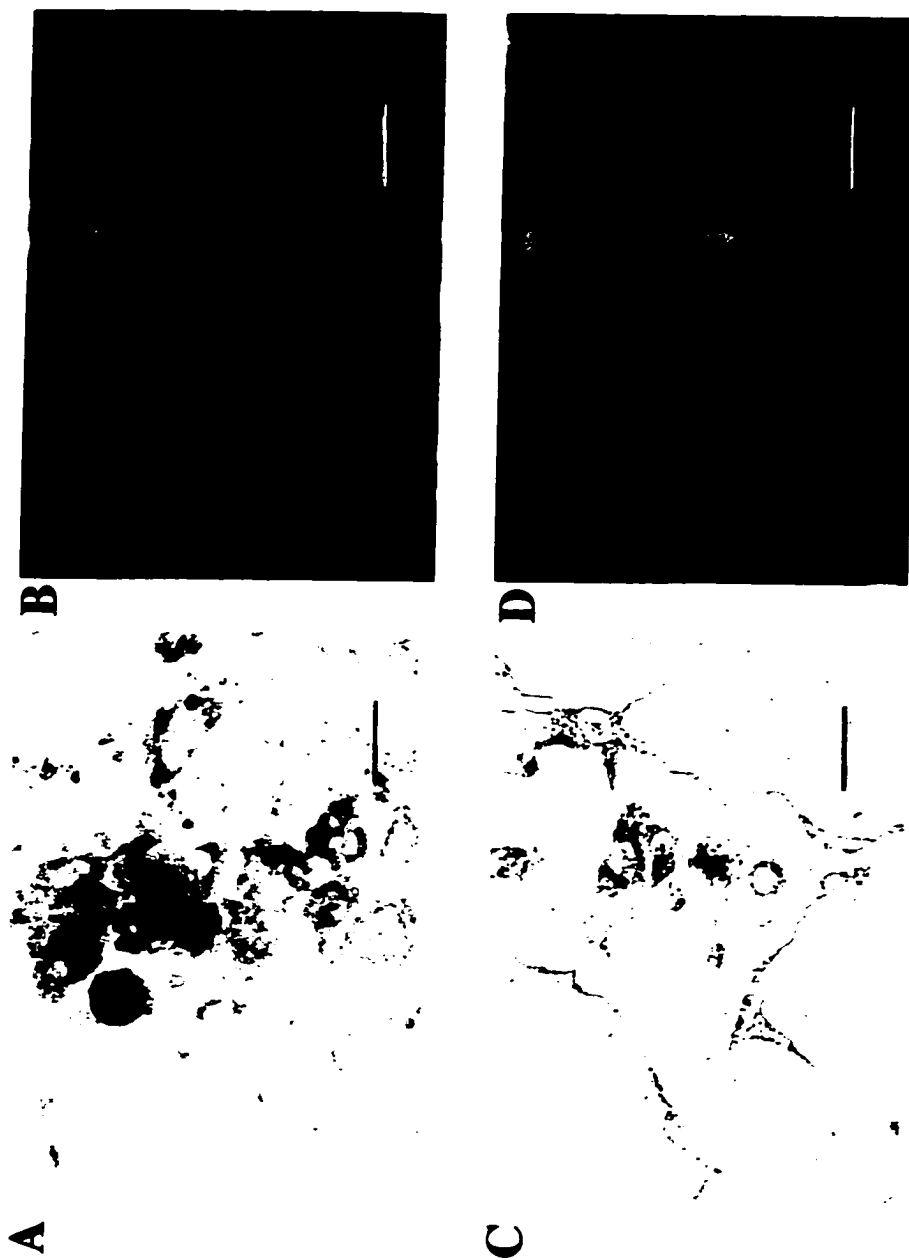


Figure 3.15

9.3 Whole-cell currents in replated RPE cells

Figure 3.16A shows macroscopic currents recorded from a representative RPE cell replated in the absence of antibody, 1 and 15 min after assuming the whole cell configuration, in 130 mM NaCl and low chloride K^+ -aspartate solution with 0.1 mM GTP γ S in the pipette. Immediately after break-in, the cell exhibits outwardly rectifying currents that resemble K^+ currents observed under normal conditions in the absence of GTP γ S (see Results, Figure 3.3). However, 15 min after break-in, large noninactivating currents are apparent (Figure 3.16B) at potentials hyperpolarized and depolarized to the holding potential (-69 mV). The activated current was present in 76 % of replated cells tested within a 15 min period following cytosolic dialysis with GTP γ S. The current-voltage relationship shown in Figure 3.16 for the GTP γ S-activated current, obtained by subtracting control current at 1 min after break-in from current at 15 min after break-in, is linear and reverses in this cell near 0 mV in standard recording solution. Thus, the replating technique does not affect whole-cell currents in rat RPE cells or the ability of GTP γ S to activate the NSC current.

Figure 3.17A, B and C show macroscopic currents from representative cells loaded with anti- $G_{\alpha s}$ (A), $G_{\alpha i/o/v/z}$ (B) or $G_{\alpha i-3}$ (C), under the same recording conditions as replated control cells. As observed in control cells, both inward and outwardly rectifying currents were recorded 1 min after assuming the whole-cell configuration in all antibody-loaded cells (Figure 3.17A-C; left panel). In those RPE cells loaded with anti $G_{\alpha s}$, GTP γ S- activation of the NSC current occurred in 74% of the cells tested (n=7) by 15 min after break-in (Figure 3.17A; right panel). In contrast, 15 min after break-in activation of the NSC current was observed in only 11% of the anti $G_{\alpha i/o/v/z}$

Figure 3.16. NSC current activation in replated RPE cells (A) Patch clamp recording from a representative replated RPE cells taken 1 (left) and 15 min (right) assuming the whole -cell configuration, in standard 140 NaCl extracellular solution and K^+ -aspartate intracellular solution with 0.1 mM $GTP\gamma S$ in the pipette. The voltage protocol is shown at the top of the figure. (B) Current-voltage plot for the traces shown in (A) for 1 (●) and 15 min (■) after break-in. The $GTP\gamma S$ – difference current (▲) was obtained by subtracting current at 1 min from that recorded at 15 min. Replating has no effect on the activation of the NSC current.

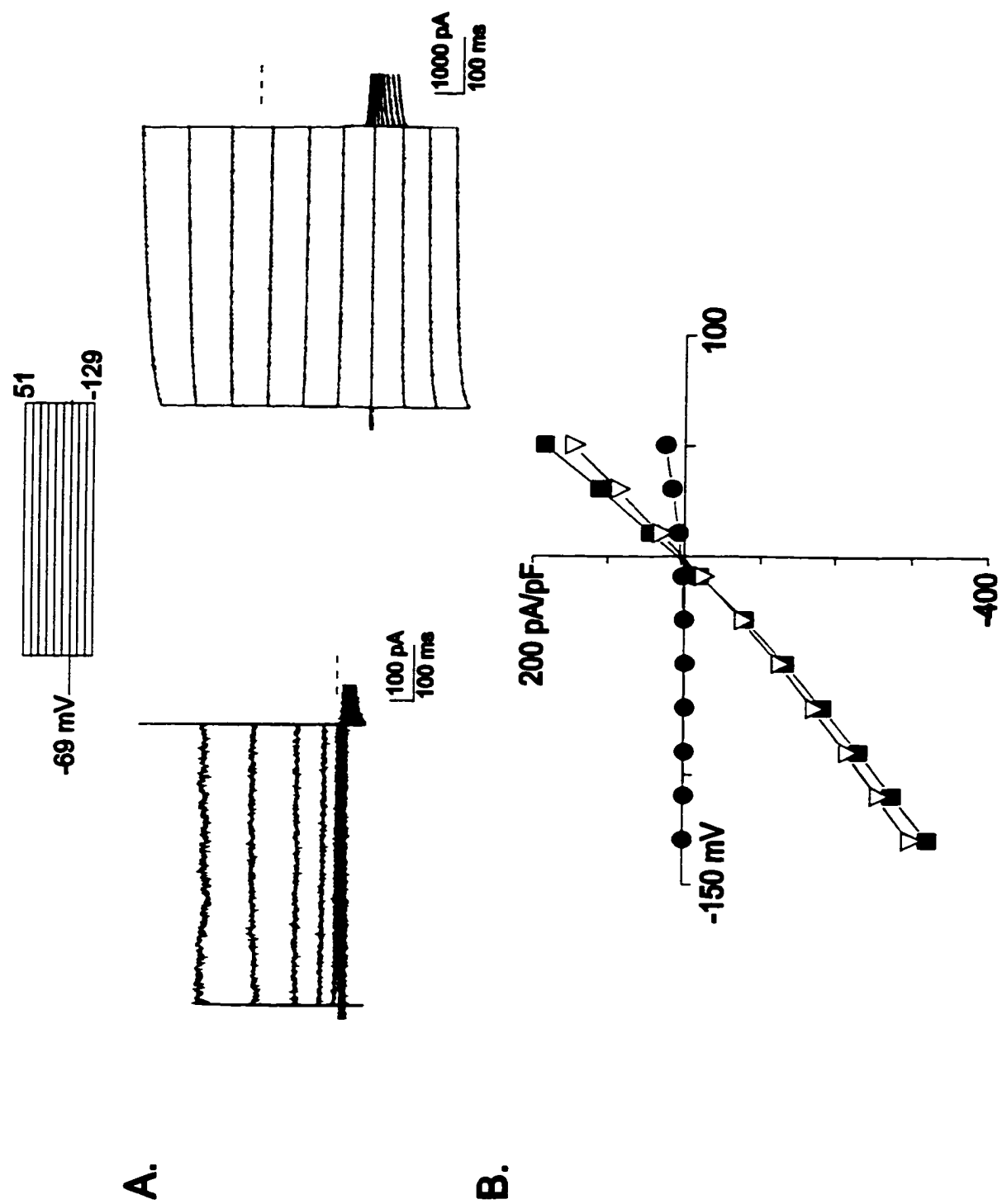


Figure 3.16

Figure 3.17. $G_{\alpha i-3}$ antibodies abolish NSC current activation. Whole-cell currents recorded from three representative RPE cells loaded with anti- $G_{\alpha s}$ (A), anti- $G_{\alpha i/o/v/z}$ (B) or anti- $G_{\alpha i-3}$ (C). Currents were recorded 1 and 15 min after assuming whole-cell configuration in standard recording solutions, with 0.1 mM GTP γ S in the pipette. (D) Mean (\pm SEM) amplitude of the difference current (current at 15 min – current at 1 min) in control RPE cells (open bar), RPE cells loaded with anti-GFAP (crosshatched bar), anti- $G_{\alpha s}$ (horizontal striped bar), anti- $G_{\alpha i/o/v/z}$ (vertical striped bar) or anti- $G_{\alpha i-3}$ (closed bar) (* $p < 0.05$). Current was measured at the end of a 500 ms step to +51 mV from $V_h = -69$ mV, and has been normalized for cell capacitance.

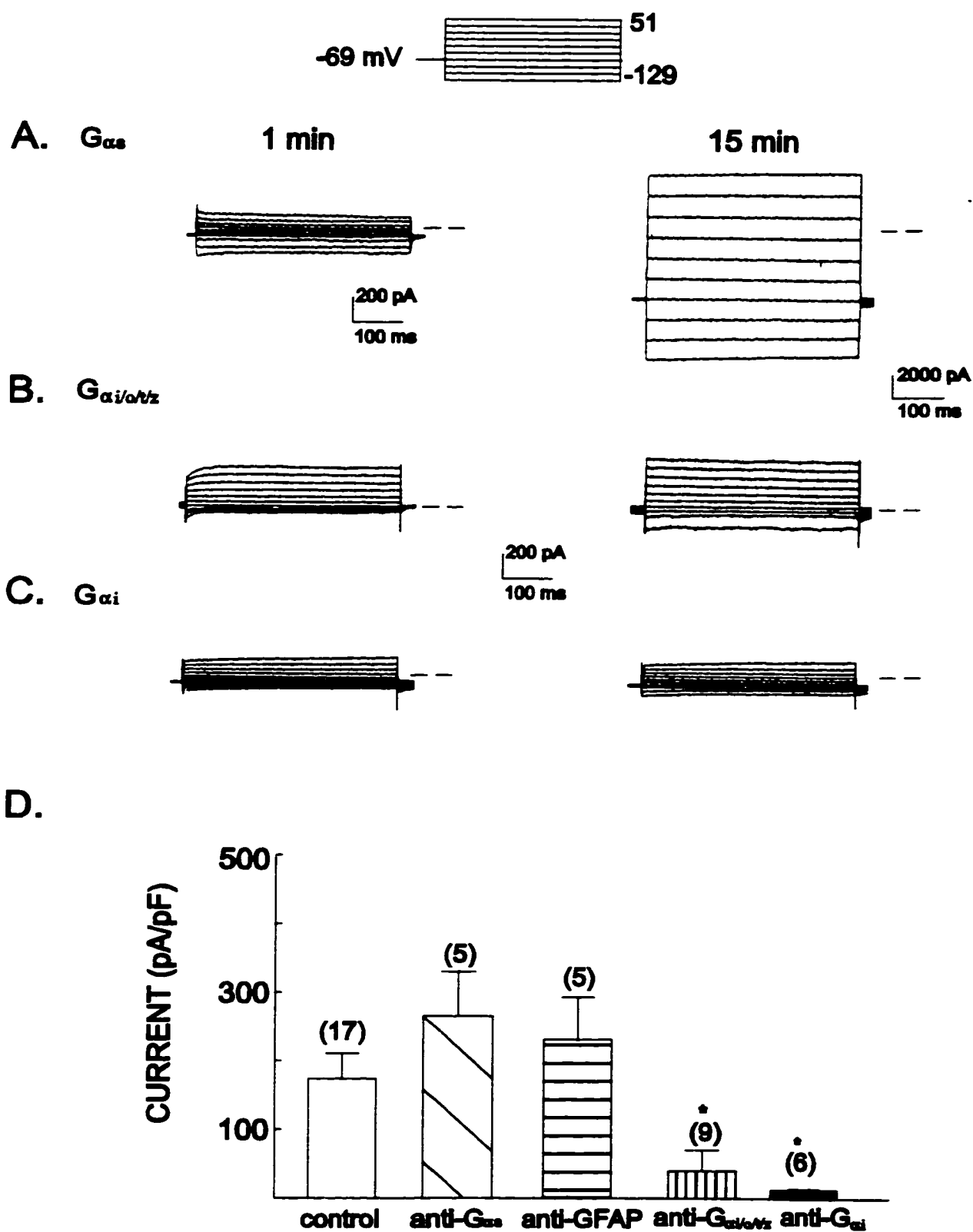


Figure 3.17

treatment group (n=9; Figure 3.17B; right panel), and the NSC current was not activated by GTP γ S in any cells loaded with G $_{\alpha i-3}$ (n=6; Figure 3.17C; right panel).

The GTP γ S-activated NSC current in control cells had a mean current amplitude at +51 mV of 174 ± 37 pA/pF (replated control; n=17) and 233 ± 62 pA/pF (anti-GFAP; n=5) 15 min after break-in. Similarly, in RPE cells loaded with anti-G $_{\alpha s}$, the GTP γ S-activated current measured at +51 mV had a mean current amplitude of 309 ± 109 pA/pF (n=7) at 15 min after break-in. In contrast, current measured 15 min after break-in at +51 mV in RPE cells replated with anti-G $_{\alpha i/o/z}$ or anti-G $_{\alpha i-3}$ had a mean current amplitude of 40 ± 29 pA/pF (n=9) and 9.9 ± 2 pA/pF (n=6), respectively (Figure 3.17 D). These results confirm that a G protein of the G $_{\alpha i}$ subtype is involved in the activation of the NSC current in rat RPE cells.

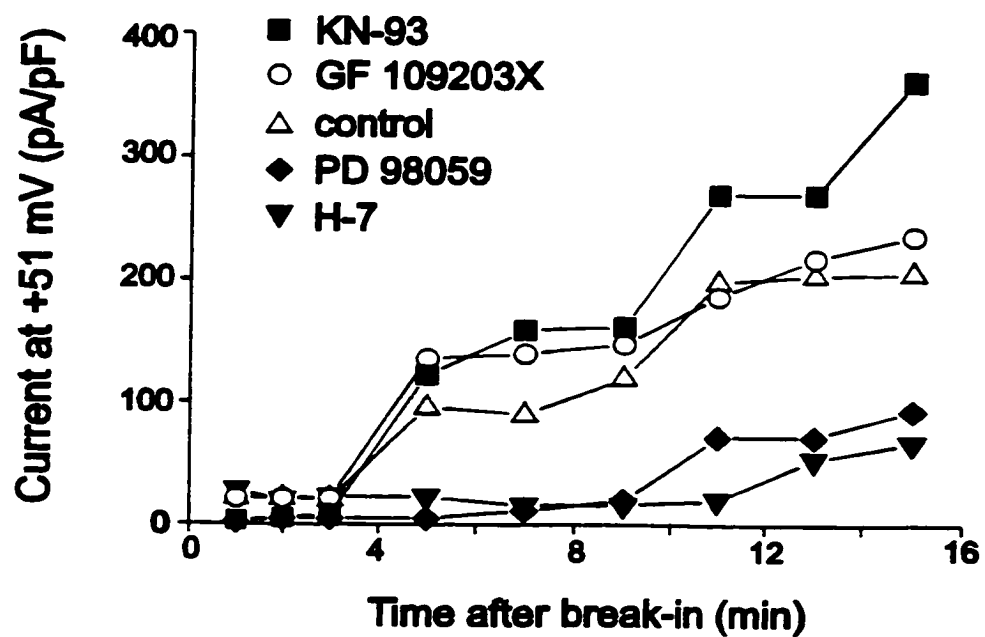
10. Involvement of Protein Kinases in Current Modulation

Figure 3.18A shows the time course for currents recorded in a control cell and 4 other representative cells, following pre-incubation and superfusion with the protein kinase inhibitors H-7, GF 109203X, KN-93 or PD 98059. H-7 is an isoquinolinesulfonamide that, at the concentration used in this study (100 μ M), is known to be a nonselective inhibitor of a number of protein kinases including: protein kinase C (PKC), cAMP-dependent protein kinase, myosin light chain kinase and cGMP-dependent protein kinase (Hidaka *et al.*, 1994). The bisindolylmaleimide GF 109203X is a selective inhibitor for PKC and inhibits PKC in intact cells at low micromolar concentrations (Toullec *et al.*, 1991). Similarly, at micromolar concentrations, the Ca $^{2+}$ /calmodulin -

Figure 3.18. Effect of kinase inhibitors on GTP γ S -activation of the NSC current.

(A) Current was measured every 20 sec from a $V_h = -69$ mV using a 100 msec step to +51 mV, in K⁻-aspartate intracellular solution containing 0.1 mM GTP γ S and standard 130 NaCl extracellular solution. Current is shown for a representative control RPE cell (Δ) and for four other cells that were pre-incubated and superfused with the protein kinase inhibitor H-7 (\blacktriangledown), GF 109203X (\bigcirc), KN-93 (\blacksquare) or PD 98059 (\blacklozenge). (B) Mean (\pm SEM) current amplitude measured at +51 and -129 mV at 15 min after assuming whole-cell configuration in control RPE cells (open bar) and in RPE cells pre-treated and superfused with the kinase inhibitors H-7 (hatched bar), GF 109203X (striped bar, vertical), KN-93 (striped bar, horizontal) or PD 98059 (closed bar). All data has been normalized for cell capacitance (* $p < 0.05$).

A.



B.

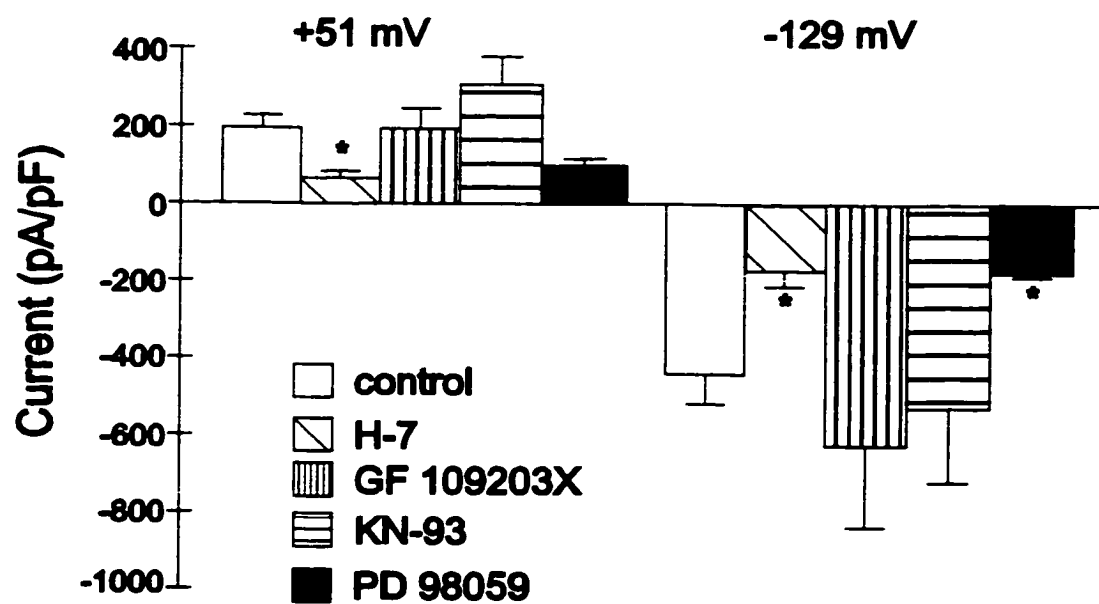


Figure 3.18

dependent protein kinase inhibitor, KN-93, inhibits a number of physiological responses associated with activation of CaM kinase II (Mamiya *et al.*, 1993; Marley & Thomson, 1996). We used PD 98059, the specific inhibitor of the MEK (Dudley *et al.*, 1995; Alessai *et al.*, 1995), to explore the possibility that mitogen-activated protein kinases (MAPKs) may be involved in NSC current activation.

To generate the time course of NSC current activation shown in figure 3.18A, current was measured every 20 sec from $V_h = -69$ mV, using a 100 msec voltage pulse to +51 mV in standard intracellular solution containing 0.1 mM GTP γ S. In the absence of kinase inhibitors, the NSC current was activated in 17/26 cells tested. The NSC current was also activated in 8/9 cells treated with either 100 μ M H-7 or 3 μ M GF 109203, in 3/4 cells treated with 50 μ M KN-93 and in 3/3 cells treated with 50 μ M PD 98059. The NSC current activated in the presence of the kinase inhibitors, GF 109203X and KN-93, had properties similar to control cells, however current activation in H-7 and PD 98059-treated cells was delayed compared to control, GF 109203X or KN-93-treated cells. In control cells, activation of the NSC current significantly increased the current amplitude measured at +51 mV from 12 ± 2 pA/pF at break-in to 135 ± 42 pA/pF at 7 min post break-in ($p < 0.05$). Current at +51 mV was also similarly increased at 7 min. post break-in, in RPE cells pre-treated with the kinase inhibitors GF 109203X (from 17 ± 6 pA/pF to 100 ± 30 pA/pF; $p < 0.05$) or KN-93 (from 16 ± 13 pA/pF to 148 ± 66 pA/pF; $p < 0.05$). In contrast, current amplitude measured at +51 mV at 7 min after break-in was not significantly different from break-in current amplitude in cells pre-treated with H-7 (10 ± 4 and 30 ± 15 pA/pF; $p > 0.05$) or PD 98050 (22 ± 15 and 32 ± 19 pA/pF; $p > 0.05$). The

decrease in current amplitude at 7 min with H-7 and PD 98059, is consistent with the delay in activation of the NSC current observed in the presence of these kinase inhibitors.

Figure 3.18B shows the mean current amplitude for the GTP γ S-activated current in control cells and in cells pre-treated with kinase inhibitors. Current amplitudes measured in control cells at +51 and -129 mV at 15 min after break-in were 195 ± 32 pA/pF and -423 ± 85 pA/pF, respectively (n=17). The mean amplitude of the current at +51 and -129 mV in cells pre-treated with H-7 (65 ± 19 and -169 ± 43 pA/pF; n=8) was significantly reduced compared to current amplitude measured in control cells ($p < 0.05$). The NSC current amplitude at +51 and -129 mV was unaffected in RPE cells treated with GF 109203X (193 ± 52 and -625 ± 212 pA/pF; n=8) or KN-93 (238 ± 86 and -528 ± 193 pA/pF; n=4). However, like H-7, pre-treatment of RPE cells with the MEK inhibitor PD 98059 also reduced the current amplitude measured at +51 and -129 mV (98 ± 20 and -176 ± 10 pA/pF; n=3) compared to control.

Figure 3.19 shows the I-V curves for the mean GTP γ S-difference current in a control RPE cell and in another cell treated with either H-7 or PD 98059. Both H-7 and PD 98059 reduced the mean current amplitude over the entire voltage range. The mean reversal potential of the NSC current however, was unaffected by treatment with H-7 or PD 98059. The lack of effect of the selective kinase inhibitors GF 109203X or KN-93 suggests that neither PKC or CaM kinase II play a role in modulating NSC current activation in rat RPE cells. However, the delay in NSC current activation and the reduced current amplitude in the presence of the nonselective kinase inhibitor H-7 and the selective inhibitor of MEK, PD 98059 suggests that some phosphorylation event, likely mediated by a MAP kinase, plays a role in NSC current modulation.

Figure 3.19. H-7 and PD 95059 decrease NSC current amplitude. Mean I-V plot for the GTP γ S-difference current in control cells (●; n=12) and for cells treated with H-7 (■; n=8) or PD 98059 (Δ;n=3). The difference current was obtained by digitally subtracting current amplitude at 1 min from current amplitude at 15 min. All data has been normalised for cell capacitance. (*p<0.05)

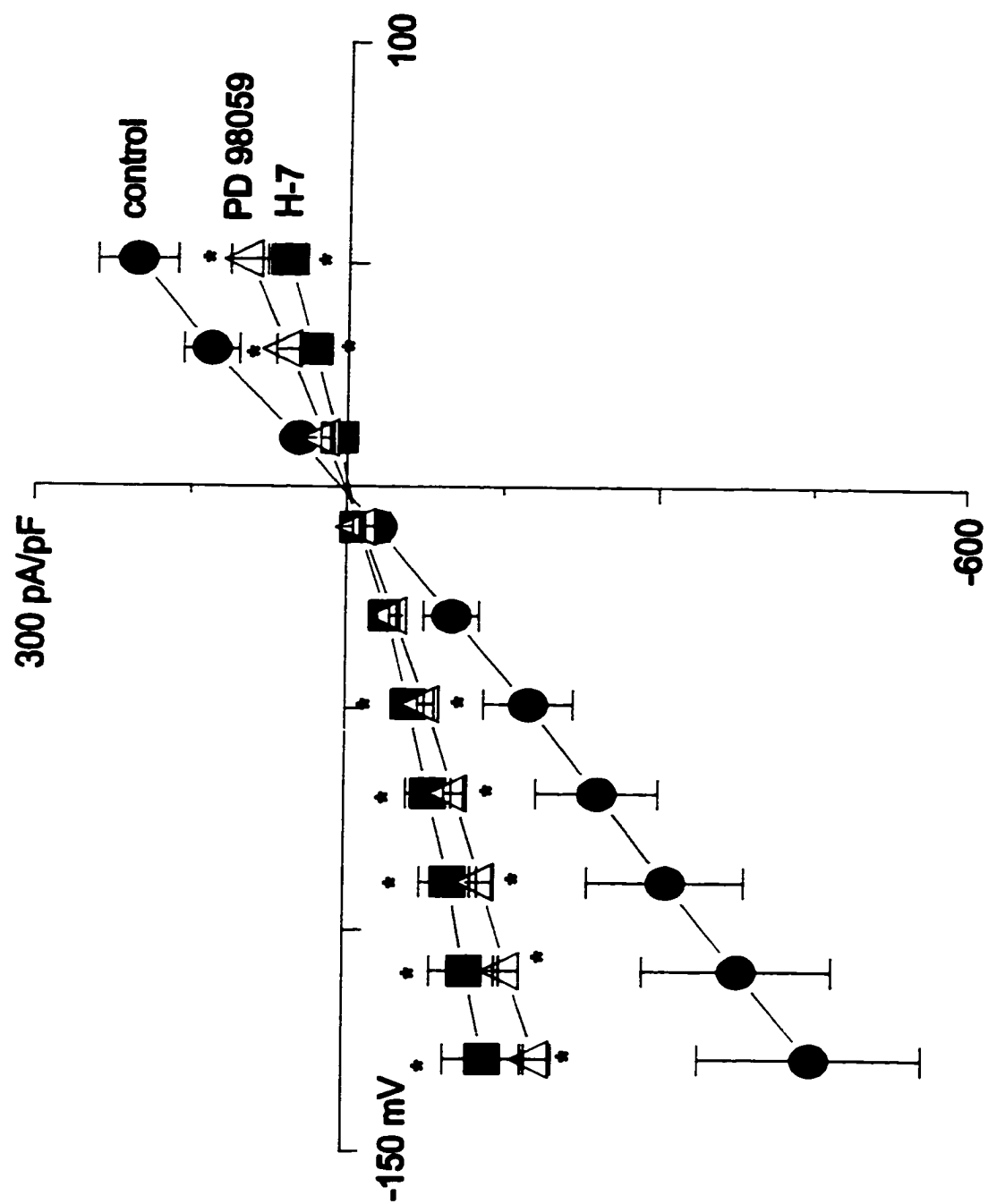


Figure 3.19

11. Involvement of Cyclic Nucleotides

The cyclic nucleotides cyclic AMP and cyclic GMP have been demonstrated to stimulate nonselective cation channels in a variety of cell types to cause membrane depolarization (for review see: Zagotta & Siegelbaum, 1996). Therefore, we investigated the possibility that signaling pathways coupled to GTP γ S-activation of heterotrimeric G proteins may generate cyclic nucleotides that could gate the NSC current in RPE cells. Figure 3.20A shows the mean current amplitude measured at break-in (1 min) and 10 min after superfusion of RPE cells with the membrane permeant adenylate cyclase activator forskolin or the membrane permeant cGMP analogue dibutyryl cGMP. Cells were recorded using Na⁻-aspartate external and Cs⁻-aspartate internal solution, in the absence of GTP γ S. Activation of the NSC current failed to occur in any of the tested RPE cells exposed to 10 μ M forskolin for 10 min (n=8). The mean current amplitudes in forskolin treated cells measured 1 and 10 min after break-in at +56 mV and -124 mV were 10 ± 4 and -13 ± 3 pA/pF and 13 ± 10 and -19 ± 15 pA/pF (n=6), respectively. The inability of forskolin to mimic activation of the NSC current in the absence of GTP γ S, suggests that cAMP is not involved in current activation and further confirms the lack of involvement of a G α_s -coupled signaling pathway.

Superfusion of RPE cells with 300 μ M dibutyryl cGMP also failed to activate the NSC current in any cells tested (Figure 3.20B; n=6). Mean current amplitudes measured at +56 and -124 mV at 1 min after break-in were 8 ± 2 and -6 ± 3 pA/pF, respectively. Similarly, 15 min after break-in, in the presence of dibutyryl cGMP, the mean current amplitude at +56 mV (11 ± 4 pA/pF) was not significantly different from break-in

Figure 3.20. Cyclic nucleotides are not involved in NSC current activation. Mean (\pm SEM) current amplitude measured in RPE cells with Cs⁻-aspartate intracellular solution minus GTP γ S and Na⁻-aspartate extracellular solution containing either forskolin (A) or dibutyryl-cGMP (B). Current was measured at +56 and -124 mV at 1 (open bars) and 15 min (closed bars) after assuming whole-cell configuration. Current amplitude at -124 mV measured at 15 min was significantly increased with dibutyryl-cGMP superfusion (* p <0.05; Student's paired t-test). All current values have been normalized for cell capacitance. (B; inset). Mean (\pm SEM) I-V relationship for dibutyryl-cGMP-activated current in RPE cells, obtained by subtracting whole cell currents measured after 15 min superfusion with dibutyryl-cGMP from those measured immediately after break-in.

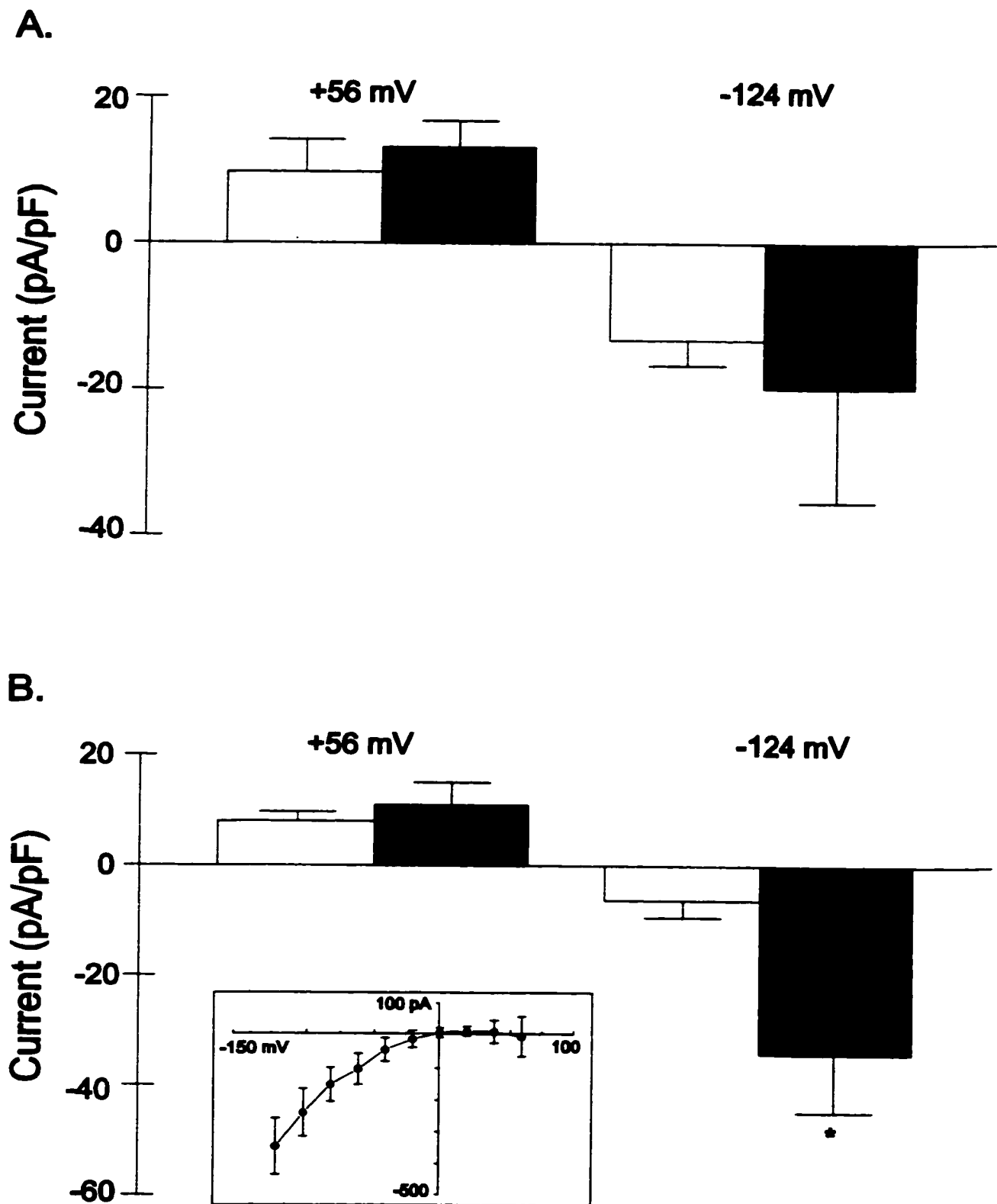


Figure 3.20

($p > 0.05$). However, in all 6 cells examined, superfusion with dibutyryl cGMP significantly increased the mean current amplitude measured at -124 mV (-34 ± 16 pA/pF; $p < 0.05$; Student's paired t-test) compared with break-in current. The mean current activated by dibutyryl cGMP (see inset Figure 3.19B) was obtained by subtracting I-Vs generated under control conditions from those obtained in the presence of cGMP. The cGMP-activated current showed inward rectification at negative potentials, with little outward current at depolarized potentials. The cGMP-activated current had a mean current reversal of 1.2 ± 3 mV and a mean whole-cell conductance of 2855 pS at -124 mV. This cGMP-activated current in RPE cells may be similar to the cGMP-gated non-selective cation currents described in other retinal cell types (Kusaka *et al.*, 1996; Wei *et al.*, 1996), but was distinct from the GTP γ S-activated NSC current being investigated in this thesis.

DISCUSSION

In this study we demonstrate, using standard whole-cell recording conditions, that the membrane conductance of rat RPE cells is normally dominated by K^+ conductances. Rat RPE cells were found to exhibit at least 3 voltage-dependent K^+ currents. Our results also demonstrate that rat RPE cells possess a nonspecific cation (NSC) current that is activated by a PTX-sensitive $G_{\alpha i}$ subunit protein. Furthermore, we show that the downstream events linked to NSC channel activation involve intracellular Ca^{2+} and a phosphorylation event that may be mediated by a MAP kinase signaling pathway. This study extends earlier electrophysiological studies in the rat RPE by identifying and characterising a NSC current not previously identified in this cell type. Details of the properties and the regulation of this G protein-activated NSC current are discussed below and compared to nonselective channels described in other cell types.

1. Membrane properties and voltage-dependent K^+ conductances in cultured rat RPE cells.

Membrane properties obtained for cultured rat RPE cells compared well with those obtained in other mammalian RPE (Hughes & Steinberg, 1990; Strauß *et al*, 1993). The average cell capacitance was 34 pF ($n=100$) and, under standard recording conditions, the average resting membrane potential of rat RPE cells cultured for 2-5 days was -47 ± 2 mV ($n=33$). The resting membrane potential of isolated RPE cells tends to be somewhat depolarized as compared to the average values obtained for intact RPE preparations which range between -70 to -80 mV (Miller & Steinberg, 1977; Joseph &

Miller, 1992). The reason for this discrepancy remains unknown but may be related to altered membrane properties, loss of epithelial polarity and/or junctional complexes between cells that occurs during RPE cell isolation and culture, and may be due to treatment with enzymes and low Ca^{2+} media (Davis *et al.*, 1995).

Under standard conditions, we found that the whole-cell current of our cultured rat RPE cells primarily consisted of at least three different voltage dependent K^+ conductances: a delayed rectifying outward K^+ current, an inactivating outward K^+ current and an inwardly rectifying K^+ current. The presence of similar K^+ currents has been demonstrated in cultured and fresh RPE cells from several amphibian and mammalian species: frog (Hughes & Steinberg, 1990), rat (Strauß, 1994), rabbit (Tao *et al.*, 1994), monkey (Wen *et al.*, 1993), and human (Strauß *et al.*, 1993; Wen *et al.*, 1993).

A delayed (outward) rectifying K^+ conductance was the predominant K^+ current observed in our cultured rat RPE cells. This current was identified on the basis of its voltage-dependence and sensitivity to pharmacological blockade (Rudy, 1988). The delayed rectifier K^+ current was activated by depolarizing the RPE cells positive to -40 mV, it showed little decay at maintained depolarization and was decreased by the blockers of voltage-dependent potassium channels, 4-AP and TEA (Cook, 1988). Tail current analysis indicated that outward current was mainly carried by K^+ ions. The delayed rectifier identified in our cultured rat RPE cells shows a similar voltage dependence and pharmacological profile to the delayed rectifier previously described in cultured primate (Wen *et al.*, 1993) and rat RPE cells (Strauß & Weinrich, 1992).

In this study on cultured rat RPE cells, 47% of the cells investigated expressed an inwardly rectifying K^+ conductance. This time and voltage-dependent inwardly rectifying

current was activated by hyperpolarizing cells to potentials negative to -70 mV. Inward current showed time-dependent inactivation at the more negative potential of -122 mV, a characteristic typically observed for mammalian inward rectifier K^+ channels (Rudy, 1988). Inward K^+ current was blocked by low concentrations of Ba^{2+} which is also typical for inward (anomalous) rectifier K^+ channels (Cook, 1988). An inwardly rectifying K^+ conductance with a similar voltage-dependence and sensitivity to blockade by Ba^{2+} as observed for rat RPE cells, has been described in rabbit (Tao *et al*, 1994).

A small percentage of rat RPE cells recorded from ($\sim 20\%$) exhibited an inactivating outward K^+ current. The threshold for activation of this current was more negative (~ -60 mV) than for the delayed rectifier and it rapidly inactivated at depolarized potentials. A similar inactivating outward current has also been observed in cultured rabbit (Tao *et al*, 1994), turtle (Fox & Steinberg, 1992) and cultured fetal and adult human RPE cells (Wen *et al*, 1993). The infrequent appearance of this transient outward current did not allow for us to test the sensitivity of this current to pharmacological blockade. In other mammalian RPE cell however, the transient outward current was sensitive to blockade by low concentrations of 4-AP, a potent blocker of transient K^+ currents (Rudy, 1988).

2. Location and function of K^+ conductances in the RPE

It is known that in most epithelial cells, there is differential expression of channel populations on the apical and basolateral surfaces (Rodriguez-Boulan & Nelson, 1989). While our whole-cell recordings did not allow us to identify whether channels were located on either the apical or basolateral membrane of RPE, studies from intact RPE-

choroid preparations have suggested that K^+ conductances are located on both the apical and basolateral membranes. Studies on the frog RPE have also provided evidence that the apical membrane K^+ conductance is comprised largely of inward rectifying K^+ current (Miller & Steinberg, 1997; Joseph & Miller, 1991).

The inwardly rectifying K^+ current we identified in cultured rat RPE cells is the predominant current active in the physiological voltage range of the RPE (Segawa & Hughes, 1994; Hughes & Takahira, 1996). Apically located inward rectifiers contribute to the establishment of the apical resting potential of RPE cells; provide an efflux pathway for K^+ that enters via the Na^+/K^+ pump; carry out transepithelial ion transport; and contribute to K^+ homeostasis in the subretinal space. Inward rectifying K^+ conductances at the basolateral membrane help set the basolateral membrane potential and provide the major efflux pathway for K^+ transport across the RPE.

In the absence of agonist stimulation, the function of the delayed outward rectifier in the RPE is unknown since it activates at potentials that are significantly depolarized (40-50 mV) to the normal resting potential of the apical and basolateral membranes. Even the depolarization (~ 12 mV) of the RPE that accompanies the onset of light would be insufficient to activate this outward K^+ current. Therefore, it seems unlikely that this conductance participates in transepithelial transport or contributes to the membrane potential under normal physiological conditions. In the face of a large transient depolarization however, this current would be well suited to restore the normal membrane potential. Outwardly rectifying K^+ conductances have been implicated in the mitogenic response of retinal ganglion cells (Puro *et al*, 1989) and T lymphocytes (DeCoursey, 1984) and in the membrane potential changes that accompany phagocytosis

in macrophages (Ypey & Clapham, 1984; Ince *et al*, 1988). Thus, the delayed rectifier K^+ conductance could play similar roles in the RPE.

The role that the transient outward K^+ current plays in the RPE also remains unknown. The infrequent appearance of this conductance and the observation that it is found mainly in dedifferentiated RPE cells in culture suggests that it does not play a physiological role under normal conditions *in vivo*. In other nonexcitable cell types the expression of transient inactivating K^+ currents has been demonstrated to be important for differentiation (Rudy, 1988) and proliferation (Mattioli *et al*, 1993).

3. Activation of the NSC current by GTP Analogues

Our results demonstrate that inclusion of $GTP\gamma S$ or $Gpp(NH)p$ in the pipette activates a large cation current in rat RPE cells. In the presence of $GTP\gamma S$ or $Gpp(NH)p$, the NSC current activates rapidly after a delay of 5-6 minutes (after assuming the whole-cell configuration). In the presence of $GTP\gamma S$, NSC current activation was not reversible. Non-reversible effects of $GTP\gamma S$ have been described for ion channel activation in other cell types (Sun *et al*, 1992), including NSC channel activation in other ocular epithelial cells (Mitchell & Jacobs, 1996a). The delay in current activation is consistent with time constant reported for $GTP\gamma S$ diffusion from the patch pipette into the cytoplasm, which has been determined to be about 4 min to reach 90% maximum concentration in the cytosol (Hescheler, 1994). Similar time-courses for current activation have been reported for $GTP\gamma S$ -mediated activation of voltage-dependent calcium currents (Oliva *et al*, 1988) and NSC channels in guinea pig chromaffin cells (Inoue *et al.*, 1991). In contrast to the effects of $GTP\gamma S$ and $Gpp(NH)p$, inclusion of $GDP\beta S$ in the pipette did not activate the

cation current. Since GDP β S is a hydrolysis-resistant GDP analogue that competes with GTP for binding sites on G proteins, the lack of activation of the cation current by GDP β S confirms the involvement of a G protein in regulation of this current.

4. Pharmacological Blockade of NSC currents

A number of agents have been reported to have some blocking actions on NSC channels including K⁺ channel blockers, such as quinine (Gogelein & Pfanmuller, 1989), and the lanthanide, gadolinium. In various cell types, including epithelial cells, gadolinium has been found to block the activation of both stretch-activated cation channels (Yang & Sachs, 1989; Davis, 1992; Naruse & Sokabe, 1993) and receptor-activated NSC channels (Schumann *et al.*, 1994) at concentrations between 50 nM to 100 μ M. Neither quinine nor gadolinium was effective in blocking the GTP γ S-activated current in rat RPE cells. Similar to our findings, 100 μ M gadolinium also had no effect on a nonselective cation current in pigmented ciliary epithelial cells (Mitchell & Jacob, 1996b). However, this study also found that the nonselective current could be blocked at higher concentrations of gadolinium (4 mM). The ineffectiveness of 100 μ M gadolinium in our study may, therefore, reflect too low a concentration of this agent for effective blockade of the NSC current in RPE cells. In addition to the above agents, the epithelial Na⁺ channel blocker amiloride (Benos *et al.*, 1995; Jacob *et al.*, 1985) was also without effect on the GTP γ S-activated current.

5. Ionic selectivity of NSC currents

The presence of non-specific cation (NSC) channels have now been described in numerous cell types including heart cells (Colquhoun *et al.*, 1981), IMCD kidney epithelial cells (Ono *et al.*, 1994), macrophages (Lipton, 1986), rat and mouse pancreatic acinar cells (Maruyama & Petersen, 1982), lacrimal acinar cells (Marty *et al.*, 1984), and subsequently in every type of exocrine gland which has been investigated (for review see, Marty, 1987). In ocular tissues, NSC channels have been described in human (Cooper *et al.*, 1990) and frog (Cooper *et al.*, 1986) lens epithelial cells and rabbit corneal endothelium (Rae *et al.* 1990). NSC channels form a heterogeneous family of pore-forming proteins whose characteristics vary, depending on both the cell system and the investigational approach used. The common denominator, as its name implies, is the selectivity of this channel for small monovalent cations, coupled with the inability to discriminate among these cations. The GTP γ S-activated current in rat RPE cells was a NSC current, because in the presence of voltage-dependent K⁺ channel blockade it showed virtually no discrimination between Na⁺ and K⁺ ions with a P_K/P_{Na} of 1.07 and had a V_r close to 0 mV in 130 mM Na⁺ or K⁺ extracellular solutions. In addition to almost complete non-discrimination between Na⁺ and K⁺ ions, large cations such as TRIS and NMDG also appeared to be able to permeate the rat NSC channel. The channel exhibited no anion permeability as alterations in extracellular [Cl⁻] produced very little change in current amplitude or current reversal potential.

In a number of cell types NSC channels have been shown to have significant permeability to the divalent cation Ca²⁺ (Benham *et al.*, 1985; Inoue & Kuriyama, 1992;

Thorn & Petersen, 1993). We did not explore the Ca^{2+} permeability of the GTP γ S-activated NSC in rat RPE cells. However, removal of extracellular Ca^{2+} still resulted in current activation and did not change the reversal potential or the amplitude of the NSC current. Thus it is unlikely that under physiological conditions that the NSC channel could represent a major pathway for Ca^{2+} entry in RPE cells.

A large nonselective channel with somewhat different properties to the NSC current recorded in rat RPE cells has been described in membrane patch recordings from cultured human RPE cells (Fox *et al.*, 1988). This nonselective channel had a unitary conductance of 300 pS, a $P_{\text{K}}/P_{\text{Na}}$ of 0.8 and showed poor selectivity between K^{+} and Cl^{-} . Investigations of the calcium and voltage-dependence of the non-selective channel in human RPE cells revealed that this channel was not dependent on either extracellular or intracellular Ca^{2+} but was voltage-dependent, with the open probability of the channel decreasing as the membrane potential increased. Similar large-conductance channels which show selectivity for several substrates but are primarily anion selective, have been described in rat Schwann cells (Gray, Bevan & Ritchie, 1983), rat muscle (Blatz & Magleby, 1983) and the apical membranes of MDCK cells (Kolb *et al.*, 1985). This poor discrimination between cations and anions and the voltage-dependency sets these channels apart from the NSC channel described in this study, which is selective for cations but has limited permeability for anions.

6. Identity of the G protein activating the NSC current

Confirmation that GTP γ S-mediated activation of the NSC current in rat RPE cells involves a heterotrimeric as opposed to a low molecular-weight (18-32 kDa) monomeric

G proteins, was carried out by dialysing cells with AlF_4^- . The AlF_4^- complex is a known activator of heterotrimeric G proteins and is able to mimic the action of GTP and thus cause dissociation of the α -subunit of G proteins (Ui, 1990). We found that AlF_4^- activated a cation current with similar properties to the $\text{GTP}\gamma\text{S}$ -activated NSC current. In the case of fluoroaluminate, however, the time-course of activation of the NSC current was somewhat slower than that found with $\text{GTP}\gamma\text{S}$ and tended to reverse more rapidly. This finding is supported by other studies which demonstrate that the effect of sodium fluoride is reversible and that it acts in a concentration-dependent manner with a K_d for G protein activation of 0.47 mM (Higashijima *et al.*, 1991).

Although fluoroaluminate has been shown to stimulate heterotrimeric G proteins in many different tissues, the results of these studies indicate that the fluoride-evoked effects were not generally mediated by a PTX-sensitive G protein (Ui, 1990). Our results are not consistent with these findings since, incubation of rat RPE cells with PTX for 24 hrs blocked $\text{GTP}\gamma\text{S}$ -activation of the NSC suggesting that the G protein involved was PTX-sensitive and of the G_i/G_o class. Several reports in the literature also demonstrate abolishment of ion channel activation after treatment of cells with PTX (Brown & Birnbaumer, 1990; Schultz *et al.*, 1990), including a muscarine-activated NSC current in guinea-pig chromaffin cells (Inoue *et al.*, 1991).

To identify the PTX-sensitive G protein subtype involved in NSC current activation we employed a modified version of the scrape-loading technique (McNeil *et al.*, 1986) to inactivate selective G protein α subunits. This technique was advantageous in the study of NSC activation in rat RPE cells because it was methodologically simple and allowed us to load >90% of the cells with antibody. Furthermore, scrape-loaded RPE

cells retained their morphological and electrophysiological characteristics indicating that viability was unaffected. Our results demonstrate that loading RPE cells with an antibody which is directed against the alpha subunit protein of all PTX-sensitive G_i proteins ($G_{\alpha i-1}$, $G_{\alpha i-2}$ and $G_{\alpha i-3}$), but has no cross reactivity with other G protein α subtypes, abolishes GTP γ S activation of the NSC current. This finding, combined with the lack of effect of antibodies directed against the PTX-insensitive $G_{\alpha s}$ subunit proteins, confirms that a G protein of the $G_{\alpha i}$ subtype is involved in NSC current activation in rat RPE cells.

In support of our findings, studies in mammalian RPE cells have identified multiple G protein species, including all 3 subtypes of $G_{\alpha i}$ proteins (Jiang *et al*, 1991), and have demonstrated that a number of light-adaptive responses, ion transport pathways and second messenger activity in this epithelium are modulated by ligands that are known to couple to G protein signaling pathways (Hughes *et al*, 1988; Dearry *et al*, 1990; Nash & Osborne, 1995). More recently, a PTX-sensitive nonselective cation channel with properties similar to the one described in this study has also been identified in human RPE cells. This NSC current is activated by lysophosphatidic acid (Thoreson & Chako, 1997), a molecule known to act via cell surface receptors coupled to $G_{\alpha i}$ protein subtypes (Moolenaar *et al*, 1997). Evidence from other studies in a variety of cell types also supports the involvement of G proteins, including PTX-sensitive ones, in the activation of nonselective cation channels. For example, muscarine-mediated activation of a nonselective cation channel in smooth muscle and guinea pig chromaffin cells is known to involve G_i/G_o proteins (Inoue & Imanaga, 1995; Wang, Fleischmann & Kotlikoff, 1997) and in HI-60 cells, a nonselective cation channel has also been described that is activated via PTX-sensitive G_i proteins (Hagelucken *et al*, 1995).

7. Signaling Pathways involved in NSC current activation

Ion channels coupled to G protein signaling pathways can be modulated both directly by activated G protein subunits and indirectly by a number of downstream signaling intermediaries (Wickman & Clapham, 1995). Signaling pathways linked to $G_{\alpha i}$ pathways have been demonstrated to be involve in phosphoinositide (PI) turnover via $PLC\beta$ activation and subsequent intracellular Ca^{2+} mobilization, inhibition of adenylyl cyclase, and activation of a host of protein kinases including: PKC; tyrosine kinases; CaM Kinase II; and MAP kinase. Second messengers and protein kinases, activated downstream of G-protein activation, can modulate the activation of a number of different ion channels (for review see, Ghosh & Greenberg, 1995; Smart, 1997), including nonselective cation channels (Braun & Schulman, 1995; Inoue & Imanaga, 1995; Inoue *et al*, 1996; Lidofsky *et al*, 1997).

7.1 Role of $[Ca^{2+}]_i$ in NSC current activation

A large number of nonselective channels have been described that are activated by elevations in the intracellular calcium concentration ($[Ca^{2+}]_i$). These channels are classified as calcium-activated nonselective cation (CAN) channels and are ubiquitous in nature, being found in virtually all cell types examined. CAN channels share three main characteristics: calcium sensitivity, nonselectivity and impermeability to anions. These channels are heterogeneous with respect to their calcium sensitivity and studies have reported that $[Ca^{2+}]_i$ as low as 50 nM and as high as 10 μ M are required to cause

significant increases in the channel open probability (for review, see Partridge & Swandulla, 1988).

The increase in $[Ca^{2+}]_i$ that activates these NSC currents is thought to arise via extracellular Ca^{2+} influx and/or release from intracellular Ca^{2+} stores. The rise in $[Ca^{2+}]_i$ that facilitates NSC current activation in RPE cells does not appear to be dependent on influx of extracellular calcium, as we observed no decrement in current amplitude when the external solution was made nominally Ca^{2+} -free (see above). This suggests that only elevations in $[Ca^{2+}]_i$ mediated by release from intracellular stores are involved in modulation of NSC current amplitude in rat RPE cells. To support this hypothesis, we observed that depletion of intracellular Ca^{2+} stores by dialysis of RPE cells with 10 mM BAPTA significantly reduced the amplitude of the NSC current without affecting its activation by GTP γ S. Thus, in rat RPE cells Ca^{2+} mobilization from intracellular stores, and not extracellular influx, facilitates channel activation but is not a prerequisite for current activation. In guinea-pig chromaffin cells, intracellular Ca^{2+} has been found play a similar role in facilitating agonist-induced NSC current activation (Inoue & Isenberg, 1990; Inoue & Imanaga, 1995).

A large body of evidence now supports two pathways for $[Ca^{2+}]_i$ to activate and/or regulate NSC channels. A number of earlier studies suggested that elevations in intracellular Ca^{2+} directly activates NSC channels by interacting with a Ca^{2+} binding site on the channel protein. Support for this hypothesis comes from studies which demonstrated that in cell-detached patches (inside-out configuration), exposure of the cytoplasmic side of the membrane to Ca^{2+} activated NSC channels (Partridge & Swandulla, 1988; Cook *et al*, 1990; Verrier & Lazdunski, 1991; Hagiuar & O'

Brodovich, 1992). More recently, several lines of evidence argue against direct binding of Ca^{2+} as a sole means for activation of CAN channels (Devin & Duffy, 1992; Braun & Schulman, 1995; Inoue & Imanaga, 1995). This finding opens up the possibility that the activation of NSC channels may be regulated by downstream signaling components of G protein pathways that are activated/inactivated subsequent to elevations in $[\text{Ca}^{2+}]_i$. For example, carbachol stimulation of a Ca^{2+} -dependent NSC current in human T84 epithelial cells was demonstrated to be mediated by the Ca^{2+} -calmodulin-dependent protein kinase, CaM kinase, which was activated secondarily to elevations in $[\text{Ca}^{2+}]_i$ (Braun & Schulman, 1995).

7.2 Protein Kinase-dependent phosphorylation in NSC current activation

Modulation of nonselective cation currents by kinase-mediated phosphorylation events have now been described in a variety of cell types. For example, in human T84 epithelial cells, phosphorylation mediated by CaM kinase was demonstrated to be required for activation of a Ca^{2+} -activated nonselective cation current (Braun & Schulman, 1995). PKA-dependent phosphorylation is also involved in the activation of a nonselective cation current in renal epithelial cells (Marunaka *et al.*, 1997) and tyrosine phosphorylation by the endogenous tyrosine kinase, Src, regulates the activity of N-methyl-D-aspartate receptors in mammalian central neurons (Yu *et al.*, 1997). Similar to our findings, a nonselective cation current has been described in chromaffin cells whose activation is sensitive to PTX, facilitated by rises in $[\text{Ca}^{2+}]_i$ and involves an H-7-sensitive and PKC, CAM kinase II-independent phosphorylation event (Inoue & Imanaga, 1995). A role for MAPK(s)-dependent phosphorylation in nonselective cation

channel activation has not yet been described, however a recent study has identified that MAPK(s) are involved in the activation of a volume-activated anion current in rat astrocytes (Crepel *et al.*, 1998).

Our current results, examining the involvement of protein kinases in NSC channel activation, indicated that neither CaM kinase II nor PKC-mediated phosphorylation is involved in NSC current regulation, as inhibitors of these kinases (KN-93 and GF 109203X) had no effect on NSC current activation or amplitude. However, in the presence of the serine/threonine kinase inhibitor H-7, or a selective inhibitor of the MAP kinase-activating enzyme MEK, (PD 98059), NSC current activation was delayed and current amplitude significantly reduced. The inhibitory effects of H-7 are mediated by direct interaction with the active center of the kinase thus competitively inhibiting ATP binding and kinase activation. PD 98059 selectively inhibits the activation of MEK (MAPKK), a dual specific kinase that is an integral part of the MAP kinase cascade. Inhibition by PD 98059 blocks subsequent MEK-dependent tyrosine/threonine MAP kinase phosphorylation and activation (Alessi *et al.*, 1995). The observation that both inhibitors had similar effects on the NSC current suggests that H-7 and PD 98059 may be blocking a common phosphorylation pathway involved in channel regulation. MEKKs (Rafs), MEKs, MAPs (ERK1/ERK2) and MAPK-activated protein kinases (MAPKAPKs) are all tyrosine/threonine or serine/threonine kinases in the MAP cascade, whose activation leads to phosphorylation of a variety of proteins (Denhardt, 1996; Robinson & Cobb, 1997). It is plausible therefore, based on the conserved sequence homology of serine/threonine kinases, that H-7 is inhibiting a kinase in the MAP cascade to produce similar effects to PD 98059-mediated MEK inhibition on the NSC current in

rat RPE cells. Our results therefore, support a role for a protein kinase-dependent phosphorylation step in the activation pathway of this current and further implicate MAPK(s)- dependent phosphorylation as a potential mediator in modulating NSC channel activity in rat RPE cells.

In support of our hypothesis that MAP kinase is a downstream effector in the $G_{\alpha i}$ cascade leading to NSC current activation in rat RPE cells, a plethora of recent studies has revealed that many receptors coupling to heterotrimeric G proteins, particularly PTX-sensitive G_i proteins, can activate the two major forms of MAP kinase in mammalian cells ERK1 and ERK2 (Luttrell *et al*, 1997). The signaling pathway(s) by which PTX-sensitive G proteins stimulate MAP kinase activation has been a topic of much research over the last 5 years. A multitude of different, yet potentially interacting, pathways have been described depending on the receptors, G proteins and effectors present in any given cell type. Despite this heterogeneity, considerable evidence now suggests that PTX-sensitive G_i -linked receptors can stimulate MAP kinase through G_i - $\beta\gamma$ subunit-mediated activation of a Ras and Raf-dependent pathway (Luttrell *et al*, 1997).

The central role of G_i - $\beta\gamma$ subunits in MAP kinase activation is supported by studies which demonstrate that G_i -coupled receptor effects on MAP kinase could be mimicked by overexpression of $\beta\gamma$ subunits, but not by activated forms of $G_{\alpha i}$ (Crespo *et al*, 1994; van Biesen *et al*, 1996). Further studies have demonstrated that $\beta\gamma$ complexes can transduce the signal downstream of G_i stimulation by activation of a number of nonreceptor tyrosine kinases including the Src family of kinases (Src, Fyn, Yes and Lyn) (Luttreil *et al*, 1997; Gutkind, 1998). Activated Src kinases can then mediate the tyrosine phosphorylation and activation of several intracellular substrates including a variety of

tyrosine kinases and the adaptor protein Src-dependent phosphorylation of Shc results in the recruitment of the Grb2-SOS complex to the plasma membrane where it activates Ras via stimulation of guanine nucleotide exchange. Activated Ras then recruits the MEKK isoform Raf-1 to the plasma membrane and initiates the phosphorylation cascade leading to MAP kinase (ERK1/ERK2) activation. Activated MAPKs can then phosphorylate a variety of cellular proteins including the MAP kinase-activated protein (MAPKAPs; e.g. Rsk-1 and Rsk-2), transcription factors, cytoskeletal elements, cytoplasmic PLA₂ and various upstream signaling elements (e.g. receptors, SOS, Raf-1 and MEK) (Denhardt, 1996).

Several recent studies, have also provided alternative pathways for MAP kinase activation by G_i-βγ subunits. In HEK-32 cells G_i-βγ mediates a PLC and calcium-dependent activation of the Ras/MAP kinase cascade (Della Rocca *et al*, 1997). In this pathway, the βγ complex activates PLCβ which liberates IP₃ and results in subsequent release of Ca²⁺ from intracellular stores. IP₃-mediated elevations in [Ca²⁺]_i lead to tyrosine phosphorylation and activation of Pyk2, a tyrosine kinase closely related to focal adhesion kinase (FAK). Pyk2 has recently received considerable attention for its involvement in linking G proteins that couple to PLC and PKC activation to the Ras-MAP kinase pathway (Luttrell *et al*, 1998). Furthermore, Pyk2 has been demonstrated, in a variety of studies, to be activated by multiple stimuli including PKC and elevated [Ca²⁺]_i. A similar pathway to the one described in HEK-32 cells has recently been proposed for PTX-sensitive Ca²⁺-dependent activation of MAP kinase by ATP/UTP in PC12 cells (Soltoff *et al*, 1998). Ca²⁺-dependent activation of MAP kinase may explain our observation that both MEK inhibition and reduction of intracellular Ca²⁺ decreased

the amplitude of the NSC current. Figure 3.21 depicts how the NSC current in rat RPE cells may be activated by the two signaling pathways linking G_i to the Ras/MAP pathway. Although we have no conclusive evidence for the presence of signaling pathway(s) linking G_i - $\beta\gamma$ activation to MAP kinase in rat RPE cells, it is possible that either pathway, or both pathways acting in concert, or an as yet unidentified pathway, could be stimulated by $GTP\gamma S$ and lead to regulation of the NSC current. In support of a role for a MAP kinase-dependent phosphorylation in regulating NSC current activity, a very recent study has demonstrated the presence of MAP kinases (ERK1 and ERK2) in human RPE cells (Hinton *et al*, 1998).

Although the factor(s) and receptor(s) responsible for initiation of the $G_{\alpha i}$ signaling pathway leading to NSC current activation have not yet been identified, several substances, including lysophosphatidic acid, muscarine, thrombin and α_{2A} -agonists have all been shown to couple G_i activation to the MAP kinase pathway (Luttrell *et al*, 1997). Recently, in cultured human RPE cells lysophosphatidic acid (LPA) has recently been shown to activate a nonselective cation current. Similar to the current described in this study, the LPA-activated NSC current was permeable to several monovalent cations, impermeable to anions and was PTX-sensitive (Thoreson & Chako, 1997). In addition to the RPE, LPA also activates a NSC current in retinal Muller cells (Puro, 1998). LPA is a simple water-soluble phospholipid that is rapidly produced and released from activated platelets. In a number of diverse cell types it exerts a wide range of biological effects including, cell proliferation, platelet aggregation, ion channel activation and neurotransmitter release (Wouter *et al*, 1997). The actions of LPA in these cell systems have been demonstrated to be primarily mediated via PTX-sensitive G_i protein activation

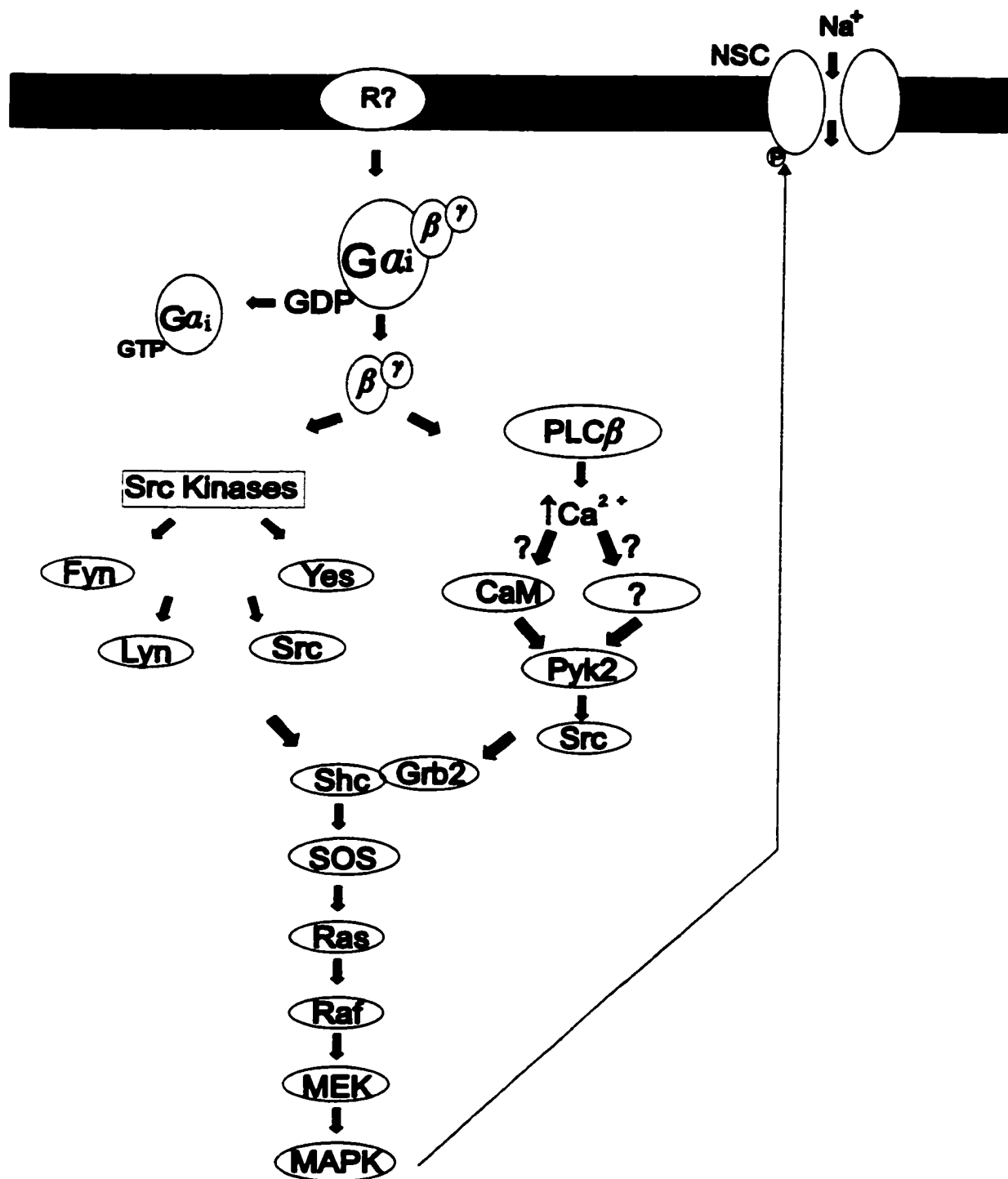


Figure 3.21. Schematic for NSC current activation by MAP kinase-dependent pathway. See text for details.

of the MAP kinase pathway. In light of these findings, the actions of LPA in modulation of cation channels in rat RPE cells warrants further investigation.

9. Function of NSC current in rat RPE cells

Macroscopic current recording does not provide information on the location of the NSC channel to either the RPE apical or basolateral membrane of RPE cells. It is therefore, difficult to propose a role for this channel in relation to current models of ion transport for this epithelium (Steinberg & Miller, 1979; Joseph & Miller, 1991; Edelman, Lin & Miller, 1994). In at least one epithelium (rat pancreatic duct), however, NSC channels are found on both the apical and basolateral membranes (Cook *et al.*, 1990). Thus, it is possible that activation of NSC channels in rat RPE cells would allow Na^+ influx, causing a depolarization of the cell relative to the resting potential. The ensuing depolarization, if sufficient, could activate other ion channels such as outwardly rectifying K^+ channels and Cl^- channels. Activation of apical K^+ conductances would provide an efflux pathway for K^+ that enters the cell via the apical $\text{Na}^+-\text{K}^+-2\text{Cl}^-$ cotransporter or the Na^+-K^+ pump. Basolateral Cl^- conductances may also be activated by NSC current-mediated depolarization altering Cl^- secretion across the epithelium and leading to changes in cell volume and transepithelial ion transport. Changes in transepithelial ion transport would alter chemical composition and hydration of the subretinal space (Joseph & Miller, 1991; Bialek & Miller, 1994).

A variety of roles for NSC currents in regulating cellular functions of non-excitable cells have been proposed. In cultured fibroblasts and colonic epithelial cells, agonist-induced activation of a NSC current has been proposed to play a role in cell

proliferation (Jung *et al* ,1992; Siemen & Gogelein, 1993). Under normal physiological conditions *in vivo* RPE cells are quiescent, having lost their mitotic ability once they have differentiated. However, in culture, or under pathophysiological conditions such as proliferative vitreoretinopathy, RPE cells have been shown to proliferate (Neill & Barnstable, 1990). Under these conditions, activation of the NSC current could play a role in stimulating the proliferative response in a similar manner to NSC channels in colonic epithelial cells. In macrophages, activation of a NCS current is involved in triggering phagocytosis and inflammatory responses (Hescheler & Schultze, 1991; Lipton, 1986; Young *et al*, 1983). In light of the central role played by the RPE in phagocytosis of shed rod outer segments roles, it is tempting to speculate that like macrophages, the activation of an NSC activation current is linked to phagocytosis in the RPE.

In summary, the present study demonstrates that activation of an NSC current in rat RPE cells is mediated by a PTX-sensitive G_{α_i} protein. We also show that elevations in $[Ca^{2-}]_i$ and kinase-dependent phosphorylation, potentially mediated by MAPK(s), are components of the signaling pathway linking G_{α_i} activation to regulation of NSC channel activity. Although the factor(s) and receptor(s) responsible for physiological initiation of the G_{α_i} signaling pathway leading to NSC current activation has not yet been identified, activation of this current *in vivo* could provide a pathway for significant Na^+ and cation influx. The resulting membrane depolarization could have important functional consequences for RPE-mediated ion transport and phagocytosis under normal physiological conditions, and may be involved in proliferative responses of the RPE in response to ocular trauma.

CHAPTER 4

Purinergic regulation of cation conductances and intracellular Ca^{2+} in cultured rat retinal pigment epithelial cells

Part of this work has been previously published in abstract form by Ryan, J.S., Baldrige, W.S. and Kelly, M.E.M. (1998). *Exp. Eye Res.* **67**(1): S.36

ABSTRACT

Extracellular ATP has been demonstrated to elevate cytosolic calcium ($[Ca^{2+}]_i$) in rat retinal pigment epithelial (RPE) cells, but its effects on ion channels have not been reported. In the present study, we used conventional whole-cell patch clamp and fluorescent $[Ca^{2+}]_i$ imaging techniques to investigate the effects of ATP on membrane currents and $[Ca^{2+}]_i$. Puffer application of 100 μ M ATP activated two cation conductances in rat RPE cells. In 62 % of the RPE cells a fast inward current was activated at negative membrane potentials. However, in 38% of RPE cells recorded from, a biphasic response to ATP was observed in which activation of the fast inward current was followed by activation of a delayed outward current. The inward current activated by ATP showed inward rectification, reversed at -1.5 ± 1 and was permeable to monovalent cations. These characteristics are consistent with activation of a nonselective cation current and involvement of P_{2X} purinoceptors. The outward current activated by ATP reversed at -68 ± 3 mV ($E_k = -84$ mV) and was blocked by Ba^{2+} ions consistent with the activation of a K^+ conductance. The outward K^+ conductance was also reduced by the maxi K_{Ca} channel blocker IbTX (10 nM) suggesting that ATP activated an outward K_{Ca} conductance in rat RPE cells via a P_{2Y} coupled signaling pathway. The nonselective cation and outward $I_{K(Ca)}$ current were activated by UTP, ADP and 2MeSATP but not by α, β methyl-ATP or adenosine. In Fluo-3 loaded RPE cells, ATP and UTP elevated $[Ca^{2+}]_i$ in a manner not dependent on extracellular Ca^{2+} influx. These results suggest that rat RPE cells express two types of purinoceptors. P_{2X} receptors gate activation of the

nonselective cation conductance and G protein coupled P_{2Y} receptors mediated Ca^{2+} release from intracellular stores and activation of a calcium-activated K^+ current.

INTRODUCTION

The retinal pigment epithelium (RPE) carries out a number of roles that are essential for the maintenance and viability of the neurosensory retina. These roles include phagocytosis of shed rod and cone outer segments, melanin synthesis and recycling and regulation of subretinal volume via ion-coupled fluid absorption (Zinn & Benjamin-Henkind, 1979; Clark, 1986; Steinberg & Miller, 1979). In order to carry out these diverse functions, the RPE must be able to detect and respond to changes in its environment via paracrine signals coming from the adjacent choroid and/or neural retina.

Regulation of RPE function via signaling molecules that act at cell-surface receptors has received considerable attention in recent years. This interest stems from evidence suggesting that defects in RPE signaling pathways may play a role in a number of ocular pathologies, including retinitis pigmentosa and central serous retinopathy (Heath *et al*, 1995; Zamir, 1997). A number of metabotropic receptors have been identified on the RPE including those for dopamine, acetylcholine, epinephrine and adenosine (Dearry & Burnside, 1988; Friedman *et al*, 1988; Friedman *et al*, 1989; Frambach *et al*, 1990). Activation of these receptors by their respective signaling molecules has been linked to changes in light-evoked responses (Dearry *et al*, 1990; Gallenmore & Steinberg, 1990), phagocytic ability (Gregory *et al*, 1994) and ion and fluid transport across the RPE (Edelman & Miller, 1991; Joseph & Miller, 1992). Recently, in monolayers of bovine and rat RPE, extracellular adenosine 5'-triphosphate (ATP) and uridine triphosphate (UTP) were demonstrated to induce changes in intracellular Ca^{2+} and transepithelial ion and fluid movement (Stalmans & Himpens,

1997b; Peterson *et al*, 1997). These findings support the presence of metabotropic purinoceptors and suggest that extracellular ATP may act as an important paracrine signal in the RPE.

Purinoceptors are divided into two main classes, P₁ and P₂, based on their selectivity for adenosine and ATP, respectively (Burnstock & Kennedy, 1985). Adenosine, or P₁, receptors, are G protein-coupled receptors that respond only to purine nucleosides and nucleoside monophosphates. They are subdivided further into adenosine A₁, A₂ or A₃ receptors based on their ability to inhibit or activate adenyl cyclase, respectively. ATP, or P₂, receptors are activated primarily by purine or pyrimidine nucleotide triphosphates. This receptor family constitutes a diverse set of proteins that are linked by their common ability to bind extracellular ATP and elicit increases in $[Ca^{2+}]_i$ and other ions. Their classification into receptor subtypes had previously been based upon pharmacological profiles of the response to ATP analogues. Recent advances in the molecular biology of P₂ receptors however, has now identified more than a dozen types of P₂ receptors and has reorganized them into two major subclasses: the P_{2X} purinoceptors and the P_{2Y} purinoceptors (Barnard *et al*, 1997). Seven P_{2X} receptor subtypes have been identified and classified on the basis of sequence homology, agonist/antagonist sensitivity and kinetics of receptor desensitization. P_{2X} receptor subtypes comprise a novel family of ligand-gated ion channels. These ionotropic receptors gate nonselective cation channels permeable to various ion, including Ca²⁺ (Barnard, 1992). The seven subtypes of P_{2Y} receptors belong to the larger superfamily of 7 transmembrane proteins that are G protein-coupled (metabotropic) receptors. Although signaling molecules downstream from P_{2Y} receptors have not been fully classified, all

subtypes to date have been linked by heterotrimeric G proteins to phospholipase C (PLC) activation, generation of inositol triphosphate (IP₃) and diacylglycerol (DAG), and subsequent release of Ca²⁺ from internal stores (Barnard *et al*, 1994).

Several lines of evidence support a role for adenosine (P₁) receptors in ocular physiology. In the rat eye, A₁, A_{2A} and A_{2B} purinoceptor mRNA is expressed in a wide variety of ocular tissues including the retinal ganglion cells (A₁ and A_{2A}), ciliary processes (A₁, A_{2A} and A_{2B}) and inner nuclear layer (A_{2A}) (Kvanta *et al*, 1997). The RPE expresses mRNA for A_{2A} purinoceptors and the presence of A_{2B} receptors has also been suggested (Blazynski, 1993; Kvanta *et al*, 1997). Functionally, activation of P₁ receptors has been found to be important in regulation of retinal blood flow (Crosson *et al*, 1994), mobilization of intracellular Ca²⁺ in retinal Muller cells and modulation of rod outer segment ingestion by the RPE (Gregory *et al*, 1994).

Pharmacological and functional data support the presence of P_{2Y} purinoceptors in the chick neural retina (Sugioka *et al*, 1996), ovine lens cells (Churchill & Louis, 1997), bovine ciliary epithelial cells (Shahidullah & Wilson, 1997) and rat and bovine RPE (Stalmans & Himpens, 1997b; Peterson *et al*, 1997). More recently, P_{2Y2} purinoceptors were found to be expressed in cultured human RPE cells (Sullivan *et al*, 1997). There is less evidence to support the existence of P_{2X} purinoceptor subtypes in the eye although P_{2X} receptor mRNA has been localized to the rat retina where it was found to be expressed in photoreceptors, inner nuclear layer neurons and retinal ganglion cells (Greenwood *et al*, 1997). In rat retinal Muller cells it has been demonstrated recently that activation of putative P_{2X} receptors mediates elevations in intracellular Ca²⁺ (Neal *et al*,

1998). However, to date, no evidence exists for the expression of functional P_{2X} purinoceptors in the mammalian RPE.

In this chapter we report that extracellular ATP, UTP and other nucleotides, but not adenosine, activate two distinct cation conductances. The rapid activation of a inwardly rectifying cation current suggests, for the first time, the presence of functional P_{2X} purinoceptors in the rat RPE. We also provide evidence for the presence of G protein-coupled P_{2Y} purinoceptors linked to activation of a Ca²⁺-sensitive outward K⁺ conductance and, with the use of nonratiometric Ca²⁺-imaging using Fluo-3, we have demonstrated purinergic-mediated increases in [Ca²⁺]_i.

Our findings that extracellular ATP (or UTP)-mediated cation channel activation and [Ca²⁺]_i mobilization in the RPE support a role for ATP and/or UTP as paracrine signals in the RPE and suggest that they may act to regulate RPE function under physiologic and/or pathologic conditions.

MATERIAL AND METHODS

1. Cell Dissociation and Culture

Rat RPE cells were dissected, cultured and identified as previously described (GENERAL METHODS, section 1.1).

2. Electrophysiological Recording

2.1 Superfusion and Solutions

Superfusion of isolated cells has been described (see GENERAL METHODS). In these experiments the standard extracellular solution contained (in mM): NaCl, 130; KCl, 5; Na⁺-HEPES, 10; NaHCO₃, 10; MgCl₂, 1; CaCl₂, 1 and glucose, 10 (solution A, table 1 in GENERAL METHODS). Replacement of extracellular Na⁺ was accomplished using equimolar substitution with either choline chloride or N-methyl-D-glucamine (NMDG) chloride (solutions B and D, table 1). In some experiments the extracellular solution was made nominally Ca²⁺-free by including 1.5 mM EGTA with 0.2 mM CaCl₂ (solution G, table 1 in GENERAL METHODS). The extracellular calcium concentration with this substitution was estimated to be <10 nM. Calcium concentration was calculated using a software program based on the algorithm of Goldstein (1979; provided by J. Kleinschmidt). The standard intracellular solution contained (in mM): K⁺-aspartate, 100; KCl, 10; HEPES acid, 20; MgCl₂, 1; CaCl₂, 0.4; EGTA, 1; ATP, 1 and 0.1 GTP (solution J, table 1 in GENERAL METHODS).

2.2 Drugs

Stock solutions of adenosine, ATP, UTP, 2MeSATP, ADP and $\alpha\beta$ methylATP were all diluted in the extracellular recording solution and applied via pressure injection from a micropipette (see GENERAL METHODS, section 3.1). The purinergic antagonists (suramin and PPADS), the potassium channel blockers (Ba^{2-} and IbTX) and the chloride channel blocker (DIDS) were all included in the extracellular solution and bath perfused. All drugs were used at the concentration cited in the RESULTS.

2.3 Electrophysiological Recording Techniques

As before (Chapter 1, section 3.2), whole-cell patch clamp techniques were used to measure currents in isolated RPE. All the data and current-voltage relationships shown have been corrected for LJP. The LJP using standard low Cl^- intracellular and standard 5 mM KCl extracellular solutions (solutions A and J, table 1 in GENERAL METHODS) or cation-substituted extracellular solutions (solutions B and D, table 1 in GENERAL METHODS).

3. Ca^{2+} Imaging

3.1 Calcium Indicator Dye Loading

RPE cells were isolated as previously described and were cultured on glass coverslips for 2-5 days before loading with the membrane-permeant (acetomethoxy ester) form of the Ca^{2+} indicator Fluo-3 (Fluo-3AM). When bound to Ca^{2+} the fluorescence

emitted by Fluo-3 increases (Kao *et al*, 1989). We chose to use Fluo-3 as the calcium indicator because of its large optical signal, which allows for very good signal-to-noise ratio. A stock solution of Fluo-3 AM was prepared by dissolving 50 μg of the dye in 50 μl of DMSO. The dye stock solution was then diluted in standard extracellular 5K^+ solution (solution A, table 1 in GENERAL METHODS) containing 0.01% pluronic F-127 to give a final concentration of 10 μM Fluo-3AM. To load RPE cells with Fluo-3, cells were incubated with the dye solution for 1 hour at RT (22-23°C), and then rinsed with 5K^+ solution.

3.2 Pharmacological Treatment

RPE cells, attached to glass coverslips, were placed in a shallow bath chamber (~1-2 ml) on the stage of Nikon UM-2 fluorescent microscope. The cells were continuously superfused with standard extracellular solution at a rate of 1-2 ml/min. The extracellular solution was made nominally Ca^{2+} -free by reducing extracellular calcium to 0.2 mM CaCl_2 and adding 1.5 mM EGTA (solution G, table 1 in GENERAL METHODS). The extracellular calcium concentration with this substitution was estimated to be <10 nM. Pharmacological agents (ATP, UTP or GTP) were dissolved directly into the extracellular solutions and bath superfused at the concentrations cited in RESULTS. A baseline intensity level was established in standard extracellular solution before addition of any drugs. All experiments were conducted at RT (20-22°C).

3.3 *Optical Recording*

Isolated RPE cells were viewed by a Zeiss 40X water immersion objective on a Nikon UM-2 fluorescent microscope. RPE cells loaded with Fluo-3 AM were imaged using a cooled Photometrics CH250 CCD camera (Photometrics, Tuscon AZ) with a 200 ms exposure time. Stimulation for the excitation and fluorescence of the Fluo-3 dye was provided by a 100W mercury-vapor lamp filtered by a -1.6 log neutral density filter, to minimize damage of the RPE cells with excessive light energy, and an appropriate filter set (Nikon B-2A, excitation wavelength of 450-490 nm; emission 520-560; dichroic 510 nm). An electronic shutter (Uniblitz, Rochester, NY) was used to limit light exposure and images (100 pixels) were recorded and saved every 5.5 sec by the IPLab Spectrum program (Signal Analytics Co., Vienna, VI)

3.4 *Quantitative Analysis*

Changes in the intensity of Fluo-3 fluorescence indicate changes in $[Ca^{2+}]_i$ (Kao *et al*, 1989; Haughland, 1992). The fluorescence intensity over the RPE cell body was measured before, during and after drug application. Changes in fluorescent intensity were quantified by determining the increase in intensity (F) during drug application and then normalizing this increase by dividing by the average baseline intensity calculated for 10 images before exposure of the cell to drug (F_{rest}). These relative changes in fluorescent intensity were expressed as:

$$\frac{\Delta F}{F} = (F - F_{rest}) / F_{rest}$$

The $\Delta F/F$ values obtained for RPE cells in response to drug application are intended only as qualitative indicators of changes in $[Ca^{2+}]_i$, as these values are not linearly related to absolute values of free $[Ca^{2+}]_i$. Using IPLab software, the $\Delta F/F$ values obtained for RPE cells in response to drug application were converted into pseudocolor image representations (see Figure 4.9 in RESULTS)

4. Materials

α,β MethylATP, 2MeSATP, suramin, PPADS and pluronic F-127 were obtained from Calbiochem (LaJolla, CA, USA). Fluo-3AM was obtained from Molecular Probes (Eugene, OR, USA). IbTX was from Peninsula Laboratories Inc. (Belmont, CA, USA). All other chemicals were from Sigma.

RESULTS

1. Effects of extracellular adenosine on whole-cell current

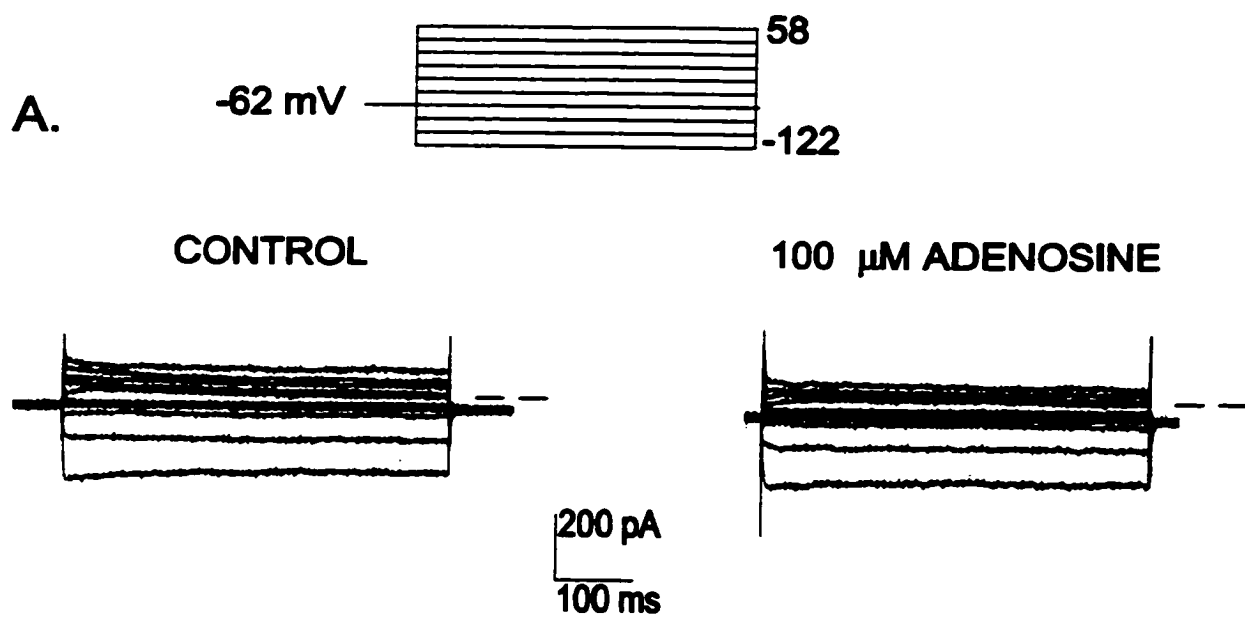
The presence of adenosine receptors on mammalian RPE cells (Hall *et al*, 1992) suggested that these purinoceptors may play a role in modulating ionic currents in these cells. We examined the effect of adenosine on whole-cell currents in isolated rat RPE cells using standard intracellular (solution I, table 1 in GENERAL METHODS) and extracellular (solution A, table 1 in GENERAL METHODS) solutions. Figure 4.1A shows whole-cell currents recorded from a representative RPE cell before and after puff application of 100 μ M adenosine. In this, and 8 other cells tested, the mean amplitude of the control current measured at +58 mV (106 ± 25 pA/pF) and -62 mV (-115 ± 12 pA/pF) was unaffected by 100 μ M adenosine (84 ± 21 pA/pF at +58 mV and -84 ± 12 pA/pF at -62 mV) (Figure 4.1B). The results suggest that activation of adenosine receptors in cultured rat RPE cells does not result in alterations in whole-cell current.

2. Effects of extracellular ATP on whole-cell current

2.1 ATP activates two conductances in rat RPE cells

In the absence of an effect of P₁ receptor activation on whole-cell currents in rat RPE, we next examined the effects of P₂ purinoceptor activation. Recent evidence supports the presence of P₂ receptors on mammalian RPE cells (Stalmens & Himpens, 1997b; Peterson *et al*, 1997). We used ATP to examine the effect of P₂ receptor

Figure 4.1 Effect of adenosine on whole-cell current in rat RPE. (A) Whole-cell current recorded from a representative RPE cell in the absence (left panel) or presence (right panel) of 100 μM adenosine. Current were recorded in standard 140 KCl intracellular (solution I, table 1) and standard 140 NaCl external (solution A, table 1) solution. Cell capacitance was 35 pF. (B) Mean \pm SE current amplitude (pA) measured at +58 and -62 mV in the absence (open bars) and presence of 100 μM adenosine. Adenosine had no effect on whole-cell current in isolated rat RPE cells (n=9).



B.

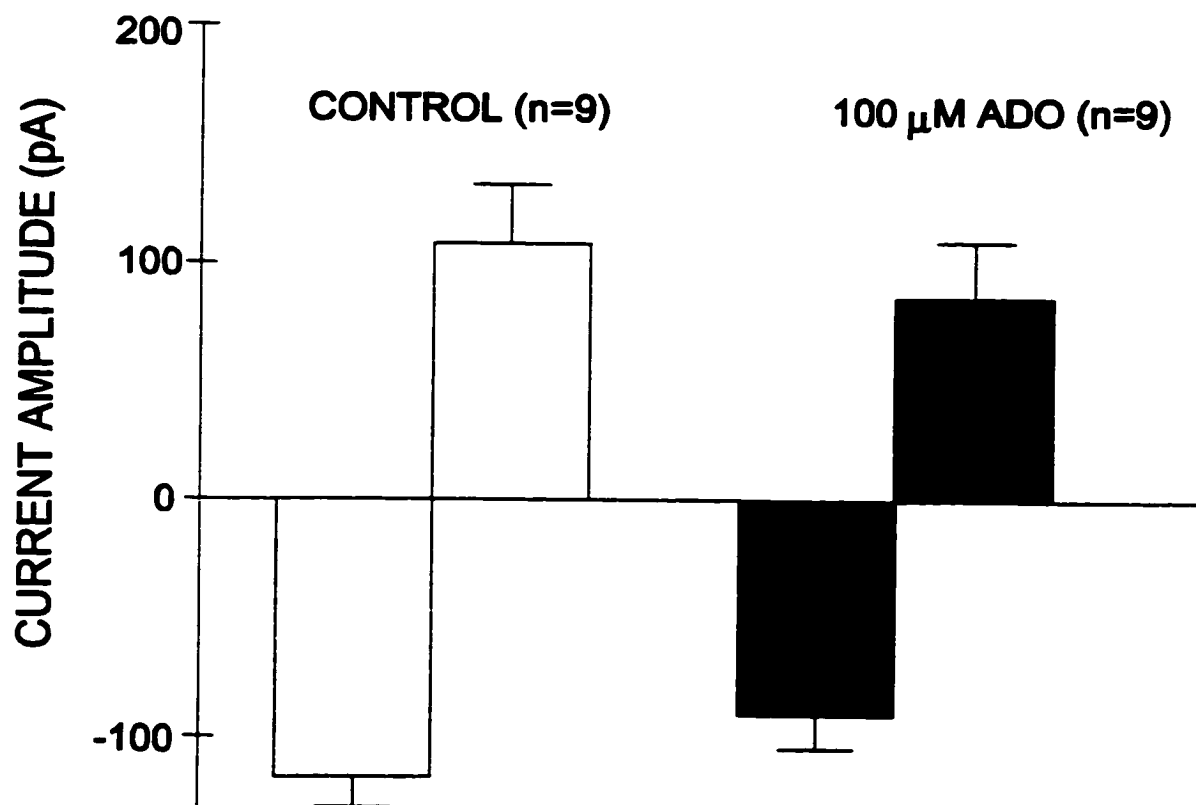


Figure 4.1

activation on whole-cell currents in cultured rat RPE cells in standard intracellular (solution I, table 1 in GENERAL METHODS) and standard extracellular (solution A, table 1 in GENERAL METHODS) recording solution. We initially chose ATP as our agonist as this nucleotide has been demonstrated to be an effective agonist at all P_{2X} and P_{2Y} subtypes described with the exception of the P_{2Y6} subtype (Barnard *et al*, 1997). Figure 4.2 shows the effects of ATP on whole-cell currents in rat RPE cells. Cells were voltage-clamped at various potentials and 100 μ M ATP was applied via 4 sec puffer application. The cells were allowed to recover for a minimum of 4 min between successive applications of ATP. Figure 4.2A shows the response of a representative RPE cells to 4 sec puffer application of 100 μ M ATP. When the cell was held at -62 mV or -22 mV, 100 μ M ATP-evoked inward current that activated rapidly and decayed only slightly during the ATP application (Figure 4.2A). At positive potentials ($+18$ mV) ATP had no effect on whole-cell current. In 57/ 92 rat RPE cells tested, ATP activated only an inward current. In this study, RPE cells were used between 2-5 days in culture as earlier experiments demonstrated that older cells which have begun to dedifferentiate and proliferate were not responsive to ATP, suggesting a change in receptor and/or ion channel expression. Loss of P_{2X} receptors with time in culture has been demonstrated for other cell types (Erlinge, 1998). The mean peak amplitude of the ATP-evoked inward current measured at -62 mV was -12.5 ± 1 pA/pF ($n=57$). The time constant (τ) for deactivation of the cation current, measured from the peak of the inward current, varied widely from 4.6 to 14 sec (8.3 ± 0.7 sec).

Figure 4.2B shows the current-voltage plot for a representative RPE cell before and after puffer application of 100 μ M ATP. The I-V plots were obtained from voltage ramp commands between -122 and $+48$ mV. Very little whole- cell current is present in this cell before drug

Figure 4.2. ATP activates two conductances in rat RPE cells. (A). ATP activates an inward cation current. The left panel shows the current activated by 4 sec puff application of 100 μ M ATP in a representative RPE cell held at -62, -22 and +18 mV. Fast-activating inward current is apparent at -62 and -22 mV with little current at +18 mV. Cell capacitance was 35 pF. (B). shows I-V curves for another RPE cell constructed from 2 sequential 8 sec voltage ramps between -122 and +38 mV in absence or presence of 100 μ M ATP. The activation of an inwardly rectifying current is apparent. (C) ATP activates a biphasic conductance change. The left panel shows the current activated by 4 sec puff application of 100 μ M ATP at -62, +22 and +38 mV in a representative RPE cell. Cell capacitance was 22 pF. Inward current is apparent at -62 mV and outward current is evident at depolarized potentials. (D). The I-V curves for 5 sequential 8 sec voltage ramps obtained from a representative RPE cell with a biphasic response to ATP is shown in the right panel. In the presence of ATP activation of fast inward current (ATP 1) is followed by activation of a large outwardly rectifying current (ATP 2).

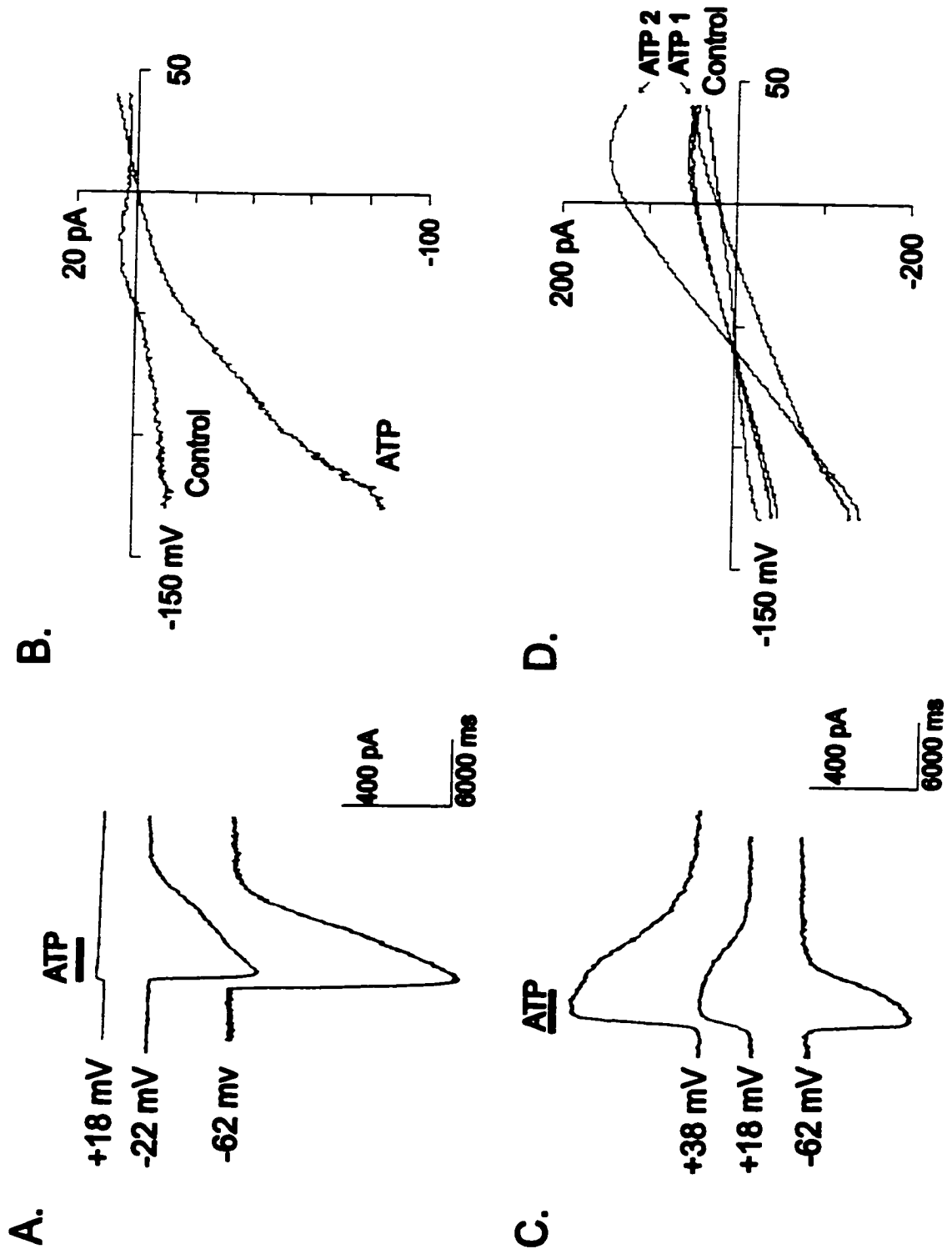


Figure 4.2

application. The I-V curve shows a small inwardly rectifying current that reverses around -52 mV. Very little outward current is apparent. Puffer application of ATP in this cell evoked a large inward current at all potentials negative to 0 mV. The ATP-activated current shown in Figure 4.2B was obtained by subtracting currents recorded under control conditions from currents recorded during ATP application. The current induced by ATP was inwardly rectifying and reversed direction close to 0 mV, suggesting the activation of a cation conductance.

In 35/92 RPE cells tested we also noted that ATP induced a biphasic conductance change. Figure 4.2C left panel, shows a representative RPE that had a biphasic response to 100 μ M ATP, suggesting activation of two conductances. At a holding potential of -62 mV the fast inward current described above is apparent. However, in contrast to Figure 4.2A, at positive potentials ($+18$ and $+38$ mV) the activation of a large outward current is apparent. The I-V relationships shown in Figure 4.2D were obtained from five sequential 8 second voltage ramps between -122 and $+48$ mV in a representative RPE cell that had a biphasic response to ATP. Control current, in the absence of drug, had both an inward and outwardly rectifying conductance that activated around -40 mV. Puffer application of ATP initially activated the fast inward current which shifted the reversal potential of the whole-cell current 25 mV positive (ramp 1). Subsequently, the ATP-induced inward current decreased at potentials between -122 and -62 mV, but began to increase at more positive potentials (ramps 2-4). When the inward current had returned to control values the outward current was still increased over control. The peak of the outward current (ramp 2) was reached within 16 sec of ATP application at which time the I-V relationship reveals an outwardly rectifying current that reverses at -56 mV. In most RPE cells

showing this biphasic response there was prominent delay between activation of the inward current and peak of the outward current. The slow shift in the reversal potential from -15 mV to -65 mV, towards the calculated reversal potential for K^+ (-84 mV) under our experimental conditions, suggested that, in addition to a cation current, ATP was also activating a K^+ -selective current in rat RPE cells.

3. ATP-activated cation conductance

3.1 Nonselectivity of the cation current

We characterize the ionic selectivity of the ATP-activated voltage-dependent inward current using low Cl^- intracellular solution (solution I, table I in GENERAL METHODS) designed to separate Cl^- currents (reversing around -40 mV) from cation currents (reversing at 0 mV). Under these recording conditions the ATP-activated current reversed closer to that expected for a cation selective channel (-1.5 ± 1 mV; $n=27$) suggesting that the current activated by ATP was carried by cations and not Cl^- . To further verify this, we also tested the sensitivity of the ATP-activated inward current to the disulphonic stilbene DIDS, which has been demonstrated to block Cl^- channels in a variety of cell types, including the RPE (Hughes & Segawa, 1993; Stauß *et al*, 1998). Micromolar amounts of DIDS have also been shown to block native $P2X$ purinoceptors in superior cervical ganglia and cloned $P2X$ purinoceptors from smooth muscle cells (Connolly and Harrison, 1995; Evans *et al*, 1995). Neither the reversal potential nor the amplitude of the ATP-activated inward current measured in 4 RPE cells at -69 mV (-225 ± 92 pA) was significantly affected after 5 min superfusion of the cells with 500 μ M

DIDS (-170 ± 57 pA). These results rule out the involvement of Cl^- current and identify the conductance activated by ATP as a nonselective cation current.

We investigated the cation selectivity of the ATP-inward current by substituting extracellular Na^+ with other monovalent cations. Figure 4.3A shows the current voltage plot for a representative RPE cell which displayed ATP-activated inward current but no outward current. The ATP-induced inward current was recorded in standard recording solution (solution A, table 1 in GENERAL METHODS) and in solution in which extracellular Na^+ was replaced with NMDG (solution D, table 1 in GENERAL METHODS). Substitution of Na^+ for NMDG shifted the reversal potential of the ATP-activated current from -5 mV to -45 mV and reduced the current amplitude measured at -62 mV from -15 pA/pF to -4 pA/pF. In cells with a biphasic response to ATP the late outward current amplitude and reversal potential were unaffected by cation substitution but in all cases substitution of extracellular Na^+ for choline or NMDG significantly reduced the amplitude of the ATP-activated inward current. The mean current amplitude for the ATP-activated inward current measured in 5-7 cells in standard Na^+ (-18 ± 2 pA/pF), choline-substituted (-9 ± 2 pA/pF; solution B, table 1) or NMDG-substituted (-5 ± 0.6 pA/pF) solutions are shown in Figure 4.3B.

The fast activating, ATP-induced inward current recorded in cultured rat RPE cells has electrophysiological characteristics identical to those described for cloned and native P2X purinoceptors (Humphrey *et al*, 1995; Soto *et al*, 1996). Similar to other P2X receptors, this current was also highly permeable to monovalent cation but not anions. These findings are consistent with the involvement of a P2X receptor subtypes in gating the inward current activated by ATP in rat RPE cells

Figure 4.3 Inward current activated by ATP is a nonselective cation current. (A) Representative current-voltage curves for the ATP-activated inward current in a representative rat RPE cell showing the effect of extracellular Na^+ replacement. When Na^+ (solution A, table 1) was substituted for by NMDG (solution D, table 1), current magnitude was significantly reduced and current reversal potential shifted from -5 to -40 mV. (B) Histogram shows mean \pm SE amplitude of the ATP-activated cation current measured at -69 mV in 5-7 cells.

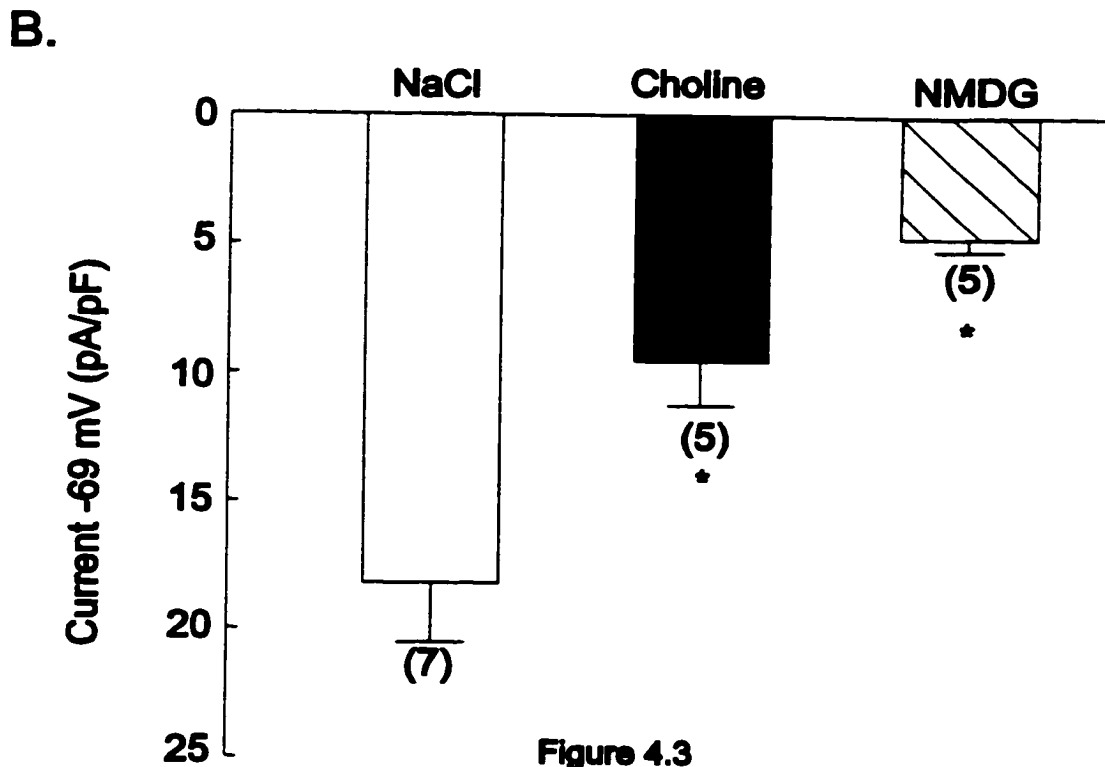
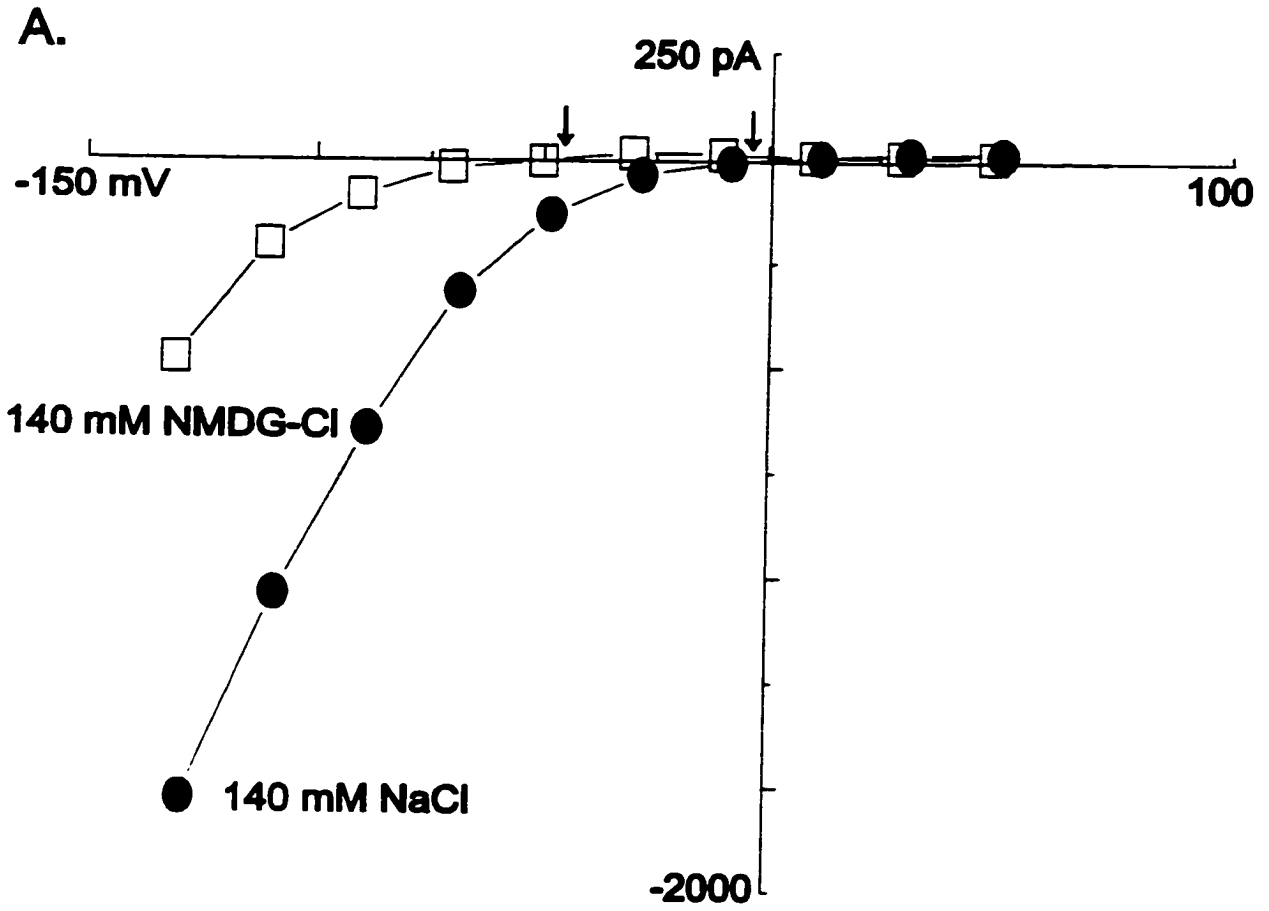


Figure 4.3

3.2 Sensitivity to extracellular Ca^{2+}

Nonselective cation channels gated by P_{2X} receptors are not only permeant to Na^+ and K^+ but also have varying degrees of permeability to larger divalent cations such as Ca^{2+} (Humphrey *et al*, 1995; Soto *et al*, 1996). We examined the effects of extracellular Ca^{2+} on the ATP-induced cation current by activating the current in nominally Ca^{2+} -free external solution ($[Ca^{2+}]_o < 10$ nM; solution G, table 1 in GENERAL METHODS). Figure 4.4 shows the mean current amplitude of the ATP-activated inward current measured at -69 V in 4 RPE cells bathed in regular (2 mM) or nominally Ca^{2+} -free (< 10 nM) extracellular solution. Removal of extracellular Ca^{2+} slightly reduced the current amplitude measured at -69 mV in 3/4 cells tested from -9 ± 1 pA/pF to -7 ± 0.8 pA/pF, corresponding to a mean decrease of 23 ± 8 % ($p > 0.05$). These results suggest that extracellular Ca^{2+} influx does not contribute significantly to the current flow through this nonselective cation channel.

3.3 Effect of the P_2 antagonists PPADS and suramin

In attempts to identify the subtype of P_{2X} purinoceptor, the sensitivity of the ATP-activated inward cation conductance to pharmacological blockade by PPADS and suramin was investigated. PPADS and suramin have been purported to act as selective antagonists at P_{2X} receptors and for many years they have been used as pharmacologic tools to discriminate between P_{2X} and P_{2Y} receptors (Surprenant *et al*, 1995; Buell *et al*, 1996). More recent evidence, however, indicates that these antagonists lack selectivity for P_{2X} receptors and are weak or ineffective blockers at certain P_{2X} receptor subtypes,

Figure 4.4. ATP-activated NSC current is not affected by removal of extracellular Ca^{2+} . Bar graph shows mean \pm SE current amplitude for the ATP-activated NSC current measured at -69 mV. Open bar is mean amplitude of the ATP-activated NSC current in 3 RPE cells bathed in 2 mM Ca^{2+} extracellular solution (Solution A, table 1). Hatched bar shows mean current amplitude of the ATP-activated NSC current measured in the same 3 cells in nominally Ca^{2+} -free extracellular solution ($[\text{Ca}^{2+}] < 100$ nM; solution G, table 1). Amplitude of the cation current is not significantly affected by removal of extracellular Ca^{2+} ($p > 0.05$). Data has been normalized for cell capacitance.

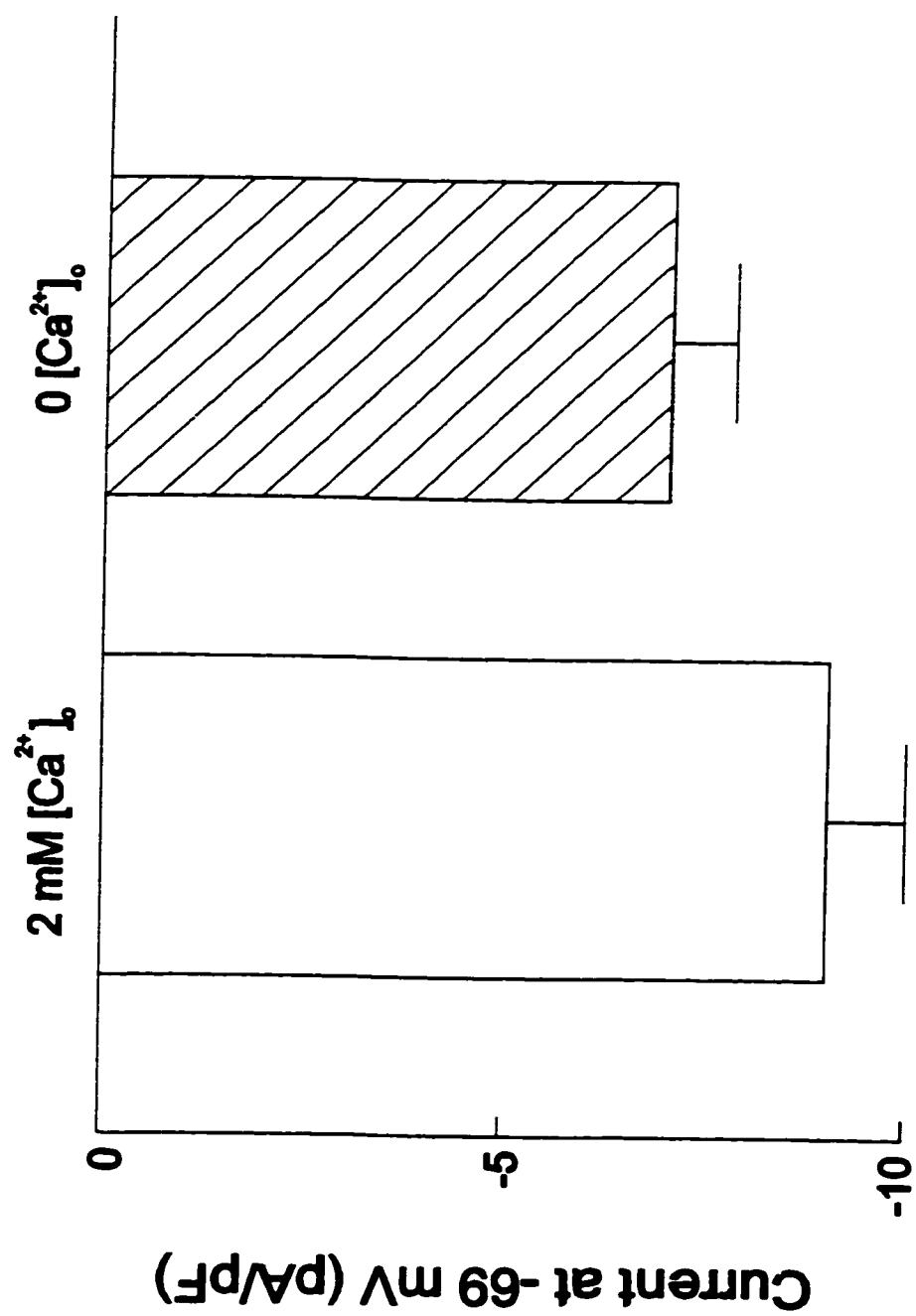


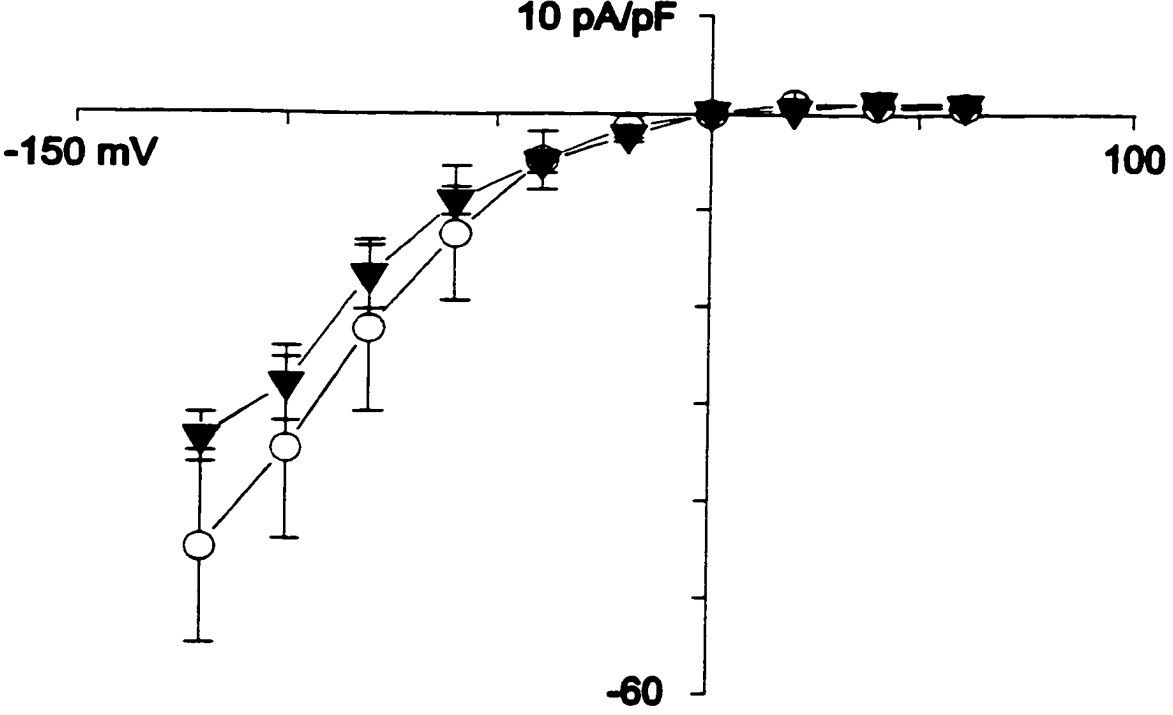
Figure 4.4

and thus their use as tools for characterizing P2 purinoceptors is limited (Humphrey *et al*, 1995; Barnard *et al*, 1997).

Figure 4.5A shows the mean I-V curve for the ATP-activated inward current measured in the presence and absence of 100 μ M of the P_{2x} antagonist suramin. In all 3 cells tested neither the amplitude nor the reversal potential of the inward cation current was significantly affected by a 15 min exposure to this antagonist. Figure 4.5B shows the mean (\pm SEM) data for the effect of 100 μ M suramin or PPADS on the inward current activated by 100 μ M ATP. Peak current amplitude for the ATP-induced inward current was measured at -69 mV in the same 3 cells in the absence and presence of antagonist. Cells were allowed 10 min period between successive ATP applications, a time that has been previously shown (see Figure 4.2) to allow for recovery from receptor desensitization. The mean amplitude of the cation current activated by ATP in the absence of either antagonist (-9 ± 1 pA/pF and -17 ± 9 pA/pF) was not significantly affected by either suramin (-13 ± 7 pA/pF) or PPADS (-15 ± 10 pA/pF). The concentration and duration of application of suramin and PPADS used in this experiment has been shown to inhibit currents through native and cloned P_{2x1}, P_{2x2}, P_{2x3} and P_{2x5} purinoceptors in a variety of cell types (Barnard *et al*, 1997). However, P_{2x4} and P_{2x6} purinoceptors have been found to be resistant, or at least partially resistant, to antagonist blockade (Collo *et al*, 1996; Soto *et al*, 1996), suggesting the possibility that one of these subtypes is involved in gating the ATP-activated cation current in rat RPE cells.

Figure 4.5. ATP-activated NSC current is insensitive to P₂ antagonists. (A) Mean \pm SE current-voltage plot for the ATP-activated inward current measured in 3 RPE cells in the absence (\blacktriangledown) or presence (\circ) of 100 μ M suramin. (B) Bar graph shows the mean \pm SE amplitude of the ATP-activated inward current measured at -69 mV in the same 3 cells before (open bars) and after (closed bars) 15 min bath superfusion with 100 μ M of the P₂ antagonist suramin (n=3) or PPADS (n=3). Neither P₂ antagonist had any effect on the amplitude of the ATP-activated NSC current. Data has been normalized for cell capacitance.

A.



B.

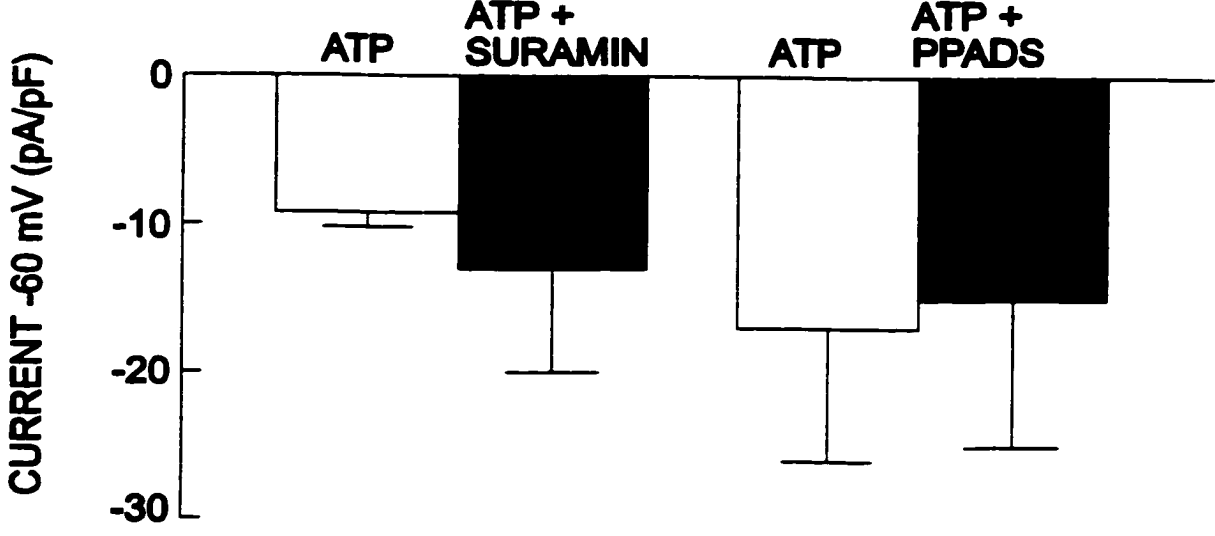


Figure 4.5

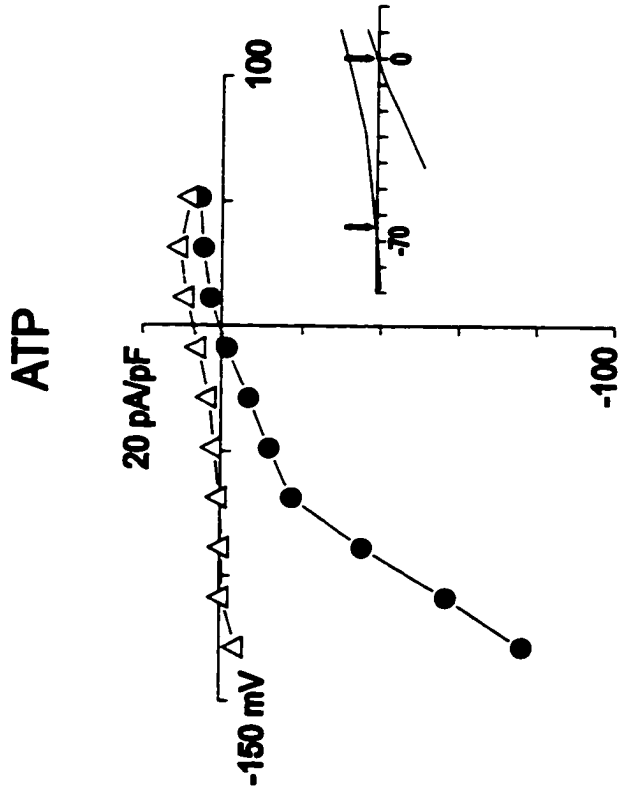
4. ATP-activated K⁺ current

4.1 Pharmacological characterization of the ATP-activated K⁺ current

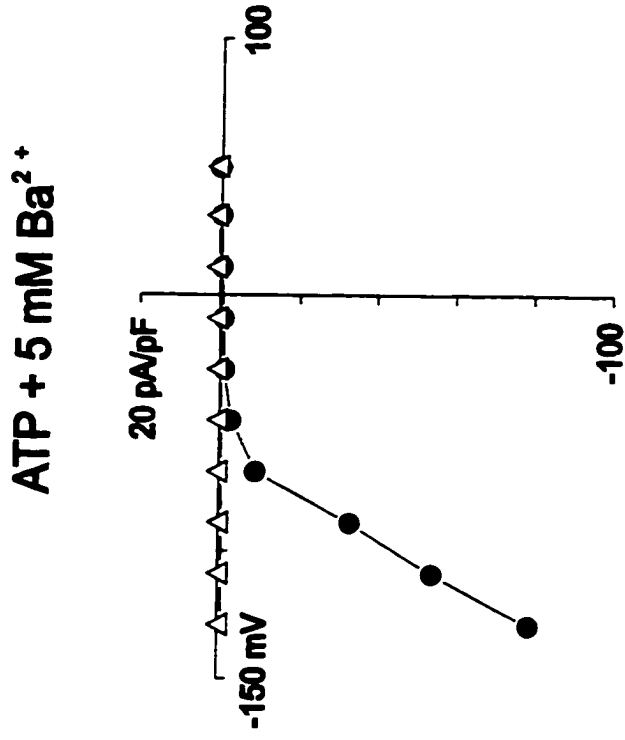
To confirm that the delayed outward current activated by ATP was K⁺-selective, we tested its susceptibility to blockade by a number of known K⁺-channel blockers. Figure 4.6A shows I-V curves for the ATP-activated cation currents in a representative RPE cell that exhibits a biphasic response to ATP. Puffer application of 100 μM ATP initially only elicited the fast inward nonselective cation current that reverses close to 0 mV. Subsequently, 10 sec after ATP application at which time the fast inward current had decayed, a delayed outwardly rectifying current activated and the reversal potential for the whole-cell current shifted to -66 mV, towards the reversal potential for K⁺ under our recording conditions (see inset). Figure 4.6B shows the I-V curve for the same RPE cell 5 min after superfusion with 5 mM Ba²⁺. This concentration of external Ba²⁺ has been shown previously to block K⁺-selective outward currents in our cultured rat RPE cells (see Chapter 3, section 4.2). Puffer application of 100 μM ATP, as before, activates the fast inward cation current in the presence of Ba²⁺ ($E_{rev} = 0$ mV). However, the second I-V plot recorded 10 sec after ATP application had very little whole-cell current, indicating that Ba²⁺ blocked activation of the ATP-activated outwardly rectifying current. Figure 4.6C shows the mean (± SE) current amplitude of the ATP-activated outward current measured at +31 mV in the same 10 cells in the absence or presence of 5 mM Ba²⁺ 10-15 sec after ATP application. The amplitude of the ATP-activated outward current under control conditions (703 ± 200 pA) is significantly reduced ($p < 0.05$) in the presence of Ba²⁺ (50 ± 14 pA). Figure 4.6D shows the

Figure 4.6. ATP activates an outwardly rectifying K^+ current in rat RPE cells. (A) Current-voltage (I-V) plots for a representative RPE cell that has a biphasic response to puffer application of 100 μ M ATP. ATP-initially activates a NSC current that reverses around 0 mV (\bullet). 10 sec after ATP application the inward cation current is inactivated and an outwardly rectifying current is now apparent that reverses at -70 mV (Δ). B. The I-V plot shows ATP-activated current measured in the same RPE cell after a 10 min bath superfusion of 5 mM Ba^{2+} . ATP still activates the initial fast inward cation current (\bullet), but the activation of the outward current is abolished (Δ). (C) The histogram shows mean \pm SE current amplitude measured at +31 mV in 10 RPE cells. ATP (black) significantly increased the outward current measured at +31 mV and this increase was blocked by 5 mM Ba^{2+} . (D) The histogram shows mean \pm SE reversal potential for the ATP-activated current measured during and 20 sec after puffer application of 100 μ M ATP in 6 RPE cells in the absence (open bar) and presence of 5 mM Ba^{2+} (black bar).

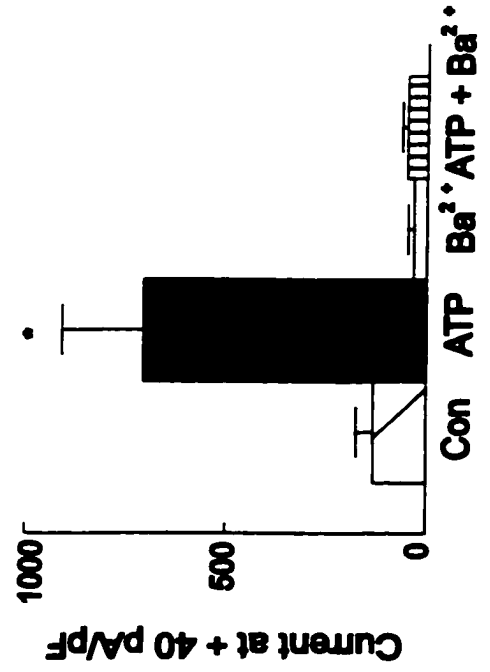
A.



B.



C.



D.

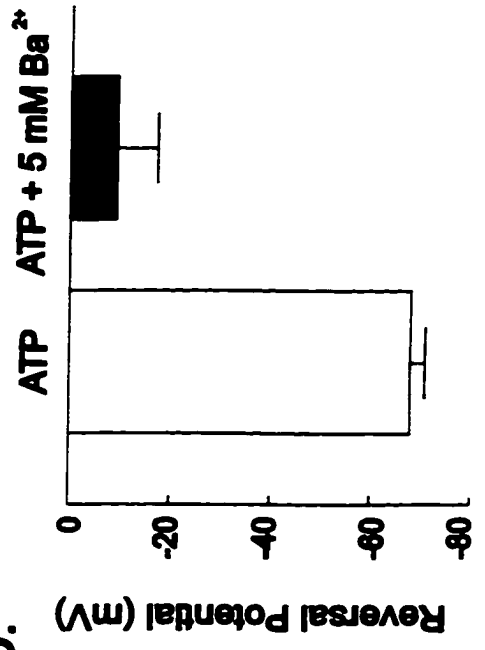


Figure 4.6

effect of 5 mM Ba^{2+} on the reversal potential of the ATP-activated outwardly rectifying K^+ current measured 40 sec after puffer application of 100 μ M ATP. In the absence of Ba^{2+} , the mean (\pm SE) reversal potential of the ATP-activated K^+ current was -68 ± 3 mV ($n=6$). In the same 6 cells superfused with 5 mM Ba^{2+} , the reversal potential of the ATP-activated current measured 40 sec after ATP application was -9 ± 8 mV indicating that Ba^{2+} blocked activation of the delayed outwardly rectifying K^+ . The shift in the reversal potential of the ATP-activated outward current towards the K^+ equilibrium potential ($E_k = -84$ mV) and the sensitivity of the outward current to Ba^{2+} ions confirms that ATP is activating a K^+ -selective current in addition to a nonselective cation current in rat RPE cells.

A least two major types of outward K^+ selective currents, a delayed rectifying K^+ current (I_{KV}) and a "maxi" K^+ or large conductance calcium-activated K^+ current ($I_{K(Ca)}$), have been described in mammalian RPE cells (Strauss *et al*, 1994; Tao *et al*, 1994; Tao & Kelly, 1995). We wanted to test the hypothesis that the delayed K^+ current activated by ATP was an Ca^{2+} -activated K^+ current. To do this we looked at the sensitivity of the ATP-activated outward current to the selective "maxi" K^+ channel blocker iberiotoxin (Giangiacomo *et al*, 1993 & 1993). IbTX has been shown to potently block agonist stimulated activation of $I_{K(Ca)}$ in ocular epithelial cells (Tao *et al*, 1995; Ryan *et al*, 1998). Figure 4.7 shows the mean increase in current amplitude of the ATP-activated outward K^+ current in RPE cells in the presence or absence of 10 nM IbTX. Puffer application of 100 μ M ATP in the absence of IbTX increased outward K^+ current between 23-110% (56 ± 27) in 3 RPE cells tested. Superfusion of the same 3 cells with 10 nM IbTX for 5 min significantly reduced the ATP-induced increase in I_K . IbTX

Figure 4.7. ATP activates an IbTX-sensitive outward K^+ current. Histogram shows mean \pm SE percentage increase in outward current measured at +31 mV. 100 μ M ATP (open box) significantly increased the outward current. In the presence of 10 nM IbTX (hatched box) the ATP-induced increase in outward current is reduced.

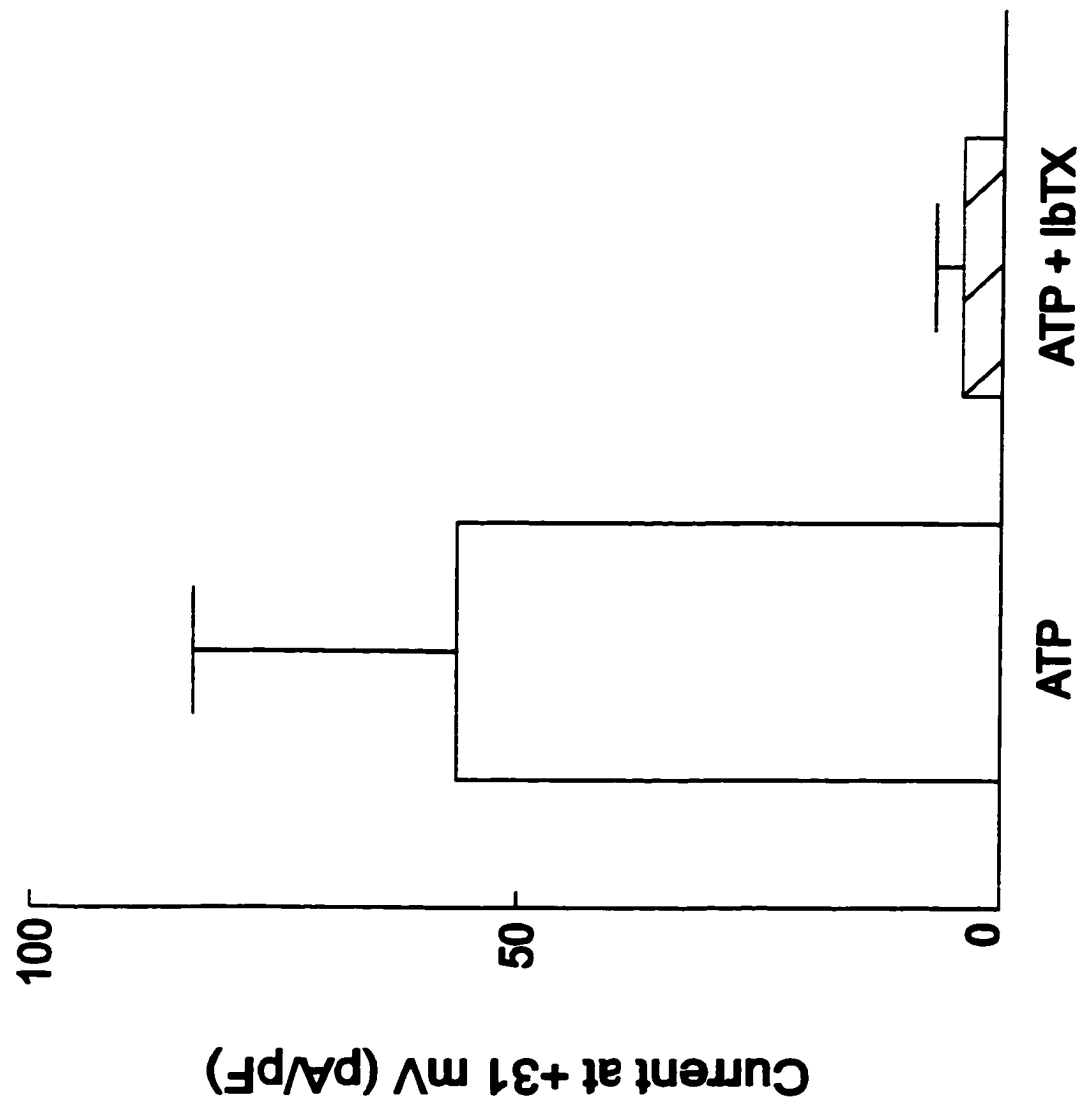


Figure 4.7

completely blocked I_K activation in one cell and reduced the increase in outward current to 2.7 and 9.6 % in the two other cells tested (4 ± 2.7). The ability of IbTX to block the effect of ATP demonstrates that the outwardly rectifying K^+ current activated by purinoceptor activation in rat RPE cells is a Ca^{2+} -activated "maxi" K^+ current (I_{KCa}).

The finding that ATP activates a calcium-activated K^+ current, suggests that purinoceptor activation in rat RPE cells is linked to a rise in $[Ca^{2+}]_i$. In a variety of cell types, including the RPE (Sullivan *et al*, 1997; Peterson *et al*, 1997), activation of metabotropic P_{2y} receptors have been shown to be coupled to elevations in intracellular $[Ca^{2+}]_i$. This suggests that a P_{2y} receptor-coupled signaling pathway may be involved in $I_{K(Ca)}$ activation in rat RPE.

5. Effect of other nucleotides

To further characterize the subtypes of purinergic receptors involved in the activation of the cation and K^+ current in RPE cells, we tested the effect of different purinoceptor agonists. Originally, the potency of these agonists at purinoceptors was used as a means to discriminate between different P_2 purinoceptor families. For example, sensitivity to 2MeSATP was previously thought to reliably indicate the involvement of P_{2y} purinoceptors and responsiveness to α,β methyl-ATP was considered indicative of P_{2x} purinoceptors. The use of these agonists to identify P_2 receptor families is now being challenged as 2MeSATP has been shown to act as a potent agonist at some P_{2x} subtypes, and its potency at P_{2y} subtypes ranges from very effective to virtually ineffective. Similarly, α,β methyl-ATP has been found to have little or no activity at some P_{2x} subtypes. Its lack of effect on virtually all P_{2y} receptors however, still makes it a useful

pharmacological tool to make putative distinctions between P₂ subtypes (Humphrey *et al*, 1995; Barnard *et al*, 1997).

Figure 4.8A, summarizes results of experiments where RPE cells were exposed to 100 μM of either ATP, UTP, 2MeSATP, ADP or α,β-methylATP. All agonists, with the exception of α,β methyl-ATP, were equally effective in activating the inward cation current. Inward current was never observed in rat RPE cells exposed to α,β methylATP. The mean current amplitude of the inward cation current measured at -69 mV evoked by UTP (-12 ± 6 pA/pF; n=7), ADP (-10 ± 2.4; n=6) or 2 MeSATP (-15 ± 3 pA/pF; n=5) was not significantly different from the inward cation current activated by ATP (-12.5 ± 1 pA/pF; n=57). Thus, all P_{2x} agonist tested in this study were equal in their ability to activate the P_{2x} receptor subtype gating the nonselective cation current.

Figure 4.8B shows the effectiveness of ATP and its analogues to activate the K⁻ current in rat RPE cells. Similar to the findings with the inward cation current, α,β methyl-ATP was ineffective in all cells tested but outward K⁻ current was activated with similar frequency in RPE cells treated with ATP, UTP, 2MeSATP, or ADP. The mean amplitude of the nucleotide-activated outward current measured at +31 mV showed no significant differences between analogues. However, the outward current activated by UTP (12 ± 3 pA/pF; n=6) was reduced in amplitude compared to that activated by ATP (23 ± 6 pA/pF; n=28), 2MeSATP (25 ± 6 pA/pF; n=3) or ADP (27 ± 8 pA/pF; n=6). This suggests that in rat RPE cells UTP may be a slightly less effective agonist for the P_{2y} receptor involved in I_{K(Ca)} activation.

The pharmacological profile (ATP=UTP=2MeSATP=ADP) for the inward cation conductances activated in rat RPE cells fits none of the described purinoceptor

Figure 4.8. Effect of other P2 agonists on whole-cell current in rat RPE cells. (A) Bar graph shows the mean \pm SE amplitude of inward NSC current measured at -69 mV activated by ATP (open bar; $n = 57$), UTP (stripped bar; $n = 7$), 2MeSATP (black bar; $n = 5$) or ADP (hatched bar $n = 6$). (B). Bar graph shows mean \pm SE amplitude of the outward K^+ current (I_{KCa}) activated by ATP ($n = 23$), UTP ($n = 6$), 2MeSATP ($n = 3$) or ADP ($n = 6$). Nucleotide-activated $I_{K(Ca)}$ was measured at $+31$ mV. All agonist were applied by puffer for a duration of 4-10 sec. All data has been normalized for cell capacitance.

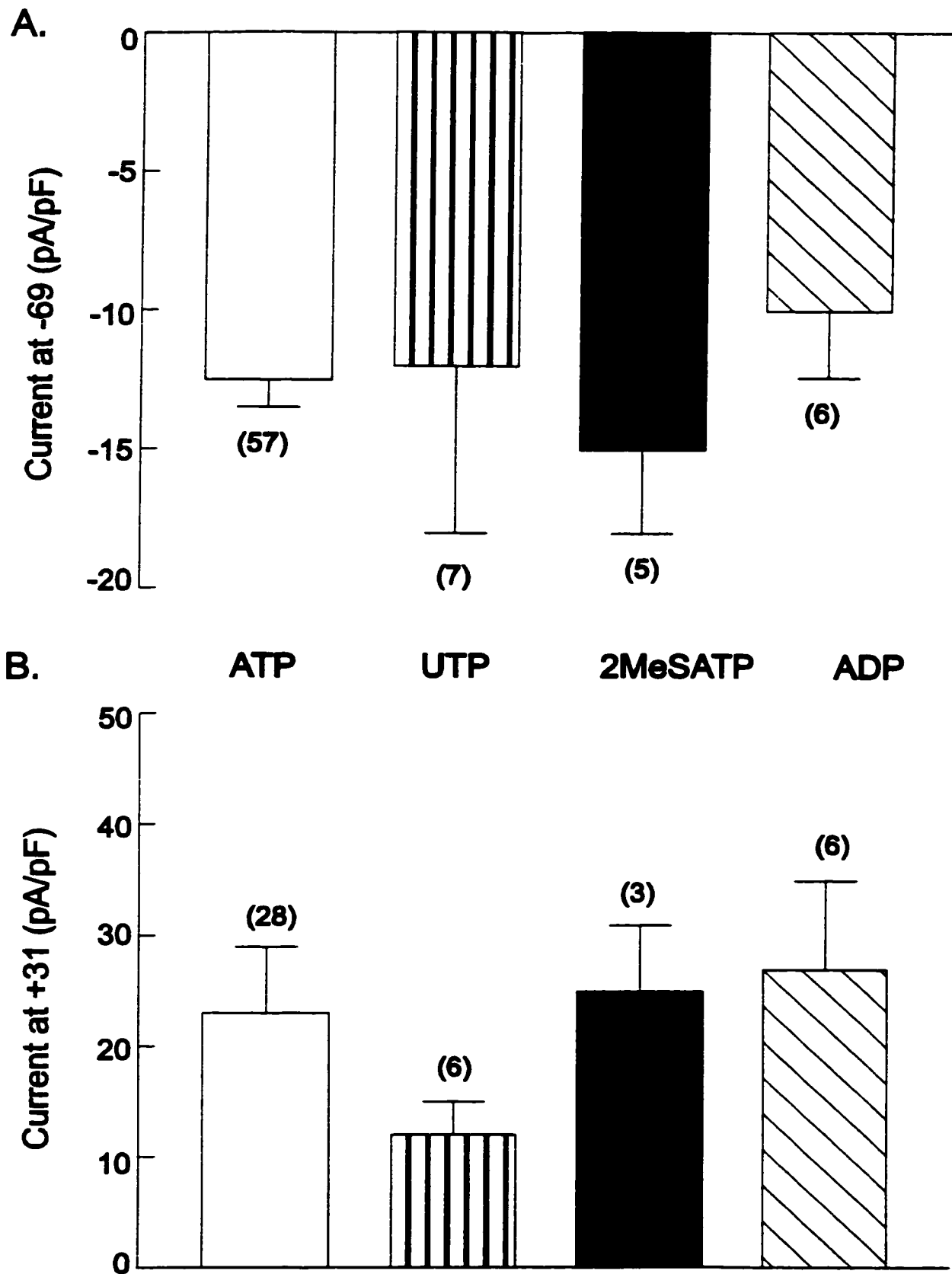


Figure 4.8

phenotypes. However, the lack of sensitivity to α,β methylATP and the antagonists PPADS and suramin, as well as the absence of receptor desensitization associated with the effects of ATP, 2MeSATP and ADP, most closely resembles the profile described for the cloned P_{2x4} or P_{2x6} receptor subtypes (Barnard *et al*, 1997). For the activation of $I_{K(Ca)}$ by a putative P_{2y} receptor in the rat RPE, the rank order of agonist sensitivity (ATP=2MeSATP=ADP>UTP) most closely resembles that described for the cloned P_{2y3} receptor subtype.

6. Intracellular calcium responses

6.1 ATP and UTP increase $[Ca^{2+}]_i$

The activation of an IbTX-sensitive $K^+_{(Ca)}$ current by ATP suggested the involvement of a G protein-coupled P_{2y} purinoceptor in the rat RPE. To determine if ATP activates Ca^{2+} -signaling pathways in the RPE we used the calcium indicator dye Fluo-3 as a qualitative measure of alterations in $[Ca^{2+}]_i$ (Kao *et al*, 1993). The top of panel of Figure 4.9 shows light microscope (A) and pseudocolor image (B) of the $[Ca^{2+}]_i$ response in a representative RPE cells in response to bath superfusion of 100 μ M ATP. ATP caused an initial transient increase in the intensity of Flou-3 fluorescence in this cell, indicative of an increase in $[Ca^{2+}]_i$. This rapid peak increase was followed by a phase of slow decrease in which $[Ca^{2+}]_i$ remained elevated above baseline for \sim 3 min. The $\Delta F/F$ for this cell was 0.27 (see lower panel, Figure 4.9 B). The mean $\Delta F/F$ (\pm SE) response to 100 μ M ATP in 7 RPE cells tested was 0.1 ± 0.03 .

Figure 4.9. ATP-evoked increases in $[Ca^{2+}]_i$. (A) Light microscope image of a representative RPE. (B) Pseudocolor image of the same RPE cell illustrating the increase in $[Ca^{2+}]_i$ in response to bath application of 100 μ M ATP. (C) Time course of the change in $[Ca^{2+}]_i$ in response to 100 μ M ATP for the same cell.

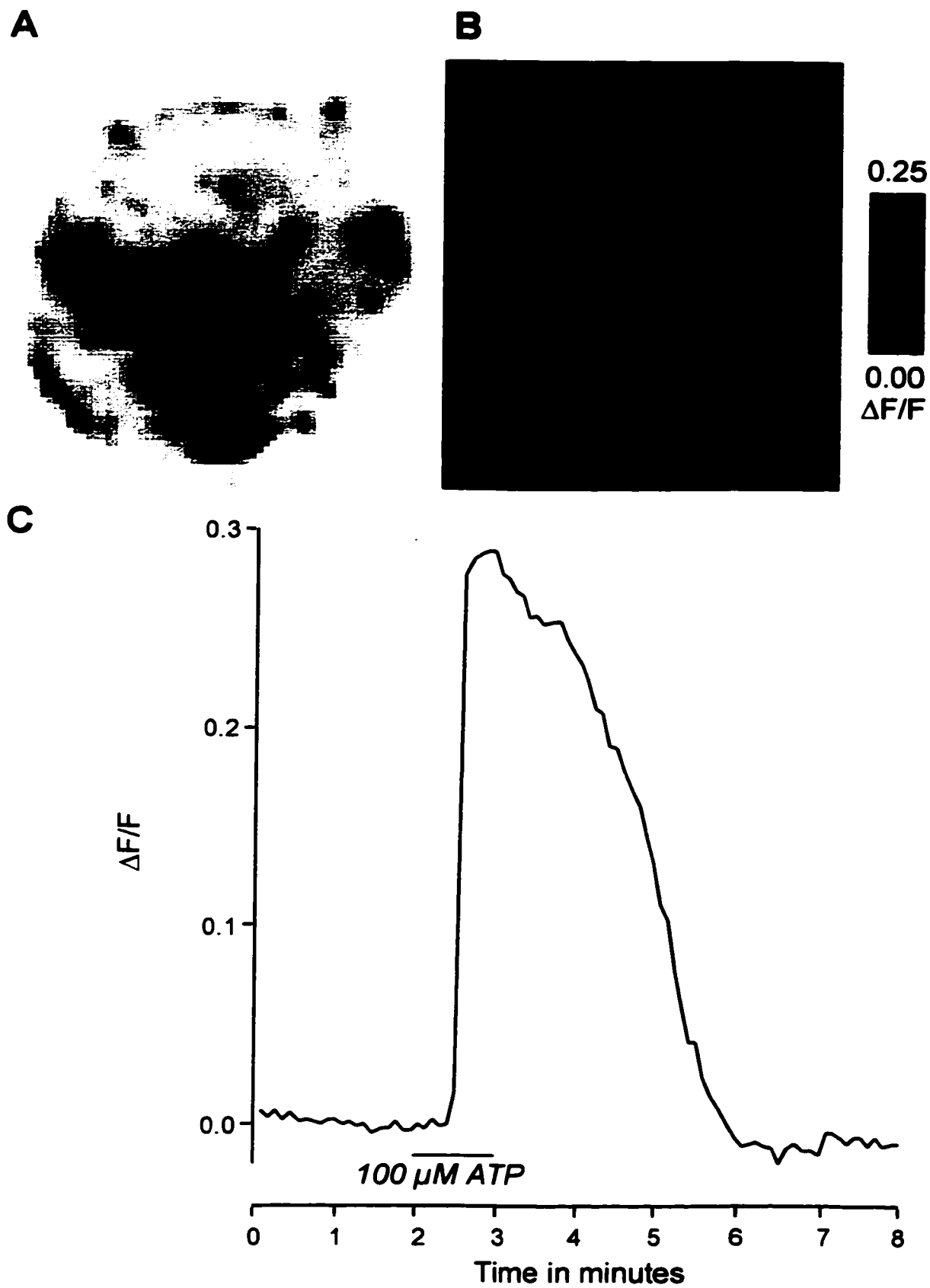


Figure 4.8

Not all RPE cells exposed to ATP responded with an increase in $[Ca^{2+}]_i$. In some cases, the dense pigmentation of the cells made it impossible to detect any significant changes in fluorescence. Similar difficulties have been reported for optical indicators, like Fluo-3, used to measure cytosolic free Ca^{2+} in pigmented tissue (Tsein, 1988). In other RPE cells, unresponsiveness to ATP was correlated with cells that had lost their pigmentation and begun to spread and proliferate. Similar heterologous Ca^{2+} responses to ATP in ocular epithelial cells have also been attributed to differentiation of cells in culture (Churchill & Louis, 1997). This observation is consistent with our finding that effect of ATP on whole-cell currents was abolished with time in culture suggesting changes in receptor-effector coupling and/or ion channel expression.

Bath superfusion of 100 μ M UTP also caused a large transient increase in $[Ca^{2+}]_i$ followed by a slow decrease back to baseline (Figure 4.10). For the representative RPE cell shown in Figure 4.11 A and B the $\Delta F/F$ was 0.1. In 2 other cells tested the mean response to 100 μ M UTP was 0.09 ± 0.02 . This mean response to UTP was not significantly different from that obtained for ATP suggesting that both agonists were equipotent in mediating elevations in $[Ca^{2+}]_i$. The mean fluorescence baseline signal or the stimulated increase in $[Ca^{2+}]_i$ did not significantly change for repeated applications of either ATP or UTP. This indicated that the calcium response was not desensitizing and that the cells were not affected significantly by photobleaching.

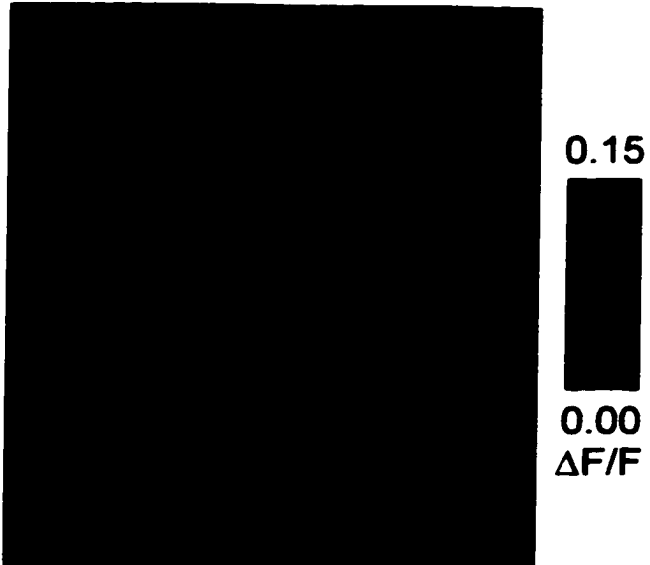
Although we did not test the effect of other P_2 agonists on $[Ca^{2+}]_i$, we did examine the effect of another purine nucleotide guanosine triphosphate (GTP). GTP has little, if any effect on P_{2x} or P_{2y} purinoceptor subtypes. Figure 4.11 shows an RPE cell that responded to 100 μ M ATP with a significant increase in $[Ca^{2+}]_i$ ($\Delta F/F = 0.1$). Bath

Figure 4.10. UTP-evoked increases in $[Ca^{2+}]_i$. (A) Light microscope image of a representative RPE cell loaded with Fluo-3. (B) Pseudocolor image of the same RPE cell showing the increase in $[Ca^{2+}]_i$ in response to bath application of 100 μ M UTP. (C) Time course of the change in $[Ca^{2+}]_i$ in response to 100 μ M UTP for the same cell shown in A and B.

A



B



C

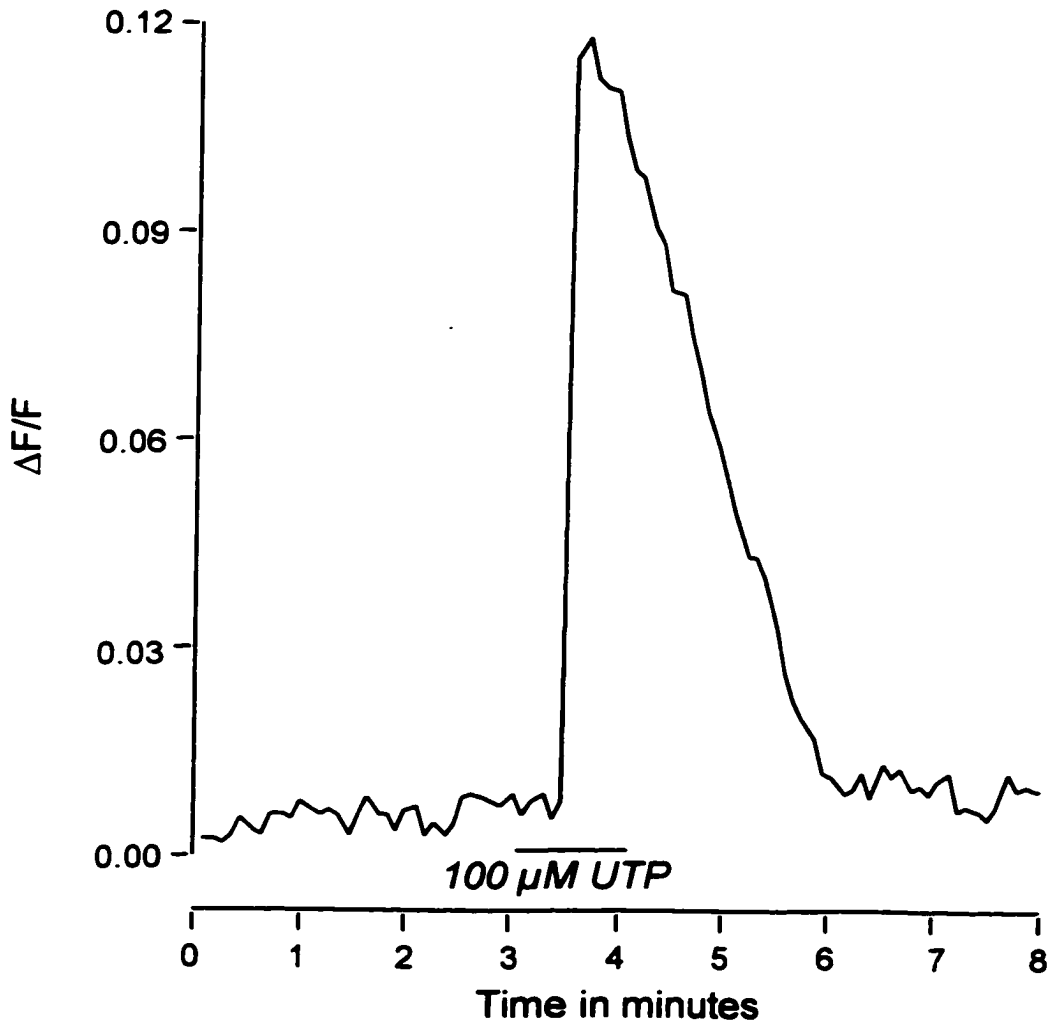


Figure 4.9

Figure 4.11. Selectivity of the ATP response. Time course of the intracellular Ca^{2+} response in a representative RPE cell loaded with Fluo-3 to bath of application 100 μM ATP (B), 100 μM GTP(C) and (D) a second application of 100 μM ATP. The $[\text{Ca}^{2+}]_i$ response in rat RPE cells is selective for adenine nucleotides.

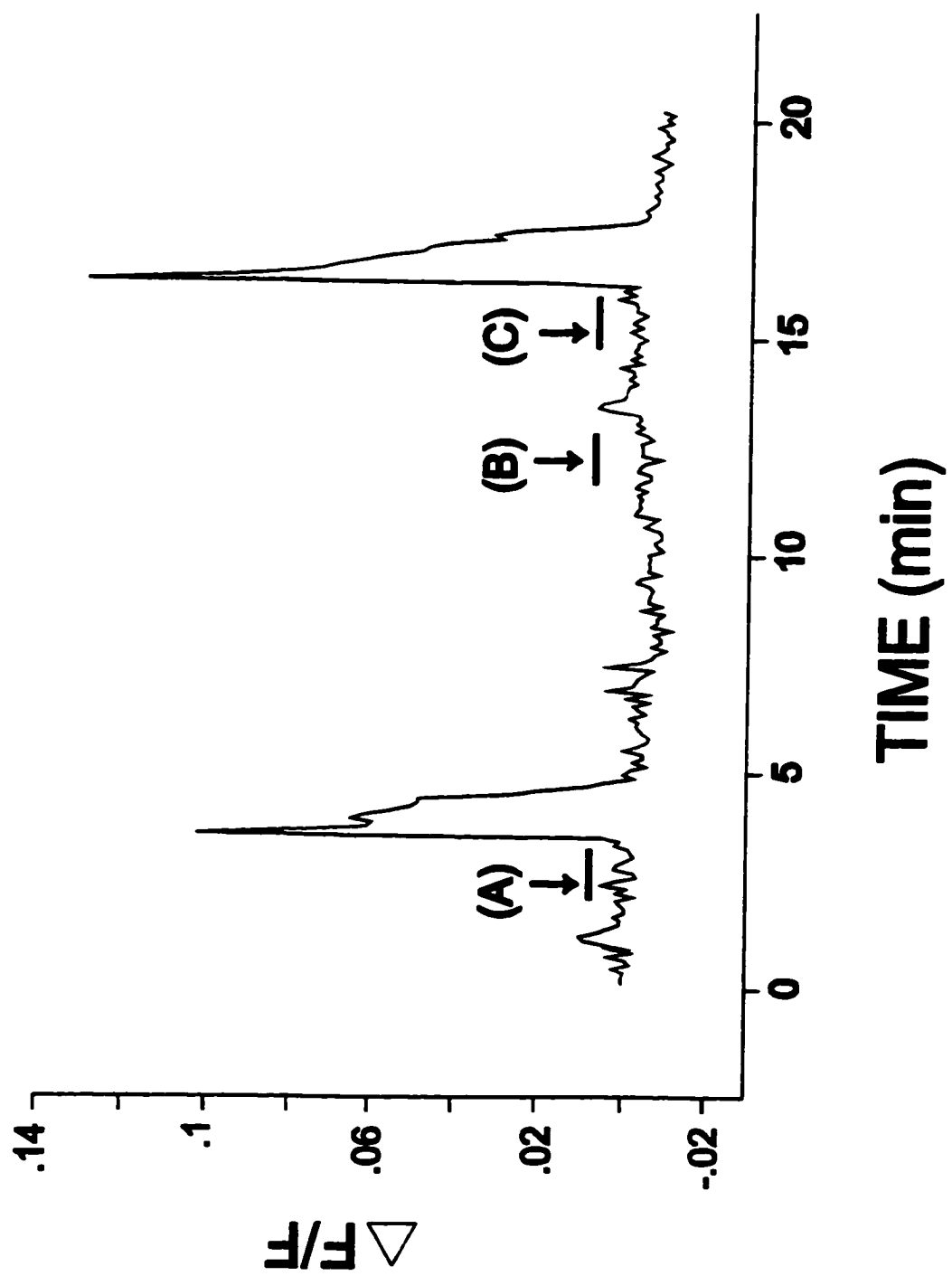


Figure 4.11

application of 100 μM GTP in the same cell failed to produce any detectable change in fluorescence. A second application of ATP however, produce a response that was undiminished from the initial change in $[\text{Ca}^{2+}]_i$ ($\Delta\text{F}/\text{F} = 0.13$). The lack of effect of GTP suggests that the Ca^{2+} response is selective for adenine nucleotides.

6.2 The role of extracellular Ca^{2+}

The increase in $[\text{Ca}^{2+}]_i$ elicited by ATP/UTP could have resulted from an influx of extracellular Ca^{2+} or from efflux of Ca^{2+} from intracellular stores. In an attempt to identify the source of Ca^{2+} mobilized in response to ATP, we measured the change in fluorescence in the absence of extracellular Ca^{2+} ($[\text{Ca}^{2+}]_o$). Figure 4.12A shows the response of a representative RPE cell to stimulation with 100 μM ATP in regular external Ca^{2+} (2mM) and nominally Ca^{2+} -free external solution with 1.5 mM EGTA added. The $[\text{Ca}^{2+}]_i$ response was slightly reduced ($\Delta\text{F}/\text{F} = 0.011$) in nominally Ca^{2+} -free solution compared to the first ATP application in 2 mM $[\text{Ca}^{2+}]_o$ ($\Delta\text{F}/\text{F} = 0.02$). With subsequent superfusion in regular external solution, the response to ATP was slightly restored ($\Delta\text{F}/\text{F} = 0.016$). The average reduction in the $[\text{Ca}^{2+}]_i$ response measured in Ca^{2+} -free solution was $38 \pm 12\%$ ($n=3$) and the ATP response recovered to $70 \pm 5\%$ of control values following reperfusion with 2 mM $[\text{Ca}^{2+}]_o$. However, figure 4.12B demonstrates that the mean $\Delta\text{F}/\text{F}$ values in nominally Ca^{2+} -free solution (0.035 ± 0.014) was not significantly different from the first (0.065 ± 0.036) or second (0.042 ± 0.021) ATP application in regular Ca^{2+} solution.

Figure 4.12. ATP-evoked increase in $[Ca^{2+}]_i$ is not dependent on extracellular Ca^{2+} influx. (A) Optical recording from a representative RPE cell illustrating the effect of Ca^{2+} -free extracellular solution on the ATP-evoked increase in $[Ca^{2+}]_i$. Removal of extracellular Ca^{2+} failed to abolish the ATP effect. (B). Histogram shows mean \pm SE data for the ATP-evoked increase in $[Ca^{2+}]_i$ measured in the same 3 RPE cells in 2 mM external Ca^{2+} (open bar), in Ca^{2+} -free external solution (stripped bar) and after reperfusion with 2 mM external Ca^{2+} (hatched bar). Removal of extracellular Ca^{2+} failed to significantly effect the amplitude of the ATP-evoked increase in $[Ca^{2+}]_i$.

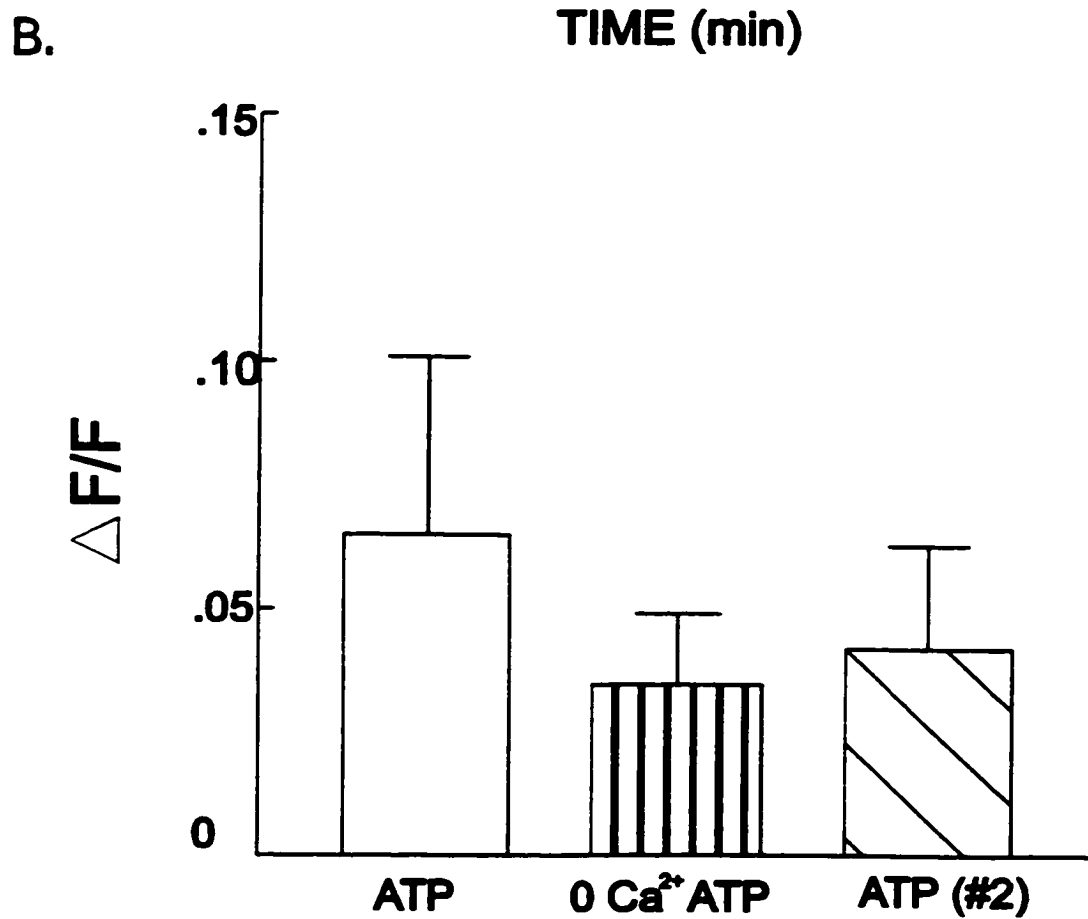
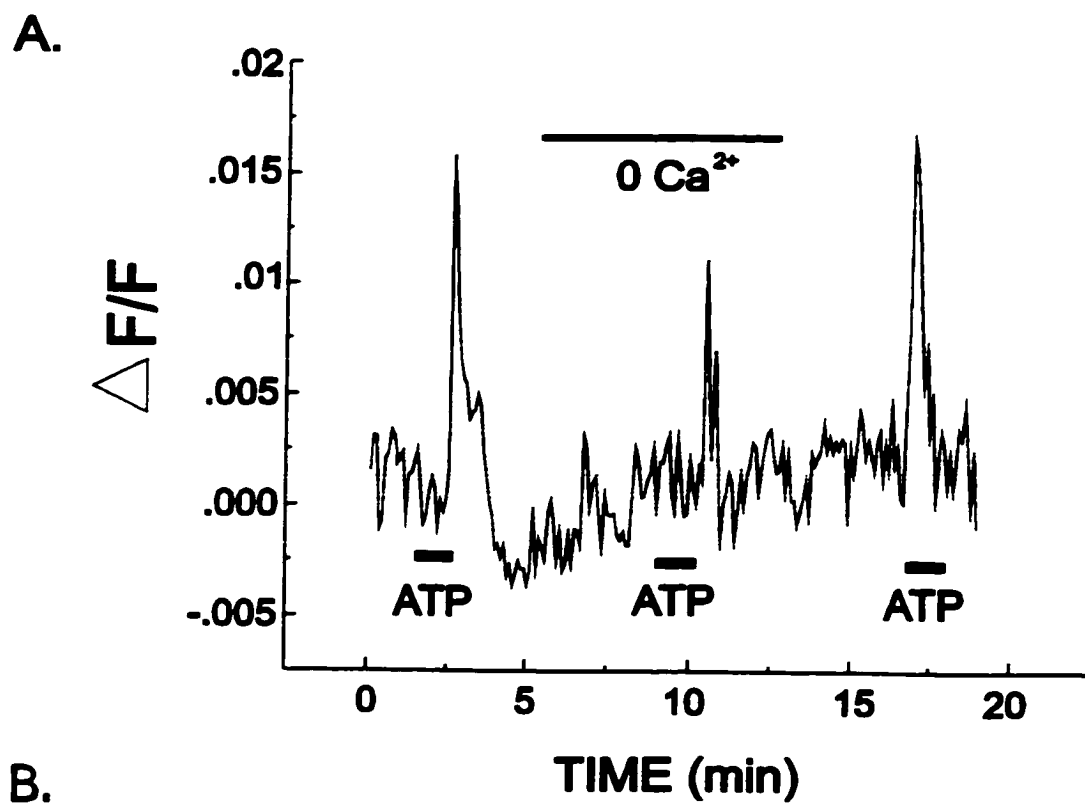


Figure 4.12

The use of heavily pigmented cells in this experiment lead to a high signal-to-noise ratio. This made it difficult to definitively determine if there were any quantitative differences in the latency to onset, peak amplitude or duration of the $[Ca^{2+}]_i$ response in the absence of external Ca^{2+} . The decline in the peak response that was observed when cells were bathed in nominally $[Ca^{2+}]_o$ -free does suggests that a small influx of $[Ca^{2+}]_o$ may contribute to the $[Ca^{2+}]_i$ response elicited by ATP. This hypothesis is supported by the observation that when Ca^{2+} was added back to the bathing solution, the $[Ca^{2+}]_i$ signal recovered slightly towards control values. This small decrease (38%) in Fluo-3 signal is comparable with the decrease in the current amplitude of the ATP-activated P_{2X} receptor (23%) we observed under similar nominally $[Ca^{2+}]_o$ free conditions. These findings suggest that some Ca^{2+} influx via P_{2X} receptors may contributed to the increased Fluo-3 fluorescence. However, the ability of ATP to evoke a $[Ca^{2+}]_i$ response in the absence of extracellular Ca^{2+} indicates that intracellular Ca^{2+} release plays a more dominant role in mediating changes in cytosolic free Ca^{2+} . These results further support the presence of metabotropic P_{2Y} receptors coupled to intracellular Ca^{2+} release in rat RPE cells. ATP and UTP were equipotent in mediated increases in $[Ca^{2+}]_i$, a characteristic that is most consistent with the pharmacological profile of cloned and native P_{2Y3} or P_{2Y4} purinoceptors (Barnard *et al*, 1997).

DISCUSSION

This study demonstrates that extracellular ATP activates two cation conductances in the rat RPE. Actions of adenine nucleotides on cation currents have not previously been described in rat RPE cells. In the majority of cells, ATP activated an inwardly rectifying nonselective cation conductance suggesting the first evidence for existence of P_{2X} purinoceptors in the RPE. In cells with a biphasic response to ATP, the activation of the inward current was followed by the activation of a calcium-activated K⁺ (I_{K(Ca)}). ATP-evoked elevations in [Ca²⁺]_i in the absence of extracellular Ca²⁺ suggested that P_{2y} purinoceptor-mediated intracellular Ca²⁺ release may be involved in I_{K(Ca)} activation. The following sections detail the effect of ATP on whole-cell current and [Ca²⁺]_i in rat RPE cells and extends the discussion to possible roles of extracellular nucleotides as autocrine and/or paracrine modulators of RPE function *in vivo*.

1. Nucleotide-activated nonselective cation current

The initial transient inward current activated by ATP was identified as a nonselective cation current based on several observations. The ATP-activated inward current reversed close to 0 mV in regular solutions and in solutions at which E_{Cl} was set at ~ -40 mV suggesting that the current was selective for cations. Nonselectivity of the current was confirmed by experiments demonstrating that large cations, such as choline and NMDG, were also able to permeate the ATP-activated channel. Removal of extracellular Ca²⁺ had no significant effect on the ATP-activated inward current but did slightly reduce the current amplitude in ¾ cells tested. Despite this small reduction, it is

unlikely that ATP-evoked Ca^{2+} influx via the NSC channel contributes significantly to the membrane currents under physiological conditions. The I-V plot for the ATP-activated nonselective cation current showed strong inward rectification. Inward rectification is a common feature of ligand-gated $\text{P}_{2\text{X}}$ channels in virtually all cell types studied (Humphrey *et al*, 1995). Thus, the electrophysiological characteristics of the ATP-activated ion channel we have identified in rat RPE cells are consistent with the presence of $\text{P}_{2\text{X}}$ purinoceptors.

$\text{P}_{2\text{X}}$ purinoceptor subtypes are classified on the basis of a number of different properties including their rate of desensitization. Of the seven subtypes characterized thus far, only $\text{P}_{2\text{X}1}$ and $\text{P}_{2\text{X}3}$ purinoceptors markedly desensitized when the application of ATP is continued for several seconds. We routinely exposed RPE cells to 4 sec puffer application of ATP without any marked desensitization over the length of the puff or during repeated drug applications. This finding suggest that $\text{P}_{2\text{X}1}$ or $\text{P}_{2\text{X}3}$ receptors do not gate activation of the ATP-evoked cation current in rat RPE. Interestingly, desensitization of $\text{P}_{2\text{X}1}$ and $\text{P}_{2\text{X}3}$ receptors is correlated with full agonist sensitivity to α,β methylATP (Surprenant *et al*, 1995). Conversely, in those subtypes where desensitization is absent ($\text{P}_{2\text{X}2}$, $\text{P}_{2\text{X}4}$, $\text{P}_{2\text{X}5}$ or $\text{P}_{2\text{X}6}$), α,β methylATP is not an effective agonist (Barnard *et al*, 1997). Consistent with these observations, our $\text{P}_{2\text{X}}$ -activated nonselective cation conductance was insensitive to α,β methylATP, suggesting the involvement of a non-desensitizing, α,β methylATP insensitive $\text{P}_{2\text{X}}$ subtype.

The identification of $\text{P}_{2\text{X}}$ purinoceptors is hindered by the lack of subtype specific blockers. Suramin and PPADS were once considered to be selective antagonists for the $\text{P}_{2\text{X}}$ receptor family. These antagonists however, are no longer considered selective for a

given P₂ purinoceptor family or subtype. They are weak or ineffective at some P_{2X} subtypes and antagonize responses to virtually all P_{2Y} subtypes identified as well as nicotinic, GABA- and glutamate- gated ion channels (Humphrey *et al*, 1995). ATP-gated nonselective cation channels in rat RPE cells were insensitive to both PPADS and suramin at a concentration of 100 μM ATP. Of the seven P_{2X} subtypes only two have been found to be resistant, or partially resistant, to antagonist blockade by suramin and PPADS. The P_{2X4} purinoceptor cloned from rat brain is virtually insensitive to suramin and PPADS at concentrations between 100 μM and 500 μM (Soto *et al*, 1996; Buell *et al*, 1996). Similarly, the cloned P_{2X6} receptor is unaffected by PPADS or suramin at concentration between 1 μM and 30 μM (Collo *et al*, 1996). Higher concentrations (>30 μM) of these antagonists however, produced a small reversible inhibition that was attributed to nonselective effects. The antagonist insensitivity of our ATP-evoked response, even at high concentrations, suggests the involvement of a P_{2X4} and/or P_{2X6} purinoceptor subtype in rat RPE cells.

Based on the pharmacological profile and desensitization characteristics, the P_{2X} receptor in RPE cells most closely resembles the cloned P_{2X4} and/or P_{2X6}. These receptors are unaffected or only weakly activated by α,β methylATP, they show little desensitization during ATP application and are not antagonized by suramin or PPADS (Barnard *et al*, 1997; Boarder & Hourani, 1998). However, comparison of the agonist profile obtained for the ATP-activated inward cation current in rat RPE cells (ATP=UTP=2MeSATP=ADP) correlates poorly with the potency profiles reported for cloned P_{2X4} (ATP> 2MeSATP >>>ADP) and P_{2X6} (ATP> 2MeSATP>>> ADP) receptors. However, it is plausible that the concentration of agonist (100 μM) used in this

study was supramaximal for the response and thus obscured any differences that existed in the potency profile. We also found that UTP was equally as effective as ATP, suggesting that this uridine nucleotide is a full agonist at the P_{2X} receptor in rat RPE cells. This finding is in direct contrast to cloned P_{2X4} receptors where UTP is completely ineffective (Buell *et al*, 1996) and in cloned P_{2X6} receptors where an effect of this pyrimidine nucleotide has not yet been reported. Very few reports, in fact, have documented effects of UTP at P_{2X} purinoceptor subtypes. Recently, in dorsal root ganglion neurons, it has been demonstrated that UTP mediates transient inward currents via stimulation of P_{2X3} purinoceptors (Rae *et al*, 1998). Similarly, UTP has been reported to activate an inward cation current gated by P_{2X1} receptors in rat vascular smooth muscle cells (McLaren *et al*, 1998). These findings support our findings that UTP gates a nonselective cation current via P_{2X} receptor activation in rat RPE cells.

A full agonist action of UTP, and other discrepancies in the agonist profile, makes it difficult to assign the nucleotide response in rat RPE cells to any one given P_{2X} subtype. Discrepancies in pharmacological profiles have also been reported between cloned and native P_{2X} purinoceptors in variety of cell types. It is plausible that our results are indicative of a combination of two or more homomeric purinoceptors, giving a novel pharmacological profile. A number of P_{2X} receptors have been shown to associate in multimers resulting in pharmacological and kinetic profiles different from homoligomeric channels. For example, in sensory neurons it has been proposed that the response to ATP is mediated via a P_{2X2} - P_{2X3} heteromultimer (Lewis *et al*, 1995). Alternatively, the pharmacological profile obtained in the rat RPE may also be indicative of P_{2X} receptor heterogeneity. In many cell types P_{2X} receptor expression is not limited to only one

subtype (Nori *et al*, 1998; Humphrey *et al*, 1995). The inward cation current in rat RPE cells could therefore be gated by multiple P_{2X} subtypes, each with subtle differences in their sensitivity to purinoceptor agonists.

In many cases the agonist activity profiles for P_{2X} receptors are affected by the activity of ectoenzymes and/or ectokinases on cells (Ziganshin *et al*, 1994; Humphrey *et al*, 1995). It is unlikely that break-down of the nucleotides was a complicating factor in our experiments since our measurements were made very quickly with short application of the agonist directly on the cell. One factor we could not control for however, was the possibility that our nucleotides were not pure. Contamination of commercially available purinoceptor agonists has been suggested as a source of error in agonist activity profiles (Barnard *et al*, 1997).

2. Nucleotide-activated calcium-sensitive K^+ current

In a subpopulation of RPE cells ATP activated an outward current whose onset was slightly delayed compared to the NSC channel. The I-V relationship indicated that the delayed current activated at negative potentials and was outwardly rectifying at depolarized potentials, indicating the activation of a K^+ current. ATP-evoked activation of this current was sensitive to the selective “maxi” K^+ channel blocker IbTX, identifying it as a Ca^{2+} -activated potassium current ($I_{K(Ca)}$). “Maxi”- K_{Ca} channels are large conductance K^+ -selective channels that have been described in a variety of cell types (reviewed by McManus, 1991). Despite their ubiquitous nature, K_{Ca} channels share common characteristics including activation by both Ca^{2+} and membrane depolarization and sensitivity to IbTX. Intracellular Ca^{2+} ions activate these channels by interacting

directly with the cytosolic surface of the channel protein and $I_{K(Ca)}$ channels are targets for modulation by a number of different agonists linked to signaling pathways that stimulate elevations in $[Ca^{2+}]_i$ (Marty, 1987 and 1989; Jacob, 1996b). An IbTX-sensitive $I_{K(Ca)}$ in rabbit RPE, similar to the one activated by ATP in rat, has been shown to be activated by α_1 -adrenergic-induced elevations in intracellular Ca^{2+} (Tao & Kelly, 1995; Tao & Kelly, unpublished observations).

ATP activation of $I_{K(Ca)}$ in rat RPE cells suggested that ATP-evoked elevations in $[Ca^{2+}]_i$ were involved in mediating channel activation. In a number of cell types purinergic agonists have been shown to regulate ion channels that are sensitive to $[Ca^{2+}]_i$. In vascular smooth muscle an ATP-mediated $[Ca^{2+}]_i$ increase has been shown to result in activation of both a Ca^{2+} -sensitive Cl^- and K^+ channel (Strobaek *et al*, 1996). Ca^{2+} -activated K^+ conductances have also been reported to be activated by ATP in colonic smooth muscle (Koh *et al*, 1997), rat osteoclasts (Weidema *et al*, 1997) and mouse microglia (Waltz *et al*, 1993). More recently, in monolayers of bovine RPE, ATP-evoked elevations in $[Ca^{2+}]_i$ were reported to be involved in mediating changes in a basolateral Cl^- and apical membrane K^+ conductance (Peterson *et al*, 1997). In all these studies, ATP-mediated activation of Ca^{2+} -sensitive ion channels was linked to P_{2Y} purinoceptor activation coupled to intracellular Ca^{2+} stores release. All P_{2Y} purinoceptor subtypes belong to the superfamily of seven transmembrane G protein-coupled receptors. Intracellular Ca^{2+} responses appear to be mediated via PTX-insensitive Gq/G11 proteins linked to a PLC/ IP_3 signaling pathway (Heilbronn *et al*, 1997; Salter & Hicks, 1995) although PTX-sensitive P_{2Y} purinoceptor responses have also been described (Dubyak *et al*, 1988; North & Barnard, 1997). Based on these studies, and our experimental findings,

we propose the presence of a functional P_{2Y} purinoceptors in rat RPE linked to increases in intracellular $[Ca^{2+}]_i$ that stimulates $I_{K(Ca)}$ activation.

Although the PLC β isoform is the primary effector mechanism for P_{2Y} purinoceptors, these receptors have also been linked to activation or inhibition of various other effector systems including: adenylate cyclase, phospholipase D, phospholipase A_2 , tyrosine kinase and mitogen-activated protein kinases cascades (Murthy & Makhoulf, 1998; Soltoff *et al*, 1998; Boarder & Hourani, 1998). In addition to second messenger-mediated signaling pathways, a possible role for membrane delimited activation of ion channels by P_{2Y} -coupled G protein subunits has also been proposed for the activation of K^+ channels in brain endothelial cells (Ikeuchi & Nishizaki, 1995 & 1996).

Functional and molecular studies support the existence of G protein-coupled P_{2Y} purinoceptors in the mammalian RPE. In bovine and human RPE cells, purinergic-mediated elevations in cytosolic-free Ca^{2+} have been linked to P_{2Y} receptor activation based on the pharmacological profile and PTX-sensitivity of the response (Peterson *et al*, 1997; Sullivan *et al*, 1997). Consistent with the presence of P_{2Y} purinoceptors in the RPE, molecular studies in human RPE cells have demonstrated the expression of mRNA for the P_{2Y2} receptor subtype (Sullivan *et al*, 1997)

In addition to a P_{2Y} second messenger-mediated increase in $[Ca^{2+}]_i$, Ca^{2+} influx via P_{2X} receptors may also contribute to $I_{K(Ca)}$ activation in rat RPE cells. We have shown that removal of extracellular Ca^{2+} has no significant effect on the amplitude or reversal potential of the P_{2X} -gated NSC current in rat RPE cells. This suggests that Ca^{2+} influx via the ATP-activated NSC current does not play a major role under physiological conditions to activation of $I_{K(Ca)}$ in rat RPE cells. However, in some cells types partial

activation of Ca^{2+} -activated K^+ currents can be elicited by intracellular Ca^{2+} increases as low as 10 nM (Marty, 1989) suggesting that even slight Ca^{2+} influx via $\text{P}_{2\text{X}}$ receptors would be sufficient to stimulate $I_{\text{K}(\text{Ca})}$. Similar to our findings with the $\text{P}_{2\text{x}}$ ligand-gated ion channel, the pharmacological profile of the $\text{P}_{2\text{Y}}$ purinoceptor in rat RPE does not correspond unequivocally to any one particular subtype. ATP, 2MeSATP and ADP were all equally effective while UTP appeared slightly less effective, although statistically its evoked response did not differ from the other agonists. Thus, the pharmacological profile of the putative $\text{P}_{2\text{Y}}$ purinoceptor in rat RPE is: 2MeSATP=ATP=ADP > UTP. Studies on cloned purinoceptors have determined that the $\text{P}_{2\text{Y}1}$ and $\text{P}_{2\text{Y}6}$ subtypes are completely insensitive to UTP whilst at the other three subtypes, $\text{P}_{2\text{Y}2}$, $\text{P}_{2\text{Y}3}$ and $\text{P}_{2\text{Y}4}$ UTP acts as a full agonist (Nicholas *et al*, 1996; Barnard *et al*, 1997). Based on these findings, it is unlikely that the $\text{P}_{2\text{Y}1}$ or $\text{P}_{2\text{Y}6}$ subtypes are involved in the electrophysiological responses of the rat RPE. Furthermore, the pharmacological profile in rat RPE is not consistent with the involvement of a $\text{P}_{2\text{Y}2}$ or $\text{P}_{2\text{Y}4}$ subtype, as 2MeSATP and ADP are purported to be ineffective agonists these receptors. Thus, the profile for $I_{\text{K}(\text{Ca})}$ activation most closely resembles that described for the cloned $\text{P}_{2\text{Y}3}$ where ATP, UTP, ADP and 2MeSATP are all effective agonists at this receptor subtype. Despite the presence of mRNA for $\text{P}_{2\text{Y}2}$ purinoceptors in human RPE (Sullivan *et al*, 1997), our pharmacological findings do not support its involvement in the electrophysiological responses evoked by purinergics in isolated rat RPE cells. Conclusive identification of the $\text{P}_{2\text{Y}}$ subtype(s) involved in $I_{\text{K}(\text{Ca})}$ activation awaits further molecular characterization of the purinoceptors in rat RPE cells. It is likely, however, that similar to our suggestion for $\text{P}_{2\text{X}}$ receptors, the response to

nucleotides in rat RPE is mediated by either a novel P_{2Y} subtypes or perhaps by heterologous expression of a number of subtypes giving a mixed pharmacological profile.

3. Role of Adenosine

In the RPE, adenosine receptor pharmacology is much better characterized than that for P₂ purinoceptors. Messenger RNA for A_{2A} purinoceptors has been demonstrated in the RPE and pharmacological data supports the presence of A_{2B} receptors that are sensitive to micromolar amounts of adenosine (Blazynski, 1993; Kvantá *et al*, 1997). A functional role for adenosine A₂ receptors in modulating phagocytosis of rod outer segments has also been proposed in the rat RPE (Gregory *et al*, 1994). Under the conditions of this study, 100 μ M adenosine had no effect on whole-cell current in the rat RPE cells examined. Thus, despite a functional role in phagocytosis, activation of adenosine receptors does not appear to play a role in modulating membrane currents in RPE cells. The lack of an adenosine effect in rat RPE cells is consistent with previous studies in which adenosine had no demonstrable effect on intracellular [Ca²⁺]_i responses in human RPE cells (Sullivan *et al*, 1997), or on fluid or ion transport in monolayers of bovine RPE (Peterson *et al*, 1997). Our findings that adenosine had no effect of whole-cell currents also supports our suggestion that ecto-ATPase activity played no role in our electrophysiological findings with ATP. Ecto-ATPase activity results in hydrolysis of extracellular ATP to adenosine, which can then activate adenosine receptors. Should this have been a contributing factor to experimental findings, we would have expected adenosine to have similar electrophysiological effects as ATP. The lack of any

effect of adenosine rules out any role of adenosine receptors in nucleotide-evoked ionic currents in the rat RPE.

4. Nucleotide-induced elevation of $[Ca^{2+}]_i$

A variety of calcium imaging techniques have demonstrated that nucleotides, acting on P_2 purinoceptors, mobilize intracellular Ca^{2+} . Our results confirm that P_2 purinoceptors activation by ATP and UTP is capable of elevating $[Ca^{2+}]_i$ in rat RPE cells. Most changes in cytosolic-free Ca^{2+} are attributed to activation of P_{2Y} receptors, although P_{2X} ligand-gated ion channels are also capable of inducing elevations in $[Ca^{2+}]_i$ (Supernant *et al*, 1995). We therefore attempted to distinguish whether our $[Ca^{2+}]_i$ response was mediated by both extracellular Ca^{2+} influx and/or intracellular Ca^{2+} -stores release. In nominally Ca^{2+} -free external solution the peak $[Ca^{2+}]_i$ response, measured by the intensity of Fluo-3 fluorescence, was reduced between 14-56%. This may indicate that at least part of the peak response may be mediated by extracellular Ca^{2+} influx. Our finding that removal of extracellular Ca^{2+} slightly reduced the amplitude of inward cation current may suggest a role for some Ca^{2+} influx via P_{2X} receptors in contributing to elevations in $[Ca^{2+}]_i$ in rat RPE cells. Additionally, ATP-activated P_{2X} receptors may lead secondarily to an influx of extracellular Ca^{2+} via depolarization-induced activation of Ca^{2+} channels. Rat RPE cells have been shown possess L-type Ca^{2+} channels which, once activated, could serve as a source for extracellular Ca^{2+} influx (Ueda & Steinberg, 1993). Our demonstration of a virtually undiminished Ca^{2+} response in nominally Ca^{2+} -free solution suggests that release from intracellular stores is the major contributor to purine-

evoked elevations in $[Ca^{2+}]_i$ and further supports the presence of P_{2Y} purinoceptors in the rat RPE.

Figure 4.14 shows a schematic of the postulated signaling pathways linking P_{2X} and P_{2Y} purinoceptor activation in rat RPE cells to changes in whole-cell current and intracellular $[Ca^{2+}]_i$.

5. Sources of ATP/UTP and role of P_2 purinoceptors

In variety of other cell types ATP, acting on cell surface P_2 purinoceptors, has been shown to regulate a plethora of biological processes including neurotransmission, vascular smooth muscle contraction, platelet aggregation, proliferation and secretion (for reviews see; Boarder & Hourani, 1998; Heilbronn et al, 1997; Zimmermann, 1994; Gorden, 1986). A number of the functions that the RPE carries out in normal retinal physiology, like cellular fluid and ion transport and phagocytosis, have been shown to be targets for P_2 purinoceptor modulation in other cell types (Ichinose, 1995; Mason *et al*, 1991). This study, and others, demonstrating a functional role for ATP purinoceptors in modulating ion transport in the RPE suggests that ATP may play an important role in regulating RPE function *in vivo*.

Within the retina, the RPE has a number of potential sources of endogenous purines. Throughout the body extracellular ATP is usually kept at very low levels due to the limited permeation of ATP across the lipid bilayer and by the action of ubiquitous ecto-ATPases and ectophosphatases. Cellular ATP levels, however, are quite high with the normal concentration in the cytosol of intact cell being in the 3-5 millimolar range.

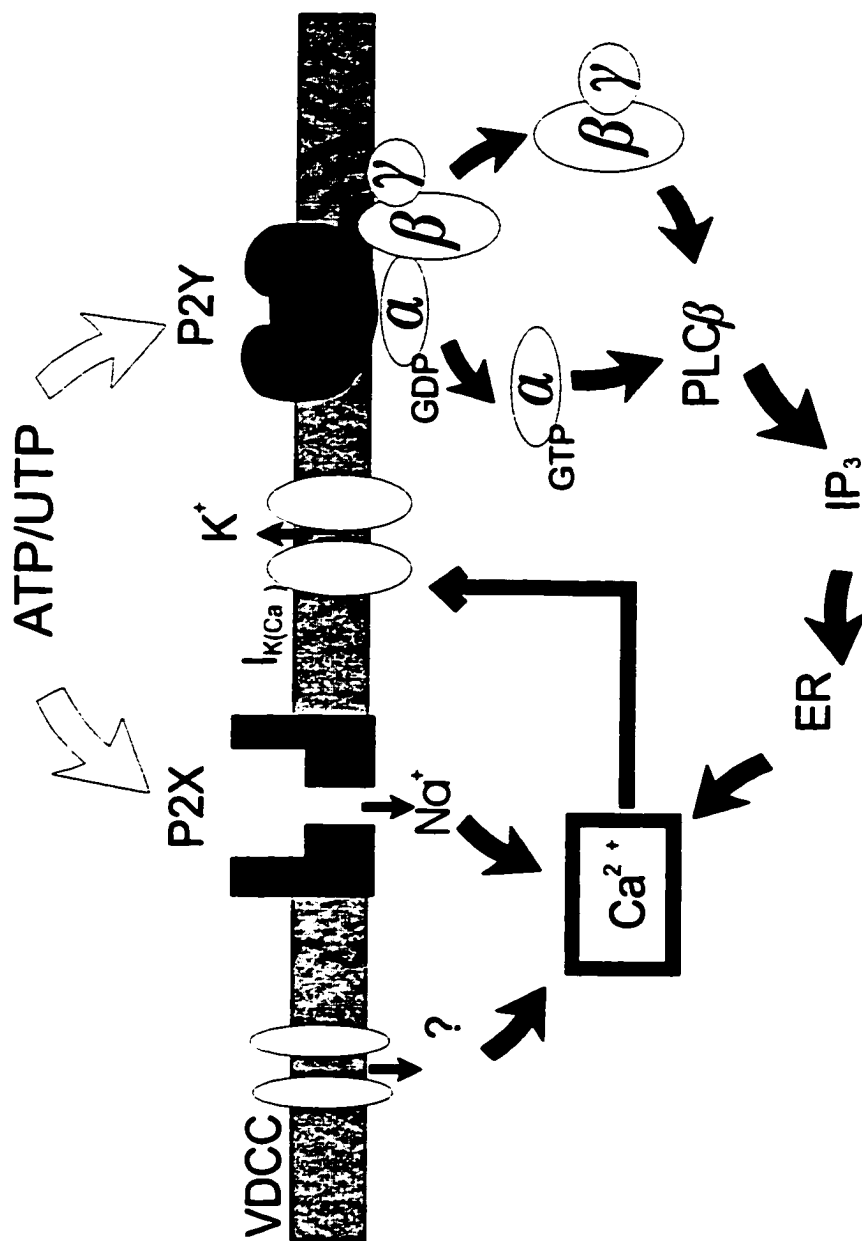


Figure 4.13. Diagrammatic summary of the possible signaling pathways for P_{2x} and P_{2y} purinoceptor activation of a NSC current and a calcium-activated K⁺ current in rat RPE cells. See text for full details.

Despite normally low extracellular concentration, ATP can reach sufficiently high levels to activate purinoceptors in response to specific physiological and/or pathophysiological stimuli. Studies have demonstrated that there are four major sources of extracellular ATP for mammalian cells: 1) ATP has been demonstrated to be stored along with adrenergic and cholinergic neurotransmitters in synaptic granules within neurons, where it is released as an excitatory co-transmitter in both the central and peripheral nervous systems; 2) ATP can also be co-stored along with serotonin in secretory vesicles within platelets, which upon activation releases significant amounts of ATP into the extracellular space; 3) under pathophysiological conditions, sudden breakage of intact cells in response to tissue trauma can release cytoplasmic ATP stores and transiently elevate the extracellular concentration to significantly high levels;. 4) cytoplasmic ATP can also be released from cells via transmembrane transport through specific plasma membrane transporter proteins on intact cells. This release has been demonstrated in both vascular smooth muscle and endothelial cells in response to receptor activation under both physiological and pathophysiological conditions (for reviews see; Gordon, 1986; Zimmermann, 1994; Boarder & Hourani, 1998)

Similar to ATP, extracellular UTP has been demonstrated to modulate a number of biological responses in a variety of cell types including epithelial fluid and ion transport (Heilbron *et al*, 1997; Mason *et al*, 1991; Petersen *et al*, 1997) and phagocytosis (Ichinose, 1995). No evidence conclusively supports synaptic release of UTP and thus, unlike ATP, it is not believed to function as a neurotransmitter or co-transmitter in neurons. However, uridine nucleotides (UTP, UDP) are stored at about 10% of the ATP concentration in chromaffin granules and platelets can be released under

pathophysiological conditions, suggesting that they too might reach sufficiently high extracellular concentrations to activate P2 purinoceptors (Anderson & Parkinson, 1998; Heilbron *et al*, 1997).

5.1 Purines in the retina

To date, there is little evidence to support a role for ATP as a neurotransmitter in the retina. However, several studies have shown however, that in response to stimuli ATP can be released from cells in the neural retina. One study has demonstrated that light flicker and/or depolarizing conditions can evoke the co- release of ATP and acetylcholine from retinal amacrine cells (Neal & Cunningham, 1994). Once released, ATP acts on neuronal P₂ receptors to provide negative feedback for ACh release and thus modulate the light response. The presence of a purine transporter has also been suggested in the retinal amacrine cells based on the observation that under strong depolarizing conditions, the evoked release of purines occurred in a Ca²⁺-independent non-vesicular manner (Blazynski & Perez, 1991). Similarly, a recent study has reported a release mechanism for stored ATP in ciliary epithelial cells (Mitchell *et al*, 1998). These studies suggest that under certain conditions ATP may be released in significantly high amounts to cross the short diffusion distance between the neural retina and RPE and activated P2 purinoceptors.

Significant concentrations of purines may also be present in the choroidal blood supply as a result of platelet activation (ATP) and/or vascular cell lysis (ATP/UTP) in response to inflammation and/or injury. Given the close approximation of the choroid to the RPE, it is plausible that under pathophysiological conditions in which the blood

retinal barrier is compromised, ATP/UTP from the choroidal vasculature could permeate in sufficiently high amounts to activate P_2 receptors on the RPE. Additionally, ATP/UTP could also be released from damaged retinal cells or RPE cells in response to ocular trauma. Under these conditions, extracellular ATP would act as an autocrine factor or paracrine factor to alert the surrounding cells to a pathological event.

5.2 Role of ATP/UTP in ion transport

In a number of transporting epithelial, ATP/UTP has been shown to modulate fluid and/or ion transport (Yan-Scott *et al*, 1995; Benali *et al*, 1994; Mason *et al*, 1991; Middleton *et al*, 1993). A recent study in isolated monolayers of bovine RPE demonstrated that stimulation of P_{2Y} purinoceptors activated a basolateral Ca^{2+} dependent Cl^- conductance, inhibited an apical Ca^{2+} -dependent K^+ conductance and increased apical fluid absorption (Petersen *et al*, 1997). The presence of a P_{2X} -activated NSC current was not suggested in this study. However, the identification of the basolateral depolarizing current as a Cl^- conductance in this study was based on the sensitivity of the current to mM concentrations of the Cl^- channel blocker DIDS. In other cell types this concentration of DIDS has been shown to virtually abolish P_{2X} -gated cation conductances (Connolly and Harrison, 1995; Evans *et al*, 1995). Thus, the presence of basolateral P_{2X} receptors in the RPE should not be ruled out as contributing to the ATP-evoked depolarization in this model.

Activation of the P_{2X} -gated NSC current in rat RPE cells would cause sufficient depolarization to activate or inactivate a variety of ion channels, pumps and transporters. The net effect on the epithelium would be altered ion/fluid transport accompanied by

changes in the composition of the subretinal space. P_{2Y} purinoceptor-stimulated Ca^{2+} -activated K^+ currents may play a similar role as the NSC current in modulating RPE ion/fluid transport. In support of this hypothesis, Ca^{2+} -activated K^+ channels have been shown to regulate transepithelial transport in a variety of epithelial cell types (Petersen & Maruyama, 1984; Sohma *et al*, 1994; Klaerke, 1997). ATP-activated K^+ current in the RPE may also play a role in the $[K^+]_o$ rebound that is observed in the subretinal space following light-induced decrease in $[K^+]_o$. ATP, potentially released from adjacent neural retina cells, may act as a paracrine signal for this rebound by stimulating apical $I_{K(Ca)}$ channels, leading to K^+ efflux and thus buffering the drop in subretinal K^+ to maintain a homeostatic environment for the photoreceptors. Alternatively, activation of $I_{K(Ca)}$ could result in hyperpolarization of the transepithelial ($TEP = V_b - V_a$) potential. This would stimulate net ion absorption by increasing the driving force for Cl^- secretion through passive ion channels in the basolateral membrane. The TEP is also known to be the driving force for ion movement through the paracellular pathway in the RPE (Edelman & Miller, 1991), and thus, $I_{K(Ca)}$ channels may also stimulate net ion/fluid movement via this route.

5.2 Potential role in phagocytosis.

In mouse peritoneal macrophages activation of P_{2Y} receptors, with concomitant elevations in $[Ca^{2+}]_i$, enhances phagocytosis (Ichinose, 1995). Although no link between P_{2Y} purinoceptor activation and phagocytosis in RPE cells has been demonstrated, experimental evidence supports at least the suggestion that purine-mediated signaling pathways may play a role. In the dystrophic Royal College of Surgeons (RCS) rats, a

genetic defect in the RPE leads to a lost ability to phagocytize shed outer segments and, as a consequence, the photoreceptors degenerate. Studies in these rats have demonstrated that there is a defect in an IP_3 signaling pathway in the RPE that normally is involved in outer segment phagocytosis (Heth & Marescalchi, 1994). Furthermore, this defect in phagocytosis could be partially elevated by treatment of RCS RPE with agonists that couple to IP_3 signaling pathways (Heth *et al*, 1995). Since our study supports the presence of P_2Y receptors linked to an IP_3 pathway in the RPE, extracellular ATP/UTP released from cells of this epithelium or other retinal cells may act a paracrine or autocrine signal for phagocytosis. The RPE initiates phagocytosis within minutes of light onset and thus, release of ATP from retinal cells by light stimuli (see above) could act lead to activation of P_2 purinoceptors in the RPE to initiate binding and ingestion of rod outer segments.

5.4 Role in inflammation and immune response

Inflammatory conditions and metabolic changes in the eye, such as those that accompany diabetes mellitus, have been shown to cause vascular leakage. Plasma leakage into the retina has recently been demonstrated to cause proliferative changes in the RPE (Shiels *et al*, 1998). This suggests that factors present in the plasma may initiate mitogenetic responses in the RPE. Proliferative effects to pathological concentrations of extracellular ATP have been demonstrated in vascular smooth muscle cells (Yu *et al*, 1996). Nucleotide-activated P_{2X} (NSC) and P_{2Y} ($I_{K(Ca)}$) currents could plausibly play a role in proliferative responses. In support of this hypothesis, activation of outwardly rectifying K^+ currents in retinal ganglion cells and a nonselective cation current in

colonic epithelial cells has been implicated in mitogenesis of these cells (Heschler & Schultz, 1993). More recently, mitogens that elevate intracellular Ca^{2+} have been linked to proliferation of RPE cells (Smith-Thomas *et al*, 1998). Thus, it is plausible that certain ocular pathologies elevate the extracellular ATP concentration to a range (0.1 to 100 μM) that could elicit mitogenesis of RPE cells.

The RPE is thought to be an important mediator in several ocular pathologies (Tso, 1988; Chader *et al*, 1988; Zamir, 1997). A role for the RPE in inflammatory and proliferative retinal disorders is suggested by the observation that the RPE produces and responds to a variety of growth factors and cytokines, including platelet derived growth factor, insulin-like growth factor, IL6 and IL8 (Planck *et al*, 1994; Gupta *et al*, 1997; Holtkamp *et al*, 1998). Furthermore, studies have suggested that many of these factors may play a role in the pathogenesis of proliferative vitreoretinopathy and uveitis (Planck *et al*, 1994). In a number of cells, ATP has been shown to modulate the release and/or activities of a number of cytokines. For example, extracellular ATP can modulate tumor necrosis factor (TNF)-induced cytolysis (Kinzer & Lehmann, 1991), and in macrophages 2MeSATP inhibits the release of IL-1 and $\text{TNF}\alpha$ protecting cells from endotoxin-induced death (Proctor *et al*, 1994). The actions of extracellular ATP in modulating cytokine action has been attributed to activation of P2 purinoceptors with subsequent changes in intracellular phospholipid and Ca^{2+} levels, as well as changes in ion fluxes (Kinzer & Lehmann, 1991). These findings support the possibility that extracellular ATP may modulate the release and/or actions of cytokines derived from the RPE. Under conditions such as ocular inflammation where cytokines and ATP may be

simultaneously produced, the activation of RPE purinoceptors may enhance or inhibit the deleterious effects of the pathological situation.

In conclusion, we have provided evidence for the presence of P_{2X} and P_{2Y} purinoceptors on cultured rat RPE cells that are functionally linked to activation of a NSC current, a calcium-activated K⁺ current and elevations in [Ca²⁺]_i. The presence of a number of different purinoceptor subtypes on RPE cells suggests that multiple signaling pathways may be activated in response to extracellular ATP or UTP to modulate various cellular functions under physiological and/or pathophysiological conditions.

CHAPTER 5

Adrenergic regulation of a calcium-activated potassium current in cultured rabbit pigmented ciliary epithelial cells

This work has been previously published by Ryan, J.S., Tao, Q-P and Kelly, M.E.M. (1998). *J. Physiol.* **511**:145-152.

ABSTRACT

The effects of adrenergic agonists on K^+ currents were studied in cultured rabbit pigmented ciliary epithelial (PCE) cells using the whole-cell patch-clamp technique. Under voltage clamp recording conditions, two distinct K^+ currents were observed: an outward rectifying K^+ current (I_K) and an inwardly rectifying K^+ current. A component of the outward K^+ current in PCE cells was found to be Ca^{2+} -activated K^+ current ($I_{K(Ca)}$). External application of the nonselective adrenergic agonists epinephrine or the α_1 -adrenergic agonist phenylephrine activated $K_{(Ca)}$ channels in PCE cells. Phenylephrine-elicited increases in $I_{K(Ca)}$ were reduced following exposure to the selective α_1 -antagonist, prazosin, implicating the involvement of α_1 -adrenoreceptors. The activation of $I_{K(Ca)}$ could be mimicked by dialysis of *D-myo*-inositol (1,4,5)-triphosphate into rabbit PCE and blocked by pre-incubation of cells in thapsigargin or the phospholipase C inhibitor U-73122. Adrenergic increases in $I_{K(Ca)}$ were reduced following dialysis with the G protein blocker, guanosine 5'-O-(2-Thiodiphosphate), but were not blocked by pertussis toxin-pretreatment. These results demonstrate that $I_{K(Ca)}$ channels in rabbit PCE cells are activated by α_1 -adrenergic receptors coupled to a PTX-insensitive G protein(s) and a PLC/IP₃ signaling pathway. Activation of these channels may modulate fluid secretion by the ciliary epithelium.

INTRODUCTION

The ciliary epithelium of the eye is a secreting epithelium comprised of two different epithelial layers; a non-pigmented ciliary epithelial (NPCE) cell layer, whose basolateral membrane faces the posterior and vitreal spaces of the vertebrate eye, and a pigmented ciliary epithelial (PCE) cell layer whose basal surface faces the stromal side. These two cell layers are coupled via gap junctions at their apical membranes (Raviola & Raviola, 1978; Cole, 1984). The formation of aqueous humor in the eye occurs primarily by electrolyte secretion across the ciliary epithelium. The rate and quantity of aqueous humor production are important determinants of intraocular pressure and are subject to autonomic modulation (Cole, 1984).

Recent transport data from intact and dispersed ciliary epithelial tissue, suggests that the PCE cells have solute uptake properties and are coupled to the NPCE cells which have solute efflux properties (Weiderholt, Helbig & Korbmacher, 1991; Edelman, Sachs & Adorante, 1994). Thus, ions and water pass from PCE cells to NPCE cells via gap junctions and are secreted at the basolateral NPCE cell membrane as aqueous humor, an isotonic solution comprised primarily of water, Na^+ and Cl^- and HCO_3^- . The mechanisms by which ion transport and fluid secretion are regulated in coupled PCE and NPCE cells remains unclear, although it is established that vectorial transport of ions and solutes between the coupled epithelial cells requires the coordinated interaction of membrane-localized transporters and intracellular signaling pathways (Jacob & Civan, 1996).

Studies of Ca^{2+} mobilization and heterocellular signal transfer in the rabbit ciliary epithelium, however, has revealed that various agonists such as adrenergic and muscarinic agonists can increase Ca^{2+} in NPCE cells in intact ciliary processes in a synergistic manner (Farahbaksh and Cilluffo, 1994). More recently, studies comparing the Ca^{2+} response in isolated ciliary body epithelial (CBE) cells and the intact ciliary body has demonstrated that with respect to Ca^{2+} mobilization the responses of isolated PCE versus NPCE cells to various agonists is different. For example, isolated PCE cells respond to α_1 -AR agonists but show little sensitivity to α_2 -AR agonists, whilst the opposite response profile is found in NPCE cells. These experiments demonstrate distinct refractory behavior in the ciliary epithelial syncytium with synergistic agonist-induced increases in Ca^{2+} in NPCE cells transferred to coupled PCE cells while the reverse does not occur (Schutte & Wolosin, 1996; Suzuki, Nakano & Sears; 1998). Further investigations are now required to identify the different cellular ion pathways responsive to agonist-induced increases in $[\text{Ca}^{2+}]_{\text{in}}$ in both PCE and NPCE cells. This information will further clarify the mechanisms contributing to vectoral fluid secretion in the ciliary body epithelium.

In the present study, we have examined the effects of adrenergic stimulation on K^+ currents in isolated rabbit pigmented ciliary epithelial (PCE) cells. Our results demonstrate the presence of a Ca^{2+} -activated K^+ current in rabbit PCE cells that is regulated by α_1 -AR stimulation. Furthermore, we confirm that the signaling pathway linking α_1 -AR to K_{Ca} channels involves a PTX-insensitive G protein coupled to IP_3 -sensitive Ca^{2+} stores. Agonist activation of K^+ channels in PCE cells would permit membrane repolarization and increase the driving force for salt secretion across the ciliary epithelium.

METHODS

1. Cell Dissociation and Culture

As described previously (Chapter 2, GENERAL METHODS, section 1.2), eyes were enucleated from 5-10 week old pigmented rabbits and isolated epithelial pieces from the ciliary body were triturated gently to yield single PCE and NPCE cells and small tissue explants. PCE cells were identified by immunofluorescent staining for cytokeratin and were differentiated from NPCE cells by the presence of pigment granules (see Results, Figure 5.1). PCE cells cultured using this isolation technique have been previously shown to be suitable for use in studies on transepithelial ion transport (Staub & Weiderholt, 1991). Rabbit PCE cells in this study were maintained in primary culture up to a maximum of 14 days before electrophysiological recording.

2. Immunocytochemistry

Isolated rabbit CE cells were stained for cytokeratin using the generalized protocol detailed in the GENERAL METHODS (Chapter 2, section 2). Specifically for rabbit CE cells, 10% sheep serum was used to block any nonspecific binding and the primary antibody was mouse anti-cytokeratin pan 8.13 (used at a 1:100 dilution in PBS). The secondary antibody for rabbit CE cell cytokeratin staining was anti-mouse immunoglobulin conjugated with rhodamine at a dilution of 1:100 in PBS (RESULTS, Figure 5.1).

3. Electrophysiological Recording

3.1 Superfusion and Solutions

For cultured CE cells the standard extracellular solution was a low $[\text{Cl}^-]$ physiological solution composed of (in mM): Na^+ -aspartate, 100; NaCl, 30; KCl, 5; CaCl_2 , 1; MgCl_2 , 1; Na_2HCO_3 , 10; HEPES, 10; Glucose 10 (solution F, table 1 in GENERAL METHODS). For low Ca^{2+} solutions, extracellular Ca^{2+} was replaced by 0.2 mM CaCl_2 and 1.5 mM EGTA (solution H, table 1 in GENERAL METHODS). The extracellular calcium concentration with this solution was estimated to be <10 nM. Standard electrode filling solution for whole-cell recordings was composed of (in mM): K^+ -aspartate, 110; KCl 30; MgCl_2 , 1; HEPES, 20; EGTA 1; CaCl_2 , 0.4; ATP (Mg), 1; GTP (Na_2), 0.1 (solution J, table 1 in GENERAL METHODS). Free internal $[\text{Ca}^{2+}]$ was estimated to be <100 nM. In some experiments intracellular Ca^{2+} was buffered to <10 nM by inclusion of 10 mM BAPTA in the electrode solution (solution M, table 1 in GENERAL METHODS).

3.2 Drugs

Potassium channel blockers, (tetraethylammonium chloride [TEA] and ibeirotoxin [IbTX], thapsigargin [TG], PLC inhibitor [U-73122] and prazosin [PZ]) were added to the extracellular solution and superfused during electrophysiological recording. Adrenergic agents (epinephrine (EPI), phenylephrine (PHe)) and the Ca^{2+} ionophore ionomycin were applied by pneumatic pressure injection. D-*myo*-inositol (1,4,5)-triphosphate (IP_3) and $\text{GDP}\beta\text{S}$ were included in the intracellular recording solution and dialysed for 10 min to allow for adequate superfusion into the cytosol. Pertussis toxin (PTX) was added to the

culture medium 24 hr. prior to electrophysiological recording (see section 3.1, Chapter 3)

All chemicals were used at the concentrations cited in RESULTS.

3.3 Electrophysiological recording techniques

Ionic currents in isolated ciliary epithelial cells were studied using whole-cell tight-seal patch-clamp recording methods (Chapter 2, section 3.2). All the data and current-voltage relationships shown have been corrected for LJP's which were 2 mV for standard low Cl⁻ external Ringers and K⁻ -aspartate pipette solution and 5.4 mV for low Cl⁻/low Ca²⁺ external and BAPTA intracellular solution.

3.4 Materials

Thapsigargin, IP₃, U-73122 and PTX were purchased from Calbiochem (LaJolla, California). Ibeirotoxin was purchased from Peninsula Laboratories Inc. (Belmont, CA). All other chemicals were purchased from Sigma Chemical (St. Louis, Mo).

RESULTS

1. Rabbit PCE cell culture: growth characteristics and identification

Primary cultures of PCE cells established from the eyes of pigmented rabbits exhibited the typical phenotype that has been described for PCE cells in culture (CocaPrados & Chat, 1986). Figure 5.1A shows a freshly isolated explant of a rabbit ciliary process tip before mechanical tirturation. The two cell types of this bilayered epithelium are clearly evident. The NPCE cells are devoid of pigment and are tightly coupled to the inner layer of pigment containing PCE cells. Tiruration of the ciliary processes yields isolated PCE and NPCE cells as well as PCE-NPCE cells that are still coupled at their apicies (Figure 5.1 B). Within 3 days of dissociation, cultures contained primarily isolated PCE, which were identified by their heavy pigmentation (Figure 5.1C). NPCE cells tended to have limited survival under the culture conditions used in this thesis and after 5 days ciliary epithelial cultures consisted only of PCE cells (CocoPrados & Chat, 1986).

Immunofluorescence was also used to identify PCE cells in culture. As mentioned previously (see section 2, Chapter 3), antibodies to cytokeratins are widely used as a means to identify cells of epithelioid phenotype including PCE cells in culture. Figure 5.1D shows a fluorescent image of PCE cells grown in culture for 12 days stained with antibodies directed against cytokeratin 8.13. Cultured PCE cells stain positive for cytokeratins, identifying them as epithelial in origin.

Figure 5.1. Isolated rabbit PCE cells in culture. (A) Phase photomicrograph of a freshly isolated explant of a rabbit ciliary process tip showing the coupled nonpigmented and pigmented epithelial cell layers. Scale bar is 10 μm . (B) Freshly dissociated ciliary epithelial cells. Arrow indicates coupled NPCE-PCE cells. Scale bar is 20 μm . (C). Isolated PCE cells grown in culture for 5 days. (D) Fluorescent image of PCE cells in culture for 12 days and stained for cytokeratin 8.13.

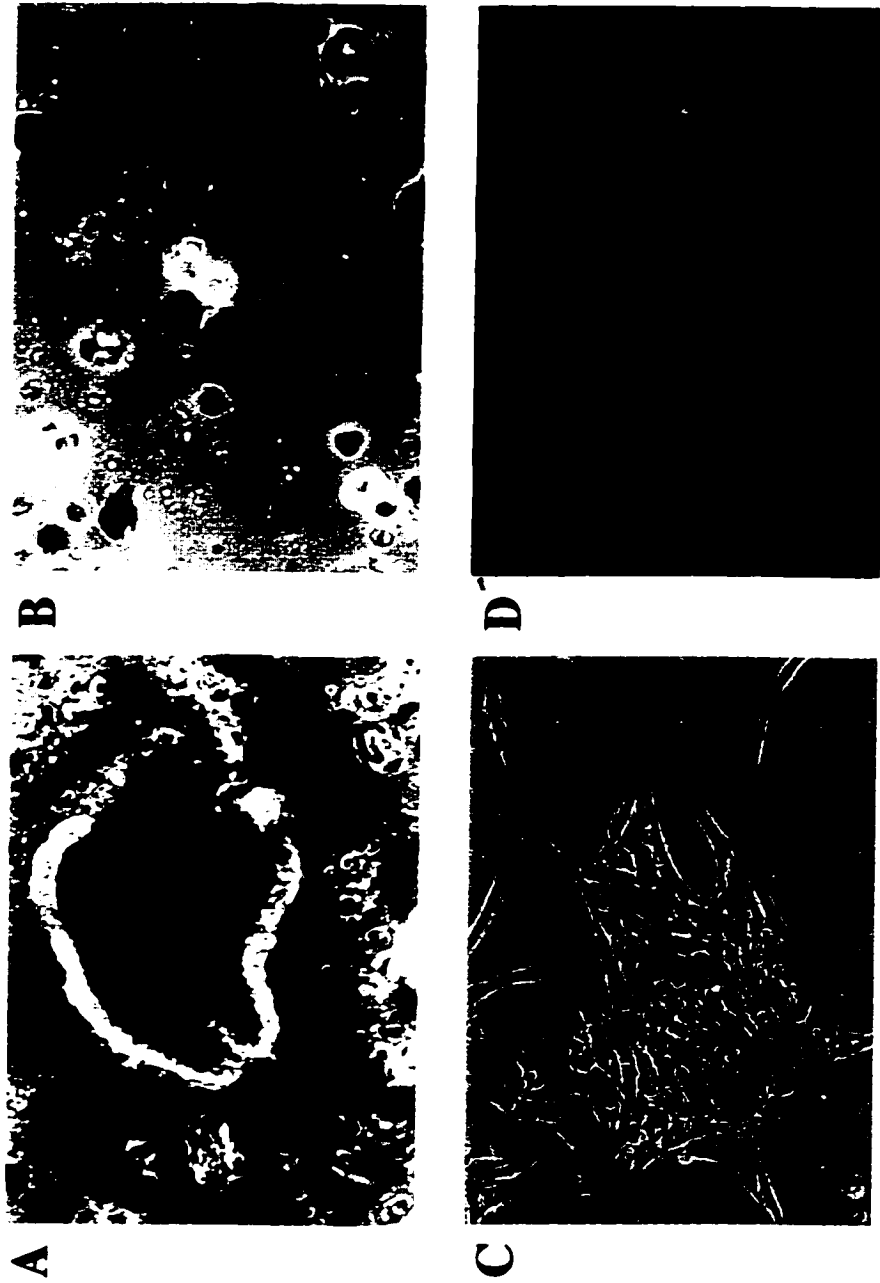
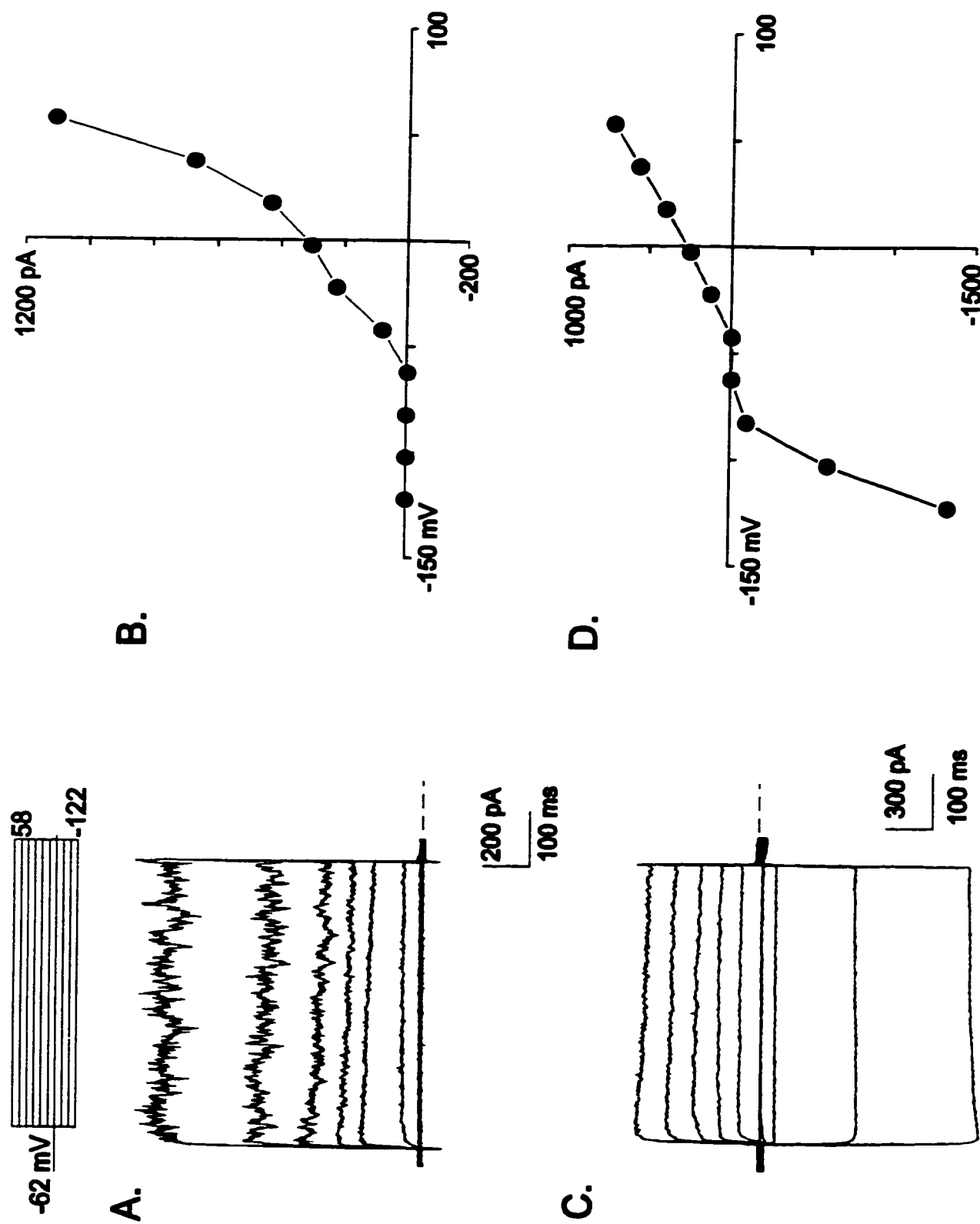


Figure 5.1

2. Membrane properties and whole cells current in rabbit PCE cells

Figure 5.2 shows typical whole-cell current recordings made from cultured PCE cells with 110 K⁻-aspartate electrode solution and standard low Cl⁻ Ringers. The mean membrane potential measured in current clamp upon break-in was -42 ± 1 mV (n=33). Cell capacitance values were obtained from the capacitance compensation circuitry on the amplifier and ranged between 10-48 pF (26 ± 0.8 ; n=108). Under voltage clamp, cells were held at -62 mV and the membrane potential was stepped in 20 mV increments to potentials negative and positive to the holding potential for 500 msec. An outward current was observed at depolarized potentials in all PCE cells recorded from (Figure 5.2A). Figure 5.2B shows the I-V relationship for the cell shown in panel A. For this and subsequent current-voltage relations current was obtained by averaging the current amplitude measured over 50 ms prior to the cessation of depolarizing step commands. The outward current activates at potentials positive to -62 mV and increases with increasing depolarization. In 31% of PCE cells recorded from, voltage steps to hyperpolarizing potentials between -130 and -80 mV also evoked an inward current. In the representative cell shown in Figure 5.2C, the hyperpolarization-activated inward current showed some time-dependent decay at the more negative potential of -130 mV. A slowly inactivating outward current is also apparent in this cell as the membrane potential was depolarized positive to -50 mV. The I-V relationship for the currents shown in panel D indicates an inwardly rectifier current which reverses at around -62 mV and an outward rectifying current which activates positive to -50 mV and increases with depolarization. These currents are similar to K⁺ currents described previously in both rabbit and bovine PCE cells (Fain & Farahbakhsh, 1989; Jacob, 1988).

Figure 5.2. Whole cell currents in cultured PCE cells. Representative whole-cell currents elicited by a series of step depolarizations from -122 to +58 mV from a holding potential of -62 mV. (A) Depolarization-induced outwardly rectifying current was observed in all PCE cells examined, while 33% displayed both inward and outward rectifying current (C). (B,D) Current-voltage relations measured from the traces shown in panel A and C. Dashed line represents zero current in this and subsequent figures.



3. Characterization of outward current in rat RPE cells

3.1 K⁺ selectivity of the outward current

The ionic selectivity of the outward current was investigated by examining time and voltage-dependent relaxations (tail currents) at potentials between -82 and 0 mV, following activation of outward current by a 100 ms voltage step to +20 mV (see Chapter 3, section 4.1). Analysis of the tail currents in 5 PCE cells in 5 mM [K⁺]_o indicated that these currents reversed direction at -76 ± 4 mV. This experimentally derived reversal potential approaches the value of -84 mV calculated for the K⁺ equilibrium potential (E_K) under our recording conditions suggesting that the outward current in PCE cells is K⁺ selective.

3.2 A component of the outward K⁺ current in PCE cells is Ca²⁺-sensitive

In 66% (58/83) of the cells recorded from, the outward K⁺ current appeared “noisy” at more depolarized potentials (+10 to +58 mV) suggesting the presence of large-conductance channels (Tao & Kelly, 1996). A representative cell is shown in Figure 5.3A. The voltage protocol used is indicated above the current traces, with the cell held at a potential (V_H) of -62 mV and stepped for 500 ms from -82 to +58 mV. A 2 min superfusion of the K⁺ channel blocker TEA (1 mM), reversibly reduced outward current. Figure 5.3B shows the I-V plot for the currents represented in panel A. In this cell, outward K⁺ current is almost completely blocked by 1 mM TEA, with a 68% ($65 \pm 10\%$; n=3)

Figure 5.3. Ca²⁺-activated K⁺ current PCE cells. Whole-cell current traces recorded from two representative PCE cells and elicited by voltage steps from -82 mV to +58 mV from a holding potential of -62 mV. Outward current was reduced in the presence of 1 mM TEA (A) and 10 nM of the maxi-K⁺ (I_{K(Ca)}) channel blocker IbTX (C). B and D: Current-voltage relations measured from the currents recorded in panels A and C in the absence (■) and presence (▼) of TEA (B) or IbTX (D). The TEA- and IbTX-sensitive current (○) was obtained by subtracting current records measured in the presence of TEA or IbTX from control currents.

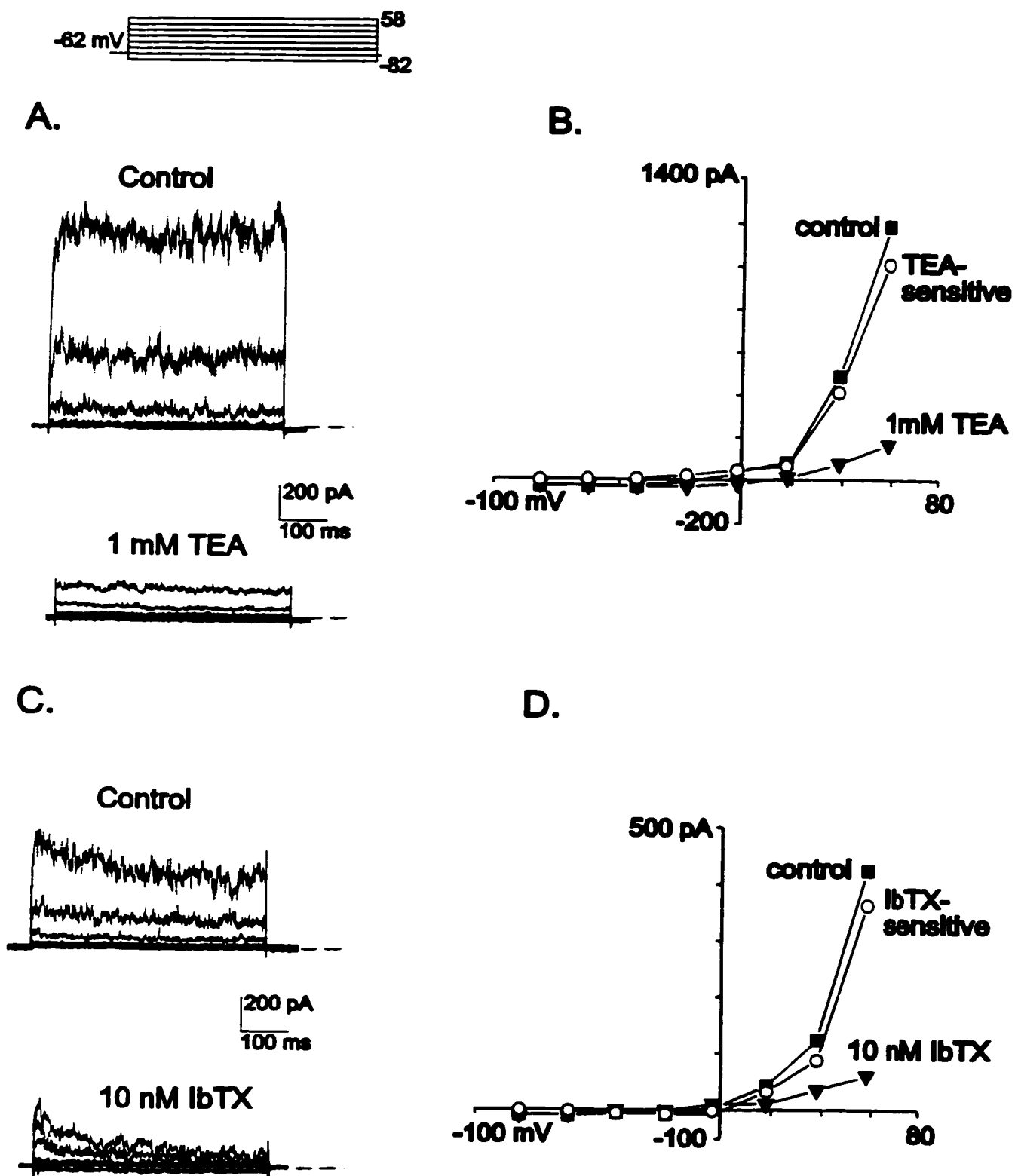


Figure 5.3

reduction in I_K measured at +58 mV and a $65 \pm 18\%$ ($n=3$) reduction at +18 mV. The TEA-sensitive current, obtained by digitally subtracting currents measured in the presence of TEA from control currents, indicates an outwardly rectifying K^+ current that activates at potentials positive to -50 mV.

A similar decrease in the outward current was also observed when the scorpion toxin, IbTX was externally applied. IbTX has been demonstrated to selectively block the large-conductance or "maxi" K_{Ca} channels in a number of cell types (Giangiacomo *et al*, 1992; Giangiacomo *et al*, 1993), including retinal pigment epithelial cells (Tao & Kelly, 1996). Figures 5.3C and D show the whole cell current recording and I-V plot for a representative cell before and after exposure to 10 nM IbTX for 5 mins. IbTX reduced I_K measured at +58 mV by 71% ($69 \pm 11\%$, $n=4$), and at +18 mV by $69 \pm 5\%$ ($n=4$). The IbTX-sensitive K^+ current (Fig. 5.3D) in this cell, as above, was outwardly rectifying with a steep increase in slope conductance at potentials depolarized to +20 mV. Superfusion of PCE cells for 15 min in nominally Ca^{2+} -free external solution also decreased the outward current ($69 \pm 17\%$ at +10 mV and $76 \pm 7\%$ at +58 mV; $n=4$). The mean decreases (\pm SEM) in current amplitude measured at +58 mV following superfusion of PCE cells with TEA, IbTX or nominally Ca^{2+} -free are shown in Figure 5.4. The TEA-, IbTX- and Ca^{2+} -sensitivity of the outward K^+ current suggests that between 50-70% of the outward current in rabbit PCE cells is mediated by "maxi" Ca^{2+} -activated K^+ ($I_{K(Ca)}$) channels.

Figure 5.4. Pharmacological Block of $I_{K(Ca)}$. Mean \pm SEM percentage decrease in outward current, measured 50 ms before the end of a step depolarization to +58 mV. Superfusion with 1 mM TEA (open bar), 10 nM IbTX (black bar) or nominally Ca^{2+} -free Ringers (hatched bar) all reduced the outward I_K by 50-70%.

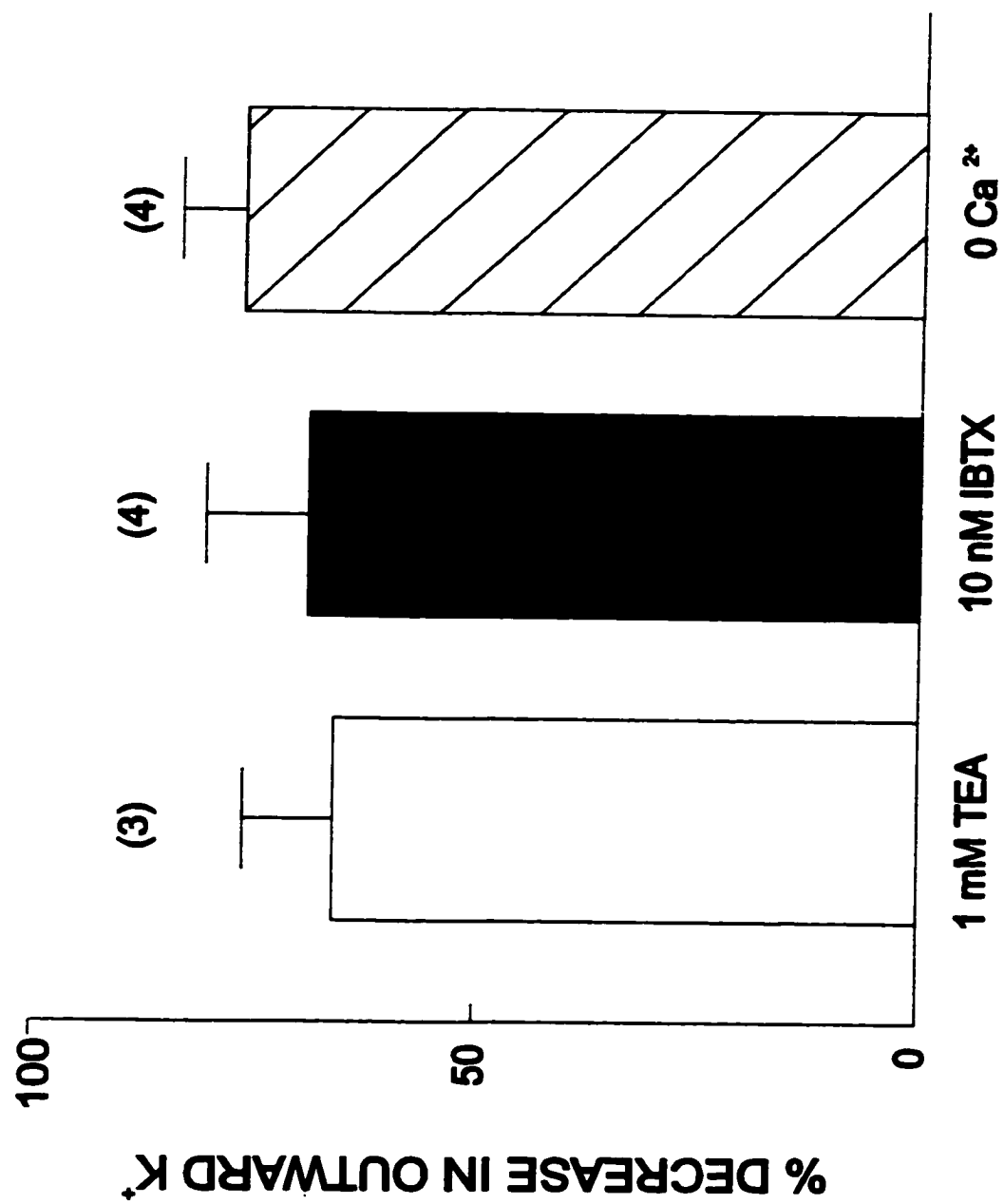


Figure 5.4

Further confirmation of the presence of K_{Ca} channels in PCE cells was obtained using the calcium ionophore, ionomycin to increase $[Ca^{2+}]_{in}$. Figure 5.5, shows outward current recorded at +58 mV from a $V_h = -62$ mV in a representative cell with 110 mM K^+ aspartate internal solution and standard low Cl^- Ringers. In this cell, pressure application of ionomycin increased outward current by 69% with concomitant qualitative increases in current noise at more depolarized potentials. In 9 additional cells, ionomycin significantly increased the outward current measured at +58 mV from 15 ± 2 pA/pF to 35 ± 5 pA/pF ($p < 0.05$; $n=9$), respectively (Figure 5.5B). The ionomycin-induced increase in the outward current was blocked by pretreatment of the cells for 10 min with 10 nM IbTX (panel B; $n=4$; $p > 0.05$), confirming that ionomycin was acting to selectively increase $I_{K(Ca)}$.

4. Adrenergic agonists activate $I_{K(Ca)}$ in PCE cells.

Ca^{2+} -activated channels in other cell types are targets for modulation by a number of transmitters and neuromodulators. Since α_1 -adrenoreceptors have been demonstrated to increase $[Ca^{2+}]_{in}$ in rabbit PCE cells (Schutte *et al*, 1996; Suzuki *et al*, 1997), we first examined the actions of the nonselective adrenergic agonist epinephrine (EPI) on whole-cell K^+ currents in PCE cells. Figure 5.6A shows whole-cell currents recorded by stepping the voltage for 500 ms from -82 to +58 mV in 20 mV increments from $V_H = -62$ mV. The cell was superfused in standard extracellular solution in the absence (control) and presence of epinephrine (100 μ M EPI). Puffer application of 100 μ M EPI substantially increased outward K^+ current activated at depolarized potentials. In addition, the I-V plot for the currents shown in panel A (Figure 5.6B) demonstrates that EPI shifted the activation potential for the outward current from -47 mV to -57 mV (-33 ± 5 mV to -52 ± 5 mV;

Figure 5.5. Activation of $I_{K(Ca)}$ by Ionomycin in PCE cells. (A) Current elicited by a 500 ms depolarization pulse to +58 mV $V_h = -62$ mV, in a representative PCE cell before () and after a 40 sec pressure application of the Ca^{2+} ionophore ionomycin (10 μ M:). Capacitance of the cell was 34. (B) Mean (\pm SEM) current measured at +58 mV for control current (n=13) and current recorded following ionomycin application in the absence (10 μ M Ion; n=9) and presence of IbTX (Ion + 10 nM IbTX; n=4). All currents were normalized for cell capacitance.

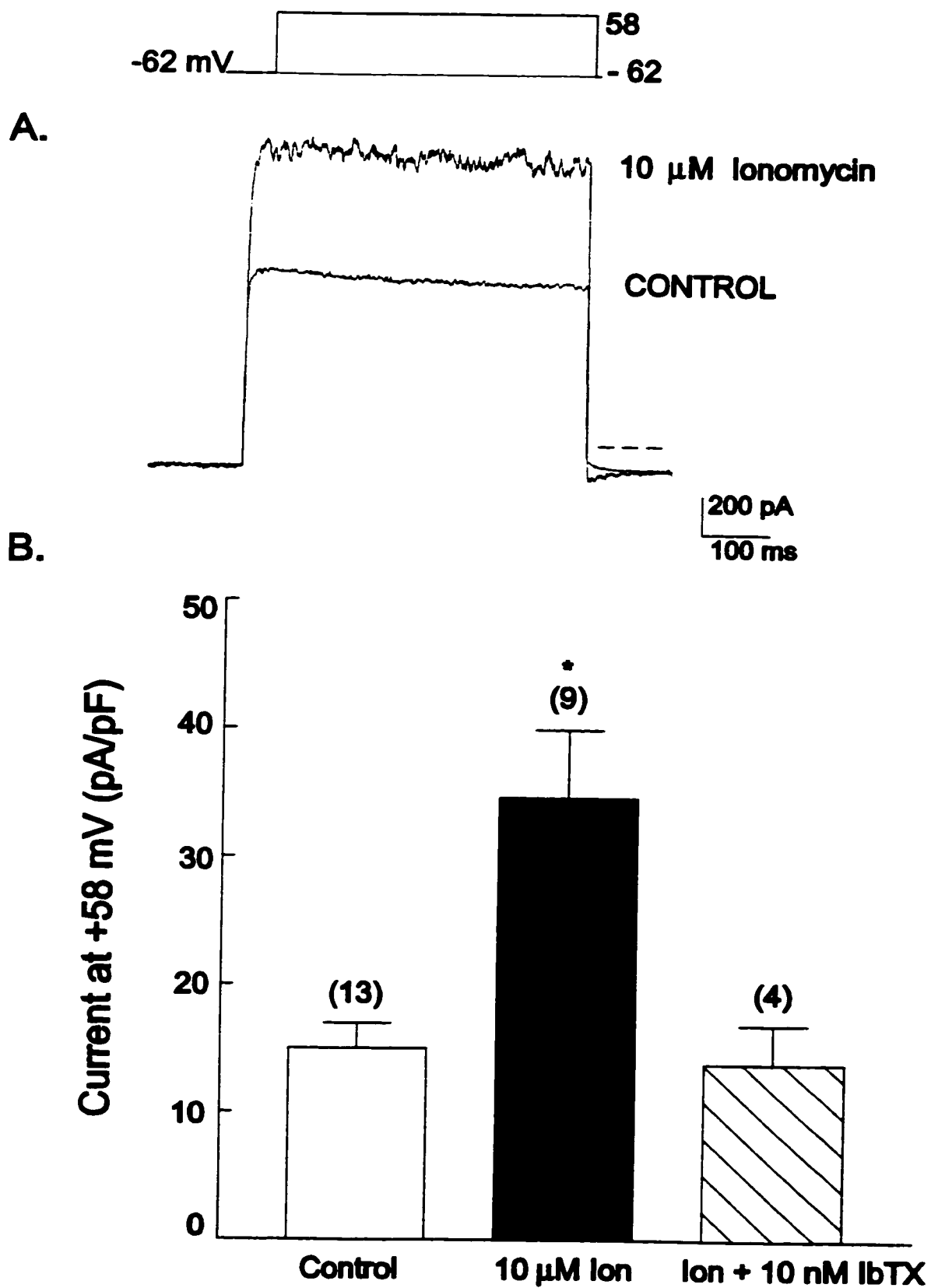


Figure 5.6. Activation of $I_{K(Ca)}$ by Epinephrine. (A). Whole-cell currents elicited from voltage steps from -122 mV to +58 mV from $V_h = -62$ mV, recorded in the absence (control) and presence of 100 μ M EPI. (B). Current-voltage relation for the cell in panel A in the absence (○) and presence of EPI (▲). (C). Mean (\pm SEM) current amplitude measured at +58 mV and normalized for cell capacitance, in 16 cells before (control) and after 40 sec pressure application of 100 μ M EPI. (D). Mean percentage increase in I_K measured at +58 mV after exposure of 4 cells to 100 μ M EPI, in absence (EPI) and presence of IbTX (EPI + 10 nM IbTX).

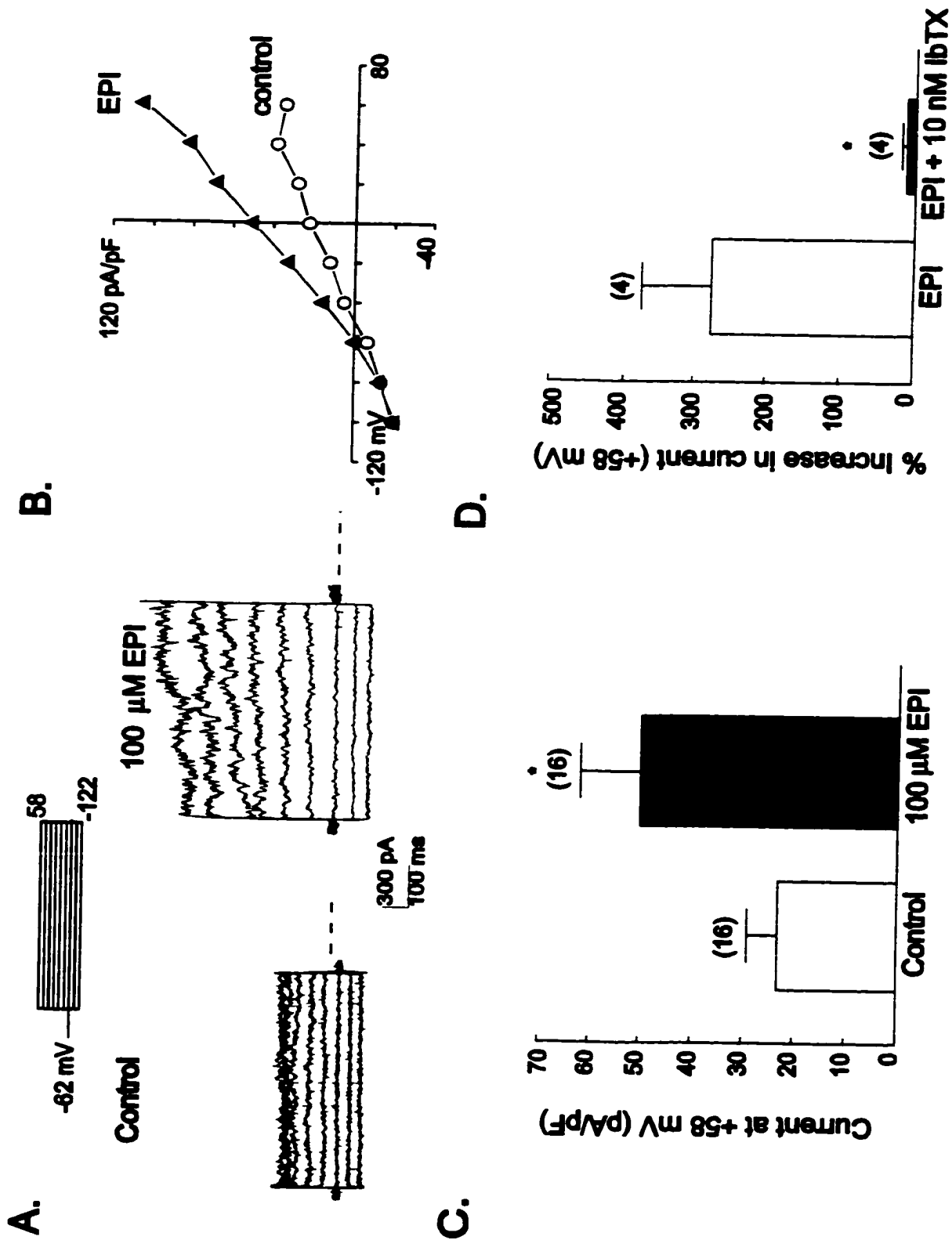


Figure 5.6

n=11), and increased whole-cell current at -52 and -42 mV by 8 and 13 pA/pF compared to control (14 ± 6 pA/pF and 21 ± 9 pA/pF; n=11). Figure 5.6C shows the mean EPI-induced increase in outward current measured at +58 mV. In the presence of EPI outward current increased from 23 ± 6 pA/pF to 50 ± 11 pA/pF (117% increase, $p < 0.05$; Student's paired t-test). In another 4 cells tested, application of EPI produced a $280 \pm 96\%$ increase ($p < 0.05$) in I_K , measured at +58 mV from $V_H = -62$ mV. In these cells, a second application (5 mins after the first application of EPI) of 100 μ M EPI in the presence of 10 nM IbTX failed to increase I_K ($12 \pm 7\%$) in comparison to the first EPI application in the absence of toxin ($p > 0.05$). These data confirm that the current activated by EPI was an IbTX-sensitive I_{KCa} (Figure 5.6D).

Activation of I_{KCa} by adrenergic agonists was via an α_1 -receptor mediated pathway. Figure 5.7A shows current records recorded from a representative PCE cell before and after application of the selective α_1 -adrenoceptor agonist phenylephrine (PHe) with 110 mM K^+ -aspartate electrode solution and standard low Cl^- Ringers. Exposure of the cell to PHe (100 μ M) increased depolarization-activated outward current. Panel B shows the I-V plots for mean current values measured in 10 cells before (control) and after exposure to 100 μ M PHe. In these cells, outwardly rectifying current activated positive to -62 mV and was increased at all potentials positive to -20 mV in the presence of 100 μ M PHe. The increase in outward current by PHe was significant ($p < 0.05$) compared to control for currents measured at +38 and +58 mV. In a total of 55 cells tested, PHe at doses of 10 and 100 μ M increased the outward current measured at +58 mV (panel C). In the presence of 10 μ M PHe, outward K^+ current increased from 20 ± 4 to 30 ± 10 pA/pF (n=5). Whilst in the presence of 100 μ M PHe, the increase in I_K was from 20 ± 2 pA/pF to 41 ± 4 pA/pF

Figure 5.7. Activation of $I_{K(Ca)}$ by α_1 -Adrenoceptors. (A). Whole cell currents recorded from a representative PCE cell. Currents were measured from a holding potential of -62 mV in response to voltage steps from -130 mV to +58 mV in the absence (control) and presence of 100 μ M of the selective α_1 - agonist phenylephrine (PHe). (B). Current-voltage relation for mean (\pm SEM) current amplitude measured in 10 representative PCE cells before (\blacktriangledown) and after a 40 sec exposure to 100 μ M PHe (\bullet). Whole-cell currents were elicited using the voltage protocol in A and normalized for cell capacitance. (C). Mean (\pm SEM) current amplitude measured at +58 mV before (control; n=5) and after 40 sec pressure application of 10 μ M (n=5) or 100 μ M PHe (n = 50). D. Bar shows mean (\pm SEM) increase in current amplitude after repeat exposure of the same 4 PCE cells to 100 μ M PHe.

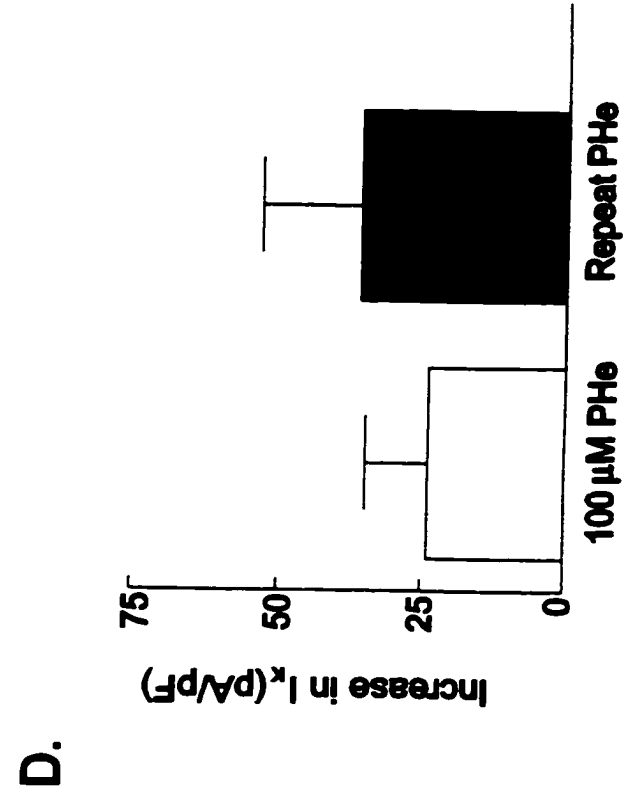
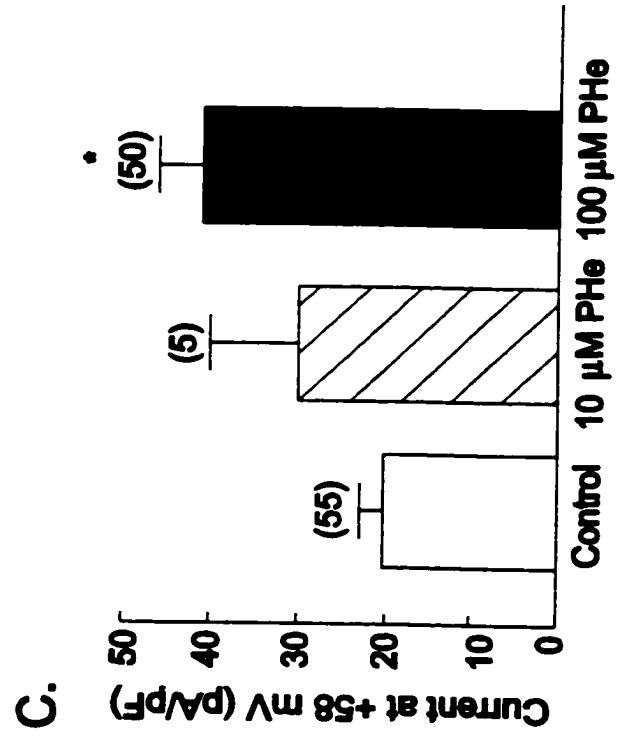
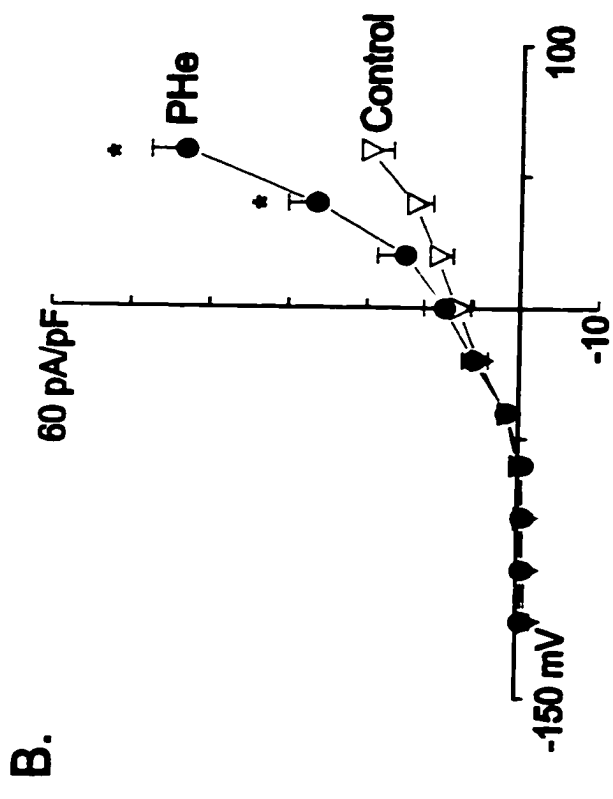
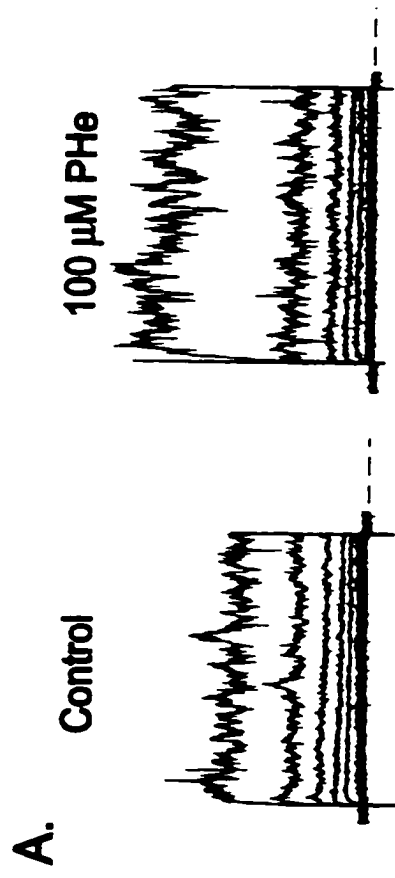


Figure 5.7

($p < 0.05$). The increase in I_K was reproducible following a repeat exposure of the cells to PHe (from 24 ± 11 pA/pF to 36 ± 17 pA/pF; $p < 0.05$, $n=4$, Figure 5.7D).

Further verification that PHe actions were mediated via α_1 -receptors was obtained when the selective α -AR antagonist prazosin (PZ) was added to the superfusate. Prazosin is a competitive antagonist of all α -ARs although its affinity for α_1 -AR subtypes is higher than for α_2 -ARs. Figure 5.8A shows whole-cell currents recorded from the same PCE cell before and after exposure of the cell to 100 μ M PHe in absence and presence of 100 μ M PZ. Figure 5.8B shows the current-voltage plot for the cell in panel A. For this and 5 other cells tested (panel C), 100 μ M PHe significantly increased outward current measured at the end of a 500 ms voltage step to +58 mV ($V_H = -62$ mV) from 15 ± 4 pA/pF to 26 ± 5 pA/pF ($p < 0.05$; Student's paired t-test). Control current recorded at +58 mV in presence of PZ, in the same 5 cells previously exposed to an initial application of PHe, was 22 ± 6 pA/pF and this value increased only slightly to 25 ± 6 pA/pF following exposure to a second 40 sec application of PHe in the presence of PZ. Thus, in the presence of 100 μ M of PZ, application of PHe failed to produce a significant increase in outward current ($p > 0.05$; Student's paired t-test) indicating that PHe modulation of $I_{K(Ca)}$ is mediated via activation of an α_1 -AR coupled pathway.

Figure 5.8. Prazosin block of PHe-mediated $I_{K(Ca)}$ increase. (A). Whole cell currents recorded from a representative PCE cell. Currents were measured from $V_h = -62$ mV in response to voltage steps from -122 mV to $+58$ mV before (control) and after exposure of the cell to $100 \mu\text{M}$ of PHe (PHe) and PHe plus prazosin (PHe + PZ). (B). Current-voltage relation for the cell shown in panel A. (C). Bar graph shows mean (\pm SEM) percent increase in current measured at $+58$ mV for the same 5 cells before and after 40 sec applications of $100 \mu\text{M}$ PHe (control; PHe) or PHe plus $100 \mu\text{M}$ prazosin (PZ; PZ + PHe)

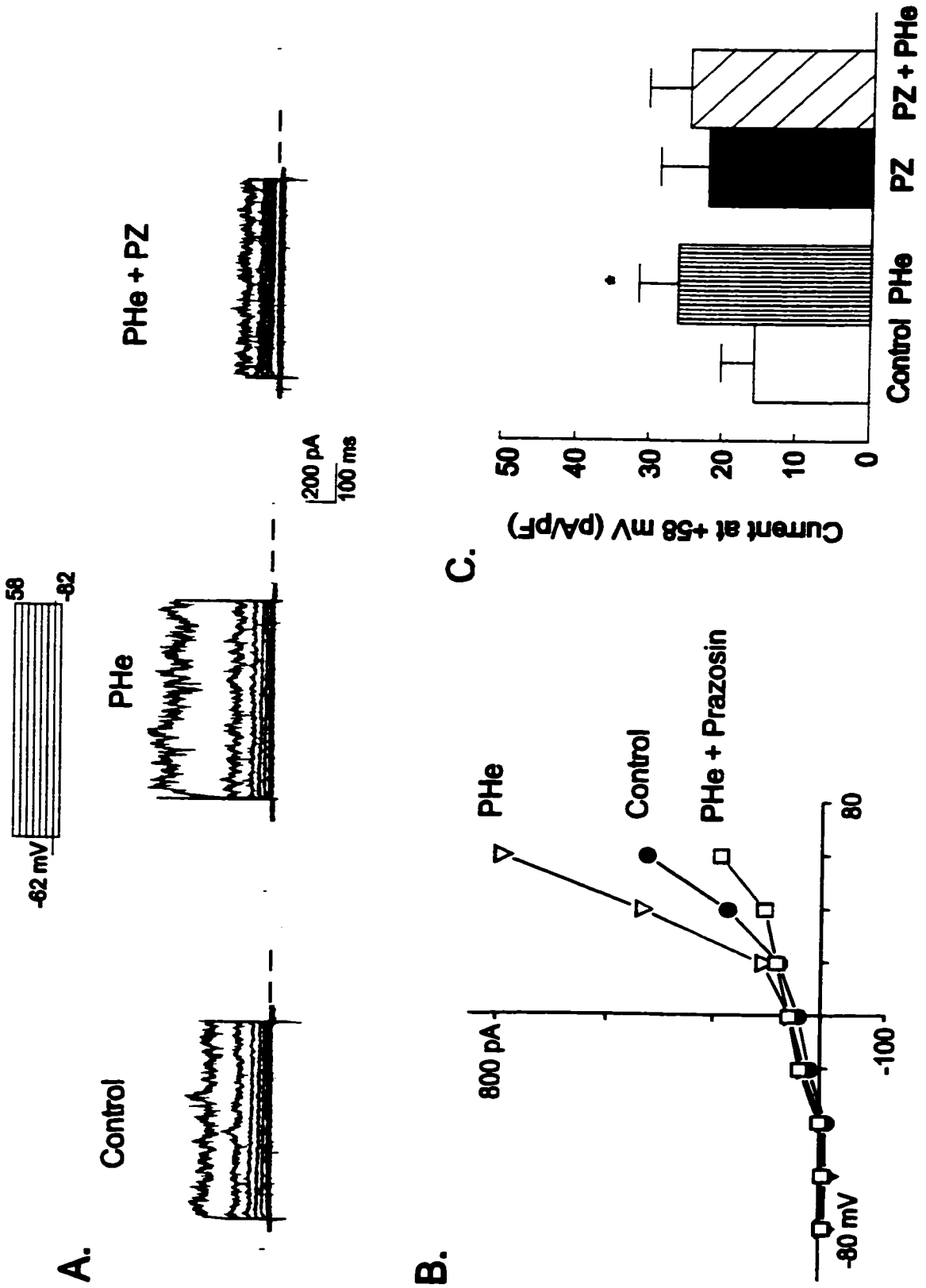


Figure 5.8

5. Signaling pathways involved in α_1 -adrenoreceptor activation

of I_{KCa}

5.1 IP_3 and intracellular Ca^{2+} -stores

In many cells, the actions of α_1 -AR agonists are associated with a rise in $[Ca^{2+}]_i$. These alterations in $[Ca^{2+}]_i$ result from agonist/receptor activation of phospholipase C-mediated hydrolysis of phosphatidylinositol 4,5-bisphosphate and liberation of IP_3 . Inositol triphosphate then mobilizes Ca^{2+} from intracellular storage sites by interacting with a specific receptor (Berridge, 1993; Minneman, 1993). We examined whether the IP_3 pathway was involved in PHe-induced activation of $I_{K(Ca)}$ in PCE cells by either dialyzing the cell cytosol with IP_3 to activate $I_{K(Ca)}$, or by exposing PCE cells to thapsigargin and nominally zero Ca^{2+} Ringers and looking for attenuation of the actions of PHe. Thapsigargin mobilizes Ca^{2+} from intracellular stores by inhibiting Ca^{2+} sequestration into IP_3 -sensitive pools (Foskett, Roifman & Wong, 1991).

Whole cell current traces are shown from a representative PCE cell immediately after break-in and after 10 min. dialysis with 10 μ M IP_3 in the standard pipette solution (Figure 5.9A). The cell was held at -62 mV and stepped to +58 mV for 500 ms to activate outward current. The mean outward current measured at +58 mV was significantly increased from 19 ± 7 to 51 ± 15 pA/pF ($p < 0.05$ Student's paired t-test; $n = 11$) after 10 min. internal dialysis with IP_3 . Current amplitude was not significantly different when cells were dialyzed for 10 min with internal recording solution in the absence of IP_3 (data not shown). Pre-incubation of PCE cells with 5 μ M thapsigargin (TG) for 30 min in nominally Ca^{2+} -free

Figure 5.9. Involvement of IP₃ and Intracellular Ca²⁺ Release in modulation of I_{K(Ca)}. (A). Representative whole-cell currents produced from voltage steps between -122 and +58 mV from V_h = -62 mV, immediately after obtaining whole-cell configuration (break-in) and after 10 min dialysis with 10 μM IP₃ in the pipette. (B). Mean (± SEM) current amplitude measured at +58 mV and normalized for cell capacitance in 5 PCE cells treated for 30 min with 5 μM thapsigargin before (TG) and after 40 sec application of 100 μM PHe (TG + PHe). Mean current amplitude is also shown for 5 cells in the absence of thapsigargin, before (control) and after PHe application (PHe) (*p < 0.05; Student's paired t-test).

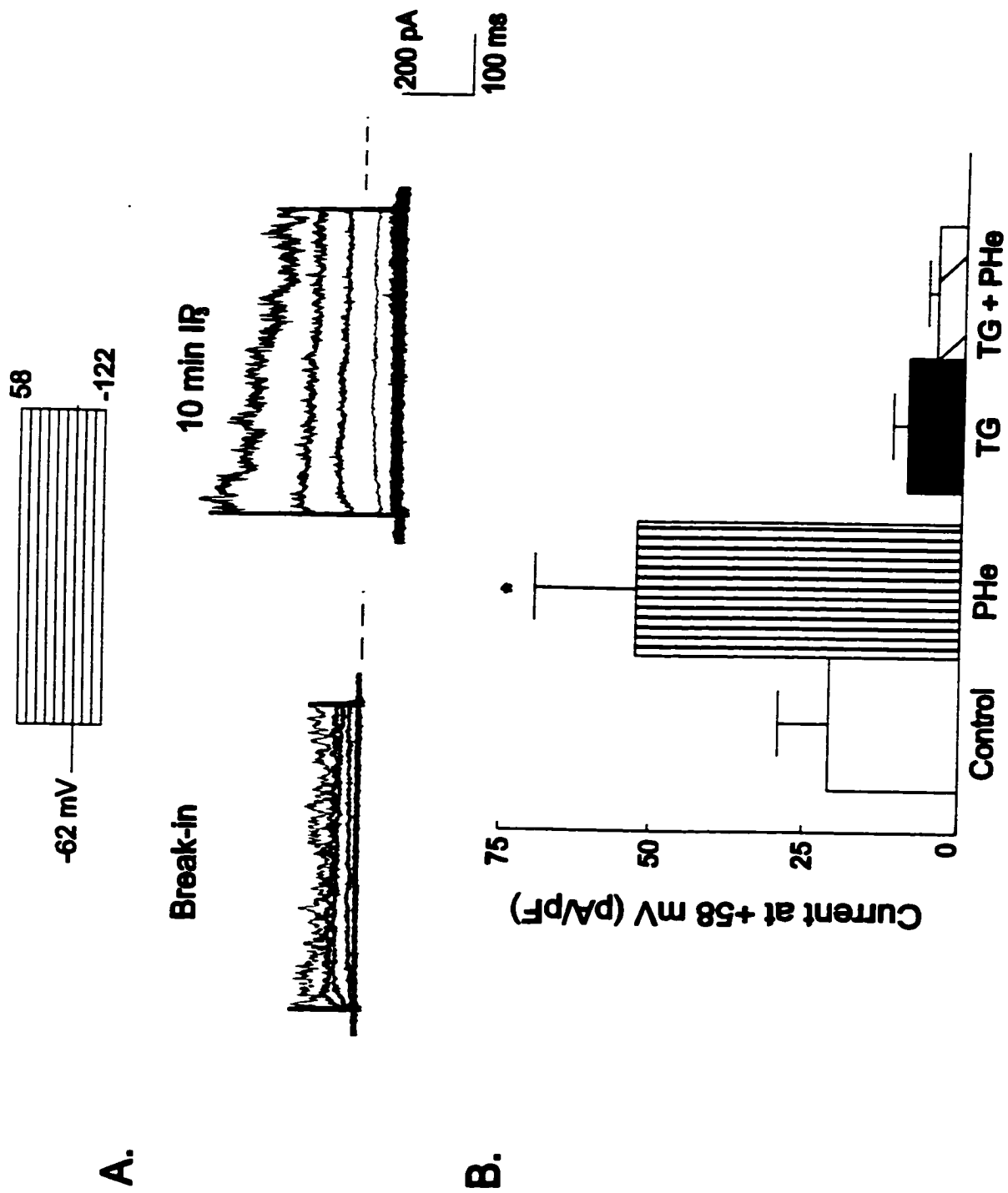


Figure 5.9

Ringer's, to empty sarcoplasmic reticular Ca^{2+} stores, blocked the PHe-mediated increase in $I_{K(\text{Ca})}$ ($n=5$; Figure 5.9B). In contrast, in PCE cells from the same culture which were not treated with thapsigargin, PHe significantly increased $I_{K(\text{Ca})}$ from 20 ± 8 pA/pF to 53 ± 17 pA/pF ($p<0.05$; $n=5$). These data support a role for IP_3 -induced intracellular calcium release in mediating the effects of PHe in modulation of $I_{K(\text{Ca})}$.

5.2 Involvement of PLC

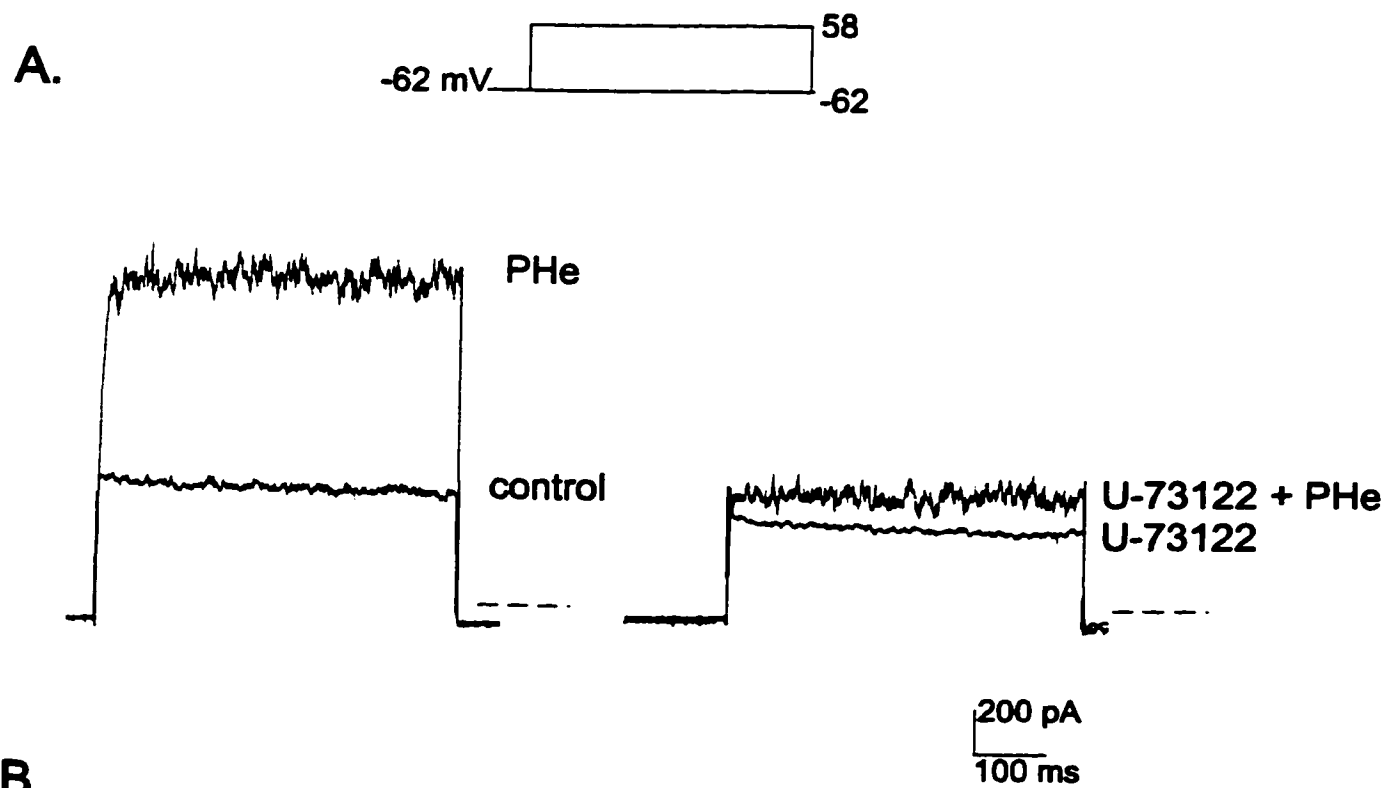
To further verify the involvement of an IP_3 pathway in the α_1 -AR increase in $I_{K(\text{Ca})}$ we exposed cells to the PLC enzyme inhibitor U-73122 (Hildebrandt, Plant & Meves, 1997). Figure 5.10A shows a PHe-induced increase in $I_{K(\text{Ca})}$ in a representative PCE cell before and after 20-30 min of superfusion with 10 μM of the PLC inhibitor U-73122. As above, the cell was stepped from $V_H = -62$ mV to $+58$ mV for 500 ms. In this cell and 3 other cells tested, PHe-mediated increases in $I_{K(\text{Ca})}$ were effectively blocked following exposure of the cells to U-73122 compared to control ($p>0.05$; Student's paired t-test) (Figure 5.10B). Thus, these results together with the findings on the effects of internal dialysis of IP_3 and pre-incubation with thapsigargin/zero Ca^{2+} on PCE cells, confirm the involvement of an IP_3 signaling pathway in mediating the PHe-induced increases in $I_{K(\text{Ca})}$.

6. The role of G proteins in $I_{K(\text{Ca})}$ activation by PHe

In many cell types α_1 -AR are coupled to PTX-insensitive heterotrimeric G proteins of the G_q class (Summers & McMartin, 1993). To confirm G protein involvement in mediating PHe increases in $I_{K(\text{Ca})}$, the standard 100 μM GTP in the pipette was replaced

Figure 5.10. Inhibition of PLC inhibits PHe-induced increases in $I_{K(Ca)}$. (A).

Representative whole-cell currents from a single PCE cell in response to a 500 ms step depolarization to +58 mV from $V_h = -62$ mV. Current is shown before and after pressure application of 100 μ M PHe and in the same cell before (control; PHe) and after 20-30 min incubation with 10 μ M U-73122 (U-73122; +PHe). (B). PHe-mediated increase in the mean current amplitude, normalized for cell capacitance, measured at +58 mV in 4 cells before (control; PHe) and after incubation with U-73122 (U-73122; U-73122+PHe) for 20-30 min (* $p < 0.05$; Student's paired t-test).



B.

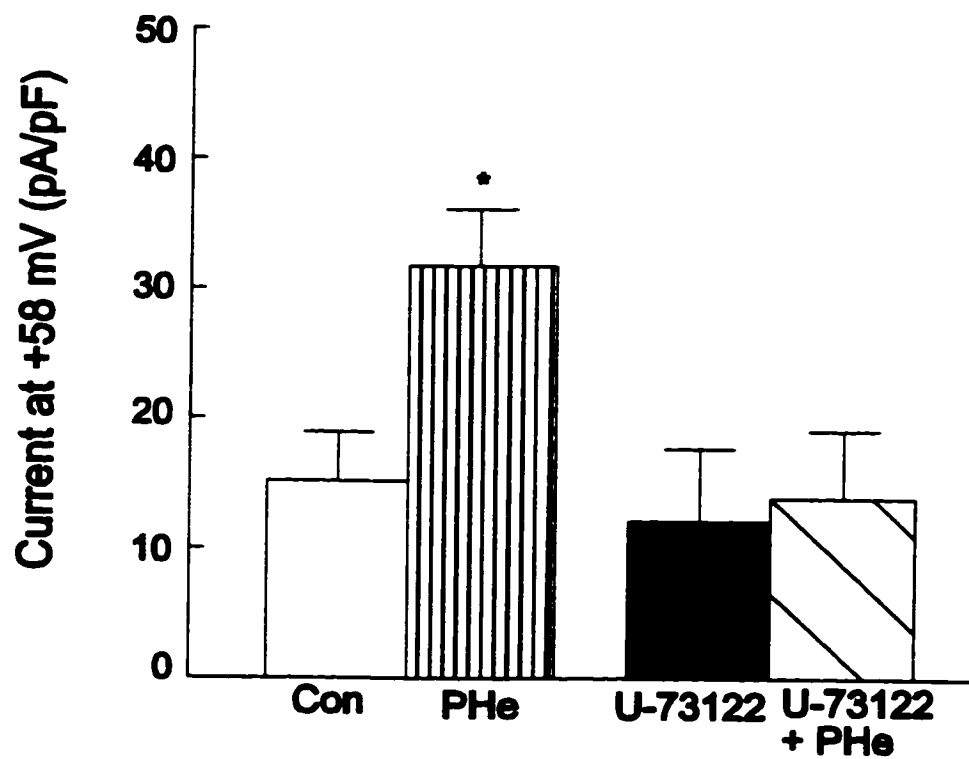


Figure 5.10

with 2 mM of the G protein blocker GDP β S. When GTP was included in the pipette PHe significantly increased $I_{K(Ca)}$ measured at +58 mV from 32 ± 11 pA/pF to 98 ± 21 pA/pF (n=5) (Figure 5.11A). However, in another 4 cells tested on the same day from the same culture before and after 10 min dialysis with 2 mM GDP β S in the pipette, 100 μ M PHe failed to significantly increase outward current measured at +58 mV over control value (24 ± 4 pA/pF vs. 30 ± 5 pA/pF; $p > 0.05$). This result confirms G protein involvement in the PHe-induced activation of $I_{K(Ca)}$ in PCE cells.

To determine whether the α_1 -AR modulation of $I_{K(Ca)}$ involved a PTX-insensitive G protein, we then pretreated PCE cells for 12 hours with 500 ng/ml of PTX, a dose previously shown to be effective in blocking PTX-sensitive G protein action in isolated ocular epithelial cells (Poyer *et al.*, 1996). The toxin inactivates G proteins of the $G_i/G_o/G_z$ class by catalyzing the ADP-ribosylation of the α subunit (Ui, 1990). Whole-cell recordings were made from control cells (not exposed to PTX) as well as from PTX-treated cells in standard intracellular and extracellular solutions. All cells were from the same culture and were plated at the same time prior to PTX treatment. Figure 5.11B shows that in 4 control cells without PTX pretreatment, a 40 sec exposure to PHe (100 μ M) significantly increased I_K measured at +58 mV ($V_H = -62$ mV) from 10 ± 3 pA/pF to 27 ± 3 pA/pF (Student's paired t-test; $p < 0.05$). In another 4 cells pretreated with PTX, a similar increase in outward current was observed following PHe application with current increasing from 20 ± 8 pA/pF to 48 ± 5 pA/pF (Student's paired t-test; $p < 0.05$). These data suggest that the G protein involved was not PTX-sensitive and therefore was not of the $G_i/G_o/G_z$ class.

Figure 5.11 G proteins are involved in PHe-mediated $I_{K(Ca)}$ Increase. (A). Bar shows mean (\pm SEM) current amplitude measured at +58 mV with 0.1 mM GTP or 2 mM GDP β S in the pipette before (GTP; GDP β S) or after 40 sec application of 100 μ M PHe (GTP + PHe; GDP β S + PHe). (B). Mean (\pm SEM) current amplitude at +58 mV in 4 untreated cells before (control) and after PHe application (+PHe), and in cells 4 pretreated with 500 ng/ml of PTX before (PTX-treated) and after PHe-application (PTX +PHe). Data has been normalized for cell capacitance. (* p <0.05; Student's paired t-test).

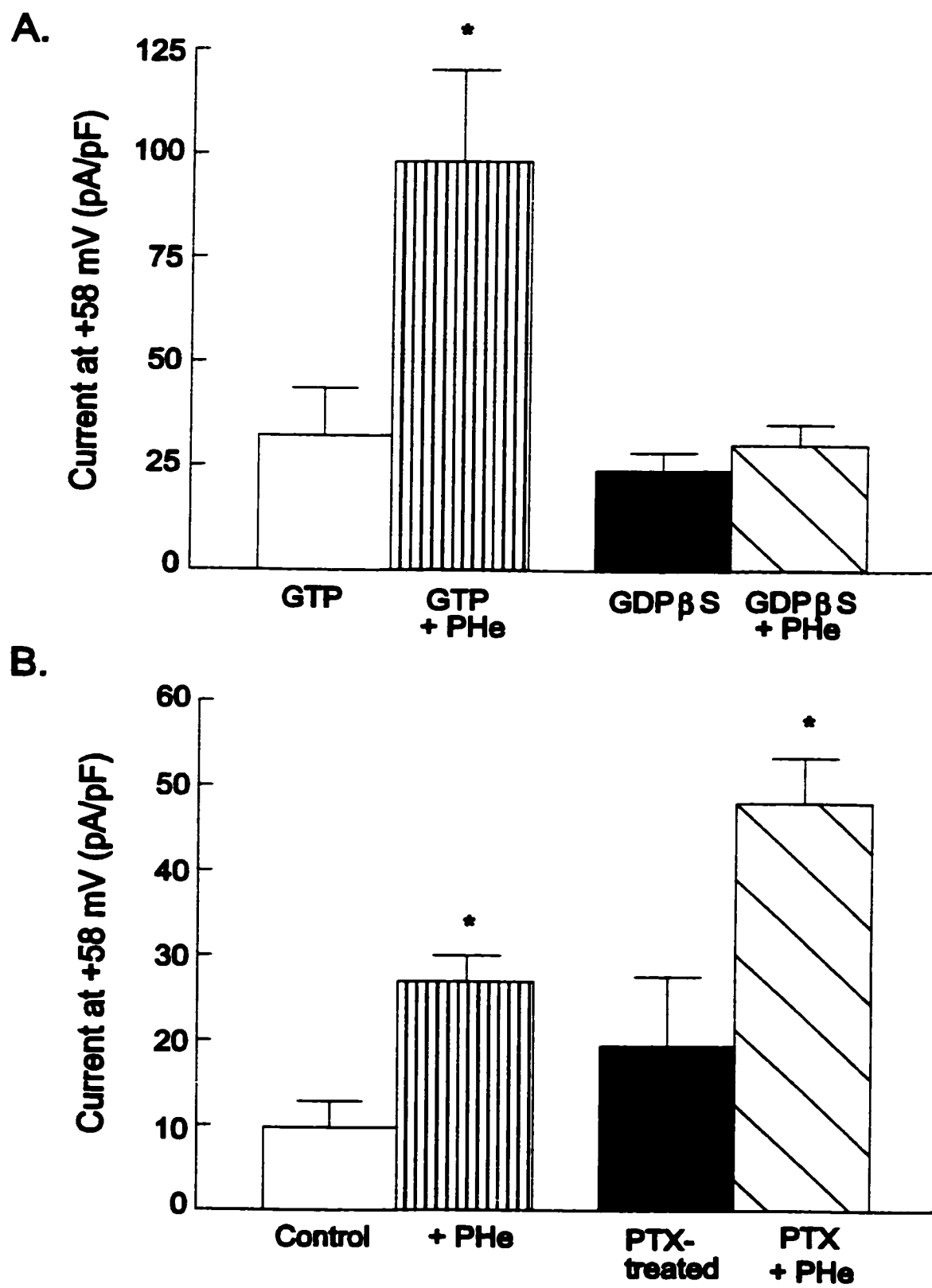


Figure 5.11

DISCUSSION

In this study we demonstrated that isolated rabbit PCE cells exhibit at least three K^+ conductances: an inwardly rectifying K^+ current, an outwardly rectifying K^+ current and a calcium-activated potassium current ($I_{K(Ca)}$). Furthermore, we have shown that $I_{K(Ca)}$ is modulated by adrenergic agonists activating α_1 -adrenoceptors which are coupled to a PTX-insensitive G protein(s) and a PLC/ IP_3 signaling pathway. To our knowledge this is the first report of α_1 -adrenergic modulation of a K^+ current in mammalian ciliary epithelial cells. This finding suggests that α_1 -adrenergic agonists may act as paracrine and/or autocrine signals to modulate ion and fluid transport across the CBE.

1. Membrane properties and voltage-dependent K^+ current in rabbit PCE cells

The average resting membrane potential (RMP= -42 mV; n=33) and cell capacitance (26 pF; n=108) of cultured rabbit PCE cells in this study compares well with those values previously reported for isolated PCE cells from a number of mammalian species (Jacob, 1991a & b; Stelling & Jacob, 1991 & 1993), but is somewhat depolarized compared with average value of -65 to -75 mV reported *in situ* for intact CBE preparations (Green *et al*, 1985). As with other isolated ocular epithelia, the enzymatic/low Ca^{2+} isolation procedure has been suggested to contribute to this discrepancy as it disrupts epithelial polarity and gap junction communication between the cells (Davis *et al*, 1995).

Previous studies in isolated PCE cells have identified a number of voltage dependent ionic currents. TTX-sensitive Na^+ current (Fain & Farahbakhsh, 1989), T and L-type Ca^{2+} current (Jacob, 1991; Farahbakhsh, Cilluffo, Chronis & Fain, 1994), Cl^- currents, a nonselective cation current (Jacob & Civan, 1996); both outwardly and inwardly rectifying K^+ currents (Fain & Farahbaksh, 1989; Jacob, 1991; Stelling & Jacob, 1991) have all been reported. Under our recording conditions the membrane of isolated rabbit PCE cells was dominated by K^+ conductances. In 33% of isolated rabbit PCE cells an inwardly rectifying K^+ current was observed. This current has properties similar to inwardly rectifying K^+ currents described previously in isolated rabbit (Fain & Farahbakhsh, 1989) and bovine (Stelling & Jacob, 1992) PCE cells. In this and other studies, the current-voltage plot for the inward rectifier K^+ current shows strong inward rectification and a time-dependent decrease in the hyperpolarizing voltage-clamp response. These characteristics identify this current in PCE cells as an anomalous type of inward rectifier K^+ channel (Stelling & Jacob, 1992; Jacob & Civan, 1996).

All rabbit PCE cells examined exhibited depolarization-activated current that was demonstrated to be K^+ selective by tail current analysis. Our observation that the outward current appeared very “noisy” at depolarized potentials in the majority of PCE cells recorded from raised the possibility of the presence of two components of the outward current. Our lab has previously demonstrated that in rabbit RPE cells such “noise” in the whole-cell current trace is indicative of the presence of a large-conductance Ca^{2+} -dependent K^+ channels ($I_{\text{K}(\text{Ca})}$) (Tao & Kelly, 1996). Consistent with this suggestion we identified that 36-87% of the outward current in rabbit PCE cells was ($I_{\text{K}(\text{Ca})}$). The remainder of the depolarization-activated outward current was most likely the delayed

rectifier current ($I_{K(V)}$) that has been observed in all isolated PCE cells examined to date (Jacob & Civan, 1996; Fain & Faranbhakhsh, 1989). Similar to our findings, in cultured bovine PCE cells the depolarization-activated outward current was also shown to be composed of both a delayed rectifier current ($I_{K(V)}$) and a Ca^{2+} -dependent K^+ current ($I_{K(Ca)}$) (Jacob, 1991). However, in bovine PCE cells, $I_{K(Ca)}$ was not as prominent as in rabbit, and constituted only 28% of the outward current. This may suggest some species differences or culture condition differences in ion channel expression. However, in contrast to our results, a study by Fain & Faranbhakhsh (1989) found no evidence for $I_{K(Ca)}$ in cultured rabbit PCE cells. The reason for this discrepancy is unknown.

2. Calcium-activated K^+ current in rabbit PCE cells

To date, all the $K_{(Ca)}$ channels identified are dependent upon Ca^{2+} for their activation. These channels have been subcategorized as big (BK or maxi- K^+) channels, intermediate (IK) channels or small (SK) channels on the basis of their single channel conductance, and their sensitivity to voltage and specific blockers (reviewed by McManus, 1991). We identified the $I_{K(Ca)}$ current that we observed in rabbit PCE cells as arising from activation of a BK or maxi K^+ type of channel based on the sensitivity of this current to voltage, to external Ca^{2+} concentration and to blockade by low concentration of external TEA (1 mM) and the selective maxi K^+ channel blocker IbTX (Giangiacomo *et al*, 1992 & 1993). The large variability in the amount of the outward current that was identified as $I_{K(Ca)}$ (36-87%) in rabbit PCE cells may reflect heterogeneity in K^+ channel expression that has been described for both fresh and

cultured ocular epithelial cells (Fain & Farahbakhsh, 1989; Stelling & Jacob, 1991; Tao *et al*, 1994; Tao & Kelly, 1996).

In bovine PCE cells, the activity of $I_{K(Ca)}$ was shown to be dependent in part on the entry of Ca^{2+} through low threshold voltage-dependent T-type Ca^{2+} channels (Jacob, 1991). This finding was based on the observation that Ni^{2+} , but not the dihydropyridine nifedipine, significantly reduced the amplitude of $I_{K(Ca)}$. Approximately 13% of the T-type channels are active at -70 mV allowing for significant Ca^{2+} entry at the physiological resting membrane potential of PCE cells *in situ* (Jacob, 1991a; Jacob, 1991b). This finding suggests that in bovine PCE cells $I_{K(Ca)}$ may be active under physiological conditions to provide a K^{+} efflux pathway. Rabbit PCE cells have been shown to possess L-type Ca^{2+} channels (Farahbakhsh *et al*, 1994), but the existence of T-type channels has not yet been demonstrated. L-type Ca^{2+} channels are active at potentials 20-30 mV depolarized from the normal range of membrane potentials found in these nonexcitable cells, and therefore would not play a role in activation of $I_{K(Ca)}$ under normal physiological conditions. Under the voltage protocol used in this study however, it is likely that Ca^{2+} entry through these L-type Ca^{2+} channels contributed to the activity of $I_{K(Ca)}$. This suggestion is supported by the observation that removal of extracellular Ca^{2+} virtually abolished the activity of $I_{K(Ca)}$.

3. Function of K^{+} currents in the CBE

Voltage-dependent K^{+} -selective channels are a ubiquitous feature of both PCE and NPCE cell membranes. The major functional role of the inward or anomalous rectifier in PCE cells, as in other cell types, is to carry outward current and thus stabilize

the membrane potential close to E_K (Fain & Farahbakahsh, 1989; Stelling & Jacob, 1992; Jacob & Civan, 1996). Hyperpolarization of the PCE cell membranes would also lead to an increased driving force for Cl^- secretion across basolateral membrane channels of the NPCE channels and theoretically, increase aqueous humor secretion. The delayed rectifier current ($I_{K(V)}$) is the most frequently observed voltage-dependent outward current in both fresh and cultured mammalian PCE cells. In excitable cells this current is responsible for membrane repolarization during an action potential. Its functional role in the CE remains undefined since this current is only activated at potentials 30-40 mV depolarized to V_m . In many epithelial cell types, inward and outwardly rectifier K^+ channels have a polarized distribution (Hunter *et al*, 1986). Under the conditions of this study we did not attempt to localize these channels to either the basal or apical membrane. However, a number of studies on isolated iris-CB preparations as well as coupled and isolated CE cells have suggested that both cell membranes possess Ba^{2+} blockable K^+ currents (Chu *et al*, 1986; Edelman *et al*, 1994a; Edelman *et al*, 1994b).

In contrast to $I_{K(V)}$, the observation in bovine PCE cells that $I_{K(Ca)}$ is active under normal physiological conditions, has led to the suggestion that it may play a role in ion transport across the CBE (Jacob, 1991; Jacob & Civan, 1996). Similar to functional role suggested for the inward rectifier, activation of $I_{K(Ca)}$ in PCE cells would lead to NPCE membrane hyperpolarization, and via alterations in transepithelial potential, provide an increased driving force for Cl^- secretion into the aqueous humor via anion channels on coupled NPCE cells (Jacob, 1991; Jacob & Civan, 1996). It has also been suggested that the coordinated interaction of $I_{K(Ca)}$ and T-type Ca^{2+} channels underlies a slow spontaneous membrane oscillation observed in bovine PCE cells (Stelling & Jacob,

1992; Stelling & Jacob, 1993; Jacob & Civan, 1996). At the normal potential of these cells, ~13% of the T-type channels would be active causing depolarization of the PCE membrane away from rest. Depolarization coupled with Ca^{2+} entry activates $I_{K(\text{Ca})}$, which acts to hyperpolarize the membrane back to rest. In this way, the repeated cycle of depolarization/hyperpolarization acts to maintain V_m .

Any factor that elevates intracellular Ca^{2+} has the potential to activate $I_{K(\text{Ca})}$ (McManus, 1991). In CE cells, a broad number of agonists linked to signaling cascades that regulate intracellular Ca^{2+} release have been documented to modulate aqueous humor formation. Probable the best-studied agents for their role in modulating aqueous formation by the CE are adrenergic drugs (Sorenson & Abel, 1996; Martin, 1996). How these drugs affect specific ion transport pathways within the CE cells to regulate aqueous formation remains undefined. However, in other cells types, including ocular epithelial cells, adrenergic drugs have been shown to change the activity of $I_{K(\text{Ca})}$ (Sato, 1996; Nara *et al*, 1998; Myraki *et al*, 1998; Tao & Kelly, unpublished observation). Altered $I_{K(\text{Ca})}$ activity in these epithelia has been proposed to play a role in the regulation of transepithelial membrane potential and ion transport (Tao & Kelly, 1996).

4. Adrenoceptors receptors in the CE

4.1 Effect of adrenergics in the CE

Adrenergic agonists control many functions in the eye. Clinical and experimental evidence from a number of mammalian species suggests that adrenergic drugs play important roles in regulating intraocular pressure (IOP) (Krupin *et al*, 1980; Chiou, 1983; Ross & Drance, 1970). For example, the β -adrenergic antagonist timolol is a commonly

used drug in the treatment of glaucoma due to its ability to reduce elevated IOP. The role of β -adrenergic agonists in regulating IOP however is less clear, with numerous studies demonstrating conflicting results probably due to actions on surrounding tissues (Caprioli *et al*, 1989; Sears, 1991). Similar to β -adrenergic antagonists, selective α_2 agonists, most notably apraclonidine, have also been used for several years in reducing elevated IOP in glaucomatous patients (Chiou, 1983). Selective α_1 agonists like phenylephrine have been shown to have effects opposite to α_2 agonists and can actually elevate IOP (Chiou, 1983).

Adrenergic drugs can alter IOP by changing the rate of aqueous humor formation, secretion and/or outflow. Identifying the exact mechanisms of action for these drugs is hampered by their notably complex effect on a variety of ocular structures including blood vessels, muscles, the trabecular meshwork and the ciliary body epithelium (CBE). In attempts to identify the effect of adrenergic drugs on aqueous humor secretion across the CBE, a number of researchers have employed the use of intact iris-CBE preparations or isolated PCE and NPCE cells. Studies in the rabbit iris-CBE have demonstrated that both α - and β -AR agonists alter ionic movement across the CBE, as measured by a decrease in short circuit current (I_{sc}) in the presence of these agonists (Krupin *et al* 1991; Shi *et al*, 1996). Although these studies did not allow researchers to deduce whether an increase or decrease in net solute transfer had occurred they did demonstrate that adrenergic agonists have a direct effect on ion flow across this epithelium. Recently, a number of studies have demonstrated increases in intracellular Ca^{2+} levels in isolated rabbit PCE and NPE cells in response to α -AR but not β -AR agonists (Schutte *et al*, 1996; Suzuki *et al*, 1997). Although these studies did not provide any evidence for functional coupling of the Ca^{2+} increase with a particular CE function, Ca^{2+} second

messenger systems in a variety of other epithelia are linked to change transepithelial ion and/or fluid transport (Leipziger *et al*, 1996; Van-Scott *et al*, 1995; DuVall & O'Grady, 1994). This suggests that adrenergic-mediated $[Ca^{2+}]_i$ increases might be involved in regulating aqueous humor formation across the CE.

4.2 Potential sources of adrenergics in vivo

Strong support for endogenous catecholamines in the regulation of aqueous production by the CE has come from a number of studies demonstrating significant levels of both NE and EPI in human aqueous humor (Trope & Rumley, 1982; Trope *et al*, 1987). Three potential sources of for these endogenous catecholamines have been proposed. The major source of NE for the eye is from ocular sympathetic nerves that are supplied almost exclusively from the superior cervical ganglion. Within the CB, the epithelial cells are richly innervated by nerves from a sympathetic fiber plexus located in the region of the ciliary process (Kramer *et al*, 1972; Stone *et al*, 1987; Streeten, 1991). The ciliary processes of the CB also receive a rich supply of blood from the anterior ciliary arteries that branch from the ophthalmic artery. Studies have demonstrated that at least one small arteriole, and sometimes several, branch into each ciliary process (Streeten, 1982). Therefore, the ciliary arteries accompanying sympathetic nerves into the ciliary processes may provide an important source of circulating catecholamines for the CE. Finally, a third potential source of endogenous catecholamines may originate from the adjacent iris tissue. The iris has been shown to synthesize EPI extra-neuronally, predominately by the action of phenylethanolamine N-methyltransferase (PNMT) (Elayan *et al*, 1990). Despite an effective uptake process for EPI into the adjacent iris

muscle and vasculature, iris-derived EPI may act on the adjacent CE cells. The demonstration that a number of potential sources for both endogenous EPI and NE exist in the CB further supports a physiological role for these catecholamines in modulation of aqueous humor formation by the CE.

4.3 α_1 -ARs in rabbit PCE cells

Very few studies have detailed the effects of adrenergic agonists on whole-cell current in isolated CE cells. This study however, has identified that the nonselective adrenergic agonist epinephrine (EPI), and the selective α_1 -AR agonist, phenylephrine (PHe), increase outward current in isolated rabbit PCE cells. The adrenoceptor stimulated outward current was identified as $I_{K(Ca)}$ based on the observations that it was mimicked by the Ca^{2+} ionophore ionomycin and blocked by the maxi- K^+ channel blocker IbTX. Our finding that the α -AR antagonist prazosin blocks PHe-mediated increases in $I_{K(Ca)}$, further supports the involvement of an α_1 -AR subtype in mediating this response.

Radioligand binding studies have identified and localized a number of adrenergic receptor subtypes to the CBE supporting a physiological role for these receptors in AH formation (Nathenson, 1981; Mittag & Tormay, 1985, Wax & Molinoff, 1987; Jin, Verstappen, Yorio, 1994). These subtypes belong to one of three recognized families of adrenergic receptors, classified as α_1 , α_2 or β . All three families share approximately 40% sequence homology and are members of the superfamily of serpentine transmembrane G protein-coupled receptors (Reviewed by Summers & McMartin, 1993). In the epithelial cells of the CB many studies support the suggestion that β_2 adreceptors are the predominate β -ARs present (Nathenson, 1981). The predominate

family of α -ARs in the CBE was thought for many years to be α_2 -ARs (Mittage & Tormey, 1985; Elena *et al*, 1989). The advent of more selective drugs and molecular cloning techniques, however has identified that the expression of α -ARs in ocular tissues, including the CBE, is more heterogeneous and includes all known α -AR subtypes.

The α adrenergic receptor family now has more than 7 different subtypes (α_{1A} , α_{1B} , α_{1C} , α_{2AD} , α_{2B} and α_{2C}) that have been identified on the basis of their sequence homology and shared (or similar) signal transduction mechanisms (Watson & Arkininstall, 1994; MacKinnon, Spedding & Brown, 1994; Daunt *et al*, 1997). Pharmacological characterization of α -AR subtypes in a given tissue is hampered by the usual presence of more than one subtype and the lack of subtype-selective drugs that can fully discriminate between subtypes (MacKinnon *et al*, 1994; Zhao *et al*, 1996). Generally, α_1 -ARs subtypes are recognized on the basis of agonist (methoxamine, BMY 7378, AH 11110A) and antagonist (prazosin, WB4101) affinity and their susceptibility to inactivation by the alkylating agent chlorethylclondine (Minneman & Esbenshade, 1994; Zhao *et al*, 1996). α_2 -ARs subtypes are similarly classified on their agonist/antagonist affinity profiles. However, α_2 -ARs can be pharmacological distinguished from α_1 -ARs on the basis of their lack of sensitivity to the α_1 -AR agonist PHe and their low sensitivity to the α_1 -AR antagonist prazosin (MacKinnon *et al*, 1994).

Detailed studies in the CBE from a number of mammalian species, including human (Huang *et al*, 1995), bovine (Bylund *et al*, 1997), rabbit (Jin *et al*, 1994) and porcine (Winkensen-Matsson *et al*, 1996), have demonstrated that there is a species specific expression pattern of both α_1 and α_2 -AR subtypes. In the rabbit CBE, all

subtypes of α_1 and α_2 -ARs have been identified. Recent studies have suggested that α_1 -ARs may be localized to the PCE cells whereas α_2 -ARs, specifically the α_{2A} -AR, are localized to the NPE cells (Shutte *et al*, 1996; Suzuki *et al*, 1997). These findings were based on functional Ca^{2+} mobilization studies demonstrating that the selective α_2 -ARs agonist brimonidine only evoked Ca^{2+} signals in NPCE cells, whereas the selective α_1 -ARs agonist PHe evoked Ca^{2+} signals exclusively in PCE cells. Furthermore, prazosin could block the PHe-mediated $[\text{Ca}^{2+}]_i$ increase in PCE cells but not the brimonidine-mediated $[\text{Ca}^{2+}]_i$ increase in NPCE cells. Our studies are consistent with these findings and support our hypothesis that PHe-evoked increase in $I_{K(\text{Ca})}$ is mediated by an α_1 adrenoceptor subtype on rabbit PCE cells.

4.4 α_1 -AR signal transduction and modulation of $I_{K(\text{Ca})}$ channels in PCE

In most cell types, α_1 -AR activation couples via PTX-insensitive G_q proteins to the activation of PLC and the initiation of the IP_3 /DAG cascade (Summers & McMartin, 1993). This signaling pathway culminates in rises in intracellular Ca^{2+} and subsequent Ca^{2+} and DAG-dependent activation of PKC. Elevated $[\text{Ca}^{2+}]_i$ is thought to occur as a result of IP_3 -mediated release of Ca^{2+} from internal stores and/or the influx of extracellular Ca^{2+} via voltage-dependent and non-voltage dependent Ca^{2+} channels (Minneman, 1988; Summers & McMartin, 1993). Several lines of evidence suggest that like other GPCRs, α_1 -ARs do not couple exclusively to an IP_3 /DAG cascade in all cell types. Studies have shown that, α_1 -ARs can also couple to other PTX-insensitive and sensitive signaling pathways to mediate activation of PLA_2 , PLD, increases in adenylate cyclase (AC) and generation of AA (Minneman & Esbenshade, 1994; Guarion *et al*,

1996). There has been some suggestion in the literature that selective α_1 -AR subtypes may be linked to these specific transduction pathways but, to date, there is no definitive correlation between subtype and signaling mechanism. In contrast to α_1 -ARs, activation of all known α_2 -ARs subtypes have been shown to couple to PTX-sensitive G_i/G_o proteins and inhibition of AC (MacKinnon *et al*, 1994). However, like α_1 -ARs, more recent studies have demonstrated that α_2 -ARs subtypes may also couple to signaling pathway linked to stimulation of AC and PLC in some cell types (Daunt *et al*, 1997).

Our findings that increases in $I_{K(Ca)}$ could be mimicked by internal dialysis with synthetic IP_3 and blocked either when PLC was inhibited, or IP_3 -sensitive intracellular Ca^{2+} stores were depleted with thapsigargin, confirmed involvement of an IP_3 signaling pathway in mediating phenylephrine's effect on $K_{(Ca)}$ channels in rabbit PCE cells. These findings, combined with our demonstration that phenylephrine couples to a PTX-insensitive G protein, suggests that in rabbit PCE cells α_1 -adrenoceptors acting via a PLC/ IP_3 pathway which leads to the activation of $I_{K(Ca)}$. In support of our findings, studies in a number of cells types, including ocular epithelia, have demonstrated that maxi- K^+ channels are targets for modulation by agonists that couple to signaling pathways linked to elevations in $[Ca^{2+}]_i$ (Marty, 1987 & 1989; Tao & Kelly, unpublished observations; Jacob, 1996b). In all cases Ca^{2+} binding to the channel protein increases channel activity. In addition to intracellular Ca^{2+} release, it should be noted that DAG-activated PKC may also play a role in modulating $I_{K(Ca)}$ in rabbit PCE cells. This suggestion is supported by the observation that the activity of $K_{(Ca)}$ channels in a number of cell types can be modulated by kinase-dependent phosphorylation (Marty, 1989; Critz *et al*, 1992; Nara *et al*, 1998; Pellegrino & Pellegrini, 1998). Figure 5.12 shows a schematic for the activation of $I_{K(Ca)}$ by α_1 -AR activation in rabbit PCE cells.

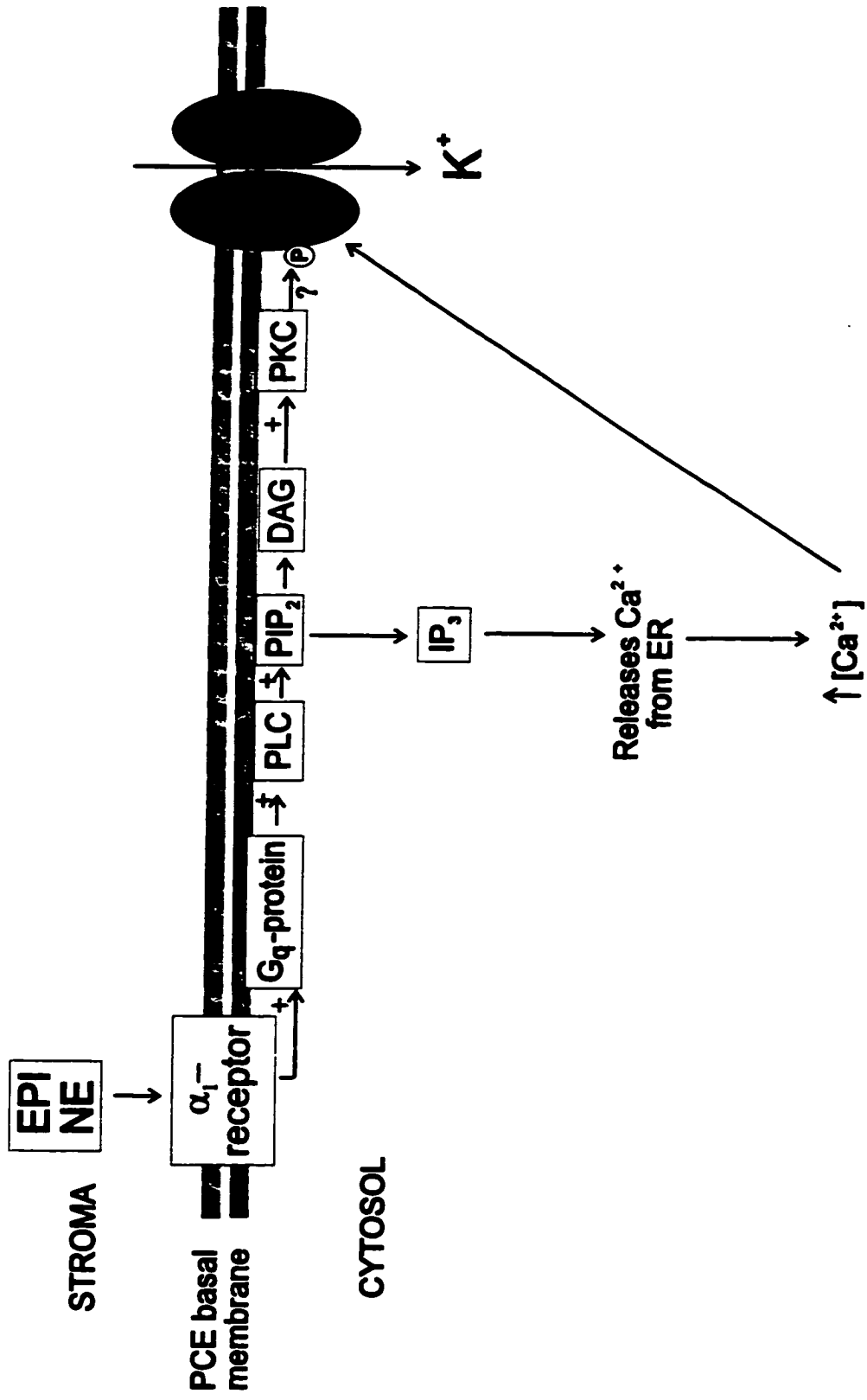


Figure 5.12. Schematic of α_1 -adrenoceptor signaling pathway linked to K_v channel activation in PCE cells. (see text for details)

4.5 Physiological implication of $I_{K(Ca)}$ modulation by α_1 -adrenoceptors

Our findings indicate that $I_{K(Ca)}$ may be activated at or near the resting membrane potential in rabbit PCE cells *in vitro* via release of receptor-coupled Ca^{2+} stores. The negative shift in the activation potential for the outward K^+ current in the presence of adrenoceptor stimulation is consistent with data reported on maxi $I_{K(Ca)}$ currents in rabbit retinal pigment epithelial cells (Tao & Kelly, 1995). These data indicate that elevations in $[Ca^{2+}]_i$ increase the probability that $I_{K(Ca)}$ channels open at membrane potentials close to the physiological resting potential of these cells. Once activated, $I_{K(Ca)}$ would lead to K^+ exit and PCE cell membrane hyperpolarization. Potential changes in the PCE cells would be relayed to NPCE cells via gap junctions between the cells resulting in hyperpolarization of the NPCE cell membrane. This membrane hyperpolarization would increase the electrical driving force for Cl^- secretion into the aqueous phase via basolateral Cl^- channels. Increased efflux of Cl^- from NPCE cells has been postulated to augment the rate of aqueous humor secretion. This hypothesis is based on the concept that Cl^- channel activity is actually a rate-limiting step in the rate of aqueous formation (Coco-Prados et al, 1995; Jacob & Civan, 1996). Therefore, our findings suggest that Ca^{2+} -activated K^+ channels on PCE cells are potential sites for adrenergic regulation of aqueous humor secretion across the CBE *in vivo*.

Several studies on aqueous humor dynamics support the suggestion that activation of α -ARs *in vivo* may augment AH formation (Krupin *et al*, 1980; Chiou, 1983). In the rabbit eye there is a circadian elevation of IOP and aqueous flow that occurs with dark onset in the normal daily light-dark environment. Concomitant with these circadian rhythms of aqueous humor dynamics is an elevated aqueous norepinephrine (NE) level

(Lui & Dacus, 1991; Gregory & Nil, 1998). Sympathectomy reduces nocturnal elevations in aqueous humor flow suggesting that release of NE from ocular sympathetic nerves is involved in this circadian regulation of aqueous humor dynamics (Gregory *et al*, 1985; Braslow & Gregory, 1987). Furthermore, circadian elevations in IOP can be reduced by prazosin, supporting the involvement of α -ARs in modulating nocturnal elevations in the rate of aqueous formation (Lui & Dacus, 1991). In light of these findings, it is plausible that modulation of $I_{K(Ca)}$ on PCE cells may be part of the adrenergic mechanism underlying circadian elevations in IOP and aqueous flow.

In conclusion, we have demonstrated that $I_{K(Ca)}$ in rabbit PCE cells can be activated by α_1 -AR coupled to IP_3 -sensitive Ca^{2+} stores release. *In vivo*, transmitters and hormones could modulate $I_{K(Ca)}$ activity providing a mechanism for both paracrine and autocrine regulation of aqueous humor secretion across the ciliary epithelium.

CHAPTER 6

GENERAL DISCUSSION AND FUTURE WORK

The specialized cells of the retinal pigment epithelium (RPE) and pigmented ciliary epithelium (PCE) perform a number of functions vital to processing the visual image. The major role of both epithelia in the vertebrate eye is in the transport of fluid and ions. RPE-mediated transepithelial transport between the choroid and sensory retina is integral for maintenance of an optimal environment for photoreceptor functioning. Electrolyte secretion across the PCE and non-pigmented cells of the ciliary body epithelium (CBE) is essential for the formation of aqueous humor, which nourishes the anterior segment of the eye and is an important determinant of intraocular pressure (IOP). Given their invaluable roles, these epithelia must be able to detect and respond to changes in the ocular environment to ensure normal physiological functioning of the eye.

Biochemical and physiological studies have identified that a variety of G protein-coupled receptors (GPCRs), including, muscarinic, purinergic and adrenergic receptors are present in both the RPE and PCE (Friedman *et al.*, 1991; Osborne *et al.*, 1993; Wolfensberger *et al.*, 1994; Nash & Osborne, 1995; Huang *et al.*, 1995; Bylund *et al.*, 1997; Jin *et al.*, 1994). Application of exogenous agonists linked to GPCR activation can modulate ion and fluid transport in these epithelia, suggesting that they may be important paracrine and/or endocrine signals *in vivo* (Dearry *et al.*, 1990; Gallemore & Steinberg, 1990; Joseph & Miller, 1992; Krupin *et al.*, 1991). The close apposition of the PCE and RPE to the underlying vasculature and sympathetic and parasympathetic nerve fibers may provide an important source of endogenous modulators which may be released from nerve endings or reach the epithelial cells via the circulation.

The goal of this thesis was to examine the role of receptor-coupled signaling pathways in the regulation of cation conductances in isolated RPE and PCE cells. Although a variety of studies have identified a number of voltage-dependent cation and anion conductances in these cells, few studies have attempted to dissect how signaling molecules may modulate the activity of individual ion channels. Elucidating the cellular and molecular mechanisms regulating ion fluxes in these epithelia provides novel information about the role of these cells in normal ocular physiology and increase our understanding of the etiology of a number of ocular pathologies linked to defects in RPE and PCE transepithelial transport.

This thesis has demonstrated receptor-coupled signaling pathways linked to modulation of cation conductances in isolated RPE and PCE cells. In rat RPE cells, a G-protein activated NSC cation current, a P_{2X} purinoceptor NSC current and a P_{2Y} purinoceptor-activated K_{Ca} channel were identified. In rabbit PCE cells, activation of α_1 -adrenoceptors linked to an IP_3 /DAG signaling pathway and intracellular Ca^{2+} stores release modulated the activity of K_{Ca} channels.

In isolated rat RPE cells, the activation of a nonspecific cation (NSC) current by G protein analogues was demonstrated to be mediated by a PTX-sensitive $G_{\alpha i}$ subunit protein coupled to intracellular Ca^{2+} and MAP-kinase-dependent phosphorylation. Activation of this conductance would cause membrane depolarization, alter the transepithelial potential (TEP), and thus, affect the activity of a variety of other ionic pumps, transporters and channels. Changes in transepithelial transport mediated by NSC channel activation may be functionally linked to changes in other RPE functions. For example, large depolarizations mediated by the activation

of NSC channels in other cell types has been linked to phagocytosis and proliferation (Young *et al*, 1983; Jung *et al*, 1992; Siemen & Gogelein, 1993).

The endogenous ligand linking NSC channel activation in rat RPE cells to the $G_{\alpha i}$ /MAP kinase pathway has not been identified. Recently, the water-soluble phospholipid, lysophosphatidic acid (LPA), was shown to activate a PTX-sensitive NSC current and to cause proliferative changes in cultured RPE cells (Thoreson & Chacko, 1997). *In vivo*, micromolar concentrations of LPA are present in serum and significant amounts may also be produced by stimulated platelets. In the eye, injury or breakdown of the blood-retinal barrier may expose the RPE to LPA and/or other serum factors. Subsequent LPA-mediated alterations in transepithelial ion transport associated with the activation of an NSC conductance, may be linked serum-induced RPE proliferation. In support of this hypothesis, the activation of an NSC current in macrophages is known to be functionally linked to mitogenesis (Lipton, 1986; Young *et al*, 1983)

Our preliminary findings suggest that LPA can activate a NSC and K^+ conductance in rat RPE cells (Ryan & Kelly, unpublished observations). Furthermore, Western blot data demonstrated LPA-mediated stimulation of MAP kinase in the rat RPE. In light of these findings we hypothesize that in rat RPE cells, LPA stimulates a PTX-sensitive G_i -coupled MAP kinase signaling pathway linked to activation of an NSC conductance. Therefore, using acutely isolated rat RPE cells, our future research objectives for this project would be to use molecular and whole-cell recording techniques to:

1. Examine the ion selectivity, voltage-dependence and kinetics of the NSC current activated by LPA to determine if this molecule is an endogenous ligand for the GTP γ S-activated NSC current;
2. Delineate the G protein-coupled signaling pathway involved in LPA-mediated NSC current activation using: i) scrape-loading techniques to inactivate selective G protein subtypes and confirm the G protein involved in channel activation; ii) Ca²⁺ imaging techniques with Fluo-3 to examine the involvement of intracellular Ca²⁺ release and iii) inhibitors of specific protein kinases (GF 109203X for PKC and PD 98059 for MEK) to determine the involvement of protein phosphorylation;
3. Confirm antibody-mediated G protein knockdown and phosphorylation-dependent activation of MAP kinase.

Our demonstration that ATP activates an NSC current provides the first evidence for functional P_{2X} purinoceptors in rat RPE cells. Although electrophysiologically distinct, this ligand-gated NSC current may subserve similar functional roles to those proposed for the G-protein activated NSC current. In addition to the P_{2X}-gated NSC current, electrophysiological and Ca²⁺ imaging data also supports P_{2Y} purinoceptor activation of a K_{Ca} channel in rat RPE cells. Metabotropic P_{2Y} purinoceptors are most commonly linked to G_q proteins coupled to an IP₃/DAG signaling pathway and subsequent release of stored Ca²⁺. Although the functional role of P_{2Y}-mediated activation of K_{Ca} channels in rat RPE is unknown, an IP₃/DAG signaling pathway has been linked to RPE-mediated photoreceptor outer segment phagocytosis (Heth & Marescalchi, 1994). It is tempting to speculate

therefore, that a P_{2Y} purinoceptor signaling pathway and subsequent K_{Ca} channel activation may provide a “molecular link” to the phagocytic function of these cells. In support of this hypothesis, activation of P_1 receptors in the RPE, P_{2Y} receptors in macrophages and K^+ channel activation have all been linked to phagocytosis (Gregory *et al*, 1992; Ypey & Clapham, 1984; Ince *et al*, 1988; Ichinose, 1995).

Therefore, we propose to:

1. Use whole-cell patch-clamp and Ca^{2+} imaging techniques to fully delineate the P_{2Y} purinoceptor signaling pathway coupled to K_{Ca} activation in rat RPE cells by: i) scrape loading RPE cells with specific G protein subunit antibodies to identify the G protein involved; ii) using inhibitors of PLC or protein kinases (U-73122 for PLC, GF 109203X for PKC and PD 98059 for MEK) to identify the downstream signaling molecules involved in P_{2Y} receptor activation; iii) simultaneously recording changes in cytosolic free $[Ca^{2+}]$ and whole-cell currents to examine the requirement for extracellular Ca^{2+} influx or intracellular Ca^{2+} stores release in K_{Ca} channel activation.
2. Use fluorescently labeled rod outer segment (ROS) and cell imaging techniques to monitor the time course and rate of phagocytosis following exposure of cultured rat RPE cells to purinoceptor agonists. If ROS phagocytosis was stimulated by purinoceptor activation, then similar techniques to those detailed above would be used to identify the signaling pathway involved.

Receptor-coupled regulation of ion channels in pigmented epithelial (PCE) cells of the ciliary body would have important functional consequences for the rate and quantity of aqueous humor secreted into the posterior chamber of the eye.

Increased aqueous secretion is associated with increases in IOP, a major risk factor leading to glaucoma (Cole, 1984). The causative relationship between elevated IOP and this disease has highlighted the importance of understanding the physiological mechanisms underlying aqueous formation by the ciliary body epithelium (CBE).

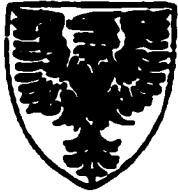
Despite the widespread use of adrenergic drugs to decrease aqueous formation in the treatment of glaucoma, there have very few studies detailing the sites and mechanisms of these agents at the level of ion conductive pathways in the CBE. This thesis has identified that an α_1 -adrenoceptor signaling pathway linked to PLC/IP₃ and intracellular Ca²⁺ stores release can modulate the activity of K_{Ca} channels in isolated rabbit PCE cells. Functionally, α_1 -adrenergic-mediated increases in K_{Ca} channel activity could augment aqueous formation by increasing the driving force for Cl⁻ secretion into the posterior chamber. Sympathetic nerve fibers present throughout the iris stroma and ciliary muscle as well as circulating catecholamines from the “major arterial circle” in the ciliary body would provide an endogenous source of agonist for regulation of PCE cell K_{Ca} channels *in vivo* (Streeten, 1991). In addition to K_{Ca} channels, modulation of other ion channels in the PCE by adrenoceptor activation may also alter aqueous humor secretion. For example, studies have demonstrated that Cl⁻ secretion across the CBE is a rate-limiting step in the formation of aqueous. We have preliminary evidence that adrenoceptor stimulation can also activate Cl⁻ conductances in rabbit PCE cells. Therefore, our future work will:

1. Identify and characterize the voltage-dependence and kinetics of Cl⁻ currents in isolated and cultured PCE and nonpigmented ciliary epithelial cells;

2. Identify the adrenoceptor subtype(s) involved in I_{Cl} activation using selective receptor antagonists;
3. Delineate the G protein(s) and downstream signaling molecules linked to adrenoceptor stimulation of I_{Cl} .

The proposed future experiments will further identify cell-signaling mechanisms involved in transepithelial transport in ocular epithelial cells. This information is essential for the design of novel pharmacological therapies for treating a number of ocular pathologies including; glaucoma, retinitis pigmentosa (RP) and central serous retinopathy (CSR), where defects in RPE or PCE-mediated fluid and ion transport have been identified.

APPENDIX



Dalhousie University

Department of Pharmacology
Faculty of Medicine
Sir Charles Tupper Medical Bldg.
Halifax, Nova Scotia
Canada B3H 4H7
(902) 494-3435
Fax: (902) 494-1388

MOSBY INC.
PUBLISHERS

NOV 05 1998

Dept. of Pharmacology
Faculty of Medicine
Dalhousie University
Halifax, Nova Scotia
B3H 4H7
FAX: 902-494-1388

10/25/98

Publisher

The C.V. Mosby Company
11830 Westline Industrial Drive
St. Louis, Missouri
63146, USA

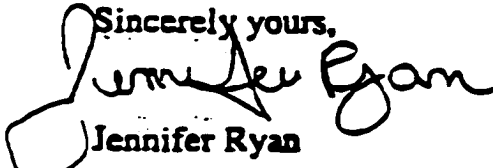
To Whom It May Concern:

I am writing to request permission to use one of your figures in a book chapter published by C.V. Mosby Co. in 1987. The chapter title is "The ciliary epithelium and aqueous humor" written by Joseph Caprioli. The figure is 7.5 on page 208. The title of the book is *Adler's Physiology of the Eye* edited by Robert A. Moses and William M. Hart Jr.

The figure is to be used in the general introduction chapter of my Ph.D. thesis.

I would appreciate your decision. I look forward to hearing from you soon.

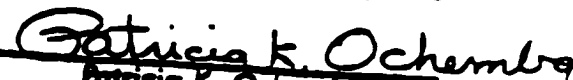
Sincerely yours,


Jennifer Ryan

Mosby, Inc.
11830 Westline Industrial Drive
St. Louis, MO 63146

Permission is granted for non-exclusive use of the material specified provided credit is given which acknowledges the author(s) or editor(s) title, edition, city, year of publication, and publisher.

11/13/98
Date


Patricia K. Ochemba



Academic Press
6277 Sea Harbor Drive
Orlando, FL 32887
Tel 407-345-2000
Fax 407-345-4058

December 4, 1998

Jennifer Ryan
Department of Pharmacology
Faculty of Medicine
Sir Charles Tupper Medical Bldg.
Halifax, Nova Scotia
Canada B3H 4H7

Re: Figure 2 at V.M. Clark's "The Cell Biology of the Retinal Pigment Epithelium" in The Retina: A Model for Cell Biology Studies, Part II (1986) edited by Adler/Farber.

Dear Ms. Ryan:

PERMISSION GRANTED to include Figure 2 from our above-referenced publication in your thesis, provided that 1) complete credit is given to the source, including the Academic Press copyright notice; 2) the material to be used has appeared in our publication without credit or acknowledgment to another source and 3) if commercial publication should result, you must contact Academic Press again.

Optional: You may wish to indicate our web site address: <http://www.apnet.com>.

We realize that University of Microfilms must have permission to sell copies of your thesis, and we agree to this. However, we must point out that we are not giving permission for separate sale of your article.



Ana D. Merced
Paralegal Department
Academic Press - Permissions
407 345 3994 (tel.)
407 345 4058 (fax)
amerced@harcourtbrace.com

REFERENCES

- Alessai, D.R., Cuenda, A., Cohen, P., Dudley, D. T. and Saltiel, A.R. (1995). PD 98059 is a specific inhibitor of the activation of mitogen-activated protein kinases *in vitro* and *in vivo*. *J. Bio. Chem.* **270**: 27489-27494.
- Ali, N. Agrawal, D.K. (1994). Guanine nucleotide binding proteins: Their characteristics and identification. *JPM* **32**: 187-196.
- Allen, T.J. and Chapman, R.A. (1996). Effects of ranolazone on L-type calcium channel currents in guinea-pig single ventricular myocytes. *Brit. J.Pharmacol.* **118**:249-254.
- Ammar, D.A., Hughes, B.A. and Thompson, D.A.(1998). Neuropeptide Y and the retinal pigment epithelium: receptor subtypes, signaling and bioelectrical responses. *Invest. Ophthamol. Vis. Sci.* **39**: 1870-1878.
- Anderson, C.M. and Parkinson, F.E. (1997). Potential signaling roles for UTP and UDP: sources, regulation and release of uracil nucleotides. *Trends Pharmacol. Sci.* **18**: 387-392.
- Barnard, E.A. (1992). Receptor classes and the transmitter-gated ion channels. *Trends Biol. Sci.* **17**: 368-374.
- Barnard, EA, Burnstock, G and Webb, TE. (1994). G protein-coupled receptors for ATP and other nucleotides: a new receptor family. *Trends. Pharmacol. Sci.* **15**: 67-70.
- Barnard, EA, Simon, S. and Webb, T.E. (1997). Nucleotide receptors in the nervous system. *Mol. Neurobiol.* **15**: 103-130.
- Barry, P. and Lynch, J. (1991). Liquid junction potentials and small cell effects in patch-clamp analysis. *J. Membr. Biol.* **121**: 107-117.
- Benali, R., Pierrot, D., Zahm, J.M., de-Bentamann, S and Puchelle, E. (1994). Effect of extracellular ATP and UTP on fluid transport by human nasal epithelial cells in culture. *Am. J. Respir.Cell Mol. Biol.* **10**: 363-368.
- Benham, C.D., Bolton, T.B. and Lang, R.J. (1985). Acetylcholine activates an inward current in single mammalian smooth muscle cells. *Nature* **361**: 345-347.
- Benos, D.J. Awayda, M.S., Ismailov, I.I, and Johnson, J. (1995). Structure and Function of Amiloride-sensitive Na⁺ Channels. *J. Membr. Biol.* **143**: 1-18.
- Berman, D.M. and Gilman, A.G. (1998). Mammalian RGS proteins: barbarians at the gate. *J. Biol. Chem.* **273**: 1269-1272.
- Berridge, M. J. (1993). Inositol triphosphate and calcium signaling. *Nature* **361**: 315-

325.

Bialek, S and Miller, S.S. (1994). K^+ and Cl^- transport mechanisms in bovine pigment epithelium that could modulate subretinal space volume and composition. *J. Physiol.* **475**: 401-417.

Bird, A.C. (1989). Pathogenesis of serous detachment of the retina and pigment epithelium. **In**: Retina diseases. M.O. Tso, editor. pp: 3-48. J.B. Lippincott Company, Philadelphia.

Blazynski, C. (1993). Characterization of adenosine A_2 receptors in bovine retinal pigment epithelial membranes. *Exp. Eye Res.* **56**: 595-599.

Blazynski, C. and Perez, M-T. R. (1991). Adenosine in vertebrate retina: localization, receptor characterization and function. *Cell Mol Neurobiol.* **11**: 463-481.

Blatz A.L., Magleby KL. (1983). Single voltage-dependent chloride-selective channels of large conductance in cultured rat muscle. *Biophysical J.* **43**: 237-241.

Boarder, M.R. and Hourani, S.M.O. (1998). The regulation of function by P2 receptors: multiple sites and multiple receptors. *TIPS.* **19**: 99-107.

Bok, D. (1988). Structure and function of retinal pigment epithelium-photoreceptor complex. **In**: Retinal diseases. M.O.M. Tso, editor. pp 3-48. J.B. Lippincott Co, Philadelphia.

Bok, D. (1993). The retinal pigment epithelium: a versatile partner in vision. *J. Cell Sci. Suppl.* **17**: 189-195.

Botchkin L.M., Matthews G. (1993). Chloride current activated by swelling in retinal pigment epithelium cells. *Am. J. Physiol.* **265**: C1037-C1045.

Botchkin LM, Matthews G. (1994). Voltage dependent sodium channels develop in rat retinal pigment epithelial cells in culture. *Proc. Natl. Acad. Sci.* **91**: 4564-4568.

Braslow, R.A. and Gregory, D.S. (1987). Adrenergic decentralization modifies the circadian rhythm of intraocular pressure. *Invest. Ophthalmol. Vis. Sci.* **28**: 1730-1732.

Braun, A.P. and Schulman, H. (1995). A non-selective cation current via the multifunctional Ca^{2+} -calmodulin-dependent protein kinase in human epithelial cells. *J. Physiol.* **488**: 37-55.

Breitwieser, G.E. (1991). G protein-mediated ion channel activation. *Hypertension* **17**: 684-692.

Brown, A.M. (1993). Membrane-delimited cell signaling complexes: direct ion channel regulation by G proteins. *J. Membr. Biol.* **131**: 93-104.

Brubaker, R.F.(1989). Measurement of aqueous flow by fluorophotometry. **In**: Glaucomas. R. Ritch, M.B. Shields and T. Krupin, editors. pp 337-344. Mosby Publishing, St. Louis.

Brubaker, R.F. (1991). *Invest. Ophthalmol.Vis. Sci.* **32**: 3145-3166.

Burke, J.M., McKay, B.S. and Jaffe, G.J. (1991). Retinal pigment epithelial cells of the posterior pole have fewer Na/K adenosine triphosphate pumps than peripheral cells. *Invest. Ophthalmol. Vis. Sci.* **32**: 2042-2047.

Burnstock, G. and Kennedy, C. (1985). Is there a basis for distinguishing two types of P2 purinoceptors? *Gen. Pharmacol.* **16**: 433-440.

Bylund, D.B., Iversen, L.J., Matulka, W.J. and Chacko, D.M. (1996). Characterization of α_{2D} adrenergic receptor subtypes in bovine ocular tissue homogenates. *J. Pharmacol. Exp. Ther.* **281**: 1171-1177.

Caprioli, J. (1992). The ciliary epithelia and aqueous humor. **In**: Adler's Physiology of the Eye: clinical application. W.M. Hart, editor. pp 228-241. Mosby Year Book Inc.

Caprioli, J., Seras, M., Mead, A., Kosley, R.W., Cherill, R.J., Hugher, F.P., Allen, R.C. and Tressler, C. (1989). Adenylate cyclase stimulation and intraocular pressure reduction by forskolin analogs. *J.Ocular. Pharm.* **5**: 181-187.

Carmen, C.V. and Benovic, J.L. (1998). G protein-coupled receptors: turn-ons and turn-offs. *Curr. Opin. Neurobiol.* **8**: 335-344.

Carre, D.A., Anguita, J., Coca-Prados, M. and Civan, M.M.(1997). Cell-attached patch clamping in the intact rabbit ciliary epithelium. *Curr. Eye Res.* **15**:192-201.

Carre, D.A. and Civan, M.M. (1994). Cation nonselective channels of intact ciliary epithelium. *Invest. Ophthalmol. Vis. Sci.* **35**: 1455.

Chader, G.J., Aguirre, G.D. and Sanyal, S. (1988). Studies on animal models of retinal degeneration, **In**: Retinal diseases. M. Tso. editor. pp 3-48. J.B. Lippincott Co., Philadelphia.

Chaug, E.L., Sharp, D.M., Fitzke, F.W., Kemp, C.M. , Holden, A.L. and Brid, A.C.(1987). Retinal dysfunction in central serous retinopathy. *Eye.* **1**: 120-125.

Chen, S, Inoue, R., Inomata, H. and Ito, Y. (1994). Role of cyclic AMP-induced Cl conductance in aqueous humor formation by the dog ciliary epithelium. *Br. J. Pharmacol.* **112**: 1137-1145.

- Chen, S. and Sears, M. (1997). A low conductance chloride channel in the basolateral membrane of the non-pigmented ciliary epithelium of the rabbit eye. *Curr. Eye Res.* **16**: 710-718.
- Chiou, G. C. Y. (1983). Effects of $\alpha 1$ and $\alpha 2$ activation of adrenergic receptors on aqueous humor dynamics. *Life Science* **32**:1699-1704.
- Chong, N.H.V. (1996). *Clinical Ocular Physiology*. pp 24-42. Butterworth-Heinemann, Oxford.
- Chu, T.C., Candia, O.A. and Iizuka, S. (1986). Effects of forskolin, prostaglandin $F_{2\alpha}$ and Ba^{2+} on the short circuit current of the isolated rabbit iris-ciliary body. *Curr. Eye Res.* **5**: 511-516.
- Churchill, G.C. and Louis, C.F. (1997). Stimulation of P_{2U} purinergic or α_{1A} adrenergic receptors mobilizes Ca^{2+} in lens cells. *Invest. Ophthalmol. Vis. Sci.* **38**: 855-867.
- Cilluffo, M.C., Cohen, B.N. and Fain, G.L. (1991). Nonpigmented cells of the ciliary body epithelium: tissue culture and voltage-gated currents. *Invest. Ophthalmol. Vis. Sci.* **32**: 1619-1629.
- Cilluffo, M. C., Fain, M. J., Fain, G. L. and Brecha, N. C. (1986). Culture of rabbit ciliary body epithelium. *Invest. Ophthalmol. Vis. Sci.* **27**: S 322.
- Civan, M.M., Coca-Prados, M. and Peterson-Yantorno, K. (1994). Pathways signalling the regulatory volume decrease of cultured non-pigmented ciliary epithelial cells. *Invest. Ophthalmol. Vis. Sci.* **35**: 2876-2886.
- Clapham, D.E. (1996). The G-protein nonomachine. *Nature.* **379**: 297-299.
- Clapham, D.E. and Neer, E.J. (1993). New roles for G protein beta-gamma dimers in transmembrane signalling. *Nature.* **365**: 403-406.
- Clark, V.M. (1986). The cell biology of the retinal pigment epithelium. **In**: *The Retina: a Model for Cell Biology Studies (part II)*. R. Adler and D. Farber, editors. pp 129-159. Academic Press Inc.
- Coca-Prados, M., Anguita, J., Chalfant, M.L. and Civan, M.M. (1995). PKC-sensitive Cl channels associated with ciliary epithelial homologue of pI_{CLn} . *Am. J. Physiol.* **268**: C572-C579.
- Coca-Prados, M. and Chat, G.(1986). Growth of non-pigmented ciliary epithelial cells in serum-free hormone-supplemented media. *Exp.Eye. Res.* **43**: 617-629.
- Coca-Prados, M. and Lopez-Briones, L.G. (1987). Evidence that the α and $\alpha(+)$ isoforms

of the catalytic subunit of (Na⁺, K⁺)-ATPase reside in distinct ciliary epithelial cells of the mammalian eye. *Biochem. Biophys. Res. Commun.* **145**: 460-466.

Coca-Prados, M., Sanchez-Torres, J., Peterson-Yantorno, K and Civan, M.M. (1996). Association of ClC-3 channel with Cl⁻ transport by human nonpigmented ciliary epithelial cells. *J. Membr. Biol.* **150**: 197-208.

Cole, D. A. (1984). Ocular fluids **In**: The Eye, Vol 1A. 3rd edit. H. Davson, editor. NY. Academic Press. pp. 269-390.

Collo, G., North, R.A., Merlo-Pich, E., Neidhart, S., Suprenant, A. and Buell, G. (1996). Cloning of P2X5 and P2X6 receptors and the distribution and properties of an extended family of ATP-gated ion channels. *J. Neurosci.* **16**: 2495-2507.

Colquhoun D, Neher E, Reuter H, Stevens CF. (1981). Inward current channels activated by intracellular calcium in cultured cardiac cells. *Nature* **294**:752-754.

Conklin, B.R. and Bourne, H.R. (1993). Structural elements of G α subunits that interact with G $\beta\gamma$, receptors and effectors. *Cell* **73**: 631-641.

Connolly, G.P. and Harrison, P.J. (1995). Discrimination between UTP – and P2-purinoceptor-mediated depolarization of rat superior cervical ganglia by 4,4'-diisothiocyanatostilbene-2,2'-disulphonate (DIDS) and uniblue A. *Br. J. Pharmacol.* **115**: 427-432.

Cook, N.S. (1988). The pharmacology of potassium channels and their therapeutic potential. *Trends Pharm Sci.* **9**: 21-28.

Cook, D.L., Poronnik, P. and Young, J.A. (1990). Characterization of a 25-pS nonselective cation channel in cultured a secretory epithelial cell line. *J. Membr. Biol.* **114**: 37-52.

Cooper K.E, Tang JM, Rae JL. (1986). A cation channel in frog lens epithelia responsive to pressure and calcium. *J Membrane Biol.* **93**:259-269.

Cooper K.E., Rae JL, Gates P, Dewey J. (1990). Electrophysiology of cultured human lens epithelial cells. *J. Membrane Biol.* **117**:285-298.

Corwin, D.J. and Gown, A.M. (1989). Review of selected lineage-directed antibodies useful in routinely processed tissue. *Arch Pathol Lab Med* **113**: 645-652.

Crepel, V., Panenka, W., Kelly, M.E.M. and MacVicar, B.A. (1998). MAP and tyrosine kinases in the activation of astrocyte volume-activated chloride current. *J. Neurosci.* **18**, 1196-1206.

Critz, S.D. and Byrne, J.H. (1992). Modulation of IK_{Ca} by phorbol ester-mediated

- activation of PKC in pleural sensory neurons of Aplysia. *J. Neurochem.* **68**: 1079-1086.
- Crook, R.B., Bazan, N.G. and Polansky, J.R. (1991). Histamine H₁ receptor occupancy triggers inositol phosphates and intracellular calcium mobilization in human non-pigmented ciliary epithelial cells. *Curr. Eye Res.* **10**: 593-600.
- Crosson, C.E., DeBenedetto, R. and Gidday, J.M. (1994). Functional evidence for retinal adenosine receptors. *J. Ocul. Pharmacol.* **10**: 499-507.
- Daunt, D.A., Hurt, C., Hein, L., Kallio, J., Feng, F. and Kobilka, B.K. (1997) Subtype-specific intracellular trafficking of α 2-adrenergic receptors. *Mol. Pharmacol.* **51**: 711-720.
- Davis, M.J., Meininger, G.A. and Zawieja, D.C. (1992). Stretch-induced increases in intracellular calcium of isolated vascular smooth muscle cells. *Am. J. Physiol.* **263**: H1292-H1299.
- Davis, P.B., Silski, C.L. and Perez, A. (1994). cAMP does not regulate [Ca²⁺]_i in human tracheal epithelial cells in primary culture. *J. Cell Sci.* **107**: 2899-2907.
- Davson, H. (1984). The intraocular pressure. In: *The Eye*, Vol 1A. 3rd edit. H. Davson, editor. NY. Academic Press. pp. 391-511.
- Dearry, A. and Burnside, B. (1988). Stimulation of distinct D2 dopaminergic and α 2-adrenergic receptors induces light-adaptive pigment dispersion in teleost retinal pigment epithelium. *J. Neurochem.* **51**: 1516-1523.
- Dearry, A., Edelman, J.L., Miller, S. and Burnside, B. (1990). Dopamine induces light-adaptive retinomotor movements in bullfrog cones via D₂ receptors and in the retinal pigment epithelium via D₁ receptors. *J. Neurochem.* **54**: 1367-1378.
- DeCoursey, T.E., Chandy, K.G., Gupta, S. and Chalan, M.D. (1984). Voltage-gated K⁺ channels in human T lymphocytes: a role for mitogenesis? *Nature* **307**: 465-467.
- Deleze, J and Herve, J.C. (1983). Effect of several uncouplers of cell-to-cell communication on gap junction morphology in mammalian heart. *J. Membrane Biol.* **74**: 203-215.
- Della Rocca, G.J., van Biesen, T., Daaka, Y., Luttrell, D.K., Luttrell, L.M. and Lefkowitz, R.J. (1997). Ras-dependent mitogen-activated protein kinase activation by G protein-coupled receptors. *J. Biol. Chem* **272**: 19125-19132.
- Denhardt, D.T. (1996). Signal-transducing protein phosphorylation cascades mediated by Ras/Rho proteins in the mammalian cell: the potential for multiplex signaling. *Biochem. J.* **318**: 729-747.

Dikic, I., Tokiwa, G., Lev, S., Courtneidge, S.A. and Schlessinger, J. (1996). A role for Pyk2 and Src in linking G protein- coupled receptors with MAP kinase activation. *Nature* **383**: 547-550.

Dolphin, A.C. (1998). Mechanisms of modulation of voltage-dependent calcium channels by G proteins. *J. Physiol.* **506**: 3-11.

Dudley, D. T., Pang, L., Decker, S.J., Bridges, A.J. and Saltiel, A.R. (1995). A synthetic inhibitor of the mitogen-activated protein kinase cascade. *Proc. Natl. Acad. Sci.* **92**: 7686-7689.

Dunbar-Hoskins, H. (1989). **In: Becker-Shaffer's Diagnosis and Therapy of the Glaucomas.** 6th edition. pp: 435-469.

Dubyak, G.R., Cowen, D.S. and Mueller, L.M. (1988). Activation of inositol phospholipid breakdown in HL60 cells by P2-purinergic receptors for extracellular ATP. Evidence for mediation by both pertussis toxin-sensitive and pertussis toxin insensitive mechanisms. *J. Biol. Chem.* **263**: 18108-18117.

DuVall, M.D. and O'Grady, S.M. (1994). cGMP and Ca²⁺ regulation of ion transport across the isolated porcine distal colon epithelium. *Am. J. Physiol.* **267**: R1026-1033.

Edelman, JL and Miller, SS. (1991). Epinephrine stimulates fluid absorption across bovine retinal pigment epithelium. *Invest. Ophthalmol. Vis. Sci.* **32**:3033-3040.

Edelman JL, Lin H, Miller SS. (1994). Potassium-induced chloride secretion across the frog retinal pigment epithelium. *Am. J. Physiol.* **266**: C957-C966.

Edelman, J. L., Sachs, G. and Adorante, J. S. (1994). Ion transport asymmetry and functional coupling in bovine pigmented and nonpigmented ciliary epithelial cells. *Am. J. Physiol.* **266**: C1210-C1221.

Ehring, G.R., Zampighi, G., Horwitz, J., Bok, D. and Hall, J.E. (1990). Properties of channels reconstituted from the major intrinsic protein of lens fiber membranes. *J. Gen. Physiol.* **96**: 631-634.

Elayan, H., Kennedy, B. and Ziergler, M.G. (1990). Epinephrine synthesis in the rat iris. *Invest. Ophthalmol. Vis. Sci.* **31**: 677-680.

Erlinge, D. (1998). Extracellular ATP: a growth factor for vascular smooth muscle cells. *Gen. Pharmacol.* **31**: 1-8.

Ernst, S.A., Palacios, J.R. and Seigel, G.J. (1986). Immunocytochemical localization of Na,K, ATPase catalytic polypeptide in mouse choroid plexus. *J. Histochem. Cytochem.* **34**: 189-195.

- Evans, R.J., Lewis, C., Buell, G., Valera, S., North, R.A. and Suprenant, A. (1995). Pharmacological characterization of heterologously expressed ATP-gated cation channels (P2X purinoceptors). *Mol. Pharmacol.* **48**: 178-183.
- Exon, J.H. (1996). Regulation of phosphoinositide phospholipase by hormones, neurotransmitters and other agonists linked to G-proteins. *Ann. Rev. Pharmacol. Toxicol.* **36**: 481-509.
- Exon, J.H. (1997). Cell signalling through guanine-nucleotide-binding regulatory proteins (G proteins) and phospholipases. *FEBS.* **243**: 10-20.
- Fain, G. L., and Farahbakhsh, N. A. (1989). Voltage-activated currents recorded from rabbit pigmented ciliary body epithelial cells in culture. *J. Physiol.* **417**: 83-103.
- Farahbakhsh, N. A. and Cilluffo, M.C. (1997). Synergistic increase in Ca^{2+} produced by A1 adenosine and muscarinic receptor activation via pertussis-toxin-sensitive pathway in epithelial cells of the rabbit ciliary body.
- Farahbakhsh, N. A. and Cilluffo, M. C. (1994). Synergistic effect of adrenergic and muscarinic receptor activation on $[Ca^{2+}]_i$ in rabbit ciliary body epithelium. *J. Physiol.* **77**: 215-221.
- Farahbakhsh, N. A., Cilluffo, M. C., Chronis, C. and Fain, G. L. (1994). Dihydropyridine-sensitive Ca^{2+} spikes and Ca^{2+} currents in rabbit ciliary body epithelial cells. *Exp. Eye Res.* **58**: 197-206.
- Finn, J.T., Grunwald, M.E. and Yau, K-W. (1996). Cyclic nucleotide-gated ion channels: an extended family with diverse functions. *Ann. Rev. Physiol.* **58**: 395-426.
- Ferguson, S.S., Barak, L.S., Zhang, J., Caron, M.G. (1996). G-protein-coupled receptor regulation: role of G-protein-coupled receptor kinases and arrestins. *Can. J. Physiol. Pharmacol.* **74**:1095-1110.
- Foskett, J. K., Roifman, C. M. and Wong, D. (1991). Activation of calcium oscillations by thapsigargin in parotid acinar cells. *J. Biol.Chem.* **266**: 2778-2782.
- Fox, J.A., Pfeffer, B. and Fain, G.L. (1988). Single-channel recordings from cultured human retinal pigment epithelium. *J. Gen. Physiol.* **91**: 193-222.
- Fox, J.A., Steinberg, R.H. (1992). Voltage dependent currents in isolated cells of the turtle retinal pigment epithelium. *Pflügers Arch.* **420**: 451-460.
- Frambach, D.A., Valentine, J.L. and Weiter, J.J. (1988). Alpha-1 adrenergic receptors on rabbit retinal pigment epithelium. *Invest. Ophthalmol. Vis. Sci.* **29**: 737-741.
- Frambach, D.A., Fain, G.L., Farber, D.B., and Bok, D. (1990). Beta adrenergic receptors

on cultured human retinal pigment epithelium. *Invest. Ophthalmol. Vis. Sci.* **31**: 1767-1772.

Friedman, Z., Hackett, S.F., Linden, J. and Campochiaro, P.A. (1988). Human retinal pigment epithelial cells possess muscarinic receptors coupled to calcium mobilization receptors. *Brain Res.* **446**: 11-16.

Friedman, Z., Hackett, S.F., Linden, J. and Campochiaro, P.A. (1989). Human retinal pigment epithelial cells in culture possess A₂ adenosine receptors. *Brain Res.* **492**: 29-35.

Friedman, Z., Delahunty, T.M., S.F., Linden, J. and Campochiaro, P.A. (1991). Human retinal pigment epithelial cells in culture possess V₁ vasopressin receptors. *Curr. Eye Res.* **10**: 811-816.

Fuch, O., Kivela, T. and Tarkkanen, A. (1991). Cytoskeleton in normal and reactive human retinal pigment epithelial cells. *Invest Ophthalmol Vis Sci* **32**: 3178-3186.

Fujii, S., Gallemore, R.P., Hughes, B.A. and Steinberg, R.H. (1992). Direct evidence for a basolateral membrane Cl⁻ conductance in toad retinal pigment epithelium. *Am. J. Physiol.* **262**: C374-383.

Fujisawa, K., Ye, J. and Zadunaisky, J.A. (1992). A Na/Ca exchange mechanism in apical membrane vesicles of the retinal pigment epithelium. *Invest. Ophthalmol. Vis. Sci.* **33**: 911.

Gallemore, R.P. and Steinberg, R.H. (1989). Effects of DIDS on the chick retinal pigment epithelium. II. Mechanism of the light peak and other responses originating at the basal membrane. *J. Neurosci.* **9**: 1977-1991.

Gallemore, R.P. and Steinberg, R.H. (1990). Effects of dopamine on the chick retinal pigment epithelium. *Invest. Ophthalmol. Vis. Sci.* **31**: 67-80.

Gether, U. and Kobilka, B.K. (1998). G protein-coupled receptors. *J. Biol.Chem.* **273**: 17979-17982.

Ghosh, A. and Greenberg, M.E. (1995). Calcium signaling in neurons: Molecular mechanisms and cellular consequences. *Science*, **268**: 239-247.

Ghosh, S., Freitag, A.C., Martin-Vasallo, P. and Coca-Prados, M. (1990). Cellular distribution and differential gene expression of the three α subunit isoforms of the Na, K-ATPase in the ocular ciliary epithelium. *J. Biol. Chem.* **265**: 2935-2940.

Giangiaco, K. M., Garcia, M. L. and McManus, O. B. (1992). Mechanism of iberiotoxin block of the large-conductance calcium-activated potassium channel from bovine aortic smooth muscle. *Biochemistry* **31**: 6719-6727.

Giangiaco, K. M., Sugg, E. E., Garcia-Calco, M., Leonard, R. J., McManus, O.

B., Kaczorowski, G. I. and Garcia, M. L. (1993). Synthetic charybdotoxin-iberiotoxin chimeric peptides define toxin binding sites in calcium-activated and voltage dependent potassium channels. *Biochemistry* **32**: 2363-2370.

Gogelein, H, Pfanmuller, B. (1989). The nonselective cation channel in the basolateral membranes of rat exocrine pancreas. Inhibition by 3',5-dichlorodiphenylamine-2-carboxylic acid (DCDPC) and activation by stilbene disulfonates. *Pflugers Arch.* **413**: 287-298.

Goldstein DA. (1979). Calculation of the concentrations of free cations and cation ligand complexes in solutions containing multiple divalent cations and ligands. *Biophys. J.* **26**:235-42.

Gooch, A.J., Morgan, J. and Jacob, T.J.C. (1992). Adrenergic stimulation of bovine non-pigmented ciliary epithelial cells raises cAMP but has no effect on K⁺ or Cl⁻ currents. *Curr. Eye. Res.* **11**: 1019-1029.

Gordon, J.L. (1986). Extracellular ATP: effects, sources and fate. *Biochem. J.* **233**: 309-319.

Gosling, M., Poyner, D.R. and Smith, J.W. (1996). Effects of arachidonic acid upon the volume-sensitive chloride current in rat osteoblastic-like (ROS 17/2.8) cells. *J.Physiol.* **493**: 613-623.

Gray PTA, Bevan S, Ritchie JM. (1983). High conductance anion-selective channels in rat cultured Schwann cells. *Proc. Royal Soc. London* **221**: 395-409.

Green, K., Bountra, C., Georgiou, P. and House, C.R. (1985). An electrophysiological study of the rabbit ciliary epithelium. *Invest. Ophthalmol. Vis. Sci.* **26**: 37-381.

Greenwood, D, Yao, W.P. and Housley, G.D. (1997). Expression of the P2X2 receptor subunit of the ATP-gated ion channel in the retina. *Neuroreport* **24**: 1083-1088.

Gregory, C.Y., Abrams, T.A. and Hall, M.O. (1994). Stimulation of A₂ adenosine receptors inhibits the ingestion of photoreceptor outer segments by retinal pigment epithelium. *Invest. Ophthalmol. Vis. Sci.* **35**: 819- 825.

Gregory, D.S., Aviado, D.G. and Sears, M.L. (1985). Cervical ganglionectomy alters the circadian rhythm of intraocular pressure in New Zealand White rabbits. *Curr. Eye Res.* **4**: 1273-1279.

Gupta, S.K., Jollimore, C.A., McLaren, M.J., Inana, G. and Kelly, M.E.M. (1997). Mammalian retinal pigment epithelial cells in vitro respond to the neurokines ciliary neurotrophic factor and leukemia inhibitory factor. *Biochem. Cell Biol.* **75**: 19-125.

Guarino, R.D., Perez, D.M. and Piascik, M.T. (1996). Recent advances in the molecular

pharmacology of $\alpha 1$ adrenoceptor. *Cell Signaling*. **8**: 232-233.

Gutkind, J.S. (1998). The pathway connecting G protein-coupled receptors to the nucleus through divergent mitogen-activated protein kinase cascades. *J. Biol. Chem* **273**: 1839-1842.

Hagelucken, A., Nurnberg, B., Harhammer, R., Grunbaum, L., Schunack, W. and Seifert, R. (1995). The class III antiarrhythmic drug amiodarone directly activates pertussis toxin-sensitive G proteins. *Mol. Pharm.* **47**: 234-240.

Hall A. (1992). Small GTP-binding proteins- A new family of biologic regulators. *Am. J. Respir. Cell Mol. Biol.* **6**: 245-246.

Hamill, O.P., Marty, A., Neher, E., Sakmann, B. and Sigworth, F.J. (1981). Improved patch-clamp techniques for high- resolution current recording from cells and cell-free membrane patches. *Pflugers Arch.* **391**: 85-100.

Hamm, H.E. (1998). The many faces of G protein signaling. *J. Biol. Chem.* **273**: 669-672.

Hart, W.M. (1992). Intraocular pressure. **In**: Adler's physiology of the eye: clinical application. W.M. Hart, editor. pp 248-261. Mosby Year Book Inc.

Heath, C.A., Marescalchi, P.A. (1994). Inositol triphosphate generation in cultured rat retinal pigment epithelium. *Invest. Ophthalmol. Vis. Sci.* **35**: 409-416.

Heath, C.A., Marescalchi, P.A. and Ye, L. (1995). IP₃ generation increases rod outer segment phagocytosis by cultured Royal College of Surgeons rat retinal pigment epithelium. *Invest. Ophthalmol. Vis. Sci.* **36**: 980-989.

Heilbronn, E., Knoblauch, B.H.A. and Muller, C.E. (1997). Uridine nucleotide receptors and their ligands: structural, physiological and pathophysiological aspects, with special emphasis on the nervous system. *Neurochem. Res.* **22**: 1041-1050.

Helbig, H., Korbmacher, C., Wohlfarth, J., Coroneo, M.T., Lindschau, C., Quass, P., Halley, H, Coca-Prados, M. and Weiderholt, M. (1989). Effect of acetylcholine on membrane potential of cultured human nonpigmented ciliary epithelial cells. *Invest. Ophthalmol. Vis. Sci.* **30**: 890-896.

Hescheler, J. (1994). Whole-cell clamp analysis for G-protein regulation of channels. *Methods in Enzymology*. **238**: 365-375.

Hescheler, J. and Schultz, G. (1993). Nonselective cation channels: Physiological and pharmacological modulations of channel activity. **In**: Nonselective cation channels: pharmacology, physiology and biophysics. Seimen & Hescheler, editors. pp 27-43.

- Hidaka, H., Inagaki, M., Kawamoto, S. and Sasaki, Y. (1984). Isoquinolinesulfonamides, novel and potent inhibitors of cyclic nucleotide dependent protein kinase and protein kinase C. *Biochem.* **23**: 5036-5041.
- Higashijima T, Graziano MP, Suga H, Kainosho M, Gilman AG. (1991). 19F and 31P NMR spectroscopy of G protein alpha subunits. Mechanism of activation by Al^{3+} and F^{-} . *J. Biol. Chem.* **266**: 3396-3401.
- Hildebrandt, J. P., Plant, T. D. and Meves, H. (1997). The effects of bradykinin on K^{+} currents in NG108-15 cells treated with U73122, a phospholipase C inhibitor, or neomycin. *Br. J. Pharm.* **120**: 841-850.
- Hille, B. (1992). Selective permeability: independence. **In**: Ionic channels of excitable membranes, 2nd Ed., pp 337-361. Sunderland, MA: Sinauer Associates, Inc.
- Hille, B. (1994). Modulation of ion channel function by G-protein coupled receptors. *Trends Neurosci.* **17**: 531-535.
- Hinton, D.R., Jin, M.L., Ryan, S.J. and Law, R. (1998). The mitogen-activated protein kinase pathway is a central regulator of the chemotactic response of retinal pigment epithelial cells to tumor necrosis factor-alpha and platelet-derived growth factor. *Exp. Eye. Res.* **67**: S.164
- Huang, Y., Gil, D.W., Vanscheeuwijck, P., Stamer, W.D. and Regan, J.W. (1995). Localization of alpha 2-adrenergic receptor subtypes in the anterior segment of the human eye with selective antibodies. *Invest. Ophthalmol. Vis. Sci.* **36**: 2729-2739.
- Hughes, B.A., Miller, S.S., Joseph, D.P. and Edelman, J.L. (1988). cAMP stimulates the Na^{+} - K^{+} pump in frog retinal pigment epithelium. *Am.J. Physiol.* **254**: C84-C98.
- Hughes BA, Steinberg RH. (1990). Voltage dependent currents in isolated cells of the frog retinal pigment epithelium. *J. Physiol.* **428**: 273-297.
- Hughes BA, Segawa, Y. (1993). CAMP-activated chloride currents in amphibian retinal pigment epithelial cells. *J. Physiol.* **466**: 749-466.
- Hughes , B.A. and Takahira, M. (1996). Inwardly rectifying K^{+} currents in isolated human retinal pigment epithelial cells. *Invest. Ophthalmol. Vis Sci.* **37**: 1125-1139.
- Humphrey, P.P.A., Buell, G., Kennedy, I., Khshk, B.S., Mivhel, A.D., Suprenant, A and Trezise, D.J. (1995). New Insights on P2X purinoceptors. *Naunyn-Schmiedeberg's Arch Pharmacol.* **352**: 585-596.
- Hunter, M., Lopes, A.G., Boulpaep, E. and Giebisch, G. (1986). Regulation of single potassium ion channels from apical membrane of rabbit collecting tubule. *Am. J. Physiol.* **251**: F725-733.

- Ichinose, M. (1995). Modulation of phagocytosis by P₂-purinoceptors in mouse peritoneal macrophages. *Japan. J. Physiol.* **45**: 707-721.
- Ikeuchi, Y. and Nishizaki, T. (1995). ATP activates the potassium channel and enhances cytosolic Ca²⁺ release via P₂Y purinoceptor linked to pertussis toxin-insensitive G protein in brain artery endothelial cells. *Biochem. Biophys. Res. Commun.* **215**: 1022-1028.
- Ikeuchi, Y. and Nishizaki, T., Matsuka, T. and Sumikawa, K. (1996). Arachidonic acid potentiates Ach receptor currents by protein kinase C activation but not by receptor phosphorylation. *Biochem. Biophys. Res. Comm.* **221**: 716-721.
- Ince, C., Coremans, J.M.C., Ypey, D.L., Leijh, P.C., Verveen, A.A. and van Furth, R. (1988). Phagocytosis by human macrophages is accompanied by changes in ionic channel currents. *J. Cell Biol.* **106**: 1873-1878.
- Inoue, M and Kuriyama, H. (1991). Muscarinic receptor is coupled with a cation channel through a GTP-binding protein in guinea-pig chromaffin cells. *J. Physiol.* **436**: 511-529.
- Inoue, M and Imanaga, I. (1993). Phosphorylation-dependent regulation of nonselective cation channels in guinea pig chromaffin cells. *Am. J. Physiol.* **265**: C343-348.
- Inoue, M. and Imanaga, I. (1995). Mechanism of activation of nonselective cation channels by putative M₄ muscarinic receptor in guinea-pig chromaffin cells. *Brit. J. Pharmacol.* **114**: 419-427.
- Inoue, M., Ogawa, K., Fujishiro, N., Yano, A., Imanaga, I. (1996). Role and source of ATP for activation of nonselective cation channels by AIF complex in guinea pig chromaffin cells. *J. Membr. Biol.* **154**: 183-195.
- Jacob TJC, Bangham JA, Duncan G. (1985). Characterization of a cation channel on the apical surface of the frog lens epithelium. *Quart. J. Exp. Physiol.* **70**: 403-421.
- Jacob, T. J. C. (1988). Inward and outward currents in isolated epithelial cells of the bovine ciliary body. *J. Physiol.* **407**: 103P.
- Jacob, T. J. C. (1991a). Identification of a low-threshold T-type calcium channel in bovine ciliary epithelial cells. *Am. J. Physiol.* **261**: C808-813.
- Jacob, T. J. C. (1991b). Two outward K⁺ currents in bovine pigmented ciliary epithelial cell: I_{K(Ca)} and I_{K(V)}. *Am. J. Physiol.* **262**: C1055-1062.
- Jacob, T. J. C. and Civan, M. M. (1996). Role of Ion channels in Aqueous humor formation. *Am. J. Physiol.* **271**: C703-720.

- Jan, L.Y. and Jan, Y.N. (1997). Receptor-regulated ion channels. *Curr. Opin. Cell Biol.* **9**:155-160.
- Jiang, M., Pandey S., Tran, V.T. and Fong, H.K.W. (1991) Guanine nucleotide-binding regulatory proteins in retinal pigment epithelial cells. *Proc. Natl. Acad. Sci.* **88**: 3907-3911.
- Jin, Y., Verstappen, A. and Yorio, T. (1994). Characterization of alpha 2 - adrenoceptor binding sites in rabbit ciliary body membranes. *Invest. Ophthalmol. Vis. Sci.* **35**: 2500-2508.
- Jonas, E.A. and Kaczmarek, L.K. (1996). Regulation of potassium channels by protein kinases. *Curr. Opin. Neurobiol.* **6**: 318-323.
- Joseph DP and, Miller SS. (1991). Apical and basal membrane ion transport mechanisms in bovine retinal pigment epithelium. *J. Physiol.* **435**: 439-463.
- Joseph, D.P. and Miller, S.S. (1992). Alpha-1 adrenergic modulation of K⁺ and Cl⁻ transport in bovine retinal pigment epithelium. *J. Gen. Physiol.* **99**: 263-290.
- Jung, F., Selvaraj, G., and Gargus, J.J. (1992). Blockers of PDGF-activated nonselective cation channels inhibit cell proliferation. *Am J. Physiol.* **262**: C1464-1470.
- Kahn RA. (1991). Fluoride is not an activator of the smaller (20-25 kDa) GTP binding proteins. *J. Biol. Chem.* **266**: 15595-15597.
- Kao, J.P., Harootunian, A.T. and Tsien, R.Y. (1989). Photochemically generated cytosolic calcium pulses and their detection by fluo-3. *J. Biol. Chem* **264**: 8179-8184.
- Kaufman, P. (1984). Cholinergics. **In**: Pharmacology of the eye. M.L. Sears, editor. Springer-Verlag, New York. pp: 149-192.
- Kenyon, E., Lin, H. and Miller, S.S. (1991). Mechanisms of pH_i regulation in the apical membrane of human RPE. *Invest. Ophthalmol. Vis. Sci.* **32**:671.
- Kinane, T. B., Kang, I., Chu, A., Chin, S.H. and Ercolani, L. (1997). G_{i(2)} mediates renal LLC-PK1 growth by a Raf-independent activation of p42/p44 MAP kinase. *Am. J. Physiol.*: F272-F282.
- Kinzer, D. and Lehmann, V. (1991). Extracellular ATP and adenosine modulate tumor necrosis factor-induced lysis of L929 cells in the presence of actinomycin D. *J. Immunol.* **146**: 2708-2711.
- Klaerke, D.A. (1997). Regulation of Ca²⁺-activated K⁺ channels from rabbit distal colon. *Comp. Biochem. Physiol. A Physiol.* **118**: 215-217.
- Koh, S.D., Dick, G.M. and Sanders, K.M. (1997). Small-conductance Ca(2+)-dependent

K⁺ channels activated by ATP in murine colonic smooth muscles. *Am. J. Physiol.* **273**: C2010-C2021.

Kolb, HA, Brown CDA, Murer H. (1985). Identification of a voltage-dependent anion channel in the apical membrane of a Cl⁻ secretory epithelium (MDCK). *Pflugers Archiv.* **403**: 262-265.

Koelle, M.R. (1997). A new family of G-protein regulators-the RGS proteins. *Curr. Opin. Cell Biol.* **9**: 143-147.

Kuntz, C.A., Crook, R.B., Dimitriev, A. and Steinberg, R.H. (1994). Modification by cyclic adenosine monophosphate of basolateral membrane chloride conductance in chick retinal pigment epithelium. *Invest. Ophthalmol. Vis. Sci.* **35**: 422-433.

Kramer, T., Potts, A.M. and Mangnall, Y. (1972). Autoradiographic localization of catecholamines in the uveal tract. I. Light microscopic study. *Am. J. Ophthalmol.* **74**: 129-133.

Krupin, T., Feitl, M. and Becker, B. (1980). Effect of prazosin on aqueous humor dynamics in rabbits. *Arch. Ophthalmol.* **98**: 1639-1642.

Krupin, T. and Civan, M.M. The physiological basis of aqueous humor formation. **In**: the Glaucomas (2nd edition). R. Ritch, M.B. Shields and T. Krupin, editors. pp: 251-280. Mosby, St. Louis, MO.

Krupin, T. E., Wax, M. B., Carre, D. A., Moolchandani, J. and Civan, M. M. (1991). Effects of adrenergic agents on transepithelial electrical measurements across the isolated iris-ciliary body. *Exp. Eye Res.* **53**: 709-716.

Krupnick, J.G. and Benovic, J.L. (1998). The role of receptor kinases and arrestins in G protein-coupled receptor regulation. *Annu. Rev. Pharmacol. Toxicol.* **38**: 289-319.

Kusaka, S., Dabin, I., Barnstable, C.J. and Puro, D.G. (1996). cGMP-mediated effects on the physiology of bovine and human retinal Muller (glial) cells. *J. Physiol.* **497**: 813-824.

Kvanta, A., Seregard, S., Sejersen, S., Kull, B. and Fredholm, B.B. (1997). Localization of adenosine receptor messenger RNAs in the rat eye. *Exp. Eye Res.* **65**: 595-602.

Leipziger, J., Greger, R. and Nitschke, R. (1996): Regulation of intracellular calcium concentration in epithelial cells. *Kid. Blood Press. Res.* **19**: 148-150.

Lewis, C., Neifhart, S., Holy, C., North, R.A., Buell, G. and Suprenant, A. (1995). Coexpression of P2X2 and P2X3 receptor subunits can account for ATP-gated currents in sensory neurons. *Nature.* **377**: 432-435.

Lidofsky, S.D., Sostman, A. and Fitz, J.G. (1997). Regulation of cation-selective

channels in liver cells. *J. Membr. Biol.*, **157**: 231-236.

Lin, H. and Miller, S.S. (1992). Basolateral membrane pH_i -dependent Cl-HCO_3 exchanger helps regulate intracellular pH (pH_i) in frog retinal pigment epithelium (RPE). *Invest. Ophthalmol. Vis. Sci. Suppl.* **33**:911.

Linsenmeier, R.A. and Steinberg, R.H. (1984). Delayed basal hyperpolarization of cat retinal pigment epithelium and its relation to the fast oscillation of the DC electroretinogram. *J. Gen. Physiol.* **83**: 213-232.

Lipton, S.A. (1986). Antibody activates cationic channels via second messenger Ca^{2+} . *Biochem. Biophys. Act.* **856**: 59-67.

Loewenstein, W.R. (1985). Regulation of cell-to-cell communication by phosphorylation. *Biochem. Soc. Symp.* **50**: 43-58.

Lui, J.H.K. and Dacus, A.C. (1991). Aqueous humor cyclic AMP and circadian elevation of intraocular pressure in rabbits. *Curr. Eye Res* **10** (12): 1175-1177.

Luttrell, L.M., van Biesen, T., Hawes, B.E., Koch, W.J., Krueger, K.M., Touhara, K. and Lefkowitz, R.J. (1997). G-protein-coupled receptors and their regulation: activation of the MAP kinase signaling pathway by G protein coupled receptors. *Adv. Second Mess. Phosphopro. Res.* **31**: 263-277.

MacKinnon, A. C., Spedding, M. and Brown, C. M. (1994). α_2 -adrenoceptors: more subtypes but fewer functional differences. *Trends Pharm. Sci.* **15**: 119-123.

Mallorga, P., Buisson, S. and Sugrue, M. F. (1988). Alpha 1-adrenoceptors in the albino rabbit ciliary process. *J. Ocular Pharm.* **4**: 203-214.

Mamiya, N., Goldenring, J.R., Tsunada, Y., Modlin, I.M., Yasui, K., Usuda, N., Ishikawa, T., Natsume, A. and Hidaka, H. (1993). Inhibition of acid secretion in gastric parietal cells by Ca^{2+} /calmodulin dependent protein kinase II inhibitor KN-93. *Biochem. Biophys. Res. Comm.* **195**: 608-615.

Marley, P.D. and Thomson, K.A. (1996). The Ca^{2+} /calmodulin-dependent protein kinase inhibitors KN62 and KN93, and their inactive analogues KN04 and KN92, inhibit nicotinic activation of tyrosine hydroxylase in bovine chromaffin cells. *Biochem. Biophys. Res. Comm.* **221**: 15-18.

Marmor, M.F. (1988). New hypothesis on the pathogenesis and treatment of serous retinal detachment. *Graefes Arch. Clin. Exp. Ophthalmol.* **226**: 548-552.

Marmor, M.F. (1991). Clinical electrophysiology of the retinal pigment epithelium. *Documenta Ophthalmol.* **76**: 301-313.

- Martin, X.D. (1996). *Glaucoma Therapy*. Hogrefe & Huber Publishers.
- Martin-Vasallo, P., Ghosh, S. and Coca-Prados, M. (1989). Expression of Na, K-ATPase alpha subunit isoforms in the human ciliary body and cultured ciliary epithelial cells. *J. Cell. Physiol.* **141**: 243-252.
- Marty A, Tan YP, Trautmann A. (1984). Three types of calcium dependent channels in rat lacrimal glands. *J. Physiol.* **357**: 293-325.
- Marty A. (1987). Control of ionic currents and fluid secretion by muscarinic agonists in exocrine glands. *Trends Neurol. Sci.* **10**: 373-377.
- Marty A. (1989). The physiological role of calcium dependent channels. *Trends Neurol. Sci.* **12**: 420-424.
- Marunaka, Y., Shintani, Y., Downey, G.P. and Niisato, N. (1997). Activation of Na⁻-permeant cation channel by stretch and cyclic AMP-dependent phosphorylation in renal epithelial A6 cells. *J. Gen. Physiol.* **110**: 327-36.
- Maruyama Y, Petersen OH. (1982). Single channel currents in isolated patches of plasma membrane from basal surface of pancreatic acini. *Nature* **299**: 159-161.
- Mason. S.J., Paridiso, A.M. and Boucher, R.C. (1991). Regulation of transepithelial ion transport and intracellular calcium by extracellular ATP in human normal and cystic fibrosis airway epithelium. *Br. J Pharmacol.* **103**: 1649-1656.
- Matsumoto, S., Yorino, T., Magnino, P.E., DeSantis, L. and Pang, I-H. (1996). Endothelin-induced changes of second messengers in cultured human ciliary muscle cells. *Invest. Ophthalmol. Vis. Sci.* **37**: 1058-1066.
- Mattioli, M., Barboni, B. and DeFelice, L.J. (1991). Calcium and potassium currents in porcine granulosa cells maintained in follicular or monolayer tissue culture. *J. Membr. Biol.* **143**: 75-83.
- Mayerson, P.L., Hall, M.O., Clark, V. and Abrams, T. (1984). An improved method for isolation and culture of rat retinal pigment epithelial cells. *Invest Ophthalmol Vis Sci* **26**: 1599-1609.
- McLaren, G.J., Sneddon, P. and Kennedy, D. (1998). Comparison of the action of ATP and UTP at P2X1 receptors in smooth muscle of the rat tail. *Eur. J. Pharmacol.* **351**: 139-144.
- McLaughlin, C.W., Peart, D., Purves, R.D., Carre, D.A., Macknight, A.D.C. and Civan, M.M. (1998). Effects of HCO₃⁻ on cell composition of rabbit ciliary epithelium: a new model for aqueous humor secretion. *Invest. Ophthalmol. Vis. Res.* **39**: 1631-1640.

- McManus, O. B. (1991). Calcium-activated Potassium Channels: Regulation by Calcium. *J. Bioener. Biomem.* **23**: 537-559.
- McNeil, P.L., Murphy, R.F., Lanni, F. and Taylor, D.L. (1984). A method for incorporating macromolecules into adherent cells. *J. Cell Biol.* **98**: 1556-1564.
- Middleton, J.P., Mangel, A.W., Basavappa, S. and Fitz, J.G. (1993). Nucleotide receptors regulate membrane ion transport in renal epithelial cells. *Am. J Physiol.* **264**: F867-873.
- Mikalsen, S.O., Husoy, T. and Sanner, T. (1995). Modulation of gap junctional intercellular communication by phosphorylation: Effect of growth factors, kinase activators and phosphatase inhibitors. *Prog. Clin. Biol. Res.* **391**: 425-438.
- Miller SS, Steinberg RH. (1977). Passive ionic properties of frog retinal pigment epithelium. *J Membrane Biol.* **36**: 337-372.
- Minneman, K. P. (1988). α_1 -Adrenergic receptor subtypes, inositol phosphates and sources of cell Ca^{2+} . *Pharm. Rev.* **40**: 87-115.
- Minneman, K. P. and Esbenshade, T.A. (1994). α_1 -Adrenergic receptor subtypes. *Annu. Rev. Toxicol* **34**:117-33.
- Mitchell, C.H. and Jacob, T.J.C. (1993). Single channel memory of the open probability of a large conductance cation channel in isolated bovine pigmented ciliary epithelial cells. *J. Physiol.* **467**: 335P.
- Mitchell, C.H. and Jacob, T.J.C. (1996a): A large-conductance chloride channel in pigmented ciliary epithelial cells activated by GTP γ S. *J. Membr. Biol.* **158**: 167-175.
- Mitchell, C.H. and Jacob, T.J.C. (1996b). A nonselective high conductance channel in bovine pigmented ciliary epithelial cell. *J. Membr. Biol.* **150**: 105-111.
- Mitchell, C.H., Carre, D.A., McGlin, A.M., Stone, R.A. and Civan, M.M. (1998). A release mechanism for stored ATP in ocular epithelial cells. *PNAS.* **95**: 7174-7178.
- Mittag, T. W. and Tormay, A. (1985). Adrenergic receptor subtypes in rabbit iris-ciliary body membranes: classification by radioligand studies. *Exp. Eye Res.* **40**: 239-249
- Moolenaar, W.H., Kranenburg, O., Postma, F.R. and Zondag, C.M. (1997). Lysophosphatidic acid: G-protein signaling and cellular responses. *Curr. Opin. Cell Biol.* **9**: 168-173.
- Mund, M.L. and Rodrigues, M.M. (1979). In: The retinal pigment epithelium. K.M. Zinn and M.F. Marmor, editors. pp-45-52. Harvard Univeristy Press, Cambridge.
- Muraki, K., Imaizumi, Y., Bolton, T.B., Watanabe, M. (1998). Comparative study of

effects of isoproterenol and vasoactive intestinal polypeptide on voltage-dependent Ca^{2+} and Ca^{2+} -activated K^{+} currents in porcine tracheal smooth muscle cells. *Gen. Pharmacol.* **30**: 115-199.

Murthy, K.S. and Makhlof, G.M. (1998). Coexpression of ligand-gated P2X and G protein-coupled P2Y receptors in smooth muscle. *J. Biol. Chem.* **273**: 4695-4704.

Nao-I, N., Gallemore, R.P. and Steinberg, R.H. (1990). Effects of cAMP and IBMX on the chick retinal pigment epithelium. *Invest. Ophthalmol. Vis. Sci.* **31**: 54-66.

Naor, Z., Harris, D. and Scacham, S. (1998). Mechanism of GnRH receptor signaling: combinatorial cross-talk of Ca^{2+} and protein kinase C. *Front. Neuroendocrin.* **19**: 1-19.

Nara, M., Dhulipala, P.D.K., Wang, Y-X and Kotlikoff, M.I. (1998). Reconstitution of beta-adrenergic modulation of large conductance, calcium-activated potassium (Maxi-K) channels in *Xenopus* Oocytes. *J. Biol. Chem.* **273**: 14920-14924.

Naruse, K. and Sokabe, M. (1993). Involvement of stretch-activated ion channels in Ca^{2+} mobilization to mechanical stretch in endothelial cells. *Am. J. Physiol.* **264**: C1037-1044.

Nash, M.S. and Osborne, N. N. (1995). Pertussis toxin-sensitive melatonin receptors negatively couple to adenylate cyclase associated with cultured human and rat retinal pigment epithelial cells. *Invest. Ophthalmol. Vis. Sci.* **36**: 94-103.

Nash, M.S. and Osborne, N. N. (1995). Agonist-induced effects of cyclic AMP metabolism are affected in pigmented epithelial cells of the Royal College of Surgeons rat. *Neurochem. Int.* **27**: 253-262.

Nash, M.S. and Osborne, N. N. (1997). Pharmacologic evidence for 5HT_{1A} receptors associated with human retinal pigment epithelial cells in culture. *Invest. Ophthalmol. Vis. Sci.* **38**: 510-519.

Nathanson, J.A. (1981). Human ciliary process adrenergic receptor: pharmacological characterization. *Invest. Ophthalmol. Vis. Sci.* **21**: 798-804.

Neal, J.M., Cunningham, J.R. and Dent, Z. (1998). Modulation of extracellular GABA levels in the retina by activation of glial P2X-purinoceptors. *Br. J. Pharmacol.* **124**: 317-322.

Neal, J.M., Cunningham, J.R. (1994). Modulation by endogenous ATP of the light-evoked release of ACh from retinal cholinergic neurons. *Brit. J. Pharmacol.* **113**: 1085-1087.

Neer, E., Schmidt, C.J., Nambudripad, R. and Smith, T.F. (1994). *Nature* **371**: 297-300.

Neer, E.J. (1995). Heterotrimeric G proteins: organizers of transmembrane signals. *Cell.*

80: 249-257.

Negi A and Marmor M.F. (1983). The reabsorption of subretinal fluid after diffuse damage to the retinal pigment epithelium. *Invest. Ophthalmol. Vis. Sci.* **24**: 1475-1479.

Negi A and Marmor M.F. (1986). Mechanisms of subretinal fluid absorption in the cat eye. *Invest. Ophthalmol. Vis. Sci.* **27**: 1560-1563.

Neher, E. (1992). Correction for liquid junction potentials in patch-clamp experiments. *Methods Enzymol* **207**: 123-131.

Neill, J.M., Thornquist, S.C., Raymond, M.C., Thompson, J.T. and Barnstable, C.J. (1993). RET-PE10: a 61 kDa polypeptide epitope expressed late during vertebrate RPE maturation. *Invest. Ophthalmol. Vis. Sci.* **34**: 453-462.

Neill, J.M. and Barnstable, C.J. (1990). Expression of the cell surface antigens RET-PE2 and N-CAM by rat retinal pigment epithelial cells during development and in tissue culture. *Exp. Eye Res.* **51**: 573-583.

Ng, B. and Barry, P.H. (1995). The measurement of ionic conductivities and mobilities of certain less common organic ions needed for junction potential corrections in electrophysiology. *J. Neurosci Methods* **56**: 37-41.

Nicholas, R.A., Lazarowski, E.R., Watt, W.C., Li-Q, Boyer, J. and Harden, T.K. (1996). Pharmacological and second messenger signaling selectivity of cloned P2Y receptors. *J. Auton. Pharmacol.* **16**: 319-323.

Nori, S., Fumagalli, L., Bo, X., Bogdanov, Y. and Burnstock, G. (1998). Coexpression of mRNAs for P2X1, P2X2 and P2X4 receptors in rat vascular smooth muscle: an *in situ* hybridization and RT-PCR study. *J. Vasc. Res.* **35**: 179-185.

North, R.A. and Barnard, E.A. (1997). Nucleotide receptors. *Curr. Opin. Cell Biol.* **7**: 346-375.

Oliva, C., Cohen, I, and Mathias, R. (1988). Calculation of time constants for intracellular diffusion in whole cell patch clamp configuration. *Biophys. J.* **54**: 791-799

Ono S, Mougouris T, DuBose TD and Sansom SC. (1994). ATP and calcium modulation of nonselective cation channels in IMCD cells. *Am. J. Physiol.* **267**: F558-565.

Osborne, N.N., Fitzgibbon, F., Nash, M., Lui, N-P., Leslie, R. and Cholewinski, A. (1993). Serotonergic, 5HT₂, receptor-mediated phosphoinositide turnover and mobilization of calcium in cultured rat retinal pigment epithelium cells. *Vis. Res.* **33**: 2171-2179.

Owaribe, K., Kartenbeck, J., Rungger-Brandle, E and Franke, W.W. (1988).

Cytoskeletons of retinal pigment epithelial cells: Interspecies differences of expression patterns indicate independence of cell function from the specific complement of cytoskeletal proteins. *Cell Tissue Res.* **254**: 301-315.

Ozanics, V. and Jakobiec, F.A. (1992). Prenatal development of the eye and its adnexa. In: Ocular embryology and teratology. F.A. Jakobiec, editor. pp 11-97. Harper & Row Publishing Inc.

Parsons, T.D. and Hartzell, H.C. (1993). Regulation of Ca^{2+} current in frog ventricular cardiomyocytes by guanosine 5'-triphosphate analogues and isoproterenol. *J. Gen. Physiol.* **102**: 525-549.

Partridge LD and Swandulla D. Calcium -activated nonspecific cation channels. (1988). *Trends Neurol. Sci.* **11**:69-72.

Pellergrino, M. and Pellegrini, M. Modulation of Ca^{2+} -activated K^+ channels of human erythrocytes by endogenous cAMP-dependent protein kinase. *Pflugers Arch.* **436**: 749-756.

Petersen, O.H. and Maruyama, Y. (1984). Calcium-activated potassium channels and their role in secretion. *Nature.* **307**: 693-696.

Peterson, WM, Meggysey, C, Yu, K and Miller, S.S. (1997). Extracellular ATP activates calcium signaling, ion and fluid transport in retinal pigment epithelium. *J. Neurosci.* **17**: 2323-2337.

Pott, L. and Mechmann, S. (1990). Large-conductance ion channel measured by whole-cell voltage clamp in single cardiac cells: modulation by adrenergic stimulation and inhibition by octanol. *J. Membr. Biol.* **117**: 189-199.

Poyer, J.F., Ryan, J.S. and Kelly, M.E.M. (1996). G protein-mediated activation of a nonspecific cation current in cultured rat retinal pigment epithelial cells. *J. Membr. Biol.* **153**: 13-26.

Proctor, R.A., Denlinger, L.C., Leventhal, P.S., Daugherty, S.K., van de Loo, J.W., Tanke, T., Firestein, G.S. and Bertis, P.J. (1994). Protection of mice from endotoxic death by 2-methylthio-ATP. *Proc. Natl. Acad. Sci.* **21**:6017-6020.

Puro, D.G., Roberge, F and Chan, C-C. (1989). Retinal ganglion cell proliferation and ion channels : A possible link. *Invest. Ophthalmol. Vis. Sci.* **30**: 521-529.

Puro, D.G. (1998). Modulation of ion channels in mammalian Muller cells. *Curr. Eye Res.* **67**: S.35.

Rae JL, Dewey J, Cooper K and Gates P. (1990). A nonselective cation channel in rabbit corneal endothelium activated by internal calcium and inhibited by internal ATP. *Exp.*

Eye Res. **50**: 373-384.

Rae, J.L. and Levis, R.A. (1984). Patch voltage clamp of lens epithelial cells: theory and practice. *Mol. Physiol.* **6**:115-162.

Rae, M.G., Rowan, E.G. and Kennedy, C. (1998). Pharmacological properties of P2X₃-receptors present in neurons of the rat dorsal root ganglia. *Br. J. Pharmacol.* **124**: 176-180.

Raviola, G. and Raviola, E. (1978). Intercellular junctions in the ciliary epithelium. *Invest. Ophthalmol. Vis. Sci.* **17**: 958-981.

Robinson, M.J. and Cobb, M.H. (1997). Mitogen-activated protein kinase pathways. *Curr. Opin. Cell. Biol.* **9**: 180-186.

Rodbell, M. (1992). The role of GTP-binding in signal transduction: From the sublimely simple to the conceptually complex. *Curr. Topics Cell Reg.* **32**:1-47.

Rodriguez-Boulan, E. and Nelson, W.J. (1989). Morphogenesis of the polarized epithelial cell phenotype. *Science.* **245**: 718-725.

Ross, R. A. and Drance, S. M. (1970). Effects of topically applied isoproterenol on aqueous dynamics in man. *Archives of Ophthalmology* **83**: 39-46.

Rudy, B. (1988). Diversity and ubiquity of K channels. *Neurosci.* **25**: 729-749.

Salter, M.W. and Hicks, J.L. (1995). ATP causes release of intracellular Ca²⁺ via the phospholipase C β IP₃ pathway in astrocytes from the dorsal spinal cord. *J. Neurosci.* **15**:2961-2971.

Satoh, H. (1996). Modulation of Ca²⁺-activated K⁺ current by isoprenaline, carbachol, and phorbol ester in cultured (and fresh) rat aortic vascular smooth cells. *Gen. Pharmacol.* **27**: 319-324.

Schumann, S., Greger, R and Leipziger, J. (1994) Flufenamate and Gd³⁺ inhibit stimulated Ca²⁺ influx in the epithelial cells line CFPAC-1. *Pflugers. Arch.* **428**: 583-589.

Schultz, G., Rosenthal, W., Trautwein, W. and Hescheler, J. (1990). Role of G proteins in calcium channel modulation. *Annu. Rev. Physiol.* **52**: 275-292.

Schutte, M., Diadori, A., Wang, C. and Wolosin, J. M. (1996). Comparative adreno-cholinergic Ca²⁺ pharmacology in the dissociated rabbit ciliary epithelial cell layers. *Invest. Ophthalmol. Vis. Sci.* **37**: 212-220.

Schutte, M. and Wolosin, J. M. (1996). Ca²⁺ mobilization and interlayer signal

transfer in the heterocellular bilayered epithelium of the rabbit ciliary body. *J. Physiol.* **496**: 25-37.

Sears, J., Nakano, T. and Sears, M. (1998). Adrenergic-mediated connexin 43 phosphorylation in the ocular ciliary epithelium. *Curr. Eye Res.* **17**: 104-107.

Segawa, Y and Hughes, B.A. (1994). Properties of the inwardly rectifying K⁺ conductance in the toad retinal pigment epithelium. *J. Physiol.* **476**: 41-53.

Selbie, L.A. and Hill, S.J. (1998). G protein-coupled-receptor cross-talk: the fine-tuning of multiple receptor-signaling pathways. *TIPS.* **19**:87-94.

Shahidullah, M. and Wilson, W.S. (1997). Mobilization of intracellular calcium by P2Y₂ receptors in cultured, non-transformed bovine ciliary epithelial cells. *Curr. Eye Res.* **16**: 1006-1016.

Shiels, I.A., Zhang, S., Ambler, J. and Taylor, S.M. (1998). Vascular leakage stimulates phenotype alteration in ocular cells, contributing to the pathology of proliferative vitreoretinopathy. *Med. Hypoth.* **50**: 113-117.

Shi, X-P., Zamudio, A.C., Candida, O.A. and Wolosin, J. M. (1996). Adreno-cholinergic modulation of junctional communication between the pigmented and nonpigmented layers of the ciliary body epithelium. *Invest. Ophthalmol. Vis. Sci.* **37**: 1037-1046.

Shuba, Y.M., Hesslinger, B., Trautwein, W., McDonald, T.F. and Pelzer, D. (1990). Whole-cell calcium current in guinea pig ventricular myocytes dialysed with guanine nucleotides. *J. Physiol.* **424**: 205-228.

Smart, T.G. (1997). Regulation of excitatory and inhibitory neurotransmitter-gated ion channels by protein phosphorylation. *Curr. Opin. Neurobiol.*, **7**: 358-367.

Smith-Thomas, L., Haycock, J.W., Metcalfe, R., Boulton, M., Ellis, S., Rennie, I.G., Richardson, P.S., Palmer, I., Parsons, M.A. and MacNeil, S. (1998). Involvement of calcium in retinal pigment epithelial cell proliferation and pigmentation. *Curr. Eye. Res.* **17**: 813-822.

Soltoff, S.P., Avraham, H., Avarham, S. and Cantley, L.C. (1998). Activation of P₂Y₂ receptors by ATP and UTP stimulates mitogen-activated kinase activity through a pathway that involves related adhesion focal tyrosine kinase and protein kinase C. *J. Biol. Chem* **273**: 2653-2660.

Sohma, Y., Harris, A., Wardle, C.J.C., Gray, M.A. and Argent, B.E. (1994). Maxi K⁺ channels on human vas deferens epithelial cells. *J. Membran. Biol.* **141**: 69-82.

Sorensen, S.J. and Abel, S.R. (1996). Comparison of ocular beta blockers. *Ann.*

Pharmacother. **30**: 43-54.

Soto, F., Guzam-Garcia, M., Gomex-Hernandez, J.M., Hollmann, M., Karschin, C. and Stuhmner, W. (1996). P2X₄: An ATP-activated ionotropic receptor cloned from brain. *Proc. Nat. Acad. Sci.* **93**: 3864-3688.

Stalmans, P and Himpens, B. (1997a). Effect of increasing glucose concentration and protein phosphorylation on intercellular communication in cultured rat retinal pigment epithelial cells. *Invest. Ophthalmol. Vis Sci.* **38**: 1598-1609.

Stalmans, P and Himpens, B. (1997b). Confocal imaging of Ca²⁺ signaling in cultured rat retinal pigment epithelial cells during mechanical and pharmacologic stimulation. *Invest. Ophthalmol. Vis Sci.* **38**: 176-187.

Steinberg, R.H. and Miller, S.S. (1979). Transport and membrane properties of the retinal pigment epithelium. **In**: The retinal pigment epithelium. K.M. Zinn and M.F. Marmor, editors. pp-192-204. Harvard Univeristy Press, Cambridge.

Stelling, J. W. and Jacob, T. J. C. (1991). The inward rectifier K⁺ current underlies oscillatory membrane potential behavior in bovine pigmented ciliary epithelial cells. *J. Physiol.* **458**, 439-56.

Stelling, J. W. and Jacob, T. J. C. (1993). Membrane potential oscillation from a novel combination of ion channels. *Am. J. Physiol.* **265**: C203-C209.

Stelling, J. W. and Jacob, T. J. C. (1996). Transient activation of K⁺ channels by carbachol in bovine pigmented ciliary body epithelial cells. *Am J. Physiol.* **271**: C203-209.

Stone, R.A., Kuwayama, Y. and Laties, A.M.(1987). Regulatory peptides in the eye. *Experimentia.* **43**: 791-800.

Strauß, O. and Wienrich, M. (1993). Cultured retinal pigment epithelial cells from RCS rats express an increased calcium conductance compared with cells from non-dystrophic rats. *Pflugers Arch.* **425**: 68-76.

Strauß, O., Richard, G. and Weinrich, M. (1993). Voltage-dependent potassium currents in cultured human retinal pigment epithelial cells. *Biochem. Biophys. Res. Commun.* **191**: 775-781.

Strauß, O., Weiser, T. and Wienrich, M. (1994). Potassium currents in cultured cells of the rat retinal pigment epithelium. *Comp. Biochem. Physiol.* **109**: 975-983.

Strauß, O., Wiederholt, M. and Wienrich, M. (1996). Activation of Cl⁻ currents in cultured rat retinal pigments epithelial cells by intracellular application of inositol-1,4,5-triphosphate: differences between rats with retinal dystrophy (RCS) and normal rats.

J. Membr. Biol. **151**: 189-200.

Strauß, O., Steinhausen, K, Wienrich, M and Wiederholt, M. (1998). Activation of a Cl⁻ conductance by protein kinase-dependent phosphorylation in cultured rat retinal pigment epithelial cells. *Exp. Eye Res* **66**: 35-42.

Streeten, B.W. (1982). Ciliary Body. **In**: Ocular embryology and teratology. F. A. Jakobiec, editor. pp 303-333. Harper & Row Publishing Inc.

Stobaek, D., Chrisophersen, P., Dissing, S and Olesen, S-P. (1996). ATP activates K and Cl channels via purinoceptor-mediated release of Ca²⁺ in human coronary artery smooth muscle. *Am. J. Physiol.* **271**: C1463-1471.

Sugioka, M., Fukunda, Y. and Yamashita, M. (1996). Ca²⁺ responses to ATP via purinoceptors in the early embryonic chick retina. *J. Physiol.* **493**: 855-863.

Sullivan, D.M., Erb, L., Anglade, E., Weisman, G.A., Turner, J.T. and Csaky, K.G. (1997). Identification and characterization of P2Y₂ nucleotide receptors in human pigment epithelial cells. *J. Neurosci. Res.* **49**: 43-52.

Summers, R. J. and McMartin, L. R. (1993) Adrenoceptors and their second messenger systems. *J. Neurochem.* **60**: 10-20.

Sun, X.P., Supplisson, S. and Mayer, E. (1993). Chloride channels in myocytes from rabbit colon are regulated by a pertussis toxin-sensitive G protein. *Am. J. Physiol.* **264**: G774-C784.

Suprenant, A., Buell, G. and North, R.A. (1995). P2X receptors bring new structure to ligand-gated ion channels. *TINS.* **18**: 224-229.

Suzuki, Y., Nakano, T. and Sears, M. (1997). Calcium signals from intact rabbit ciliary epithelium observed with confocal microscopy. *Curr. Eye Res.* **16**: 166-175.

Tao, Q.-P., Rafuse, P.E. and Kelly, M.E.M. (1994). Potassium currents in rabbit retinal pigment epithelial cells. *J. Membr. Biol.* **141**: 123-138.

Tao, Q-P. and Kelly, M. E. M. (1996). Calcium-activated potassium current in cultured rabbit retinal pigment epithelial cells. *Curr. Eye Res.* **15**: 237-246.

Thorn, P. and Petersen, O.H. (1992). Activation of a nonselective cation channel by physiological cholecystokinin concentrations in mouse pancreatic acinar cells. *J. Gen. Physiol.* **100**: 11-25.

Thorn, P. and Petersen, O.H. (1993). Nonselective cation channels in exocrine gland cells. **In**: Nonselective cation channels: pharmacology, physiology and biophysics. D. Seimen and J. Hescheler, editors.

- Thoreson, W.B. and Chacko, D.M. (1997). Lysophosphatidic acid stimulates two ion currents in cultured human retinal pigment epithelial cells. *Exp. Eye Res.* **65**: 7-14.
- Topping, T.M., Abrams, G.W. and Machemer, R. (1979). Experimental double-perforating injury of the posterior segment in rabbit eyes. *Arch. Ophthalmol.* **97**: 735-742.
- Toullec, D., Pianetti, P., Coste, H., Bellevergue, P., Gran-Perret, T., Ajakanes, M., Baudet, V., Boissin, P., Boursier, E., Loriolle, F., Duhamel, L., Charon, D. and Kirilovsky, J. (1991). The bisindolylmaleimide GF 109203X is a potent and selective inhibitor of protein kinase C. *J. Biol. Chem.* **266**: 15771-15781.
- Trope, G. and Rumley, A.G. (1985). Catecholamines in human aqueous humor. *Invest. Ophthalmol. Vis. Sci.* **26**: 399-401.
- Trope, G.E., Sole, M., Aedy, L and Madapallimattam, A. (1987). Levels of norepinephrine, epinephrine, dopamine, serotonin and N-acetylserotonin in aqueous humor. *Can. J. Ophthalmol.* **22**: 152-154.
- Tsein, R.Y. (1988). Fluorescence measurement and photochemical manipulation of cytosolic free calcium. *Trends Biochem.* **11**: 419-424.
- Tso, M.O.M.(1988). Comparison of pathologic changes in retinal photic injury and age-related macular degeneration. **In**: Retinal disease. M. Tso, editor. pp:207-208. J.B. Lippincott Co, Philadelphia.
- Twitchell, W.A., Pena, T.L. and Rane, S.G. (1997). Ca^{2+} -dependent K^+ channels in bovine adrenal chromaffin cells are modulated by lipoxygenase metabolites of arachidonic acid. *J. Membrane Biol.* **158**: 69-75.
- Ueda, Y. and Steinberg, R.H. (1993). Voltage-operated calcium channels in fresh and cultured rat retinal pigment epithelial cells. *Invest. Ophthalmol. Vis. Sci.* **34**: 3408-3418.
- Ueda, Y. and Steinberg, R.H. (1994). Chloride currents in freshly isolated rat retinal pigment epithelial cells. *Exp. Eye Res.* **58**: 331-342.
- Ui, M. (1990). Pertussis toxin as a valuable probe for G-protein involvement in signal transduction. **In**: ADP-Ribosylating Toxins and G proteins. Insights into Signal Transduction. J. Moss and M. Vaughan, editors. pp. 45-77. American Society for Microbiology Press, Washington, D.C.
- Van Biesen, T., Luttrell, L.M., Hawes, B.E. and Lefkowitz, R.J. (1996). Mitogenic signaling via G protein-coupled receptors. *Endo. Rev.* **17**: 698-709.

- Van-Scott, M.R., Chinet, T.C., Burnette, A.D. and Paradisio, A.M. (1995). Purinergic regulation of ion transport across nonciliated bronchiolar epithelial (Clara) cells. *Am. J. Physiol.* **269**: L30-L37.
- Von-Tschanner, V., Prod'hom, B., Baggiolini, M and Reuter, H. (1986). Ion channels in human neutrophils activated by a rise in free cytosolic calcium concentration. *Nature* **324**: 369-372.
- Wang N, Koutz CA, Anderson RE (1993). A method for the isolation of retinal pigment epithelial cells from adult rats. *Invest. Ophthalmol. Vis. Sci.* **34**: 101-107.
- Waltz, W., Llscher, S., Ohlemeyer, C., Banati, R. and Kettenmann, H. (1993). Extracellular ATP activates a cation conductance and a K⁺ conductance in cultured microglial cells from mouse brain. *J. Neurosci.* **13**: 4403-4411.
- Wang, Y.X., Fleischmann, B.K. and Kotlikoff, M.I. (1997). M₂ receptor activation of nonselective cation channels in smooth muscle cells: calcium and Gi/Go requirements. *Am. J. Physiol.* **273**: C500-C508.
- Watson, S. and Arkininstall, S. (1994). Adrenaline and noradrenaline. In: The G-Protein Linked Receptor Facts Book. pp 32-54. Academic Press INC., San Diego, CA.
- Watson, S. and Arkininstall, S. (1994). The G-protein linked receptor facts book. pp: 1-219. Academic Press, London.
- Wax, M. (1991). Signal transduction in the ciliary epithelium. In: Adler's Physiology of the Eye. 2nd edition. W.M. Hart, editor. pp 184-210. Mosby Year Book Inc.
- Wax, M. B. and Molinoff, P. B. (1987). Distribution of beta-adrenergic receptors in human iris-ciliary body. *Invest. Ophthalmol. Vis. Sci.* **28**: 420-430.
- Wei, J.Y., Cohen, E.D., Yan, Y.Y., Genieser, H.G and Barnstable, C.J. (1996). Identification of competitive antagonists of the rod photoreceptor cGMP-gated cation channel: beta-phenyl-1,N2-etheno-substituted cGMP analogues as probes of the cGMP-binding site. *Biochemistry*, **35**: 16815-16823.
- Wen R, Lui GM, Steinberg RH. (1993). Whole cell K⁺ currents in fresh and cultured cells of the human and monkey retinal pigment epithelium. *J. Physiol.* **465**: 121-147.
- Wess, J. (1997). G-protein-coupled receptors: molecular mechanisms involved in receptor activation and selectivity of G-protein recognition. *FASEB.* **11**:346-354.
- Wiederholt, M., Helbig, H. and Korbmacher, C. (1991). In: Carbonic Anhydrase. F. Botre, G. Gross, and B.T. Storey, editors. pp 232-244.
- Wickman, K. and Clapham, D.E. (1995a). Ion channel regulation by G proteins. *Physiol.*

Rev. 75(4): 865-885.

Wickman, K. and Clapham, D.E. (1995b). G-protein regulation of ion channels. *Curr. Opin. Cell Biol.* 5: 278-285.

Wikberg-Matsson, A., Wikberg, J.E.S. and Uhlen, S. (1996). Characterization of $\alpha 2$ -adrenoceptor subtypes in the porcine eye: Identification of $\alpha 2$ -adrenoceptors in the choroid, ciliary body and iris, and $\alpha 2A$ - and $\alpha 2C$ -adrenoceptors in the retina. *Exp. Eye Res.* 63: 57-66.

Wolfensberger, T.J., Holz, F.G., Ationu, A., Carter, N.D. and Bird, A.C. (1994). Natriuretic peptide and their receptors in human neural retina and retinal pigment epithelium. *German J.Ophthalmol.* 3: 248-252.

Wolosin, J.M., Bonanno, J.A., Hanzel, D. and Machen, T.E. (1991). Bicarbonate transport mechanisms in rabbit ciliary body epithelium. *Exp. Eye Res.* 52: 397-407.

Yan, Z., Song, W.J. and Surmeier, J. (1997). D₂ dopamine receptors reduce N-type Ca²⁺ currents in rat neostriatal cholinergic interneurons through a membrane-delimited, protein kinaseC insensitive pathway. *J. Neurophysiol.* 77: 1003-1015.

Yang, X.-C and Sachs, F. (1989). Block of stretch-activated ion channels on *Xenopus* oocytes by gadolinium and calcium ions. *Science* 243: 1068-1071.

Ypey, D.L. and Clapham, D.E. (1984). Development of a delayed outward-rectifying K⁺ conductance in cultured mouse peritoneal macrophages. *Proc. Natl. Acad. Sci.* 81: 3083-3087.

Yu, X-M., Asklan, R., Keill I.G, and Salter, M.W. (1997). NMDA channel regulation by channel-associated protein tyrosine kinase Src. *Science*, 275: 674-678.

Yu, S-M., Chen, S-F, Lau, Y-T, Yang, C-M. and Chen, J-C.(1996). Mechanism of extracellular ATP-induced proliferation of vascular smooth muscle cells. *Mol. Pharmacol.* 50:1000-1009.

Zagotta, W.N. and Siegelbaum, S.A.(1996). Structure and function of cyclic nucleotide-gated ion channels. *Ann. Rev. Neurosci.* 19: 235-263.

Zamir, E. (1997). Central serous retinopathy associated with adrenocorticotrophic hormone therapy. A case report and a hypothesis. *Graefes-Arch-Clin-Exp-Ophthalmol.* 235: 339-344.

Zauberman, H. (1979). Adhesive forces between the retinal pigment epithelium and sensory retina. In: The retinal pigment epithelium. K.M. Zinn and M.F. Marmor, editors. pp-192-204. Harvard Univeristy Press, Cambridge.

Zhao, M.M., Hwa, J. and Perez, D. M. (1996). Identification of critical extracellular loop residues involved in $\alpha 1$ -adrenergic receptor subtype-selective antagonist binding. *Mol. Pharmacol.* **50**:1118-1126.

Zhu, M., Galband, C.H., Moore, J.M., Posner, P and Summers, C. (1998). Angiotensin II type 2 receptor stimulation of neuronal delayed-rectifier potassium current involves phospholipase and arachidonic acid. *J. Neurosci.* **18**: 679-686.

Zimmermann, H (1994), Signaling via ATP in the nervous system. *TINS.* **17**: 420-425.

Zinn, K.M. and Benjamin-Henkind, J.V. (1979). Anatomy of the human retinal pigment epithelium. **In**: The retinal pigment epithelium. K.M. Zinn, M.F. Marmor, editors. pp: 3-27. Harvard University Press, Cambridge, MA.